NISTIR 5373

Report on the Workshop on Manufacturing Polymer Composites by Liquid Molding

September 20 - 22, 1993

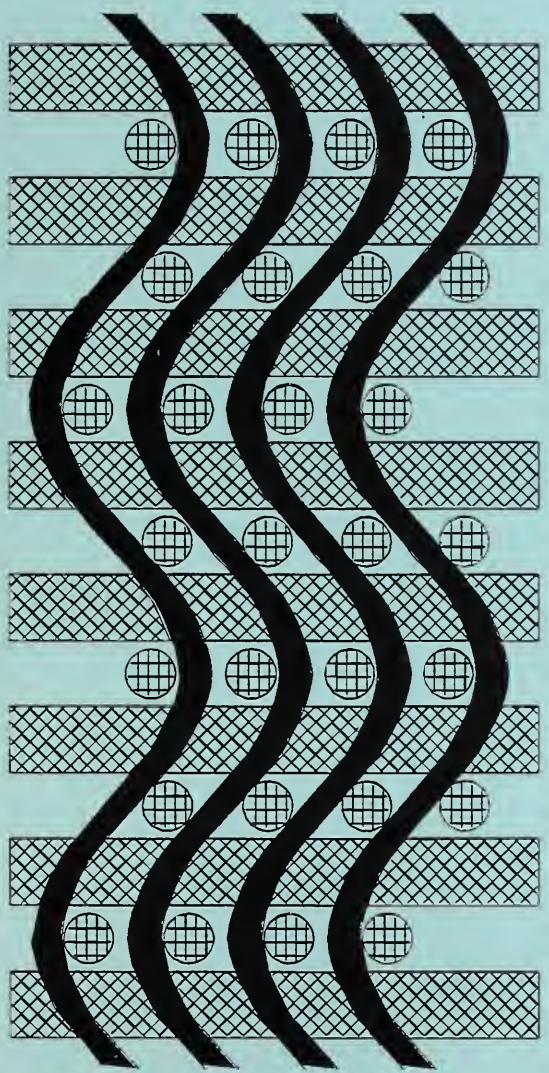

Richard S. Parnas
NIST, Polymers Division

Andrew J. Salem
General Electric Corporate Research & Development

Kenneth N. Kendall
Ford Motor Company

Michiel V. Bruschke
Unilever Research Laboratorium

U.S. DEPARTMENT OF COMMERCE
Technology Administration
National Institute of Standards and Technology
Gaithersburg, MD 20899

NIST

About the cover:
A cross section of the 3-dimensionally woven fabric NIST is proposing as a standard reference material for permeability. An original image was produced by casting the fabric in epoxy, sectioning the composite, and photographing the exposed surface. The schematic diagram on the cover was developed from the original image by digitizing and curve fitting the fiber trajectories for a mathematical model of the fabric.

NISTIR 5373

Report on the

Workshop on Manufacturing Polymer Composites by Liquid Molding

September 20 - 22, 1993

Richard S. Parnas
NIST, Polymers Division

Andrew J. Salem
General Electric Corporate Research & Development

Kenneth N. Kendall
Ford Motor Company

Michiel V. Bruschke
Unilever Research Laboratorium

U.S. DEPARTMENT OF COMMERCE
Technology Administration
National Institute of Standards and Technology
Gaithersburg, MD 20899

February 1994

U.S. DEPARTMENT OF COMMERCE
Ronald H. Brown, Secretary

TECHNOLOGY ADMINISTRATION
Mary L. Good, Under Secretary for Technology

NATIONAL INSTITUTE OF STANDARDS AND TECHNOLOGY
Arati Prabhakar, Director

Executive Summary

The *Workshop on Manufacturing Polymer Composites by Liquid Molding* was convened at the behest and with the cooperation of General Electric and Ford Motor Co. The workshop concept originated in the Advanced Technology Program (ATP) with Ford, GE and NIST, and the ATP office generously provided funding for this meeting. The workshop goals were to define the major issues facing industry, open lines of communication between those working on each issue, and focus attention on those thought most critical. The workshop included eight invited lectures introducing the major topics, five discussion sections devoted to defining the critical challenges presented by each major issue, and a number of posters.

The five discussion groups convened on the second day of the workshop focussed on model validation and test methods, high speed processing, preform architecture and permeability, reinforcement / resin interactions during flow, and heating and rheokinetic effects during flow. Although the discussions produced vigorous debate, especially between the academic and industrial communities, on the priorities of the various issues, there was nearly complete agreement on which issues deserved further attention. One issue deemed critical is the deformation process a fibrous reinforcement undergoes when it is preformed, and the effects of the deformation process on the permeability tensor for fluid flow. One may also ask if the preform deformation effects the mechanical properties of the finished part. A second issue also considered essential to the progress of the liquid molding industry is the establishment of standard materials and procedures for permeability measurements, as well as the development of a data base of permeability and related processing information. Of overriding concern to the representatives from the automotive industry was the issue of high speed processing, and the production of high quality preforms in rapid cycle times.

Table of Contents

1. Workshop description and results

This report documents the *Workshop on Manufacturing Polymer Composites by Liquid Molding*, held September 20-22, 1993 at the National Institute of Standards and Technology in Gaithersburg, MD. The workshop was organized at the request of industry and co-sponsored by Ford Motor Co., General Electric Corporate Research & Development, and the National Institute of Standards and Technology. Although it has been recognized that Liquid Composite Molding (LCM) has a high potential for cost effective manufacturing of structural composites, there remain a number of technological hurdles to overcome. The wide range of issues facing the composite manufacturer who produces parts via LCM includes a number of fluid flow problems. For example, the complex reinforcement structures used in LCM preforms lead to nonuniform flows, and therefore require sophisticated mold design procedures to ensure complete part wetout and filling of the mold. Solving problems such as these are crucial for the successful industrial application of LCM.

The goals of the workshop were to define clearly the major theoretical and practical issues facing the industry, open lines of communication between those working on each issue, and focus attention on those issues deemed most critical at the present time. The workshop included eight invited lectures introducing the major issues, five discussion sections devoted to defining the critical challenges presented by each major issue, and a number of posters. The meeting agenda allowed 45 minutes for each lecture and approximately 4 hours for each discussion group. A total of 69 people, predominantly from industry, but also from universities and governments, attended the meeting. Papers summarizing the lectures and workshop discussions, poster abstracts, and a participants list follow these introductory remarks.

The five discussion groups convened on the second day of the workshop focussed on model validation and test methods, high speed processing, preform architecture and permeability, reinforcement / resin interactions during flow, and heating and rheokinetic effects during flow. Although the discussions produced vigorous debate, especially between the academic and industrial communities, on the priorities of the various issues, there was nearly complete

agreement on which issues deserved further attention. One issue deemed critical is the deformation process a fibrous reinforcement undergoes when it is preformed, and the affects of the deformation process on the permeability tensor for fluid flow. One may also ask if the preform deformation effects the mechanical properties of the finished part. A second issue also considered essential to the progress of the liquid molding industry is the establishment of standard materials and procedures for permeability measurements, as well as the development of a data base of permeability and related processing information. Of overriding concern to the representatives from the automotive industry was the issue of high speed processing, and the production of high quality preforms in rapid cycle times.

The workshop on model validation and test methods discussed the issues and requirements for validating computer models for liquid molding design. Perhaps the most important issue raised was the uncertainty introduced into validation studies by the sensors used to make measurements. For example, pressure transducers are prone to errors as large as 20% when the pressure falls in the lower 10% of the transducer measurement range. Flowmeters and thermocouples suffer related problems that call for very careful sensor selection and experimental design. An equally serious issue that was raised concerns the expense of model validation. Most validation studies have been incomplete due to the cost of conducting realistic experiments in molds of complex geometry, repetitive experiments to generate statistical information, and using curing systems to produce realistic thermal effects. The third major issue raised in the model validation workshop was the permeability. While it was widely agreed that knowledge of the permeability is necessary for proper model validation, it was also widely agreed that the permeability is difficult to measure reliably.

The most important conclusions reached in the validation workshop were that sensitivity of the liquid molding process to material properties such as permeability should be determined in order to place the appropriate priority on material property measurements. Assuming that properties such as permeability and thermal conductivity are important, standard test methods and standard reference materials should be developed with all possible speed. Specifically, the workshop recommended that new permeability measurements be accompanied by data obtained

with the NIST permeability SRM.

The workshop on high speed processing focused on an assessment of current processing technology and enabling technologies that would permit the use of SRIM in the automotive industry. The state-of-the-art is concisely summarized in the figure on the report cover, and included in the workshop report on p.??74??. Only geometrically simple, nonstructural parts (i.e. spare tire covers) can currently be manufactured by SRIM in large quantities. Enabling technologies of the highest priority, required to produce geometrically complex parts with high structural performance, include preform processing models and reinforcement characterization. The underlying scientific issue in both the preform processing and characterization tasks is the nearly complete lack of understanding of the deformation process the fibrous materials undergo during the preforming operation and during the resin injection process. Preform deformation is known to have a large effect on the flow behavior of the resin either through changes in the permeability tensor or by opening flow channels within the mold. Addressing that issue calls for a large effort since most previous work in the area of flow through porous media has assumed the media to be rigid. Work in the area could begin with an effort to combine a flow model with a solid mechanics model of the reinforcement.

The workshop on permeability and fiber architecture attracted a great deal of interest since the conference focused on fluid flow related issues. Much of the workshop focused on permeability measurement methods and more recent efforts on predicting the permeability from a knowledge of the preform architecture. The most urgent need in the area of measurement is the establishment of a standard reference material and a permeability data base. It was suggested that NIST lead these efforts, and a project to establish a permeability SRM is currently nearing completion. Additionally, the development of a permeability data base is underway with sample data currently being tested in a prototype data base structure.

Efforts to predict the flow behavior are currently quite crude, but the avenues for future work appear to be well known. Current work is mostly limited to the prediction of the permeability in unidirectional and homogeneous model media, with very limited work on

heterogeneous media. Future work needs to address more complex structures such as woven, braided and 3-D fiber architectures. The issues of structural heterogeneity will need to be addressed to understand void formation mechanisms, and microscopic effects such as surface interactions should be included in such models to account for the effects of wicking.

The workshop on reinforcement/resin interactions brought out two important issues that can effect both the processing and performance of composites manufactured by liquid molding, namely binder or sizing dissolution, and capillary forces. Both of these issues link the chemistry of the surface finish applied to the reinforcing fibers to the flow behavior obtained during processing. In the case of binder or sizing dissolution, the resin viscosity, the resin cure kinetics, and the cured resin properties may be substantially changed by dissolved material. This issue has not been widely recognized but may be quite important if the time scale for dissolution is not much longer than the time scale of processing. In the case of capillary forces, both the fiber architecture and the fiber surface chemistry are expected to play a role. The fiber architecture becomes important because capillary forces grow as the interstitial spaces become smaller. Both the surface chemistry of the fiber and the resin chemistry affect the degree of wetting, or contact angle, between the resin and fiber, and the contact angle plays an important role in determining capillary forces. Good wetting of the fiber by the resin is a necessary condition for achieving a strong adhesive bond at their interface, and a strong bond is necessary for composite performance.

The workshop on heating and rheokinetic effects stressed the fact that the resin viscosity is just as important as the permeability in determining resin flow behavior during liquid molding. Nonisothermal behavior caused by heat transfer from the mold wall or by fast, exothermic chemical reactions can lead to resin viscosities that are highly nonuniform in both space and time. Although models have been formulated to address nonisothermal behavior, data are lacking for the required thermal parameters. Two types of data are required, rheokinetic data on the resin, and heat transport data on the preform, mold, and resin. Measurement methods to acquire some of these parameters do not even exist, and therefore the importance of these parameters must be assessed to determine if the large effort required to develop measurement methods is justified.

Before proceeding to the workshop reports and lecture manuscripts, a participant profile and the results of a questionnaire distributed to the workshop particpants is included.

Table. Number of attendees, by occupation.

Industry		**Government**		**University**	
Auto.	10	DoD	5	Chem.E.	3
Aero.	7	DoE	1	Mech.E.	6
Chemical	8	Foreign	2	Math.	2
Textile, etc.	5	NIST	8	Students	12
Total	30	Total	16	Total	23

Eight of the participants were from outside the United States, including two from Europe and one from Australia. Finally, we must note that only two representatives from molding companies took part, and a larger representation of molders should be attained at future liquid molding conferences. One reason for the low level of participation by molders may be that most molding companies are small, and attending conferences is beyond their budgets.

Thirty-two questionnaires were returned, which represents about half the conference participants. The respondents agreed that the workshop was beneficial for a wide variety of reasons, and also thought that a similar meeting should be held in one or two years. Each question asked on the questionnaire is indicated by large type preceeded by a "bullet."

Questionnaire Tabulation

- Was this workshop beneficial to you?

  31 yes 1 blank

  Why? (Reported reasons in order of vote count)

  The discussion groups.
  Interaction with other industries.
  Interaction between industry and university.
  Focussed meeting on liquid molding.
  Most major players attended.

Compare results with others.

- How important was the technical information presented in the lectures to your work. (Numbers in table indicate the number of respondents that gave each lecture a particular score, with 1 being the least important and 5 the most.)

Score	1	2	3	4	5	avg
Critical issues in model validation.	1	3	7	7	12	3.9
RTM - Design for processing.	0	1	3	12	13	4.3
Predicting Permeability from Preform Structure.	0	3	8	11	8	3.8
Permeability: Theoretical and experimental considerations.	0	1	6	9	15	4.3
Permeability measurements and void formation.	0	2	8	13	8	3.9
Dynamics of binder displacement in liquid molding.	1	6	10	11	3	3.3
Fluid mechanics issues in SRIM with highly reactive resins.	0	6	10	7	7	3.5
Rheokinetics during mold filling in SRIM.	1	3	5	9	12	4.0

- Please rate the workshops you attended? (Numbers in table indicate the number of respondents that gave each lecture a particular score)

Score	1	2	3	4	5	avg
Model validation and test methods.	0	0	4	6	4	4.0
High speed processing.	2	1	0	6	7	4.0
Preform architecture and permeability.	0	2	4	5	4	3.7
Reinforcement/resin interaction during flow.	0	0	5	6	3	3.9
Heating and rheokinetic effects during flow.	1	1	4	5	3	3.6

- Are there additional topics in liquid molding that should have been covered at this conference?
  - Preforming (deformation in mold, modeling)
  - Molding (actual parts, using cut fiber)
  - Rheokinetics & heat transfer
  - Process monitoring & control
  - High speed resin flow
  - Needs of industry (both small and large companies)
  - Traditional flow-thru-porous media
  - Thick composites

- Would you attend a second liquid molding workshop held in: (Numbers indicate vote count)

  14 - One year 17 - Two years 1 - Three years

The most notable response to the questionnaire urged that future meetings on LCM include **preforming** as a major topic. Although this meeting focussed on processing issues, the discussions repeatedly touched on preforming issues, and the connection between preforming and processing.

Questions concerning this report or the meeting should be directed to the organizing committee:

Richard S. Parnas
Polymers Division
NIST
(301) 975-5805
(301) 869-3239 FAX

Andrew J. Salem
Polymer Composites Program
General Electric CRD
(518) 387-7255
(518) 387-5812 FAX

Kenneth N. Kendall
Materials Research Laboratory
Ford Motor Company
(313) 248-1730
(313) 390-0514 FAX

2. Participant List

Nitin Anturkar
Ford Motor Co.
Rm. 2219, P.O Box 2053
20000 Rotunda, Maildrop 3198
Dearborn, MI 48121
USA

Jimmy Barron
Dow Chemical
B-2009
Freeport, TX 77541
USA

Edward Bernardon
Draper Lab.
555 Technology Sq.
MS #20
Cambridge, MA 02139
USA

John Berwald
Vetrotex Certainteed
1720-C Indianwood Circle
Ste. C
Maumee, OH 43537
USA

Linda A. Brown
U.S. Army
220 7th Street NE
ATTN: IAFSTC-PM
Charlottesville, VA 22901-5396
USA

Richard Brown
Atlantic Research Corp.
Bldg.300, Rm.162
5945 Wellington Rd.
Gainesville, VA 22065
USA

Daniel Buckley
American GFM
1036 Russellville Rd.
Shrewsbury, VT 05738
USA

Daniel Butrymowicz
NIST
Bldg. 224, Rm. B309
Gaithersburg, MD 20899-0001
USA

Daryl Calhoun
Dow Chemical
Central Research
1712/1714 Bldg.
Midland, MI 48674
USA

Gil Carpenter
Grumman Aerospace &
Electronics
MS A08-35
Bethpage, NY
USA

Jose Castro
Gencorp Research
2990 Gilcrest Rd.
Akron, OH 44305
USA

Albert Chan
Michigan State Univ.
2203 Eastman Ave.
Midland, MI 48640
USA

Mark Condon
Draper Lab.
555 Technology Sq.
MS #20
Cambridge, MA 02139
USA

David DeGuiseppi
Hercules, Inc.
500 Hercules Rd.
MTC Bldg., Rm. 26
Wilmington, DE 19808
USA

Steven DeTeresa
Lawrence Livermore National Lab.
7000 E. Ave.
Lawrence, CA 94550
USA

Douglas Denton
Chrysler Corp.
12800 Chrysler Dr.
CIMS 418-17-05
Highland Park, MI 48309
USA

Richard Dessenberger
Univ. of Illinois
1206 W. Green St.
Urbana, IL 61801
USA

Mohamadou Diallo
Ecole Polytechnique
CP 6079, Succ. A
H3C 3A7
Montreal, Quebec,
CANADA

Lawrence Drzal
Michigan State Univ.
College of Engineering
East Lansing, MI 48824
USA

Michael Durham
Northrop Corporation
One Northrop Ave.
Dept. N5995/WI
Hawthorne, CA 90250
USA

James Early
NIST
Bldg. 224, Rm. B309
Gaithersburg, MD 20899-0001
USA

Renata Engel
Penn State Univ.
45 Hammond Bldg.
University Park, PA 16802
USA

Kurt Fickie
U.S. Army
B394
Attn: AMSRL-CI
Aberdeen PG, MD 21008-5067
USA

Raymond Gauvin
Ecole Polytechnique
C.P 6079, Succursale "A"
Montreal, Quebec, H3C 3A7
Canada,

Rikard Gebart
Swedish Institute Of Composites
Box 271
S-941 26 Pitea
Sweden

James G. Glimm
Univ. of Stony Brook
Stony Brook, NY 11794
USA

Sunil Gupte
Univ. of Delaware
Dept. of Mechanical Engineering
Newark, DE 19716
USA

Kerang Han
Ohio State Univ.
2075 Robinson Lab.
Columbus, OH 43210
USA

Greg Hasko
Lockheed/NASA Langley
144 Research Dr.
Hampton, VA 23666
USA

Kenneth Heitzmann
Univ. of Illinois
1206 W. Green SE
Urbana, IL 61801
USA

Donald Hunston
NIST
Bldg. 224, Rm. A319
GAITHERSBURG, MD 20899-0001
USA

Stanley Iobst
General Motors Corp.
30500 Mound Rd.
Polymers Dept.- RSB
Warrren, MI 48090-9055
USA

K. Jayaraman
Michigan State Univ.
Dept. of Chemical Engineering
East Lansing, MI 48824
USA

Kenneth Kendall
Ford Motor Co.
P.O Box 2053, MD 3182
20000 Rotunda Dr.
Dearborn, MI 48121
USA

Yann LeMenn
Ecole Polytechnique
Campus de L'Univ.
Montreal, Quebec,
CANADA

Gilbert Lebrun
Ecole Polytechnique
C.P. 6079, Succ. A
H3C 3A7
Montreal, Quebec,
CANADA

Bob Lee
Specialty Plastics
530 Sherwood Ave.
Dunmore, PA 18512
USA

L.J. Lee
Ohio State Univ.
Dept. of Chem. Eng.
140 W. 19th Avenue
Columbus, OH 43201
USA

Richard Leek
Grumman Aerospace &
Electronics
Rm. A02-026
Bethpage, NY 11714-3580
USA

Baichen Liu
Univ. of Delaware
Center for Composite
Engineering
Newark, DE 19716
USA

Robert Maier
AHPCRC
1100 Washington Ave.
Minneapolis, MN 55415
USA

Bernard Malofsky
Loctite Corp.
705 N. Mountain Rd.
Newington, CT 06111
USA

Andrew Mark
U.S. Army
ATTN: AMSRL-CI-S
Aberdeen Prov. Grnd, MD 21005
USA

Fred Phelan
NIST
Bldg. 224, Rm. A213
Gaithersburg, MD 20899-0001
USA

John McGeehan
General Motors Corp.
30300 Mound Rd., Box 9040
Monf. Bldg. A/MD-24
Warren, MI 48090-9040
USA

Laura Piechowski
Ford Motor Co.
PO Box 2053, MD 3182
20000 Rotunda Dr.
Dearborn, MI 48121
USA

John Morley
General Motors Corp.
30300 Mound Rd.
MC MD-24, Bldg. 1-9
Warren, MI 48090-9040
USA

Krishna Pillai
Univ. of Delaware
126 Spencer Lab.
Ctr. for Composite Materials
Newark, DE 19716
USA

Richard Parnas
NIST
Bldg. 224, Rm. A105
Gaithersburg, MD 20899-0001
USA

Timothy Rohaly
U.S. Army
ATTN: AMSRL-CI-S
Aberdeen PG, MD 21005
USA

Niraj Patel
Ohio State Univ.
140 W. 19th Ave.
425
Columbus, OH 43210
USA

C.D. Rudd
Univ. Of Nottingham
Univ. Park
Nottingham, NG7 2RD
England

Rowan Paton
CRC-AS
506 Lorimer St.
Port Melbourne, 3207,
AUSTRALIA

Robert Sadler
North Carolina A&T State
1601 E. Market St.
Mech. Engr. McNair
Greensboro, NC 27411
USA

Erin Perry
GE-CRD
1 River Road
KWD-273
Schenectady, NY 12301
USA

Andrew Salem
General Electric CR&D
Bldg.K-1, 4B21
PO Box 8
Schenectady, NY 12301
USA

Muhammad Shafi
Dow Chemical Co.
2301 N. Brazosport
B2009
Freeport, TX 77541-3257
USA

Jay G. Shukla
Lockheed Aerospace Co.
86 S. Cobb Dr.
Dept/73-C3 Zone 0648
Marietta, GA 50063
USA

Leslie E. Smith
NIST
Bldg. 224, Rm. A309
Gaithersburg, MD 20899-0001
USA

Rajgopal Subramanian
PPG Industries-Fiber Glass
P.O. Box 2844
Pittsburgh, PA 16001
USA

Folkert Tangerman
Univ. of Stony Brook
Stony Brook, NY 11794-3600
USA

Charles Tucker
Univ. Of Illinois
144 Mechanical Eng. Bldg.
1206 W. Green
Urbana, IL 61801
USA

Deanna Venzke
General Motors Corp.
30300 Mound Rd.
MC MD-24, Bldg. 1-9
Warren, MI 48090-9040
USA

Jeffrey Vogel
Univ. of MN
111 Church St., SE
Minneapolis, MN 55455
USA

Robin Wilson
Dow-UT Composite Products
15 Sterling Dr.
Wallingford, CT 06492-1843
USA

Ming Xie
Concordia Univ.
1455 Maisonneuve W.
H-0025
Montreal Quebec, H3G 1M8
CANADA

Victor Yagi
Boeing
P.O. Box 3707
MS 4H-79
Seattle, WA
USA

Selim Yalvac
Dow Chemical
Central Research
1712/1714 Building
Midland, MI 48674
USA

3. Workshop reports by discussion group leaders

Model Validation & Test Methods, Selim Yalvac, Dow Chemical.

High Speed Processing, Kenneth Kendall, Ford Motor Co.

Preform Architecture and Permeability, L. James Lee, Ohio State University.

Reinforcement / Resin Interactions During Flow, Lawrence Drzal, Michigan State U.

Heating and Rheokinetic Effects During Flow, Nitin Anturkar , Ford Motor Co.

MODEL VALIDATION AND TEST METHODS

Selim Yalvaç
The Dow Chemical Company
Advanced Composites Laboratory
Central Research and Development
Midland, MI 48674

INTRODUCTION

A working group was convened during the workshop held at the National Institute of Standards and Technology (NIST) on September 21, 1993 to discuss the state of the art, issues, needs and challenges in the resin transfer molding (RTM) model verification area. It was decided by this work group to focus entirely on the macroscopic modeling aspect of the RTM process since this was considered to be of more interest for the participants from a manufacturing point of view. The participants also thought themselves to be more qualified in macroscopic modeling than microscopic modeling. Furthermore, time was a factor in determining the extent and depth of the discussions on any given subject.

This work group reported back to the workshop participants the following day with their results, summaries and prioritization of critical issues which was followed by a floor discussion. Several additional issues raised and comments made during this reporting session are also included in this report.

It is important to note that the diverse background of both the work group and the work shop participants resulted in the participants being generally divided on a wide variety of issues, although several conclusions were arrived at with a consensus. The general feeling was that more questions were raised than solutions offered as this was the stated objective of the workshop.

STATE OF THE ART

The first task was to establish the state of the art in the RTM model verification

efforts. The group accomplished this by discussing the subject on several platforms. These were: in-situ sensors, materials, mold design, experiment design, and complex geometries.

Currently, the most widely used method of validation is visualization of the injection fluid through a transparent mold. Although the method is simple, it has severe shortcomings. It is generally limited to non-reactive fluids and flat plate geometry. The transparent mold top can not sustain high pressures without deflection and is, therefore, not suitable for constant flow rate systems where unpredictable pressure spikes are common. Furthermore, the system is prone to non-Darcian type flow due to channeling of the fluid if the transparent mold top deflects.

The state of the art for in-situ sensors was described as using fine diameter thermocouples at many points, preferably located where the action is, to measure temperature profiles during injection into the mold. Similarly, pressure distribution in the mold is measured using transducers at many points along the flow direction. Intentional short shots are sometimes used to compare flow front progression with that predicted from models. Dielectric sensors are occasionally employed to track viscosity development and to measure the degree of cure, however, one can only determine general trends with this type of a sensor.

Precise flow metering can be attained using commercial equipment if the fluid is non-reactive. However, if resin and hardener are premixed these flow measuring devices become useless due to resin curing inside the flow meter. Instead, the method of flow rate calibration as a function of DP would be the preferred alternative. This method requires a careful, timed dispensing of resin into a container while measuring the pressure drop.

Other types of sensors tried on an experimental basis include electrochemical sensors, use of carbon fibers to monitor electrical resistance changes due to flow front progression, and fiber optic visualization within the mold cavity. The reproducibility and accuracy of data obtained with these methods are not well defined.

The current state of the art, as far as materials are concerned, is to use both reactive and non-reactive fluids. The emphasis is more on the non-reactive fluids in

academic validation studies, whereas this emphasis shifts to reactive fluids in industrial studies. Unfortunately, due to the lack of a standard injection fluid a computer code's weakness or strength is not properly ascertained when validation experiments are done. The differences observed between validation experiments of similar nature may be disguised since the resin related experimental error changes from one laboratory to another.

Most of the published validation experiments have been performed using flat panels with one-dimensional flow. Several participants reported a few studies using a square box geometry, indicating that the extent of complexity of part and mold shapes used in validation studies is still primitive. The difficulty in the transition from flat panels to complex geometries appears to stem from the fact that the reproducibility of data obtained on flat panels continues to be a problem. Most experimentalists become quite apprehensive in moving on to the next level of code validation in complex geometries when their efforts with simpler flat panel molds face difficulties. On the other hand, the degree of realism associated with experiments conducted with flat panels still seems to be unacceptable by many of the potential code users in the industry.

A majority of the current experimental work is conducted with constant pressure injection equipment. The simplicity of the equipment design and the comparatively low costs associated with the experimental setup make this type of injection very attractive. On the other hand, constant injection rate experiments have the advantage of being able to study the RTM process at a scale dictated by the requirements of large volume/low cost manufacturing. The cost of constant injection rate equipment is generally much higher than the constant pressure equipment. A few researchers have been said to try an injection method which is a combination of both constant injection rate and constant pressure, utilizing the advantages of both methods.

The variables that are most widely traced during validation experiments are pressure distribution in the mold, temperature profiles during both mold filling and part cure, resin/hardener injection rate, and mold deflection. The use of active versus passive vacuum (i.e., vacuum applied throughout the fill time as opposed to shutting off the vacuum once a desired pressure is reached prior to injecting resin) has also been studied

in several laboratories. Finally, the effect of part thickness on temperature distribution, specifically due to reaction exotherm, has been studied by a number of researchers.

ISSUES AND NEEDS

The reproducibility of data from run-to-run and the uncertainty of measurements using sensors were reported to be serious concerns by many of the participants. A study investigating sensor related errors detailing measurement sensitivity is much needed.

The cost of model validation experiments was indicated to be significant when reactive fluids are used in complex geometry molds. Therefore, assessing the cost of experiments remains to be very critical for the successful completion of any experimental program.

The significance of being able to measure variations in *local* permeabilities and preform porosities was recognized, yet currently no feasible method is known for measuring local permeabilities in-situ. In addition to this need, in-situ monitoring of void formation and transportation is very desirable. These issues will be further compounded when validating models in complex geometry molds.

It is generally necessary to know the pressure distribution in a mold *a priori* for the proper selection of pressure transducers with correct range. This is almost impossible to predict in a versatile validation mold where all parameters being studied span large ranges, since the purpose of the validation experiments is to demonstrate the usefulness of the model for all molding conditions. It is, therefore, desirable to have pressure transducers with increased sensitivity over a larger range of pressures.

Many of the participants stated that reliable permeability measurement is essential for effective computer code validation. It was suggested that fabric manufacturers should assume more responsibility for reporting to molders or design engineers permeability and porosity data as a function of preform compression. This can be greatly aided by the industry wide acceptance and use of a standard test for permeability measurements. It is also important to develop a fundamental understanding of how the permeability of hybrid preforms manufactured by intermixing of different forms and types fiber beds or plies of fabrics change with various configurational parameters.

The measured permeability of the preform will change during injection of the resin if the preform is compressed in the plane of the preform. When the injection pressures are high or the local velocities reach some critical value, several researchers have reported observing this behavior. It is not yet known what critical values the parameters that drive fiber wash should assume before this behavior is observed. More work is needed to determine the range of operating parameters one should avoid to prevent fiber wash. When validation experiments are conducted under conditions that cause fiber wash, a non-Darcian behavior may erroneously lead the researchers to question the applicability of the theory.

The draping of fabric in complex geometry parts changes the permeability of the fabric measured using flat geometries. The degree of stretching of the fabric and the individual tow will have serious effects on the in-situ permeability of the preform. Innovative techniques are needed for measuring local permeability changes as a function of drape, draw, stretch, etc., or use other techniques during manufacturing, such as ply stepping to reduce the degree of stretching. It is equally important to find ways of incorporating the local permeability variations in the model.

A need also exists in developing resin systems that would allow accurate metering and delivery of each component (resin and hardener) within the capabilities of the control system for a wide variety of constant injection rate equipment. For instance, a resin/hardener system requiring a mix ratio of 50:50 wt % is much easier to meter and deliver than another system requiring 15 phr hardener since the metering and delivery of hardener at small injection rates can be inaccurate.

One of the fiercely debated issues among the workshop participants was the difficulties encountered during filling of the mold in maintaining a pseudo-linear flow front in one-dimensional flow due to race tracking or channeling of the resin. This phenomenon is especially prevalant when low permeability fabrics are used. Race tracking is generally a non-issue for the manufacturer, yet presents a great challenge for the experimentalist trying to generate data for the purpose of computer code validation. Many members of the work group shared the frustration that the degree of race tracking was largely an uncontrollable phenomenon. It was pointed out that preform-mold surface

contact could never be made perfect and tiny channels were created at random along the mold surface where the resin, due to higher permeability in this region, would advance faster than elsewhere in the preform. Entering a variable difficult to quantify into the computer model, such as the permeability along the mold edges, renders the model ineffective. Several studies assumed several orders of magnitude higher permeability values in the edge region of the flow domain to fit the predicted flow front with that observed experimentally. This type of approach turns the modeling efforts into a trial-and-error fit-to-data method and defeats the main purpose of trying to predict flow activities.

Opponents of the view that race tracking was uncontrollable, a "ghost variable," suggested that through proper mold design race tracking can be controlled. In fact a large number of experiments conducted in their laboratories have shown that highly linear and reproducible flow fronts were obtained with no evidence of race tracking. Further discussions, however, revealed that the participants' experience with the presence of race tracking or lack of it, depended on several factors such as the fiber volume fraction, injection rate, type of preform (random mat versus woven fabric, or satin versus plain), etc. The issue of race tracking remains unsettled and the reader is cautioned about comments based on experience limited to a single experimental set-up, such as a certain type of preform or injection rate, etc. It was generally agreed that more work is needed to clarify the issue.

The need for realism in validation experiments resurfaced with the discussion of how to experiment with flows in complex geometry preforms (3-D and 2.5-D) with ribs, deep draws, contoured surfaces, etc. Unless a computer code is capable of at least predicting trends in complex geometry molds, it will be useless for the design and production engineer. More work is needed with complex geometry molds and the major part of this responsibility should be shouldered by industry with close cooperation of academia or other organizations.

The work group wanted to stress that assuring a rigorous experimental program to eliminate biased error in experimental set-up is very critical to the success of the validation experiments. This often implies that similar but independent experiments need

to be conducted in several laboratories and the results compared statistically. This requires a long term commitment and financial leadership of a major industrial or government organization.

COMMENTS MADE DURING THE REPORTING SESSION

Many workshop participants reacted to the work group's presentation during the reporting session by commenting and questioning several aspects of the group's recommendations or observations. These are included in this section in the order they were discussed:

1. Non-isothermal modeling is not being used as extensively as is necessary to get at the heart of the issue. Validation experiments should include this facet.

2. Researchers need to set a new level of goals. There are too many variables at this time.

3. Model validation experiments should take into account resin-fiber interactions, especially at higher pressures (higher flow rates) where some deformation of the preform may be important. Perhaps accurate interaction measurements are necessary, but ballpark figures are generally sufficient for dimensional analysis. Poor quality data can still qualify or disqualify an issue as important.

4. The value of fundamental theory to the practicing engineer lies in telling him what not to worry about. This should be the aim of the code developers.

5. The quality of communication must improve to bridge the gap between model generators and model validators. Workshops, such as this one, serve this purpose very nicely.

6. A physical understanding of what goes on in the mold is needed by the model user. One needs to know how to use the sensitivity of the model.

CONCLUSIONS

The following were recommended by the work group for devising a strategy for validation of any new code:

1. Determine the importance of material property interactions and develop a standard procedure for validating a computer code.

2. It was recommended that any new permeability measurement should be accompanied by data obtained using the new NIST standard permeability kit.

3. The conditions that cause fiber-wash should be well characterized and the effect of fiber wash on local permeability changes should be studied.

4. For validation experiments with flat plate geometry, the use of peripheral or center injection is recommended. This eliminates edge effects and race tracking, although the flow becomes a 2-D flow.

5. Validation of the experimenter via round-robin testing is highly recommended for each new computer code.

6. Researchers are encouraged to use analytical solutions when possible to determine the limits and bounds of the numeric solutions. Encourage software developers to publish comparisons of numeric solutions with those obtained from analytical solutions whenever possible.

7. Decouple computational fluid mechanics from heat transfer and cure in 1-D flow for comparison of numerical and analytical solutions.

HIGH SPEED PROCESSING

Kenneth N. Kendall
Ford Research Laboratory
Dearborn, MI 48121

Introduction

It would be difficult to evaluate the issues that present the greatest challenges in high speed liquid composite molding (LCM) processing, without first obtaining a clear understanding of what is meant by a high speed LCM process.

In aerospace composite processing, a typical LCM process may take several hours. One order of magnitude decrease in the molding cycle time to one hour, could therefore be considered high speed. Similarly, some very low volume automotive applications (< 1000 parts per year) tolerate a component cycle time in the order of one hour. In this instance a 6 minute molding cycle could be considered high speed. However, an order of magnitude decrease in the molding cycle time for a high volume application (> 100,000 parts per year), where a component cycle time of 2 or 3 minutes may dictate a molding cycle time of 1 minute or less, is unlikely. A high speed LCM process could therefore be defined as that required to manufacture parts at the upper limit of the process capability. It should be stated that this includes all processes required in the manufacture of components by liquid composite molding, such as preforming.

Challenges in High Speed Composite Processing

Factors to consider when assessing the challenges facing high speed LCM processing include component geometry, application, state-of-the-art and cost.

A simple planar geometry would present fewer processing difficulties than a complex two dimensional geometry. The same is true for a component without cores in comparison to one with cores. Thus a complex geometry with cores would present the greatest geometrical challenge in a high speed process.

There is a greater potential for sacrificing part performance in favor of processing

speed in non-structural or semi-structural applications than in structural applications. Hence, a challenge in a high speed process would be to maintain structural properties at a level equal to or greater than those which could be obtained by processing at slower speeds.

State-of-the-art is an important consideration as this is used to measure the successful implementation of a process in production and focus efforts in research and development. However, current implementation of a process may not correspond with the level of fundamental understanding in the processing science. Indeed, there is a great deal of evidence to suggest that there is a significant disparity between state-of-the-art in research and development laboratories and state-of-the-art in manufacturing facilities. This highlights a shortcoming in technology transfer.

Cost is an important criterion in the selection of any manufacturing process. It would be possible to justify a high manufacturing cost for an essential component that could be manufactured by no other means. It is more usual, however, to have several manufacturing options with cost being a prime selection criterion. Volume is also a consideration in regard to cost since a small cost saving on a high volume item could yield greater cost benefits than a large cost saving on a low volume item. Therefore the challenge in high speed LCM processing is to produce a component in high volumes at a cost competitive with alternative manufacturing processes.

It is not difficult to identify several automotive components (body sides, floorpans, chassis components, etc) which would provide the necessary challenges to a high speed LCM process, based on the description above. This provides confidence that the challenges identified are realistic in terms of demand, even if they are not achieveable in terms of supply.

State-of-the-art/State-of-implementation in LCM Processing

A review of automotive composite components currently in production could be considered to be the most candid method of assessing state-of-the-art. Rather, this reveals the current state-of-implementation. Figure 1 summarizes the current status of LCM component production.

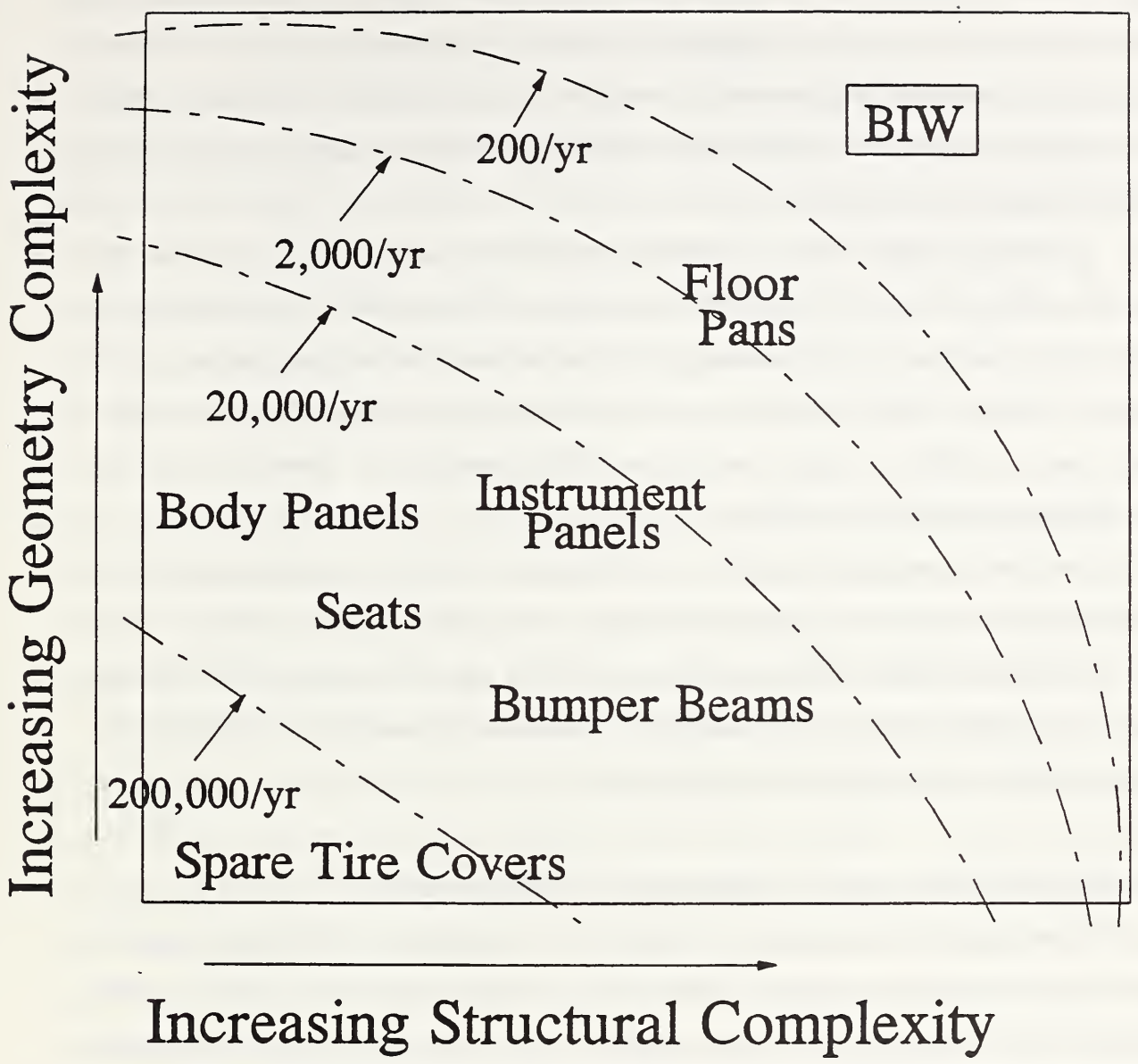

Figure 1. Current LCM Production Status.

There are several examples of non-structural and semi-structural body panels in production. Lotus, BMW, Renault, Citroen, Alpha Romeo, Chrysler, Mack, Iveco and Ford employ body panels in low volumes (1,000's per year). While issues such as poor out-of-the-mold surface finish remain, non of the components could be considered challenging in the context of high speed LCM processing. GM and Ford use non-structural, non-appearance components (spare tire covers, sound shields) in reasonably

high volumes (100,000's per year) but these components fail to meet the high speed processing criteria of complex geometry and structural property requirements. GM and BMW employ semi-structural bumper beams and seat backs in similar volumes but again the components fail to meet the high speed processing criteria of complex geometry and demanding structural properties.

To achieve high volume production, preforming and molding processes are required which can meet the cycle time requirement. This has been accomplished for simple, planar geometries with preforming cycles less than 45 seconds and molding cycles less than 2 minutes. While there are a number of foam cored components in production, these are all low volume and/or non-structural RTM applications; there are no foam-cored SRIM applications in production.

In terms of analytical capability, several process models are reaching maturity in research establishments and verge on becoming commercially available. Most of these will, if not presently then within the next year, offer a non-isothermal mold filling and resin cure capability. There is, however, little evidence of this analytical capability being harnessed by the majority of LCM manufacturers.

Obstacles to the Introduction of High Speed LCM Processing

There are several obstacles to the widespread introduction of LCM for high speed processing of composite components. Preforming complex shapes to acceptable quality standards and cost targets in a fast repeatable cycle presents perhaps the greatest challenge. Net-shape or near net-shape preforming would help reduce component cycle times and reduce overall cost while improving process control during molding. Net-shape molding of complex shapes would improve part quality and reduce cost by eliminating post-molding operations. Core manufacturing technology requires development to improve core quality, reduce component weight and reduce cost. Molding-in inserts and attachments and adhesive technology also require greater understanding.

Enabling Technology

Current research and development activities in the molding aspects of LCM

processing are relatively advanced. With the exception of reinforcement permeability characterization, aspects relating to preform processing remain comparatively neglected. To help develop a better understanding of preform processing and aid with the design of preforms, process models are required. These models should be developed to predict the deformation characteristics of both random mats and engineered fabrics, the re-orientation of fibers during deformation, the formation of defects such as thinning, tearing, and wrinkling, the effect deformation has on the mechanical and processing properties of the preform and to provide a link between preforming process models and molding process models. A significant amount of raw materials characterization will be required to furnish such process models with accurate materials behavior data. Included would be compaction/relaxation behavior, drape/conformability behavior and the identification of deformation mechanisms under the range of high speed processing conditions required. Current reinforcement permeability characterization techniques should be developed to account for the changes that occur when transforming reinforcements into preforms.

Secondary in importance to preform modelling and characterization would be improvements to existing flow models. While resin race tracking and film flow during mold fill may present production problems, they are undesirable in terms of process control and should therefore be eliminated, not modelled. A better understanding of the preforming process may permit this. Non-linearities during mold filling such as fiber movement and/or deformation may present a more desirable avenue of pursuit. In addition, process models for core manufacturing processes would improve core quality, help to reduce weight and improve subsequent LCM process control. Design aids, such as composite component design guides, design rules, materials databases and processing databases would also assist. Finally, improvements in Class A surface finishes would be of benefit to a high speed LCM processing strategy if complete body sides, providing both structural performance and external body surfaces, were to be considered.

The required technologies are summarized in Table 1.

Table 1. Enabling Technologies Required for High Speed LCM

Enabling Technology	Priority
Preform Processing Models	**HIGH**
Reinforcement Characterization	**HIGH**
Flow Modelling	**MEDIUM**
Core Process Modelling	**MEDIUM**
Design Aids	**MEDIUM**
Class A Surface Finish	LOW

Conclusions

A high speed LCM process would be one which produces composite components at the limit of the process capability. This is suggested to be represented by a component manufacturing cycle time of two minutes or less. All elements of the component manufacturing process must be achieved within this cycle time, while remaining competitive in terms of cost and performance with alternative materials and manufacturing processes. A structural component with a complex geometry requiring cores would provide a credible challenge for such a process.

Technology transfer between research and development laboratories and the molding industry should be improved. The development and distribution of design aids would be an element of such an improvement. However, the molding industry should also be pro-active in the technology transfer.

There is a lack of understanding in the preforming process which is presently a major barrier to the introduction of structural composite components manufactured by high speed LCM processes. Preform process models are required to help develop understanding in preform processing and the design of preforms for high speed LCM.

An appreciable amount of materials characterization is required to provide the necessary data for preform process models. This data should be collected under

representative process conditions.

Core manufacturing processes require greater understanding to improve core quality, LCM process control and ultimately the composite component quality.

The focus of research projects, particularly those in which automotive companies participate, should be directed toward addressing issues raised by this workshop.

PREFORM ARCHITECTURE AND PERMEABILITY

L. James Lee and Niraj Patel
Department of Chemical Engineering, 140 W. 19th Avenue
The Ohio State University, Columbus, OH 43210

The relationship between fiber preform architecture and permeability was discussed on September 21, 1993 during a workshop on LCM organized by NIST. Various topics discussed and conclusions reached during this workshop are summarized below. The purpose of this working group discussion was to address various issues pertaining to the measurement, prediction and usage of fiber preform permeability in the manufacture of composite parts by liquid composite molding technology. The working group consisted of 20-25 participants representing several industries, universities and other organizations. Three major topics were discussed during this workshop : (1) permeability measurement techniques and data base, (2) modeling of permeability, and (3) applications of permeability models / data in liquid composite molding.

(1)Permeability measurement techniques and data base

In the last 5-8 years a substantial amount of permeability data have appeared in the literature. The permeability measurement involves either a unidirectional flow or a radial flow through a fiber preform. The raw data obtained during a typical measurement include pressure as a function of time at constant flow rates, or flow rate / flow front progression as a function of time at constant pressures. One advantage of the unidirectional flow device is that the analysis of raw data is relatively easy. This method directly gives permeability of fiber preform in the direction of flow. The major disadvantage of this technique is that elimination of race tracking, i.e. channeling near the side walls of the mold, is not easy. Some researchers have been able to eliminate race tracking by carefully designing the measurement tool. In general, it was felt that for low fiber volume content race tracking can be minimized to an insignificant level during permeability measurement. However, for fiber preforms of high fiber volume content

race tracking could be a major issue. Control and / or quantification of race tracking is the key to a successful measurement of permeability by unidirectional flow technique. The radial flow technique eliminates the race tracking. This technique, however, requires a more complex treatment of raw data. This is because in-plane permeabilities in the two principal directions (K_{xx} and K_{yy}) play major roles during radial flow. This technique, thus, requires either a separate flow visualization experiment to determine the ratio of the two in-plane permeabilities, or measurement of pressures in the fiber preform at three locations with different angles.

The equipment for liquid injection during permeability measurement includes either a constant inlet pressure or a constant inlet flow rate device. Analysis of data is easier for the constant inlet flow rate device. However, this type of device is generally more expensive compared to the constant inlet pressure device. Another problem in the constant inlet flow rate experiment is that system elasticity (e.g. deformation of tubing or flow cell under an increasing injection pressure) may play a major role during the transient flow experiment leading to gradual built up of flow rate to its final steady state value. This effect does not alter the final steady state P-Q relationship but will affect pressure increase with time during mold filling. This problem can be reduced to an insignificant level by taking proper precautions to ensure delivery of liquid at constant flow rate throughout the permeability measurement.

Based on the discussion in the working group it was observed that consistent permeability values have been obtained in the same laboratory by different researchers, however, there is a lack of good inter-laboratory comparison. It was felt that the reasons for this lack of agreement among various laboratories include leakage in the measurement device (i.e. race tracking or channeling between the sides of the mold walls and fiber preform, and channeling between the upper and bottom mold walls and fiber preform), system elasticity, change of cavity thickness, and other variations in the measurement equipments and test liquids. One notable exception was, for example, the continuous random fiberglass mat, OCF M8610. Permeability data of this fiber reinforcement from several laboratories agree with each other quite well. Perhaps the relatively low flow resistance (i.e. high permeability) and a weak dependence of permeability on the porosity

of this fiber reinforcement make it more tolerable to various artifacts.

Darcy's law seems to work well for describing macroscopic flow behavior through a fiber preform. This is evident from the fact that the permeability values calculated using transient flow data (unsteady state permeability) and using the final steady state P-Q data (steady state permeability) are in good agreement within the experimental limits. Darcy's law, however, can not describe the microscopic resin flow behavior. For example, analysis of wicking and void formation can not be carried out based on Darcy's law alone.

Some of the key issues identified in this session of the discussion include the need of inter-laboratory comparison of the permeability data and standardization of permeability measurement techniques. The following organizations were asked and agreed to participate in such a task : National Institute of Standards and Technology (NIST), Swedish Institute of Composites (SICOMP), University of Delaware, Ecole Polytechnique de Montreal, University of Illinois, Michigan State University, The Ohio State University, Boeing Company, and Lockheed Aerospace Company. It was suggested that several model porous materials need to be identified; wire screens, continuous random fiberglass mats, e.g. OCF M8610 which is nearly isotropic and has high permeability, and Injectex fabric or 8 harness graphite fiber mat which have low permeability and are anisotropic are possible choices. A model fluid for permeability measurements should be Newtonian and stable. Model fluid to be used, however, could not be agreed upon during the discussion. Several fluids were suggested, such as Dow Corning's silicone oils, DOP oil and glycerin-water mixtures. The problem with using silicone oils is their volatile nature. DOP oil, on the other hand, is not stable, whereas viscosities of glycerin-water mixtures are very sensitive to temperature and moisture absorption. It was decided that the participating organizations should perform permeability measurement experiments using the same type of fiber preforms but self-chosen liquids. Furthermore, in order to minimize batch to batch variations, fiber mat samples should be provided by the same vendor. The purpose of this exercise is to identify equipment artifacts that cause lab-to-lab variations. Towards this goal the participating organizations will be requested to report raw data such as pressure versus

time (during constant inlet flow rate experiment), or flow rate versus time and flow front position versus time (during constant inlet pressure experiment), in addition to the permeability data.

Another issue identified in this session of the workshop was flow behavior through saturated versus unsaturated fiber preform. This is especially important in the study of micro-scale flow behavior, such as fiber wetting, void formation and movement, and dry spot formation, movement and changes.

(2) Modeling of permeability

Most studies available on permeability and resin flow behavior through fiber preforms involve experimental determination of permeability. Some analytical and numerical models are available today for the idealized fiber bed. These models assume a particular regular arrangement of fibers or fiber tows for the estimation of permeability. The actual fiber preforms, however, are heterogeneous in nature, and may have inhomogeneties and random variations of porosity, fiber arrangement and orientation. Because of these complex features, models to predict permeabilities of actual fiber mats, that can completely replace experiments seem to be not feasible at present. Modeling efforts are useful from the point view of fundamental understanding of flow behavior and design of fiber mat architecture. Qualitative and correlation type permeability modeling, however, could be very useful. For example, measurement of permeabilites of a 3-dimensional braided fiber preform with complicated geometry is very difficult if not impossible. Qualitative modeling in conjunction with experimental data correlation seems to be the only solution in this situation.

Kozeny-Carman equation is not applicable for the prediction of permeability because Kozeny constant varies with porosity. However, in absence of more rigorous models, Kozeny-Carman equation may be used to correlate the experimental data. Inclusion of capillary forces is probably not necessary for the macro-scale models. However, in micro-scale modeling such as void formation studies, capillary forces may have to be included.

(3) Applications of permeability models / data in LCM

The ultimate goal of permeability measurements / modeling is to use this information in mold filling simulation studies and LCM process design. It was concluded that flow models developed by various organizations and the available permeability data are useful when dealing with composite parts with simple geometry and without race tracking. Control and quantification of race tracking was identified as one of the key issues in modeling and model validation by molding experiments. Other important issues in the application of permeability data and flow models are summarized below.

- Effects of preforming on permeability and local resin flow behavior in complicated mold geometry should be studied. These include fiber reorientation, porosity changes, and thickness reduction (leading to channeling) that are inevitable in most preforming operations. In the fiber free region, the applicability of Darcy's law is disputable.

- Mold deflection that takes place when the mold pressure is greater than the clamping pressure should be considered. This also leads to channeling.

- Prediction of defect related issues, such as fiber wetting, void formation, dry spot formation, and warpage should be considered. This would require micro scale flow measurements and modeling.

- Binder / tackifier dissolution during molding should be analyzed. This would affect viscosity and surface tension of the resin and permeability of the fiber preform.

- Gel coat effect is important in some applications.

- Fiber wash-out and deformation of fiber preform (compressibility) are important in high speed processes. Most models developed so far assume fiber preform to be incompressible.

REINFORCEMENT/RESIN INTERACTIONS DURING FLOW

Lawrence T. Drzal
Michigan State University
East Lansing, MI 48824

I. INTRODUCTION & BACKGROUND

Liquid composite molding of polymer composites is a manufacturing process which has the potential for creating a cost-effective approach for the fabrication of structural polymer composite materials. The ability to place fiber preforms in their final designed position in a net shape mold prior to mold filling offers a significant increase in flexibility to design and produce large complex shapes(1).

This process of filling the net shape mold with the liquid resin matrix after the dry fibers have been inserted is the key area where process improvements need to be made. The infiltrated mold must be thoroughly "wetted" by the resin in which the resin is distributed around each fiber for optimum mechanical performance. Attention is being directed to increase the speed of filling as the key to reducing manufacturing cost. The structure of the fiber preform, the sizings and binders applied to the fibers and the nature of the resin pose some difficulties however. Fibers are typically in the 10 micron size range. The positioning of fibers next to each other creates a very fine series of capillaries which must be thoroughly infiltrated for optimum composite mechanical properties. The fibers themselves are fabricated into bundles which can contain from several hundred to several thousand individual filaments. These larger bundles or tows create larger spaces when placed in the mold. Liquid resin being forced into the mold will flow through the larger spaces preferentially then the smaller volumes. This can create regions where the resin does not infiltrate as well as the trapping of volatiles which reduce the mechanical properties and part quality.

Most attention at the mold filling process has been directed at the infiltration of the liquid resin at the macroscopic level (1,2). A simple relationship (Darcy's Law) has been proposed (equation 1) relating the velocity (v_x) of the infiltrating resin to its viscosity (η), the permeability of the fiber preform (K_x) and the pressure gradient (dp/dx) in the flow direction.

$$v_x = \frac{K_x}{\mu} \frac{dp}{dx} \quad (1)$$

Most resins are not simple Newtonian fluids making the applicability of Darcy's law difficult without modification to the viscosity for the non-Newtonian character of the liquid polymeric matrix and the directional character of the permeability of the fiber prefrom.

At the microscopic level (i.e. between fibers within a bundle) the capillary forces generated by the attractiveness of the fiber surfaces to the resin aid the flow within these very small regions. A measure of this attractiveness is the contact angle given by the balance of surface tensions in equation 2. The contact angle (θ) can be related to the surface tensions (or surface free energies) of the solid surface (γ_{SV}), the liquid molding resin (γ_{LV}), and the interfacial surface tension (γ_{SL}) by the relationship

$$\cos \Theta = \frac{\gamma_{SV} - \gamma_{SL}}{\gamma_{LV}} \quad (2)$$

The surface tensions of the solids are difficult to determine but the liquid resin surface tension can easily be measured. The contact angle itself is a direct measure of the atractiveness and is measured for a given matrix and fiber. Ideally the contact angle should be zero but any value less than 90° is acceptable.

In general, for a given surface tension (γ) and contact angle (θ), the capillary forces aiding flow (represented by a pressure drop ΔP) increase inversely with the radius of the capillary (r). Equation 3 analytically expresses this relationship and is known as Young's equation.

$$\Delta P = 2\gamma \frac{(\cos \theta)}{r} \quad (3)$$

In general capillary flow is a slower process that the macroscopic flow generated by the resin pumps. However it is important to utilize capillary flow to insure complete infiltration and elimination of voids and inclusions within the fiber bundles. The relative importance of capillary

versus viscous flow in the mold filling process can be quantified by use of the Capillary Number (equation 4), a dimensionless number that is the ratio of the viscous forces i.e., the product of velocity (v) and viscosity (η), to the interfacial surface tension (1).

$$Ca = \frac{v\,\eta}{\gamma} \qquad (4)$$

While modifications to both macroscopic and microscopic models are being pursued, the materials used in liquid composite molding and their interactions with each other have not been considered as a potential contributing factor to both understand and improve the liquid molding process. For example, the polymeric resins used in liquid composite molding are multicomponent, non-Newtonian formulated systems and can exhibit changes in viscosity with filling conditions. These matrices are also reacting systems whose viscosity will increase with temperature and time (2).

While the glass fibers themselves are inert, the commercial fibers used are packaged in bundles which also contain other chemical constituents. Glass fibers are naturally susceptible to corrosion upon exposure to atmospheric moisture. Even minute amounts of moisture exposure results in serious loss in fiber strength. Glass fiber manufacturers always protect the fibers surface with a proprietary sizing applied at the point of manufacture to protect the fiber surface. This sizing is formulated to contain coupling agents (e.g. silanes) that chemically bond to the fibers surface and the matrix, film formers to produce a uniformly thick coating, antistatic agents and lubricants to aid in the fiber handling (2). The manufactured fiber bundle contains many fibers each surrounded by this sizing. (Table 1 lists some potential components that could be used in commercial sizing systems as listed in the patent literature.) The sizing is formulated to be compatible with the matrix chemistry so that it dissolves away into the infiltrating matrix during liquid composite molding. Another constituent of commercial glass fibers is a binder. The fiber prefrom requires a method to hold the fiber bundles in place during the liquid resin infiltration process. Usually a thermoplastic binder is added in the form of small droplets which are melted during the fiber prefrom shaping process. When the binder particles solidify, they adhere to adjacent bundles causing them to be rigidly fixed in a three dimensional network,

making the prefrom easier to handle and less susceptible to rearrangement during the mold filling process. These binders are also selected to be soluble in the infiltrating matrix.

Table 1. Typical Compositions of Polyester, Polyvinyl Acetate and Polyurethane Fiber Sizings

Common Sizing Name	Polyester	Polyvinyl Acetate	Polyurethane
Components	**Pat.# 4,752,527 Example 2**	**Pat.# 4,027,071 Example 1**	**Pat.# 3,803,069 Example 1**
Solvent	water	water	water
Coupling Agent	gamma-methacryloxy-propyltrimethoxy silane	1. gamma ethylene diamine propyl trimethoxy silane 2. methacrylic acid complex of chromic chloride	gamma aminopropyltriethoxy silane
Film Former	unsaturated bisphenolic glycol-maleic polyester	polyvinyl acetate	curable, blocked polyurethane resin emulsion
Antistatic Agent	cationic organic quaternary ammonium salt		
Lubricant	polyethyleneimine polyamide	1. cationic fatty acid amide 2. tetraethylene pentamine	
Strand Hardening Agent	aqueous methylated melamine-formaldehyde resin		
pH Control	acetic acid	acetic acid	
Emulsifying Agent			condensate of polypropylene oxide with propylene glycol

It is the interaction between the reacting matrix with the sizing and binders under the time constraints and the process thermal profile that have the potential for unsuspected interactions that can significantly affect the mold filling process and the quality of the resulting composite that

must be considered in developing a model of the liquid molding process. For example, it has been shown that the dissolution of a thermoplastic polyester binder into a vinyl ester resin can increase the viscosity by 200%[1]. Sizing dissolution into an epoxy matrix has been reported to increase the modulus but decrease the matrix fracture toughness (2). Void generation is strongly affected by the interfacial free energies resulting from the contact of the resin with the sizing[2]. Even the adhesion that results from the interaction of a fully compatible sizing with the matrix can be affected by process temperatures resulting in a significant reduction compared to thermal and temporal equilibrium values (4,5,6).

Complete and thorough infiltration of the fiber preforms then depends both on the compatibility of the matrix with the sizing as well as on the liquid composite molding conditions of time and temperature. Figure 1 illustrates the dynamics of the events taking place at the sizing/matrix infiltration front. If these conditions are not optimum, partial or incomplete dissolution may result in incomplete wetting, poorly structured interphases, enhanced void generation, less than optimum adhesion and reduced composite mechanical properties (4).

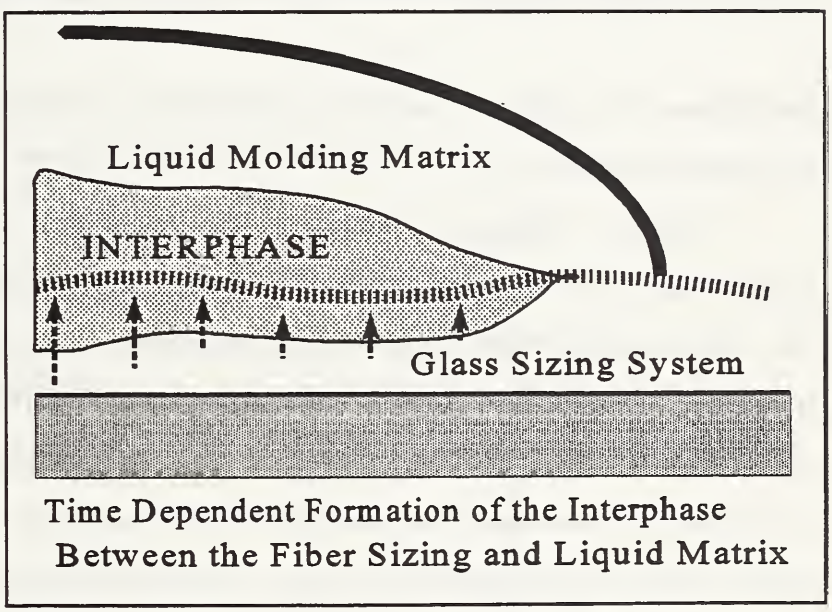

Figure 1

II. STRUCTURE OF WORKING GROUP

Objectives of Working Group. The Objectives of the working group were to assess the reinforcement/resin area and seek to identify the importance of various possible interactions on structure-processing-property relationships for liquid composite molding and in particular to assess the role of the sizing, binder and fiber architecture.

Discussion Format. The session was structured so that the three areas (sizings, binders and fiber architecture) were discussed in the context of the processing and performance stages that are to

be encountered by a composite that is manufactured by liquid molding (i.e. mold filling, composite curing and composite long-term mechanical performance). Participants were first asked to identify potential important factors without regard to the level of their importance. Once an exhaustive list had been prepared, the group went through each factor individually with the purpose of identifying whether the factor was Important (I), Moderately important(M), Unimportant (U) or of unknown importance (?). Published literature citations, corporate and personal experience and anecdotal information was used to formulate the final assessment. Since this process reflects the background of the working group participants, and since only a few hours were available for discussions, the results reported here should be viewed as an initial starting point for the review of this area. The results of this discussion were recorded and are reported here according to the identified focus of the group, i.e. sizing, binder and fiber architecture.

Definitions. In order to conduct this assessment, the group adopted some common definitions of sizing and binder.

Sizing. Sizing is defined as the formulated coating applied to glass fibers at approximately 1% by weight immediately after glass manufacture. Sizing formulations are for the most part proprietary. The main ingredients of the sizing consist of a coupling agent (typically a silane), film former, antistatic agent and lubricant. The film former is nominally selected to be compatible with the matrix resin with which it is to be used. Sizings are applied for corrosion protection of the glass fibers (from moisture), to provide chemical bonding with the matrix and to provide physical integrity of the fiber bundle.

Binder. Binder refers to a thermoplastic or thermoset 'B' or 'C' staged material applied to the external surfaces of fiber bundles to mechanically stabilize the preform architecture during handling, mold filling or other operations which could result in a rearrangement of the fibers. Binder is usually applied at 3-10% by weight.

III. SUMMARY OF FINDINGS

The objective of this exercise was to identify those reinforcement/resin interactions and factors which are necessary to develop comprehensive structure-processing-property relationships for liquid composite molding.

SIZING. Since all glass fibers are sized, the sizing itself is a critical material which has not been heretofore considered in the development of structure-processing-property relationships for liquid composite molding. As discussed previously, sizing is defined as the formulated coating applied to glass fibers at approximately 1% by weight immediately after glass manufacture. The main ingredients of the sizing consist of a coupling agent, film former, antistatic agent and lubricant. The film former is nominally selected to be compatible with the matrix resin with which it is to be used. Sizing formulations are proprietary. Sizings are applied for corrosion protection of the glass fibers (from moisture), to provide chemical bonding with the matrix and to provide physical integrity of the fiber bundle. The results of the assessment of fiber sizing were discussed as to their influence during mold filling, processing and performance. The following factors were identified as being improtant or moderately important during the workshop.

SIZING	
Thermodynamic Wetting by Matrix	I
Solubility of Sizing in Matrix	I, ?
Effect on Viscosity	I, ?
Effect on Matrix Reaction Kinetics	I, ?
Effect on Cured Matrix Properties	I, ?
Effect on Fiber "Wash"	M, ?
Ageing of the Sizing	I, ?

Thermodynamic Wetting. The most important factor in the interaction between sizing and matrix in liquid composite molding is thermodynamic wetting. This quantity is the change in interfacial free energy that takes place when the matrix is brought in contact with the sized fiber

surface. This free energy change must be negative to insure that the fiber and matrix are in thermodynamic equilibrium. This in turn is a necessary condition for optimum adhesion between fiber and matrix. A decrease in interfacial free energy will allow for displacement of volatiles from the fiber surface by the infiltrating resin.

Solubility. Properly formulated and processed sizings are designed to dissolve into the infiltrating matrix and be transported away from the fiber surface. Therefore, under the constraints of the liquid composite molding cycle, the time for dissolution should be short compared to some time characteristic of matrix reaction. In theory solubility and diffusional mobility will decrease with increasing matrix viscosity. but for the most part studies to establish causal relationships between solubility of the sizing in the matrix and its relationship to liquid molded composite processing and mechanical properties is an unknown and should be investigated. Solubility of the sizing into the matrix may manifest itself in many process and performance issues such as:

Effect of Sizing Solubility on Resin Matrix Viscosity. The constituents of typical sizings are expected to have a significant effect on the local viscosity of the matrix near the fiber surface. Since such changes can have an effect on the viscous flow models such as those based on Darcy's law, the effect of sizing on matrix viscosity is considered to be an important factor.

Effect of Sizing Solubility on Matrix Reaction Kinetics. It has been shown that some of the ingredients in sizings are themselves reactive with the matrix. Variations in matrix properties caused by effects of the sizing ingredients on the matrix reactivity have been reported. These effects can be both inhibitive and accelarative depending on the matrix chemistry and sizing constituents. An inhibitative effect could increase process time required to obtain a full cure while an acceleratory effect could raise the matrix viscosity and contribute to lower fill rates and perhaps void entrapment.

Effect of Sizing Solubility on Cured Matrix Properties. Studies have been reported where sizing has been mixed into some generic matrices and bulk coupons have been fabricated. Measurements have shown that such large amounts of sizings might be present near the fiber surface and can cause significant changes in the glass transition temperature (Tg) in that region. This change in local concentration can have either positive and negative effects on the matrix

tensile modulus and increase the extent of trapped voids.

Effect of Sizing Solubility on Fiber 'Wash'. It is possible for the sizing to be very soluble in the infiltrating resin under processing conditions. In such circumstances a secondary effect might be that the removal of the sizing would allow the fibers to reposition themselves under the influence of the flow fields associated with resin infiltration. This could result in 'nesting' of the fibers which would reduce the size of the inter and intra fiber spaces and thereby increase the infiltration pressure. The effect was rated as moderate and much mre important and low volume fractions of fiber tha at high volume fractions.

Ageing of the Sizing. Another factor that could affect sizing/resin interactions could be ageing of the sizing. Most sizings are formulated with the idea that they will be used within a relatively short period of time. Lengthy periods of storage or storage under very dry conditions could 'age' the sizing either by reducing the residual moisture content or allowing some of the constituents to react prematurely. This would reduce the solubility of the sizing in the matrix, perhaps change the surface free energy and affect void generation or removal.

BINDER. Since the binder is viewed as a separate constituent from the sizing, its role was disucssed and assessed independently of the sizing. As explained earlier for purposes of this discussion a binder is defined as either a thermoplastic or thermoset 'B' or 'C' staged material applied to the external surfaces of fiber bundles to mechanically stabilize the preform architecture. Binder is usually applied at 3-10% by weight to the external surfaces of the fiber bundles. The binder may be distributed as either discrete particles or continuous coatings on the fiber bundles.

BINDER	
Thermodynamic Wetting of Binder	**I**
Particle Size and Distribution	**U**
Soluble Binder	
Effect of Viscosity	**I, ?**
Effect on Matrix Reaction Kinetics	**I, ?**
Effect on Cured Matrix Properties	**I, ?**
Effect on Fiber Wash	**M, ?**
Insoluble Binder	
Stress Concentrator	**U**
Inhibits Impregnation of Fiber Bundle	**M, ?**
Source of Porosity	**M, ?**

Thermodynamic Wetting. Thermodynamic wetting is again a very important factor for optimum adhesion between a continuous binder film or a discrete bonder particle applied to the fiber bundle and subject to interaction with the infiltrating matrix. If discrete binder particles are used, wetting is still important since unwetted binder particles could act as stress concentrations in the composite. A decrease in interfacial free energy brought about by proper interaction between the binder surface and the matrix will allow for displacement of volatiles from the binder surface by the infiltrating resin. The contact angle is a direct measure of this quantity.

Particle Size and Distribution. Binders may be applied in different ways resulting in either continuous films or discrete particles. Particles can vary in size from the micron scale to several

hundred microns. Since in all applications the mechanical integrity of the preform is the criterion for effectiveness of the binder, it was felt that this is not an important factor. Glass manufacturers will select the from of the binder consistent with a potential application.

Soluble Binder. Some binders are selected to be soluble in the infiltrating matrix. Properly selected, they are designed to dissolve into the infiltrating matrix and be transported away from the fiber surface after the mechanical strain on the preform during the filling operation has been reduced. Under the constraints of the liquid composite molding cycle, the time for dissolution should be greater than the time for mold filling but less than some time associated with significant matrix reaction as in the case for sizings. Solubility and diffusional mobility will decrease with increasing matrix viscosity. Solubility of the binder into the matrix manifests itself in many process and performance issues similar to sizings.

Effect of Bonder Solubility on Resin Matrix Viscosity. The constituents of typical binders are expected to have a significant effect on the local viscosity of the matrix near the fiber surface. Since such changes can have an effect on the viscous flow models such as those based on Darcy's law, the effect of binder on matrix viscosity is considered to be an important factor.

Effect of Binder Solubility on Matrix Reaction Kinetics. It has been shown that some of the ingredients in binders are themselves reactive with the matrix. Variations in matrix properties caused by effects of the binder ingredients on the matrix reactivity have been reported. These effects can either inhibit or accelerate the matrix curing reaction depending on the matrix chemistry and binder constituents. An inhibition of the curing reaction could increase process time required to obtain a full cure while an acceleration of the reaction raise the matrix viscosity and contribute to lower fill rates and perhaps void entrapment.

Effect of Binder Solubility on Cured Matrix Properties. Studies have been reported where binder has been mixed into some generic matrices and bulk coupons have been fabricated. Measurements have shown that large amounts of binders as might be present near the fiber surface can cause significant changes in the glass transition temperature (Tg), have both positive and negative effects on the tensile modulus and increase the extent of trapped voids. Thermoplastic binder dissolved in the matrix can reduce the local properties as well.

Effect of Binder Solubility on Fiber 'Wash'. It is possible for the binder to be very soluble in the infiltrating resin under processing conditions if the selection is not optimum. In such circumstances a secondary effect might be that the removal of the binder would allow the fibers to reposition themselves under the influence of the flow fields associated with resin infiltration. This could result in nesting of the fibers which would reduce the size of the inter and intra fiber spaces and thereby increase the infiltration pressure. This effect would be greatest in low volume fraction or short discontinuous fiber composites. Fiber architecture would tend to stabilize the structure at higher fiber volume fractions.

FIBER ARCHITECTURE. Since the placement of fiber bundles is the result of any of a number of textile operations, the fiber architecture itself is viewed as a factor which can affect the interactions that take place during liquid composite molding. The expected geometric arrangement of fibers and bundles of fibers is further complicated by the presence of sizing and/or binder.

FIBER ARCHITECTURE	
Capillary Forces (Intra Bundle)	**I**
Capillary Forces (Inter Bundle)	**I**
Fiber/Bundle Crossover Points	**U**
Closed End Pores	**M, ?**
Cure Shrinkage	**U**
Volume Fraction of Fiber	**M**
Surface Area of Fiber	**M**

Capillary Forces. The spacing of fibers within the bundles and the spacing of bundles in the preform are important factors in the development of capillary forces which can aid in infiltration. Flows through the prefrom must be balanced so that inter-bundle flow does ot exceed intra-bundle flow and result in trapping of volatiles and void formation.

Fiber Bundle Geometry. Weaving or braiding of fiber bundles creates contact points where the bundles are forced into mechanical contact. At these junctures, the fibers are bent out-of-plane and there is a large compressive force induced by the fabric that forces these overlapping bundles into close contact. The presence of these contact points can create stress concentrations. The density of these points will vary with the nature of the weave. Since this effect is reflected in the design parameters for a given fiber architecture, it is not considered important in the context of this discussion.

Closed End Pores. In addition to the stress concentration, the compressive force at these junctures will reduce the spacing between fibers to the lowest possible value in effect closing off the capillaries. This in turn can create closed end pores (microvoidage) which will not fill with matrix during the liquid molding operation if any gas phase material is captured in them.

Cure Shrinkage. Most liquid molding resins undergo a certain amount of shrinkage depending on their chemistry and process conditions. This can in severe cases lead to microcracking. Although this is an important factor in the performance of the final composite part, it is not a factor to be considered under this workshop.

Volume Fraction and Surface Area of Fiber. The total amount of fiber in each composite part strongly affects the interactions through a concentration effect. At high fiber contents, the amount of sizing and binder is large and must be given a greater degree of consideration in the design of the process. Likewise the spacing between bundles would be expected to decrease. Overall the effect would be moderate but nonetheless it should be considered.

IV. RECOMMENDATIONS

The working group concluded that the factors identified in the discussions vary in importance as well as understanding. However, the discussion pointed out that a fundamental problem exists which must be solved through joint cooperation of all groups involved in liquid composite

molding. It is very important to know what the composition of the sizings and binders are so that appropriate research could be conducted to develop predictive composition-processing-property relationships. This is not practical since the glass manufacturers depend on the proprietary formulations to differentiate their products in the marketplace. However, if a comprehensive research program was supported and conducted by both glass manufacturers and fabricators through the auspices of the NIST, a set of evaluation protocols may be specified to aid in the optimization of the sizing/resin interaction and thereby define the limitations imposed by the interactions between the sizings and binders with the reacting liquid molding resin. Based on the discussions in this worskop, the following three areas are considered to be very important to improving the speed and quality of the composite formed in the liquid molding process.

Thermodynamic Wetting. The measurement of the **contact angle** formed between the sized fiber and the fiber bundles with binders would directly assess the thermodynamic interactions. A value less than 90° would insure wetting and the closer the value was to 0°, the better filling and displacement of volatiles would occur. This would also provide a figure of merit for determining the changes in the thermodynamic interaction as a function of the reaction of the matrix system.

Sizing/Binder Solubility in the Matrix. Solubility of the sizing and/or binder in the matrix is often a desired goal during liquid molding. Standard procedures are available for determining the solubility parameter (i.e. square root of the cohesive energy density) for both the sizing and the matrix. If this quantity was specified by the glass fiber manufacturer, selection the fabricator could compare values with the liquid molding resin and insure that the selection is optimum.

A second equally important factor is the time for dissolution of the sizing and/or binder in the reacting matrix. This can be measured and coupled with the known kinetic expressions for most liquid molding resins.

Mechanical Properties. Beyond the obvious direct measurement of the composite mechanical properties, the most sensitive mechanical property affected by these interactions would be fiber-matrix adhesion. Methods exist for the direct measurement of this quantity in-situ. Such measurements should be conducted to assess the effect on material interactions on this

property. With the cooperation of the fiber manufacturers, it should be possible to obtain bulk quantities of the sizings and binders for evaluation with liquid molding resins. Compositions with varying amounts of sizings and binders should be interrogated to determine their effect on Tg and modulus.

In summary, although it may not be possible or even necessary to obtain fundamental scientific information about the exact nature of the sizing and/or binder interactions with the liquid molding resins, it would be beneficial to conduct an effort to develop protocols to insure maximum compatibility and optimum processing. If such a result can be achieved, it may be possible to develop a set of criteria that define and optimize the process limits based on the interactions of sizings and binders with resins in liquid composite molding as illustrated by the process window of Figure 2.

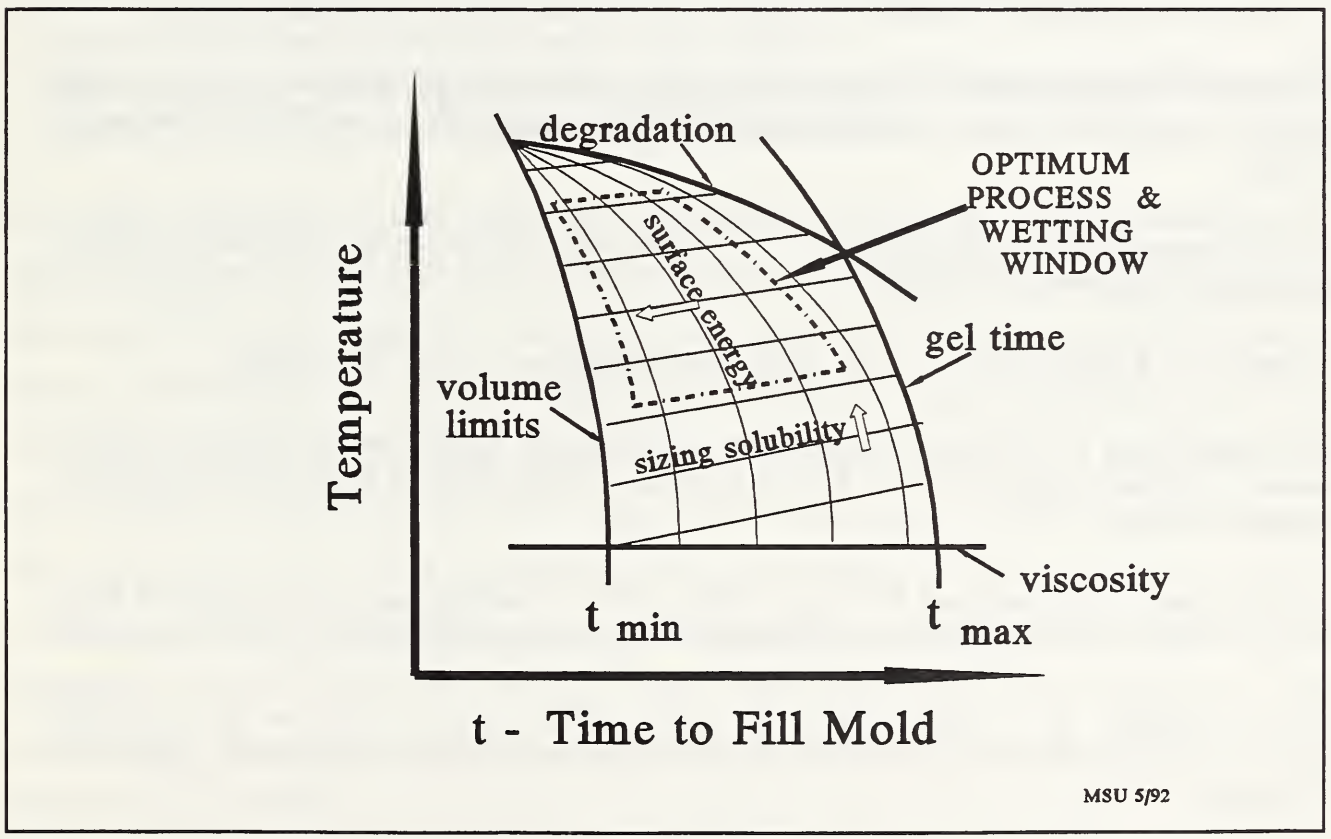

Figure 2

REFERENCES

1. ***Polymer Composite Processing, 2nd Industry Workshop, NISTIR 4461***, National Institute of Standards and Technology, C. Johnson, S.S. Chang and D. Hunston, ed., May (1990).

2. R. S. Parnas and F. R. Phelan, Jr., *The Effect of Heterogeneous Porus media on Mold Filling in Resin Transfer Molding,* ***SAMPE Quarterly***, 22, p 53-60, (1991).

3. A. W. Chan and R. J. Morgan, *Modelong Preform Impregnation and Void Formation in Resin Transfer Molding of Unidirectional Composites,* ***SAMPE Quarterly***, 23, pp 48-52 (1992).

4. C.W. Macosko, ***RIM, Fundamentals of Reaction Injection Molding***, Hanser Publishers, (1989).

5. J. Chen, K. Jayaraman and C. A. Petty, *A Process Model for Liquid Molding: Effects of Binder Dissolution, Heat Transfer and Reaction,* ***Proc. 9th Ann. Advanced Composites Conference and Exposition***, Dearborn, MI (1993).

6. E. Plueddemann, ***Silane Coupling Agents***, p. 20, Plenum Press, New York, (1982).

7. D. Backes. K. Jayarman and C. A. Petty, *The Effects of Resin Soluble Binder on Flow Through Continuous Strand Glass Mats,* ***Society of Automotive Engineers***, Paper No. 930175, Dearborn, MI (1993).

8. H. AlMoussawi, E. K. Drown and L. T. Drzal, *The Silane/Sizing Interphase,* ***Polymer Composites***, 14, pp.195-200 (1993).

9. N. Patel, V. Rohatgi and L. J. Lee, ***Polymer Composites***, 14 , pp. 161 (1993).

10. B. Larson and L. T. Drzal, *Glass Fiber Sizing-Matrix Interphase Formation in Liquid Composite Molding: Effects on Fiber-Matrix Adhesion and Mechanical Properties,* ***Composites***, (to appear in 1994).

11. T. H. Cheng, F. R. Jones and D. Wang, *Effect of Fibre Conditioning on the Interfacil Shear Strength of Glass-Fibre Composites,* ***Composites Science and Technology***, 48, pp. 89-96 (1993).

12. K. A. Lindsey, C. D. Rudd and I. M. Fraser, *Effects of Post-Cure on the Interfacial Properties of Glass Fibre-Urethane Methacrylate Composites,* ***J. Matr, Sci. Letters***, 12 pp. 894-897 (1993).

13. E. K. Drown, H. AlMoussawi and L. T. Drzal, *Glass Fiber Sizings and Their Role in Fiber Matrix Adhesion,* ***J. Adhesion Sci. Technol.***, 5, pp. 865-881 (1991).

HEATING AND RHEOKINETIC EFFECTS DURING FLOW

Nitin Anturkar
Ford Motor Company
Dearborn, MI 48121

Introduction

The workgroup on Rheokinetics and Heat Transfer was convened during the workshop on Manufacturing Polymer Composites by Liquid Molding (LCM) to define the critical challenges in the areas of rheokinetics and heat transfer, with particular applications to LCM. The discussion was focused on the following major issues:

* Define critical research topics in the areas of rheokinetics and heat transfer.
* Review current state-of-the-art for each of these topics.
* Build consensus on prioratizing the issues within these research topics with respect to their importance to LCM and difficulty in addressing the issues.

In the past, significant extent of efforts have been directed towards permeability measurements, model simulation and validation and reinforcement/resin interactions, at least within an academic community (There were separate workgroups, which addressed these issues in the workshop.). However, with increasing emphasis on high-speed processing for large volume applications, there is a rising strong demand for better understanding of rheokinetics behavior of the resins and of heat transfer for improving the LCM process. In fact, participants identified applications of rheokinetics and heat transfer themselves to be the key research topic that needs further attention for the enhancement of the LCM process. We will first review various possible applications of rheokinetics and heat transfer in LCM. The other critical topics that will be addressed in this report include rheokinetics measurements, rheokinetics models, heat transfer coefficients and thermal dispersion effect. In this report, all the discussions are arranged under the headings of these *five* individual research topics.

Applications

A potential for low-cost high-volume applications of composites by liquid molding will increase with reduction in the cycle time. Fundamental understanding of cure kinetics and its effects on the final mechanical properties is, however, essential for reducing the cycle time. Ideally, one prefers low, constant viscosity during injection and rapid rise in viscosity after injection. However, in reality, viscosity starts rising as soon as reactants are mixed. Therefore, one undesired side-effect of faster cure kinetics is the reduction in the injection time. Whether the reactions are activated by employing hot mold walls (Resin Transfer Molding or RTM) or by impingement mixing (Structural Reaction Injection Molding or SRIM), the heat transfer effects on moldability and final properties of the parts are very important in LCM, and are tied with rheokinetics behavior of the resins. Note also that newer, faster reactions are highly exothermic, and create large temperature gradients in composite parts. Therefore, the emerging trends in the LCM process require more in-depth, fundamental understanding of rheokinetics and heat transfer to address the above-mentioned issues. The other conventional applications of these two areas include:

(1) modeling and simulation of LCM with desired accuracy,
(2) establishing operating windows for given resin/reinforcement combinations and part geometry,
(3) developing process control strategies and process integration, (4) designing resins for ease of processability, while maintaining desired final properties.

Several researchers have devoted efforts in studying the effects of viscosity and heat transfer parameters on the process defects, such as microvoids and race tracking. Such studies are also required for newer resins with faster, highly exothermic reactions.

Rheokinetics Measurements

It would be difficult to identify the challenges in the rheokinetic measurements without first defining the reaction rate and associated build-up in viscosity in terms of some simplistic, practical process parameter. One possible, loosely defined choice of such process parameter is the time it takes for viscosity to rise to a level, where no further injection is possible. Note that this time *does not* necessarily correspond to the gel time as defined in the classical thermoset

rheometry or to the apparent gel time encountered in the phase-separating resins. Table 1 lists three classes of resins in terms of these limiting injection times (t_{inj}), the current level of expertise in the measurements of their rheokinetic behavior and the importance of these resins in LCM applications.

Table 1: Three classes of resins.

Reaction Rate	Level of Expertise	Importance in LCM
Slow ($t_{inj} > 20s$)	Good	Important
Moderate ($20s > t_{inj} > 2s$)	Poor	Important
fast ($t_{inj} < 2s$)	Poor	Not Important

Although the resins with the lowest t_{inj} offer the most serious challenge in the measurements of the rheokinetic behavior, the applications of these resins are limited in the LCM process in the near future. The resins with the highest t_{inj} are already investigated by various researchers. However, resins with moderate reaction rates ($2s < t_{inj} < 20s$) have started playing an important role in LCM, and pose a difficult task in the measurements of viscosity and kinetics.

Various techniques have been used to characterize viscosity and kinetics of resins used in RTM and SRIM. Research activities related to SRIM derive largely from the activities in the area of Reaction Injection Molding (RIM). Although direct measurements of viscosity of fast-reacting systems are difficult, pressure traces during molding can be used to derive the "average" viscosity profile in the mold. The conventional and on-line viscometers have been modified to facilitate rapid injection and data acquisition. Solution polymerization is also used to slow down the reaction so that broader window is available for the measurements. Subsequent extrapolation to the bulk systems from the experiments at various solvent concentrations provides the estimate of viscosity. Conventional kinetics measurement techniques, such as FTIR spectroscopy, differential scanning calorimetry and dielectric measurements have their limitations in faster, highly exothermic reactions. However, a temperature rise in adiabatic conditions can be followed in exothermic reactions to derive the lumped kinetic rate expressions. Recently, in-

mold fiber-optic FTIR has been used to follow kinetics in complex molds.

However, viscosity of the resins with faster reactions has been estimated from the indirect measurements such as in neutral solvents and from pressure traces, rather than from the direct measurements. Besides, viscoelasticity and the shear-rate dependence of viscosity are generally neglected in reactive molding. However, these effects may play major roles in rapid LCM processing, particularly due to small gaps around fibers and through porous media, which give rise to complex local flows. Measurements of these effects is a difficult task using existing experimental techniques. The other important issue is to correlate the modulus development with the extent of reaction. This correlation is strongly influenced by parameters such as thermal history and morphology. The development of flexural modulus is ultimately responsible for the duration of part to stay in the mold.

Rheokinetics Models

Once the rheokinetic behavior of the resins is successfully measured, generalized models need to be developed for the viscosity and kinetic rate expressions, so that they can be used in various applications for process improvements as described in the earlier section. Several ad-hoc models, such as Castro-Macosko model and dual Arrheneous model, have been developed to correlate the viscosity with the temperature and the extent of reaction. In these models, shear-rate dependence and the interactions between parameters related to temperatures and extent of reaction are neglected, such that

$$\eta(T,\chi) = \eta_T(T) \cdot \eta_\chi(\chi) \qquad (5)$$

However, if the viscosity varies during molding inside the mold, then incorporating Darcy's law in the simulation poses a new challenge. An exercise of deriving the governing equations in LCM processes from the fundamentals is a necessary first step in addressing a proper, consistent interpretation of Darcy's law and to eliminate any confusions amongst the researchers. This was a recurring comment within participants for the research topics discussed in the following sections as well. Note that such efforts are already initiated within LCM community by Tucker and Dessenberger (1994). As discussed earlier, viscoelasticity and shear-rate dependence of viscosity may need to be incorporated in the rheological models for these resins. Finally, the

assumption of weak interaction between the temperature, conversion and shear-rate effects (as shown in eqn. 1) need to be carefully examined for resins used in LCM.

Heat Transfer Coefficients

Heat transfer always played a critical role in earlier LCM processes such as in RTM, because reactions are thermally activated in these processes by heating the mold walls. In new generation LCM processes such as SRIM, the reactions are induced by impingement mixing. However, these reactions are highly exothermic, and build high temperatures gradients in the parts. Besides, the thermal history of the resins influences the morphology within the resin matrix, bonding between the resin and fibers, and the rheokinetics behavior. Although the importance of heat transfer has been identified for a long time, state-of-the-art in understanding the effects of various parameters on the heat transfer coefficients has involved considerable empiricism.

Participants felt that resin to wall heat transfer coefficient (h_w) plays more critical role in modeling heat transfer, whereas resin to fiber heat transfer coefficient (h_f) is more important in understanding microscopic phenomena in LCM processes. Empirical measurements of h_w for simplified geometries have been performed. However, the following moderately difficult issues need to be further addressed:

* Effects of materials, the presence of porous media near the walls and geometric shape factors on h_w.
* Effects on race-tracking and other processing issues.
* Development of generalized experimental techniques.

The measurements of h_f, however, pose a difficult task. Although state-of-the-art thermographic imaging and fiber optics have been used in estimating the heat transfer from resin to fibers, little is known at the fundamental level. The experimental techniques are still emerging and the basic definition of this heat transfer coefficient needs to be clarified and agreed upon by the researchers (Tucker and Dessenberger, 1994). Such exercise is also expected to help in understanding how to incorporate this "microquantity" in the "macromodels". Besides, the importance of this heat transfer coefficient in the LCM process can not be determined until above issues are addressed.

Thermal Dispersion Effect

Thermal dispersion occurs in the porous media because microscopic velocities and temperatures are different from the average values. If the fluid experiences a temprature gradient while moving through the fiber matrix, it will convect heat locally and if these temperature gradients are different from the gradients of the average temprature then there will be the heat dispersion effect.

Mathematical description of this effect has been concisely reported by Tucker and Dessenberger (1994). Unfortunately, some microscopic model, such as unit cell model or some empirical model, is necessary to correlate the dispersion term (which contains only local quantities) with the average temperatures and velocities. It is equally difficult to perform reasonably accurate experiments to estimate the extent of thermal dispersion. The influence of various process and resin parameters on thermal dispersion is also unknown. Besides, simulation of this phenomenon strongly depends on the type of model chosen. It is postulated that for non-periodic media, the dispersion term in the energy equation depends on the local Peclet number. Thus, for fast, highly exothermic reactions, the dispersion effect can be significant enough to adversely affect the moldability and final properties of the part. Therefore, this relatively brand new, difficult area is definitely ripe for in-depth investigation.

Summary

Although several research topics were identified in our "wish-list" in the areas of rheokinetics and heat transfer, the participants reached consensus on five topics, which were considered critical challenges in enhancing high-volume low-cost applications of LCM. These topics were rheokinetics measurements, rheokinetics models, heat transfer coefficients, thermal dispersion effect and the applications of rheokinetics and heat transfer in LCM. New emerging trends of resins with faster, highly exothermic reactions for rapid processing are definitely a catalyst in increasing necessity for better understanding of the above research topics. In addition, the existence of fiber matrix in the LCM process offers unique challenges among all polymer processes in terms of uniqueness of phenomena such as thermal dispersion effect, and in terms of the direct impact of the above topics on the processability and final properties of the

composite parts. Therefore, apart from the measurements and analysis of the key rheokinetic and heat transfer parameters, their applications in the enhancement of the LCM process beyond conventional modeling and simulation was also included as a critical research topic in our discussion. Eventually, like many other research areas, increased activities in rheokinetics and heat transfer are directly tied with the further commercialization of LCM.

Reference

Tucker, C. L. and R. B. Dessenberger, "Governing Equations for Flow and Heat Transfer in Stationary Fiber Beds," to appear in *Flow and Rheology in Polymer Composites Manufacturing*, ed. S. G. Advani, Elsevier, New York (1994).

4. Poster Abstracts

Draper Lab Poster. E. Bernardon, Draper Labs.

Rheokinetics of Cyclic Carbonate Oligomer Polymerization, A.J. Salem, General Electric.

Permeability of Glass Fiber mat for Resin Transfer Molding. M. Xie et al., Concordia U.

Grumman Poster. G. Carpenter and R. Leek, Grumman Aerospace.

A Standard Reference Material for Permeability. R.S. Parnas, NIST.

State-of-the-Art Survey of Process Monitoring Sensors for Composite Fabrication. D.L. Hunston et al., NIST.

Dry Spot Formation and Changes in Liquid Composite Molding, K.Han et al., Ohio State U.

Micro-scale Flow Behavior and Void Formation and Removal in Resin Transfer Molding, N.Patel et al., Ohio State U.

Thermal Dispersion Effects in Resin Transfer Molding, R. Dessenberger and C. Tucker, U. Illinois.

Draper Lab Poster Board Abstract
NIST RTM Workshop 9/93
Ed Bernardon

Draper's RTM technologies include a new process called Flexible Resin Transfer Molding (FRTM®) which combines the cost-saving capability of double diaphragm forming with RTM. Other developments include design, construction, and delivery of automated preforming machinery to reduce RTM part cost. Preforming knowledge has been incorporated into design guides and CAD tools that improve preform design. Other new preforming methods under development, include geometrically smart braiding.

Systems with in-mold or in-part sensors for control of cure and resin injection, inspection of ply distortion and positioning, fiber stitching and tension-control have also been developed.

RHEOKINETICS OF CYCLIC CARBONATE OLIGOMER POLYMERIZATION

Andrew J. Salem

Polymer & Inorganic Materials Laboratory
GE Corporate Research & Development
Schenectady, NY 12301

Cyclic thermoplastic oligomers can be processed as low viscosity melts and them polymerized to high molecular weight, combining the processability similar to that of thermosets while yielding the final properties of a thermoplastic. One of the key elements in a comprehensive processing technology for cyclic resins is the ability to measure and predict the time-dependent changes in melt viscosity during the polymerization reaction. This paper presents a model of the rheokinetic behavior of cyclic resins for the limited reaction extent that maintain the low viscosities of interest for efficient processing. Kinetic expressions for the ring-opening polymerization reaction are combined with a dilute polymer solution rheological model to yield expressions for the time-dependent viscosity during the polymerization reaction. The results are compared with rheological data at several temperatures with several polymerization initiators for cyclic BPA carbonate oblogmers. A simplified version of the model is shown to predict the effects of temperature and initiator concentration reasonably well.

PERMEABILITY OF GLASS FIBER MAT FOR RESIN TRANSFER MOLDING

M.XIE, S.V.HOA, S.LIN and X.R.XI\AO
Concordia Center for Composites
Department of Mechanical Engineering
Concordia University
Montreal Canada

ABSTRACT: The permeability of motor oil in dry and wet glass fiber mat (M8610 owens-corning) has been measured. Permeabilities determined by Darcy's law increase with the velocity of the flow. The transient phenomenon has been observed. The variation of permeability from dry to saturated state can be expressed by an empirical equation:

$$K(t)/K_s = 1 + (K_{dry}/K_s - 1) * \exp[-c * t/(1-t/t_s)]$$

where: K: permeability;
K_s: permeability at saturated state;
t: time ($0 \le t \le t_s$);
t_s: time reaching saturated state;
c: system constant.

G. Carpenter and R. Leek
Grumman Aerospace and Electronics
Corporate Research Center
Bethpage, N.Y.

Poster Abstract

The objective of the Grumman Manufacturing Science Initiative Program for resin transfer molding is to establish a scientific basis for understanding and predicting the process in order to optimize component design, mold design and processing conditions. Flow behavior visualization experiments using transparent molds are coordinated with validation of computational models. A building block approach is being used to sequentially determine the effect of material and process variables on macro-flow behavior, cure, void formation and void transport. In-plain directional unsaturated permeability (K_u) values for an anisotropic plain weave fiberglass were determined in flat plate molds using the 'end fill' technique at room temperature. An oil with a viscosity of 0.08 Pa's (80 cP) was injected at 1.38 x 10^5 Pa (20 psi). K_u values were determined for 2 fiber volume fractions (Vf; 40.8% and 51.0%) and 2 fiber orientations (global flow parallel to warp or fill yarns) which were repeatable within ± 10%. Flow behavior was then determined for more complex geometries using the same preform architectures, fluid and processing conditions used in the flat plate experiments. Flow was determined through performs having a lower Vf edge (Edge Flow Study) of constant widths and through a 5 faced cube shell geometry (Cube Shell Study) with and without open channels between adjacent faces. Finite element models (FEM) were generated and appropriate K_u value(s) were input to predict flow for the Edge Flow and Cube Shell Studies. Comparison of experimental and predicted results indicated that there was an impediment to flow across the transition zone on the 'edge flow' experiments possibly due to the discontinuity of fibers, and through the corners of the 'cube shell' due to an increased in Vf observed during mold closure and preform compaction. A parametric study was conducted on the models for both geometry studies to obtain good agreement with experimental results. A zone was created i the 'edge flow' FEM to represent the transition from lower to higher Vf, and a refinement of the mesh in the 'cube shell' FEM to represent corners with either a higher Vf or open channels. A series of different K_u values were then input to the models for only the areas newly defined to provide the best fit to the experimental result.

A Standard Reference Material for Permeability

Richard S. Parnas, NIST

Liquid molding has been identified as a versatile and economical manufacturing process for the production of composite materials. The resin injection strategy is a critical part of the process design and ensures that the reinforcement is completely impregnated with resin. Preform permeability and fluid viscosity are the two important material properties required for characterizing the resin flow during the injection stage of the process. Measuring the permeability tensor can be quite difficult for many preform materials, therefore a calibration standard is expected to be valuable to composite manufacturers.

Two materials are proposed to comprise the SRM package, a relatively high permeability random mat and a lower permeability 3-dimensionally woven fabric. The random mat is included primarily as a "practice" material to provide an easy measurement with a low level of accuracy. Once a user gains confidence with the random mat, then the more difficult measurements with the 3-D woven fabric can be attempted with a higher probablility of success.

Both saturated and unsaturated 1-dimensional flow, as well as radial flow experiments were conducted with both materials. The saturated permeability of the random mat was found to vary from approximately 10^{-4} to 10^{-5} cm^2 as the fiber volume fraction was increased from approximately 7% to 22%. Additionally, the in-plane permeability of the random mat was found to be nearly isotropic. The saturated permeability of the 3-D woven fabric varied from approximately 10^{-6} to $6 \cdot 10^{-7}$ cm^2 as the fiber fraction increased from about 52.4% to 53%. However, the in-plane permeability of the 3-D woven fabric was clearly anisotropic. The permeability of both materials was also measured for flow in the through-thickness direction, and in each case the through-thickness permeability was approximately 15% of the in-plane permeability.

Unsaturated flow experiments, both radial and 1-D, consistently showed large deviations from the saturated flow behavior, but the unsaturated flow behavior in each material differed from the corresponding saturated flow behavior in opposite directions. In the random mat, the differences could be attributed to wicking since the "unsaturated permeability" initially increased above the saturated permeability, and then gradually decreased towards the saturated permeability as the mold filled. In the 3-D woven fabric, the differences could be attributed to preform structural heterogeneities since the "unsaturated permeability" initially decreased below the saturated permeability, then increased and overshot the saturated permeability before finally decreasing to the saturated value after the mold appeared filled.

State-of-the-Art Survey of Process Monitoring sensors for Polymer Composite Fabrication

D. L. Hunston, W. G. McDonough, B. M. Fanconi, and F. I. Mopsik
Polymers Division
National Institute of Standards and Technology
Gaithersburg, MD 20899

ABSTRACT

A variety of techniques have been applied to monitoring the changes that occur in the resin during composite processing. All these methods have advantages and disadvantages, and the best technique for a given application will depend strongly on the materials and processes involved. This poster will discuss these techniques and compare them in the areas of measurement speed, sampling volume, sensitivity to different resins, effects of fiber type, resistance to the manufacturing environment, interpretation of the data, adaptability for other uses, and temperature capabilities. The most important comparison, however, concerns the research and development work that is needed to achieve the full potential of each technique in applications on the factory floor.

The three classes of methods with the most potential for on-line application are electrical measurements, wave propagation techniques, and optical and spectroscopic methods implemented by fiber optics. The first two classes have an advantage in that commercial equipment designed for process monitoring is already available. The various spectroscopic and optical methods are generally in an earlier stage of development, but their great potential makes it highly desirable to actively pursue their developments as well.

Although each of the monitoring techniques has its own research and development needs, the most important technical and scientific issues are common to all. The major short term need is to build more rugged and reliable equipment that can withstand the harsh manufacturing environment. The scientific issues are equally important and more difficult to resolve. The two major issues are interpretation of the sensor output, and correlation of the resulting data to process control information through processing models. A wide range of empirical correlations have been developed between the various process monitoring measurements and a variety of material parameters, but few studies have attempted to develop a fundamental understanding of these correlations. As a result, such relationships must be used with care since they are generally resin specific, and their ranges of applicability and validity are unknown.

The future for process control is very bright. Many programs are currently underway in this area, but despite the critical role that sensors play, much of the on-going research focuses primarily on the process control aspects of the problem. Consequently, research and development on sensors is badly needed if we are to take full advantage of process control technology.

Title : Dry Spot Formation and Changes in Liquid Composite Molding

Authors : K. Han*, C. H. Wu* and L. James Lee**

*** Department of Mechanical Engineering, 206 W. 18th Ave.**

**** Department of Chemical Engineering, 140 W. 19th Ave.**

The Ohio State University, Columbus, OH 43210

Abstract submitted to NIST workshop on LCM

Dry spots are the most serious defect in the parts made by liquid composite molding (LCM). Local permeability variation of the fiber preform due to the preforming process, race tracking, and inappropriately placed inlets or outlets are the primary reasons to form dry spots. Although many computer models have been developed to simulate the mold filling process, none of them is capable of predicting the dry spot formation and changes. The goal of this work is to analyze and model the dry spot formation and changes in LCM.

Visualization experiments were conducted to investigate the dry spot formation and changes. Based on the experimental results, dry spot can be reduced in three ways : (I) Air in the dry spot may be compressed as the resin pressure increases in the saturated region around the dry spot. This leads to the reduction of the dry spot size. (II) If there is a pressure difference around the dry spot, air in the dry spot may escape as small bubbles through the saturated region with the lowest pressure. Eventually, the dry spot disappears. (III) When the hydropressure is at equilibrium between the dry spot and the surrounded saturated region, the resin may wick into the dry spot by the capillary force, which may also reduce the dry spot size. A centrifuge device has been developed to measure the relationship between the capillary pressure and saturation. The results showed that the capillary pressure depends strongly on the fiber architecture. A computer model has been developed based on the control volume - finite element method. Using this model, the number of dry spots, dry spot sizes and locations can be predicted. The calculated results agreed well with the experimental results.

Title : **Micro scale flow behavior and void formation and removal in resin transfer molding**

Authors : **Niraj Patel, Vivek Rohatgi, and L. James Lee**
Department of Chemical Engineering, 140 W. 19th Avenue
The Ohio State University, Columbus, OH 43210

Abstract submitted to NIST workshop on RTM

The resin injection process in Resin Transfer Molding (RTM) consists of two types of flow that occur simultaneously. One is bulk mold filling or the macro flow and the other is local penetration of resin into the fiber tows or the micro flow. The complexity of the injection step often results in flow induced defects such as formation of voids and poor fiber wetting. These defects have a detrimental effect on the performance of composite part. In this work, flow visualization experiments were carried out to investigate micro scale resin flow behavior through glass fiber preforms with an aim to correlate it to void formation and removal. Glass fiber mats used include unidirectional and bidirectional stitched, continuous random and 4 harness woven. Several reactive and non-reactive liquids with a wide range of viscosity and surface tension were used. Mechanisms of flow front progression and void formation, movement and removal were proposed. The study revealed that at low capillary numbers, macro voids between the fiber tows or crossing one or more tows were formed, whereas, at high capillary numbers micro voids were formed between the fiber filaments. The macro voids trapped in the fiber mats could be purged by bleeding resin at high flow rates. Macro void removal involved void stretching, breaking and movement. Micro void removal on the other hand, required void coagulation followed by removal. The effect of fiber mat architecture on micro scale flow pattern and void formation and removal were also discussed.

Thermal Dispersion Effects in Resin Transfer Molding

Richard B. Dessenberger and Charles L. Tucker III
Department of Mechanical and Industrial Engineering
University of Illinois
1206 W. Green St., Urbana, IL 61801 USA
(217) 333-2692 fax: (217) 244-6534

In the resin transfer molding (RTM) process a reactive liquid resin is injected into a mold that contains a preform of reinforcing fibers. The recent literature reports the development of several computer simulations for modeling the fluid flow, heat transfer and chemical reaction during RTM mold filling. The underlying mathematical models are based on the theory of flow through porous media; typically they use Darcy's law as the momentum balance, together with mass conservation and equations for the average temperature and cure. We have carefully studied the governing equations for RTM, and discovered the potential importance of *dispersion* effects in the governing equations for energy and curing.

We have derived governing equations based on the method of local volume averaging [1]. This method starts by writing the classical single-fluid equations for each point in the fluid and solid phases. Next, these equations are averaged over a small representative volume, using a rigorous mathematical procedure. Some mathematical manipulations then produce balance equations for the average velocity, pressure, temperature and degree of cure in the representative volume. The advantages of this approach are that the average values are precisely defined, and the governing equations are rigorously derived from accepted principles. This guarantees that no effects will be left out. This approach produces some terms that are not present in less formal derivations; one of these is the dispersion term. Dispersion is an enhanced transport of heat or mass caused by small-scale differences between the local velocity and its average value. An order-of-magnitude analysis shows dispersion to be important in both the energy and cure equations.

Using this approach, the equation governing heat transfer in RTM can be written as

$$\left\{\varepsilon_f (\rho C_p)_f + \varepsilon_s (\rho C_p)_s\right\} \frac{\partial \langle T \rangle}{\partial t} + (\rho C_p)_f \langle \mathbf{v}_f \rangle \cdot \nabla \langle T \rangle$$

$$= \nabla \cdot \left\{ \left(\varepsilon_f \mathbf{k}_f + \mathbf{K}_D + \varepsilon_s \mathbf{k}_s \right) \cdot \nabla \langle T \rangle \right\}$$

$$+ \varepsilon_f \rho_f H_R f_c \left\{ \langle c_f \rangle^f, \langle T_f \rangle^f \right\} + \mu \langle \mathbf{v}_f \rangle \cdot \mathbf{S}^{-1} \cdot \langle \mathbf{v}_f \rangle$$

One key idea used in the derivation of this equation is the assumption of local thermal equilibrium. Here it is assumed that the overall temperature changes slowly enough that in any given locale the fibers and the resin are essentially at the same temperature. Our estimates show that this is true for most RTM conditions, but may not be the case for very fast filling. In this equation the subscripts s and f denote the solid (fiber) and fluid (resin) phases, respectively. Angle brackets with no subscript, $\langle..\rangle$, represent a local average taken over the entire representative volume; angle brackets with a superscript f, $\langle..\rangle^f$, represent a local average over the fluid phase only. The primary variables are fluid velocity $\mathbf{v}_f$, temperature T, and degree of resin cure c_f. ε_f and ε_s are the volume fractions of the fluid and solid. μ is the viscosity of the fluid and $\mathbf{S}^{-1}$ is the inverse of the permeability tensor. f_c is a function describing the dependence of the chemical reaction rate on cure and temperature, and H_R is the heat of reaction per unit mass of the fluid. $\mathbf{k}_f$ and $\mathbf{k}_s$ are effective thermal conductivity tensors for the fluid and solid, which may not be equal to the intrinsic values. $\mathbf{K}_D$ is an effective conductivity tensor due to the dispersion effect.

Physically, dispersion occurs because the microscopic fluid velocities and temperatures are different from the average values. On the microscopic scale, the fluid moves up and down as it flows around the solid particles. If the fluid experiences a temperature gradient at the same time it will convect heat locally, and if these temperature gradients are different from the gradient of the average temperature then there will be a net heat flux. Dispersion produces an "effective" thermal conductivity that increases greatly with the average velocity.

An order of magnitude analysis on the governing equations shows that dispersion will be significant compared to the average convective terms when the "dispersion number" $\frac{\sqrt{S}L}{H^2}$ is greater than unity. S is the scalar permeability of the preform, H is one-half the gap-height and L is the length of the mold cavity. When this number is large, dispersion will dominate in regions containing large temperature gradients.

We have incorporated dispersion into a numerical simulation of flow and heat transfer in RTM mold filling. The simulation shows that dispersion significantly changes the temperature profile during filling, especially near the gate. These predictions will be compared to experimental measurements of temperature histories in RTM mold cavities. Our results show that it is important to include dispersion effects to get accurate predictions of RTM mold filling behavior.

[1]. Tucker, C. L., and R. B. Dessenberger, "Governing Equations for Flow and Heat Transfer in Stationary Fiber Beds, *"Flow and Rheology in Polymer Composites Manufacturing,* S. G. Advani, ed., Elsevier, Amsterdam (1994).

5. Lecture Manuscripts

Critical Issues in Model Verification for the Resin Transfer Molding Process. D. Calhoun.

Liquid Composite Moulding - Design for Processing. C.D. Rudd.

Permeability Measurement and Flow Simulation through Fiber Reinforcement. R. Gauvin.

Measurement of in-plane permeability of anisotropic fibre reinforcements. R. Gebart.

Dynamics of Binder Displacement in Liquid Molding. K. Jayaraman.

Mold Filling Issues in High Speed Reactive Liquid Molding. J. Castro.

Heat Transfer and Reaction Issues in Liquid Composite Molding. C.L. Tucker.

CRITICAL ISSUES IN MODEL VERIFICATION FOR THE RESIN TRANSFER MOLDING PROCESS

D. R. Calhoun, S. Yalvaç, D. G. Wetters, C. A. Raeck

The Dow Chemical Company
Central Research and Development
Advanced Composites Laboratory
Midland, MI 48674

INTRODUCTION

There is a constant effort in the composites industry to lower the manufacturing cost of parts primarily due to recent changes in the defense industry and a new emphasis on developing non-defense related markets. The resin transfer molding (RTM) process, which offers the potential of lower cost than related manufacturing processes, is attracting attention in composites engineering circles. The cost reduction of composites made by RTM primarily stems from increased production rates due to automation. However, lower scrap rates and relatively low capital expenses also significantly contribute to lowering fixed and operating costs.

Historically, the RTM process has been more art than science. Only recently have inroads been made into the computer modeling of the process which have the potential to be of real use to the industry. However, many of the computer codes recently developed have been based solely on theory, or have had little connection to real world experimental research. Verification studies have often been based on non-realistic mold designs or have utilized non-reactive idealized fluids. The present study has attempted to provide experimentation closer to reality by using a reactive resin system and production style mold. Complex issues such as pressure distribution and temperature profiles during filling of the mold, temperature profiles during cure, time to fill the mold, the most efficient method of locating vents, avoiding race tracking and dry spots were studied to develop a science base for meaningful process optimization. Many other issues such as multiple injection ports, weld lines, permeability changes both locally and on a contoured surface, void formation and transportation were not addressed since they were beyond the scope of this initial work.

It is the intention of this study to share with the new experimentalist some of the problems and critical issues encountered and solutions provided during the RTM validation experiments. It is also the intention of this study to provide researchers with data for code validation. The data presented serves as unbiased experimentation as it was done without knowledge of the inner workings of any specific code.

CONSIDERATIONS AND EXPERIMENTAL VERIFICATION

Verification of a flow code must attempt to include all viable operational parameters while limiting the interaction effects of parameters which may lead to erroneous data or incorrect conclusions. These considerations will naturally lead to an appropriate mold geometry for study. Two-dimensional analyses generally involve structures with square, rectangular, or circular geometries. Although flow modeling can assume a wide variety of two-dimensional patterns, an increase in pattern complexity can also introduce an increase in flow dependent variables.

The mold design for RTM is vital to successful verification of a flow model. It is necessary to have at least a basic understanding of how the flow front will progress through the mold cavity before the mold is cut. Also, it is important to take into consideration the injection and cure conditions and how they impact or may be impacted by the design of the mold.

In most cases the progression of the flow front through a flat plate mold can easily be assumed by examining the injection port and vent sites and taking into consideration the directionality of the fiber preform. A center gate option will allow the resin to infiltrate the mold in the center of the cavity and advance in a radially outward progression of the flow front. An end injection port will fill similarly with a semi-radial progression, due to left-right symmetry of the center gate option described above. By modifying the simple end injection port to include a runner along the length of the mold on the injection end, and assuming no race tracking along the preform/mold edges, a quasi-linear progression of the flow front through the mold can be achieved. Lastly, if the runner described above is extended about the perimeter of the mold cavity with a center vent, the resulting flow is opposite to that of center injection and the flow front progresses radially inward.

In the present study, several types of flow progression were studied. To provide maximum flexibility to the capabilities of the mold, injection ports were machined for end gate and center gate injection. Vent location with respect to the injection site influences the shape of the advancing flow front as well as governs the quality of fill of the cavity. The mold for the present study was designed with nine possible vent locations. One in each corner (4), one equi-spaced between each corner (4), and one in the center of the mold. Plugs which sit flush with the surface of the mold allowed selection of any combination of vents desired. An inexpensive, disposable ball valve was connected to each vent port to allow opening and closure of the port as desired during injection. A disposable valve was used due to its being infiltrated with resin during injection. Similarly, the injection port was closed with a ball valve and cooled with dry ice immediately following injection. The dry ice and distance from

the mold allowed the injection valve to be easily disassembled for cleaning. A disposable valve at the injection port was inappropriate due to high pressure.

Instrumentation of the mold was necessary for the collection of data used to track the progression of the flow front, monitor pressure distribution, and record temperature profiles. The mold was designed to allow the introduction of thermocouples into the mold cavity and a thermocouple permanently mounted to monitor the mold surface temperature. Placement of the thermocouples was planned to be determined on a run-to-run basis, so the option of permanent mounting within the cavity was dismissed. Thirteen grooves were milled into the top of the picture frame with dimensions slightly larger than the thermocouple wire. These grooves, perpendicular to the cavity wall, allowed the thermocouple cable to pass into the mold cavity from the exterior, directly under the o-ring used to seal the mold. In order to provide seal integrity, all grooves, whether occupied by a thermocouple cable or not, are filled with RTV silicone prior to closing the mold for injection.

The thermocouple layout should be designed by considering the intended flow progression. For center injection, the thermocouples should be placed in a V-shape, extending outward from the resin inlet. Laying the thermocouples linearly along the flow direction can determine the extent of the exotherm and rate of reaction of the progressing flow front in an end injection configuration. Placement of thermocouples at various points throughout the thickness of the panel can provide information on dissipation of the exotherm in the z-direction. Also, placing thermocouples in the mold corners and the anticipated last point to fill can also give valuable exotherm information. It is expected that the resin at the last point to fill will display a higher temperature than at the injection port due to a longer residence time in the mold and more advanced reaction. This temperature measurement can be compared to the original resin inlet temperature by placing a thermocouple at the mold inlet or, depending on the length of the transfer line, at the injector mix head.

In this study, the position of the thermocouples was generally decided before the experiment was run. It was essential to place the thermocouple such that they would not move during injection. This was accomplished by raising one roving from the woven preform and locking the thermocouple under it. Each of the thermocouple cables was positioned in a mold thermocouple port filling one of the 13 grooves machined on the surface of the picture frame. After the curing step, these thermocouple wires were cut as close to the laminate as possible to release the composite panel. It was, therefore, necessary to start each new experiment with newly welded thermocouples. This could be done economically if the initial wire leads were sufficiently long to allow trimming of a few inches for each experiment.

Seven of the eight thermocouples used in the experimentation were used to measure temperature in the composite during fill and cure. These were 0.076 mm (0.003 inch) thick type-J thermocouples (Omega Engineering, TT-J-36 SLE). This thickness was selected because it is thin enough not to interfere with the flow pattern yet could be positioned anywhere on the preform without much difficulty in terms of handling and breakage. All of these thermocouples were ungrounded and required a special configuration on the terminal panels of the data acquisition hardware. The eighth thermocouple, also type-J, was used to monitor the bottom mold surface temperature. This thermocouple was shielded. The thermocouples were selected based on the response time of these sensors being faster than the sampling rate, and their sensitivity being greater than that of the data acquisition system. Since graphite fibers are conductive, the standard approach would be to configure the terminal board for grounded thermocouples or to use specially ordered, grounded thermocouples. However, when resin is injected it encapsulates the thermocouples and prevents them from contacting the fibers, changing the grounded thermocouples to ungrounded. Therefore, the terminal panels had to be reconfigured for sometimes grounded and sometimes ungrounded use.

Injection via constant flow rate can generate high pressures within the mold cavity. For accurate flow progression, safety, and dimensional stability of the cavity the mold must be securely clamped. A hydraulic press provides easy control and reliable clamping force as the mold can be secured to the platens and raised and lowered safely. A distinguishing feature of the present study over most previously reported work was the reliance on data acquisition by sensors as opposed to visual observations through a transparent mold. A 150-ton Wabash press was used to clamp the mold. It was necessary to include a spacer plate between the mold and the platens to allow access to the vent and injection ports on the top and bottom of the mold. This plate was machined from aluminum and contained various cut-out portions for the ports while still providing sufficient transfer of the clamping force to the mold.

The Wabash press includes electrically heated platens which, initially, were to be used to control the mold temperature. Due to the various cut-out sections of the spacer plate, efficient heating of the mold through conduction was not possible. The cut-out portions allowed significant convective cooling resulting in non-uniform temperatures across the mold surface. For this reason, electrical heating of the mold was supplemented by hot oil lines machined into both the top and bottom halves of the tool.

The mold was designed and fabricated from high carbon tool steel with an inside cavity measuring 33 cm x 45.7 cm. These dimensions were chosen anticipating poor quality edges for the manufactured panel. These edge effects can be attributed to washing of the fibers during injection, fiber misalignment leading to resin rich or resin poor areas, and

damaged fibers from the preform construction. By trimming the poor quality edges from the cured panel, a panel of approximately 30.5 cm x 40.6 cm could be obtained. The thickness of the mold cavity could be chosen as either 2.8 or 5.6 mm by selecting the appropriate picture frame corresponding to preforms containing approximately 50% fiber volume fraction.

The selection of pressure transducers for the mold cavity requires some information *a priori*. With most pressure transducers, the accuracy of the pressure measurement is within the sensor specification only in the upper 80% of its range. Within the first 20% of the sensor range, the measurement is accurate only to ± 15%. If injection is to occur under constant pressure, the transducers should be purchased such that the highest injection pressure is near the upper limit of the pressure transducer. This provides system versatility of injection pressures while remaining within the upper 80% of the transducer range. Similarly, pressure transducers used with constant injection rate should be sized for the highest expected pressure within the range of experimental flow rates. Experience gained over the course of the experiments with constant flow rate indicated that *a priori* knowledge of the maximum pressure in the mold is difficult since pressure is the most sensitive variable in the RTM process. In two separate runs with fiber preforms prepared identically pressure could vary by as much as 3-fold. Ideally, the pressure transducers could be changed over the course of the experimentation so as to match the upper limits of the transducers to the highest expected pressure at any given flow rate. As was the case with the thermocouples, the pressure transducers response time and signal must be congruent with the capabilities of the data acquisition system.

The six pressure transducers used for monitoring pressure were placed in six pressure transducer ports along the flow direction. The remaining three unused ports were plugged. For end or perimeter injection, the transducers are equi-spaced along the center line running the length of the mold cavity. This was sufficient to measure either linear flow progression or to compare symmetry of radially inward (from perimeter injection) flow progression. For center injection it may be necessary to measure resin pressure off of the x- or y-axes. Therefore, while three transducers remain along the centerline the other three transducers are placed along the diagonal between the center gate and a corner. This V-shape configuration allows determination of the flow front location taking into account the directionality of the preform. The pressure transducers used in this study (Dynisco, Sharon, MA, Model PT435A-5C) were mounted flush to the surface of the mold cavity and have a pressure range of 0 to 3.45 MPa gauge (500 psig). These transducers were connected to an external signal conditioning/readout instrument with a six-wire shielded cable assembly. The transducers were zeroed and calibrated after the preform was placed in the mold, the mold closed, and heated to the injection temperature. Calibrating at this point eliminated

thermal effects and compression of the preform on the transducer surface, and enabled recording of only hydrostatic pressure.

In most cases, a vacuum is applied to the mold to lower the internal gas pressure and assist in proper wet out of the fiber preform. Most pressure transducers do not report accurate measurements in the presence of a vacuum. This fact must be taken into account when analyzing the data. Data below 0 Pa should not be interpreted as real, but can be used to determine the elapsed time from injection initiation to the flow front reaching the transducer.

Some considerations for the selection of the data acquisition hardware and software should include: sufficient I/O ports for the number of measurement devices used in the study, sampling and accuracy rate matched to the measurement devices, synchronization of injection and data collection events, and desirability of control capability. The acquisition system must be able to address the conductive, non-conductive fiber differences for the grounding, or not grounding, of thermocouples. Lastly, the ease of post collection data analysis (i.e., format, compatibility with post processor or spreadsheet, etc.) should be strongly considered.

Analog Connection WorkBench from Strawberry Tree was used for both fill and cure data acquisition during the present study. It displays and logs data on a Macintosh® computer unattended when the engineering units and the input ranges are specified.

The interface card used was a 16 channel, 16-bit card (ACM2-16-16) allowing 16 digital or analog I/O's. One counter/timer is available on each card for counting pulses or events, precision timing, or pulse output. The first 8 analog channels were used for temperature measurements, the eighth one measuring the temperature of the bottom mold surface. Six of the remaining analog channels were used to display and log pressure data during fill. One of the digital channels was used to synchronize the start of data logging with resin injection. When the injection head is open the signal from this channel is 1 and 0 when it is closed. Data logging could be turned on manually from the software menu but would not start until this signal from the injection head is 1, i.e., injection head opens.

Injection of the resin into the mold can be sourced from either a constant pressure system or a constant flow rate system. Each system has inherent good and bad attributes. Constant pressure is generally a cheaper, less complex system mainly requiring a pot which can be pressurized, a resin transfer tube, and related mixers, heaters, and control equipment. The resin and hardener are usually premixed before loading into the pot, leading to the possibility of the resin advancing during injection and temperature and viscosity being inconsistent throughout the supply pot. Also, a back pressure is applied to the pot via compressed gas. At high pressures the injection gas may be dissolved into the resin leading to a

poor quality part. Constant flow rate equipment utilizes mechanical pumps or hydraulic systems to cycle the resin and catalyst to the injection head where impingement mixing joins components immediately before injection into the mold. Sufficient back pressure on the components is necessary to allow adequate impingement mixing and, if a hydraulic system is used, the cylinder size should be sufficient to fill the mold in one stroke. If multiple strokes are necessary, the second stroke is injected into a partially saturated, partially dry preform which must be accounted for in the flow code. Regardless of injector type, the resin system must be degassed before injection.

Many resin systems have a two component system where the proper mix ratios are not one-to-one (i.e., four-to-one, etc.). For this reason, certain considerations are necessary before using a constant flow rate injector. Minor variations in the resin to catalyst ratio will affect the final part quality by changing not only the resin viscosity but also the time to gel and the degree of cure. Flow meters up-stream from the mix head can give accurate control of the final mixture ratio. Also, the meter controlling the smaller volume component (usually the catalyst) should have sufficient accuracy to remove uncertainty from the mixture ratio, especially at slow injection rates.

Either injection condition, constant pressure or constant flow rate, has inherent safety concerns. Constant flow rate may raise a safety issue due to its capability of generating high pressures throughout the system, including transfer tubing and at mold seal locations. For this reason, proper pressure relief devices (i.e., frangibles, valves, automatic shut down, etc.) should be engineered into the system. The constant pressure systems have a bulk of catalyzed resin residing in the supply pot which can result in a runaway reaction if conditions are not carefully monitored. Also, many hardeners used today are corrosive and highly toxic demanding proper handling and cleaning procedures. Installation and use of proper safety equipment is situational, but paramount to successful research and experimentation.

For the present study, injection was via an impingement head mixing machine (Admiral Equipment Co., Akron, OH) which is capable of injecting a liquid with a melting temperature of up to 150°C. The apparatus, specifically designed for this study, includes a hydraulic system used to pressurize and circulate the resident liquids (i.e., resin or catalyst) within the system. Initial preparation for injection included charging the machine with resin in the "A" side and catalyst in the "B" side, adjusting the system motion controls to the desired flow rate and mixing ratios, adjusting the system heating controls to the desired temperature set points, and degassing the resin components with an applied vacuum. Agitation of the components was accomplished using air driven mixers suspended in the material holding tanks on either side of the machine.

After the machine and resin components reached the set point temperature, vacuum was removed from the system and replaced by a nitrogen blanket. This served to slow any reaction with oxygen the components may have been susceptible to and significantly reduce the possibility of forcing gas back into the degassed components.

The components originally resided in the material holding pots during heat-up and degassing. Upon reaching the set point temperature, the machine was set to continually recirculate the components through the system to maintain a thermal steady state. This was accomplished through a computer controlled series of solenoids and pistons. During both recirculation and injection, the first solenoid was activated to allow material to be drawn into the piston cylinder from the material holding pot. The first solenoid was then closed and the second opened. Actuation of the piston forced the material in the cylinder to flow through the system and into the impingement head. In the impingement head, the liquid streams were forced through an orifice to increase the liquid velocity and induce sufficient mixing of the components. During injection, the two streams from the individual components were allowed to mix at this point and flow into the mold. If recirculation was desired, the individual streams would not mix, but rather be redirected into their corresponding systems and the material would drain back into the material holding pots.

During the recirculation period prior to injection, it was required to adjust the orifice openings in the impingement head to create a back pressure in the system which would induce proper mixing of the resin components during injection. The machine controls maintained this set point and would disallow injection of the resin into the mold if this minimum pressure was not maintained.

Using a reactive resin system differs from an idealized fluid in terms of the amount of *a priori* information necessary for modeling. System characteristics such as viscosity, pot life, injection temperature, and degree of exotherm are needed for evaluation of the resin as a candidate for a given structure. The heat of reaction will affect the process by limiting the maximum part thickness since charring can deteriorate the final part quality. The quality of the part is very important since most advanced composite applications are performance driven. Modeling the flow is also dependent on the reaction kinetics of the resin, a parameter which cannot be modeled with an idealized fluid. Resin choice is also driven by the physical set-up of the injection apparatus. The mixture ratios and injection temperature of the resin must be within the equipment capability, and cleaning solvent availability and situational compatibility must be considered.

The resin and catalyst systems used in the present study are TACTIX® 123 resin (The Dow Chemical Company) and Millamine 5260 (Diaminocy-

clohexane from Milliken Chemical) and E905L, a two part system (BP Chemical, Hitco Division) designed for RTM. The properties of these resin systems are shown in Table 1. TACTIX® 123 is a high purity bisphenol A epoxy resin. This two part system is specifically developed for the RTM process to give exceptionally low color and low viscosity. Pot life is suitable for many small RTM parts and mechanical properties exceed MIL-R-9300B requirements. TACTIX® 123 and Millamine 5260 are generally formulated to 17 phr to yield the optimum T_g (152°C by DSC). E905L, being a 100 phr system, allowed experimentation with injection rates lower than those for TACTIX® 123.

The issues involving selection and characterization of the preform are of the greatest importance. The two sources found to cause the greatest inconsistencies in the data are race tracking and permeability measurement, both of which are preform dependent. Race tracking occurs in the filling stage when the resin finds a path of resistance lower than the bulk resistance offered by the preform. This path generally is found between the edge of the preform and the mold cavity wall, but can also be a channel within the preform caused by a misaligned roving or an inconsistency in stacking and nesting of the fabric layers. Also, large RTM structures can have internal fabric edges where race tracking could occur. Permeability measurement techniques are still in the development stages to the extent that a general trend is evident and comparisons can be made between "tight" preforms and "loose" preforms (i.e., woven vs. non-woven, open vs. closed weave), but accuracy and precision of measurement is not yet attainable.

Fabric style and type is not inherent to model verification. Woven or non-woven preforms can be used as long as the fiber can be accurately characterized. If a woven fabric is chosen, the weave should be of consistent quality to maintain the permeability of the fabric and, ultimately, the preform. Consideration should be given as to whether the measurement instruments can be configured for use with conductive fibers.

The fiber preform used consisted of Celion G105 (G30-500) carbon fabric in an 8-harness satin weave interspersed with Kevlar® (DuPont) tracers for alignment. The fabric is available in 106.7 cm wide rolls with an areal weight of 375 g/m^2 and is characterized in Table 2. Seven layers were cut to size using a manual paper cutter and stacked in the 0° direction inside the mold. The paper cutter (Ideal Paper Cutter, model 4700A, Michael Business Machines, SC), with a vertical acting blade and a dial scale was designed to cut 47.6 cm wide and 7.9 cm thick paper with little effort. Cuts with this paper cutter were clean and precise causing little damage to the preform edge. Once the preform was stacked in its final orientation, holes were punched in the fiber corresponding to the mold vent locations. Failure to include the holes in the fiber results in z-

TACTIX® 123 is the trademark of The Dow Chemical Company
Millamine 5260 is the Trademark of The Milliken Chemical Company

direction flow at the vents causing excessive pressure spikes. The holes were filled with brass wire mesh to keep the preform from moving during injection. The runners on the preform edge were also filled with brass wire mesh prior to closing the mold.

In the present study, with injection at one end attempting a quasi-linear flow front progression, race tracking was a random, uncontrollable problem. Small misalignment of the fabric layers, rovings coming loose along the trimmed edges, gaps between the preform and the mold walls that are very difficult to control, and preform layer nesting all contributed to the race tracking. Since all these varied in a random fashion from run to run, reproducible pressure distributions were a rarity and those with similarities could not be considered representative with any certainty. The injection condition was changed to eliminate the possibility of race tracking by changing the flow from one-dimensional (quasi-linear flow front progression) to two-dimensional (perimeter injection, center vent). The injected resin first filled the transfer line and a runner about the perimeter of the preform and then started impregnating the preform from the outer edge in a radially decreasing direction. As a result of this change in the flow pattern, the preform size was reduced from 34.9 x 43.2 cm to 30.5 x 43.2 cm to allow room for the runner.

As described above, after the resin has fully saturated the preform, it must converge upon itself below the vent and also change from x-y flow to z-direction flow to exit the mold cavity. Resistance to flow can be lowered at this point by locally removing the preform with a punched hole. The size of the hole at the vent port is important as this determines the magnitude of the pressure drop during the converging flow. This pressure drop can be calculated using the relation:

$$\Delta P = \frac{\mu Q \ln \frac{r_o}{r_i}}{2\pi H k} \qquad (1)$$

where r_o and r_i are the outside and the inside radii of the flow front, H is the cavity gap height, Q is the flow rate, μ is the viscosity, and k is the permeability. In a two-dimensional flow pattern one needs to know three permeabilities, k_{xx}, k_{yy} and k_{xy}, instead of a single permeability, k_{xx}, for one-dimensional flow.

Regardless of the injection conditions, the injection procedure was common for all runs. The temperature settings for both the press platens and the oil heater were set to 65.6°C before the resin was injected. The mold was closed and allowed to reach the steady state as monitored by the thermocouples, at which time the pressure transducers were zeroed and calibrated. The injector was then connected to the mold via a quick connect coupling. The already degassed resin and catalyst were allowed to reach their steady state injection temperature of 65.6°C. The amount of resin necessary to fill the transfer tubes and the perimeter runner was calculated and dispensed with a brief injection period preceding the first

stroke into the fiber preform. This ensured that during injection the resin was used to infiltrate the preform, not fill the runners.

Before the first stroke was started and after the transfer tubes and perimeter runners were filled, the fill data acquisition program was activated from the Macintosh computer.

Each stroke of the injection was timed so that the amount of resin injected and time to see the first drop of resin venting could be verified with that of the computer. This could also be used to determine if there was race tracking or not. By simple mass balance and knowing the flow rate into the mold and the mold volume, the time to fill the cavity could be calculated. Resin appearing at the vent prior to the calculated fill time indicated some race tracking or channeling had occurred, and the mold was not properly filled.

The vent was closed after the escaping resin ran relatively bubble free and pressure distributions within the mold leveled off. The injection port was then closed. Halting the injection in this fashion kept a positive pressure inside the mold cavity for the cure cycle. The injector was disconnected from the mold and the mix head and nozzles cleaned.

In order to start the cure cycle, the temperature settings of the oil heater and press were increased to 176.7°C. Data collection during the cure cycle was activated from the computer. The laminate was removed from the mold when the cure was completed and allowed to cool to room temperature.

RESULTS AND DISCUSSION

The results presented are representative of 31 separate experimental trials. These trials were split between (1) end injection with a width-wise runner for quasi-linear flow progression and (2) end injection with a perimeter runner for concentric, radially inward flow progression. In most cases the resin and mold temperatures were allowed to reach a steady state before an isothermal injection at a temperature of 65.6°C. Resin temperature was monitored by thermocouples inside the mold cavity as described above for approximately half the experiments. Due to the thinness of the panels no significant exotherm was measured (Figure 1) and the use of thermocouples was discontinued.

The thermal history of the panels during the cure cycle was recorded for those injection experiments where thermocouples were present for the injection. Figure 2 gives a representative example of the data generated during a typical cure cycle. No information pertinent to verification of a flow model was gained from these data and the practice was discontinued along with injection temperature monitoring.

Isothermal injection generally assumes either a latent or slow reacting resin system which does not advance significantly during the injection of the part. Thus, simulation of injection under isothermal conditions does not include consideration of the cure kinetics of the resin. Elimination of the cure kinetics from the simulation results in a less complex, less numerically intensive model which is little more than a computational mass balance and is of limited use to the manufacturer. For this reason experimentation was done where the resin, preheated to 65.6°C, was injected into a mold preheated to the cure temperature of the resin in an attempt to generate data that can be used to model the reaction kinetics of resin systems during injection. The mold temperature was 176.7°C, the mold filled with seven layers of fabric (345 g), and the thermocouples distributed as shown in Figure 3.

The temperature profiles during fill are shown in Figure 4. The resin / hardener mixture reacted significantly faster at 176.7°C than at 65.6°C. Gelation occurred during the injection stroke thereby shutting down the injector with the mold only partially filled due to high pressures. Successive injection strokes were not possible. The thermocouples measured a substantial reaction exotherm resulting in instantaneous local temperature increases up to 30°C in the mold. In fact, thermocouple 3 registered a 30°C temperature increase within 5 seconds of resin entering the mold. The speed of the reaction also affected the pressure distribution, but this data is not reliable due to gelation of the resin. The cure temperature profiles for this run are similar to that shown in Figure 2 except that the ramp section is missing. Non-isothermal injection starts to blur the definition between RTM and reaction injection molding but, as was evidenced by the large dry sections in the cured part and incomplete resin flow during injection, forcing the kinetics to this extent is unreasonable.

In the first half of the experimentation scheme resin was end injected with a width-wise runner to propagate quasi-linear flow progression. Three vents at the opposite end of the mold were used to vent the resin out. Figure 5 shows the pressure transducer measurements recorded during an experiment in this configuration. A total of four injection periods were used. The flow rate for the first two strokes was set at 4.0 cc/sec and the last two strokes at 6 cc/sec. The preform was trimmed to 43.2 cm in length allowing space for a 1.9 cm width of brass mesh to be inserted at the vent end of the mold. The mold, resin, and catalyst were heated to a steady-state of 65.6°C prior to injection, and the 7-layer preform weighed 378 g.

Although the ΔP between the pressure transducers was constant, as it should be during the lower flow rate strokes, it was highly variable for the higher flow rate. A small ΔP between PT1 and PT2 in the second two strokes (Figure 5) constantly increased to a very large ΔP between PT5 and PT6. This was attributed to both a change in the permeability of the

preform with an increased flow rate and the effect of injecting into a saturated preform.

As discussed previously the race tracking effect between the preform edge and the mold cavity wall caused most of the end injection experiments to have a parabolic flow front instead of the intended linear progression. This effect is shown in Figure 6. Many efforts were made to eliminate race tracking from the experiments. These include: addition of RTV along the edges to seal the gaps, modifications to the mold picture frame to allow compression of the preform along the edges thus lowering the permeability, and addition of O-ring cord stock to further compress the preform at the edges. In each case, race tracking was not eliminated and was evident by the presence of resin at the vents before sufficient time had passed to fill the cavity. Further supporting the presence of race tracking was the fact that resin was first observed at the two corner vents before it could be seen at the center vent.

It was at this point in the experimentation that the injection condition was changed to include a runner about the perimeter of the preform and a vent in the center. As a result of this change in the flow pattern, the preform size has changed from 34.9 x 43.2 cm to 30.5 x 43.2 cm. In these perimeter injection experiments the flow front advances by radially decreasing ellipses. Therefore, pressure transducers 1 and 6, 2 and 5, 3 and 4 should register the same pressures and the flow front progression should be determined by these pressure transducer pairs simultaneously (i.e., the rise times for these pressure transducers should be identical). For purposes of comparison from run to run, the transducer rise time is defined by the time from injection initiation until the transducer crosses it's zero reading (recall injection is initiated with the mold under vacuum).

Figure 7 is a graph of the pressure transducer measurements for a perimeter injection at 3 cc/sec. The resin, hardener, and mold reached a steady-state of 65.6°C prior to injection, and the 7-layer fiber preform weighed 337 g. As indicated in Figure 7, the pressure transducer pairs (1 and 6, 2 and 5, etc.) measured rise times together, as expected. Also, pressure measurements for the transducer pairs were equivalent within the accuracy of the sensors and leveled off indicating the mold was filled and resin was flowing at a steady state. The perimeter injection experiments were more successful than the linear progression experiments in that the results were regularly duplicated. This can be seen from the comparison of rise times for several injection rates shown in Table 3.

This configuration eliminated the race tracking due to the edge effects, but channeling due to fabric motion and nesting and local permeability variations due to fiber wash could still be present. The radially inward flow of this configuration tended to cause constriction of the preform, thus lowering permeability due to local compression of the weave. This resulted in an increased resistance to flow and constantly increasing

mold pressures as shown in Figure 8. The type of pressure history shown was seen in several of the experimental runs. After removal of the cured panel from the mold, loose fibers could be seen in the brass mesh under the vent port, and many times wrinkles in the fiber layers were visible near the vent. The high pressures were attributed to this fabric motion and fiber wash.

CONCLUSIONS

Accurate and precise permeability measurements are the core of the issue. Under present capabilities, only trends or comparative results can be obtained. This leads to trial and error and retrial for the flow model so that simulated results can be fit to experimental data. The authors believe that, contrary to most modeling assumptions, the preform is not a rigid static structure during wet out, but rather one that can be stretched and compressed causing local variations in permeability. Current measurement techniques do not take into account any fiber or roving motion during wet-out, inconsistency in the stack nesting, minor roving misalignment during preform manufacture, or local weaving imperfections. These seemingly slight differences in local permeability, when compared to the bulk permeability, can vary the final fill pressures up to an order of magnitude.

Since permeability increases non-linearly with decreasing fiber volume fraction, a small reduction in fiber volume fraction of the composite will significantly reduce the resistance to flow. For instance, decreasing fiber volume from about 58% to 50% increases permeability by approximately an order of magnitude, greatly facilitating impregnation.

Race tracking is a real effect for the manufacturer, but cannot yet be accounted for by the flow model in a predictive fashion. The inability to accurately predict *a priori* the extent of race tracking invalidates the model to the manufacturer for use in tool design. Unfortunately, race tracking could not be predicted with current modeling techniques until layer nesting, inter-layer channeling, and wall-edge effects can be accounted for or eliminated in the preform manufacturing step.

REFERENCES:

1. C. L. Tucker, The University of Illinois, private communications.

2. L. J. Lee, The Ohio State University, private communications.

TABLE 1.
Properties of TACTIX® 123/Millamine 5260 System

Viscosity Data

Time, Minutes	VISCOSITY, Cps		
	Temperature, °C		
	38	52	66
0	175	94	33
5	176	78	44
10	191	97	98
12			164
15	213	131	389
16			537
17	224	155	758
18			1086
19			1577
20	238	193	2366
21			3623
22	255	230	5537
23			8628
24			13986
25	272	299	22921
26			39404
30	310	498	
35	363	996	
40	422	1927	
43		2981	
45	503	4076	
46		5680	
48		8060	
50	606	11452	
53		19815	
55	743	29399	
60	913		
65	1179		
70	1480		
75	1915		
80	2511		
85	3427		
90	4500		
95	6666		
100	9155		
105	12962		
110	19734		
115	28858		
120	42445		

TABLE 1. (Continued)
Properties of TACTIX® 123/Millamine 5260 System

Density	
Resin Density, g/cc	1.16
Hardener Density, g/cc	0.946
17 phr Millamine 5260+Resin Density, g/cc	1.1224

Specific Heat of TACTIX® 123/Millamine 5260 System:
C_p (J/g-°C) =1.053+5.469 X 10^{-3}T(°C)
Specific Heat of TACTIX® 123/T105 Composite:
C_p (J/g-°C) =0.7572+3.556 X 10^{-3}T(°C)

Thermal Conductivity

Material	**Temperature, °C**	**Thermal Conductivity kcal/hr.m.°C**
TACTIX® 123 MONOMER	29.6	1.481
	38.7	1.478
	47.5	1.480
	51.4	1.478
	60.2	1.469
	68.6	1.452
	77.0	1.451
TACTIX® 123/Millamine 5260 POLYMER	33.6	2.425
	42.9	2.507
	51.6	2.559
	60.1	2.649
TACTIX® 123/G105 COMPOSITE	33.7	11.481
	42.9	12.033
	51.6	12.364
	60.2	12.682

Residual Exotherm

Time at Temperature, min	37.8°C	48.9°C	65.6°C
Residual Exotherm, Joules/g			
0	454	454	454
10	435	362	
15	420	384	317
20	399	352	
30	366	332	126
60	302	225	12
90	242	160	
120	164	65	
150	161		
180	146		
210	115		

TABLE 2.
Properties of G105 Fabric

Property	
Density, g/cc	1.78
Porosity (in 110 mil mold cavity), %	48.97
Permeability, m^2	
k_{xx}† (Warp Direction)	6.78×10^{-11}
k_{xy}†	0.45×10^{-11}
k_{yy}† (Fill Direction)	5.77×10^{-11}
k_{11}††	9.03×10^{-12}
k_{22}††	5.78×10^{-12}

† Reported by The University of Illinois
†† Reported by The Ohio State University

TABLE 3.
Pressure Rise Times for Selected Runs in Seconds

Inject. Rate	PT1	PT6	PT2	PT5	PT3	PT4
3 cc/sec	24	24	45	43	52	52
	28	27	44	41	51	50
	32*,†	32*,†	49*,†	49*,†	58*,†	58*,†
3.5 cc/sec	18	18	41	42	53	54
4 cc/sec†	10	9	30	22	37	35
5 cc/sec†	15	15	25	25	31	31
	12	12	28	24	32	30

* Resin leakage during injection
† These runs not presented in the results section

FIGURE CAPTIONS:

Figure 1. Temperature distribution during fill in isothermal end gated-3-point sink linear flow. Resin was injected into a 65.6°C mold at an injection rate of 5 cc/sec.

Figure 2. A typical temperature-time plot during cure. Oscillations are due to on/off cycle of the oil heater.

Figure 3. Thermocouple layout for both linear end convergent flow patterns.

Figure 4. Temperature-time plot in a non-isothermal end gated-center vented perimeter flow. Resin was injected into a 176.7°C mold at an injection rate of 4 cc/sec.

Figure 5. Pressure-time plot of an end gated-3 point sink linear flow. Resin was injected into a 65.6°C mold at an injection rate of 4 cc/sec during the first two strokes and 6 cc/sec during the last two strokes.

Figure 6. A photograph of a short-shot showing a parabolic flow front instead of the intended linear progression indicating severe race tracking along the length of the mold between the preform edge and the mold cavity wall.

Figure 7. Pressure-time plot of an end-gated center vented perimeter flow. Resin was injected at 3 cc/sec into a 65.6°C mold.

Figure 8. Pressure-time plot showing fabric motion during fill due to increased radial velocity of the resin near the vent. Resin was injected at 3.5 cc/sec into a 65.6°C mold.

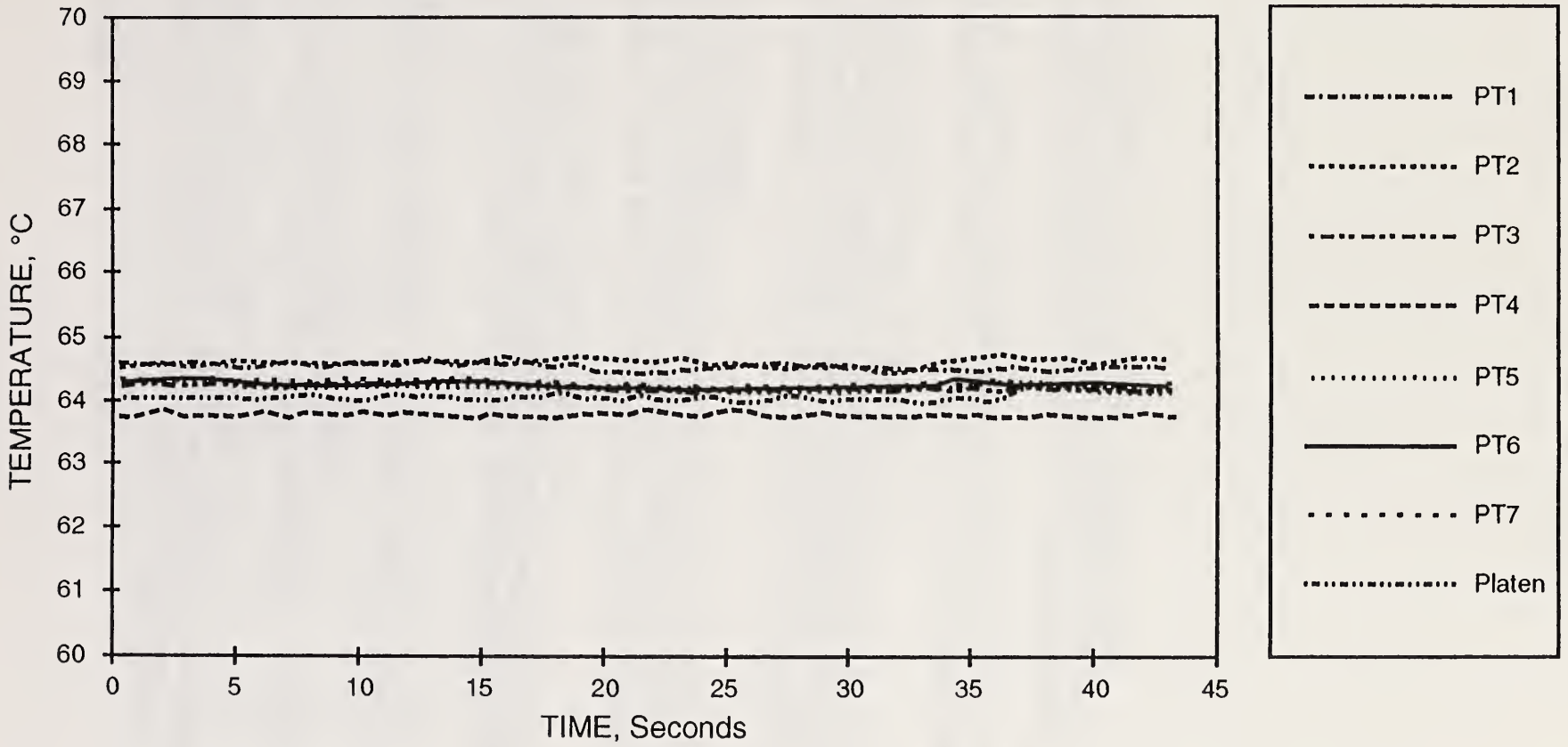
70
69
68
67
66
65
64
63
62
61
60
TEMPERATURE, °C
0
5
10
15
20
25
30
35
40
45
TIME, Seconds
PT1
PT2
PT3
PT4
PT5
PT6
PT7
Platen

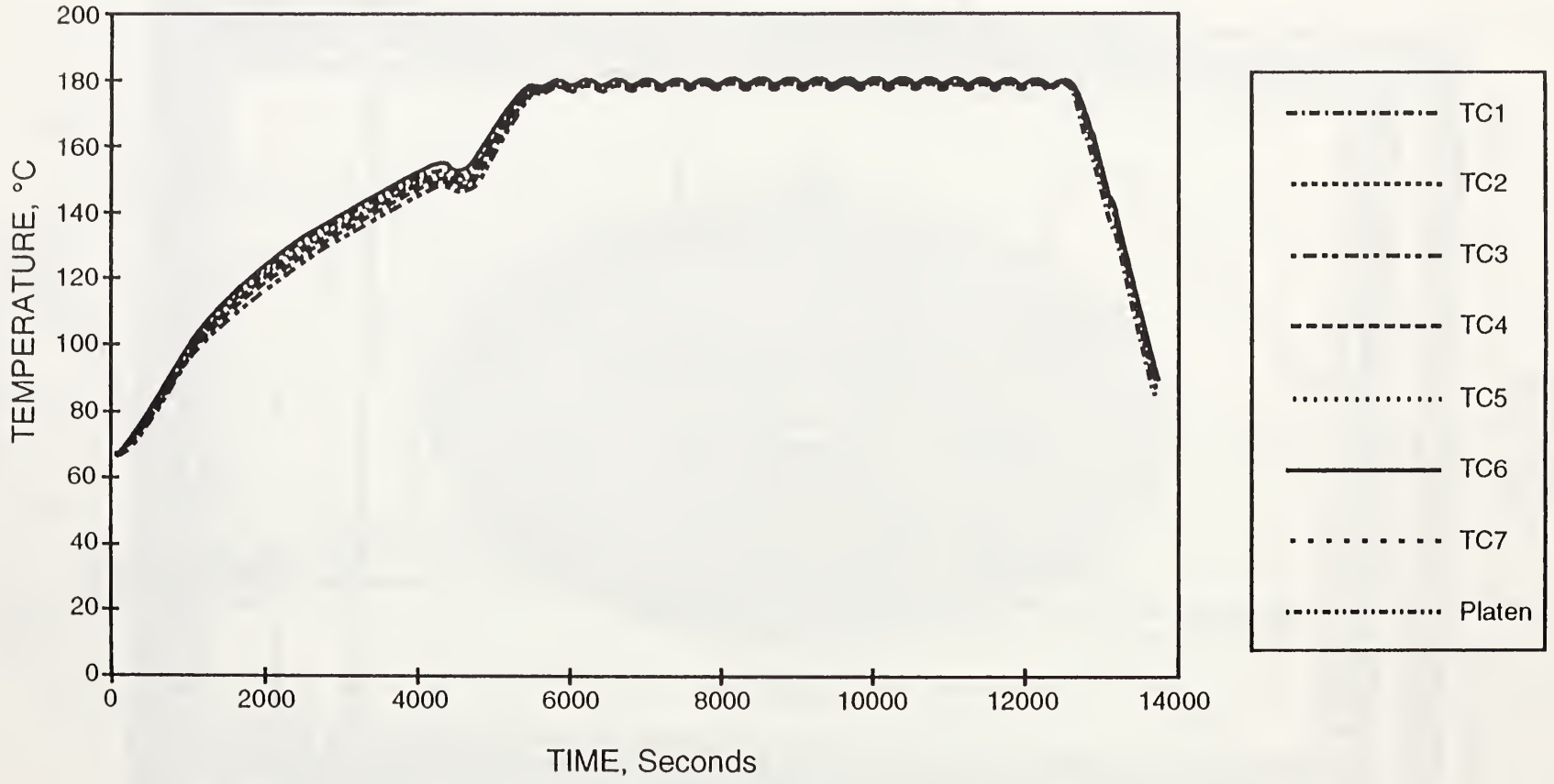
TEMPERATURE, °C
200
180
160
140
120
100
80
60
40
20
0
0
2000
4000
6000
8000
10000
12000
14000
TIME, Seconds
TC1
TC2
TC3
TC4
TC5
TC6
TC7
Platen

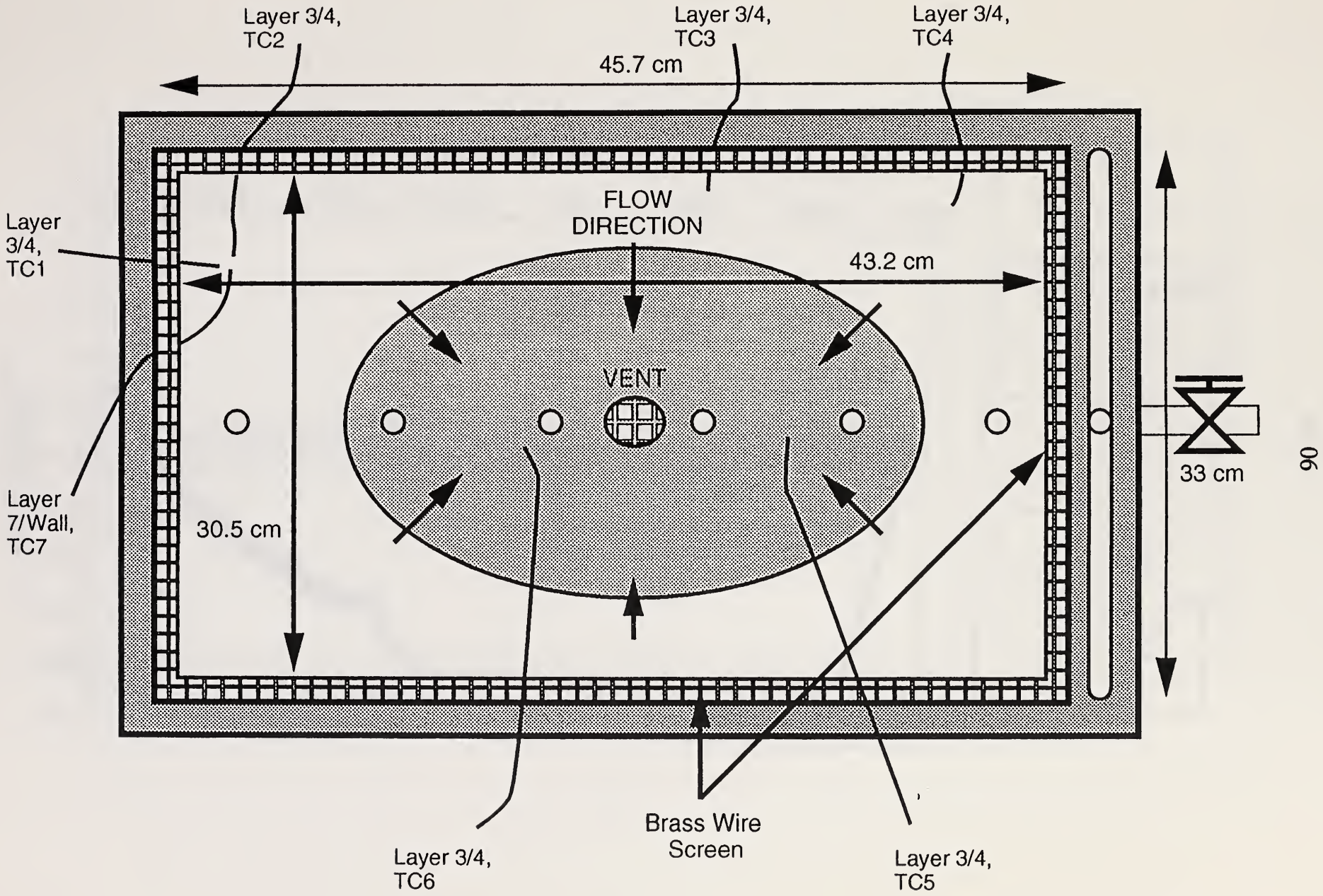
Layer 3/4, TC2
Layer 3/4, TC3
Layer 3/4, TC4
45.7 cm
FLOW DIRECTION
Layer 3/4, TC1
43.2 cm
VENT
Layer 7/Wall, TC7
30.5 cm
33 cm
Brass Wire Screen
Layer 3/4, TC6
Layer 3/4, TC5

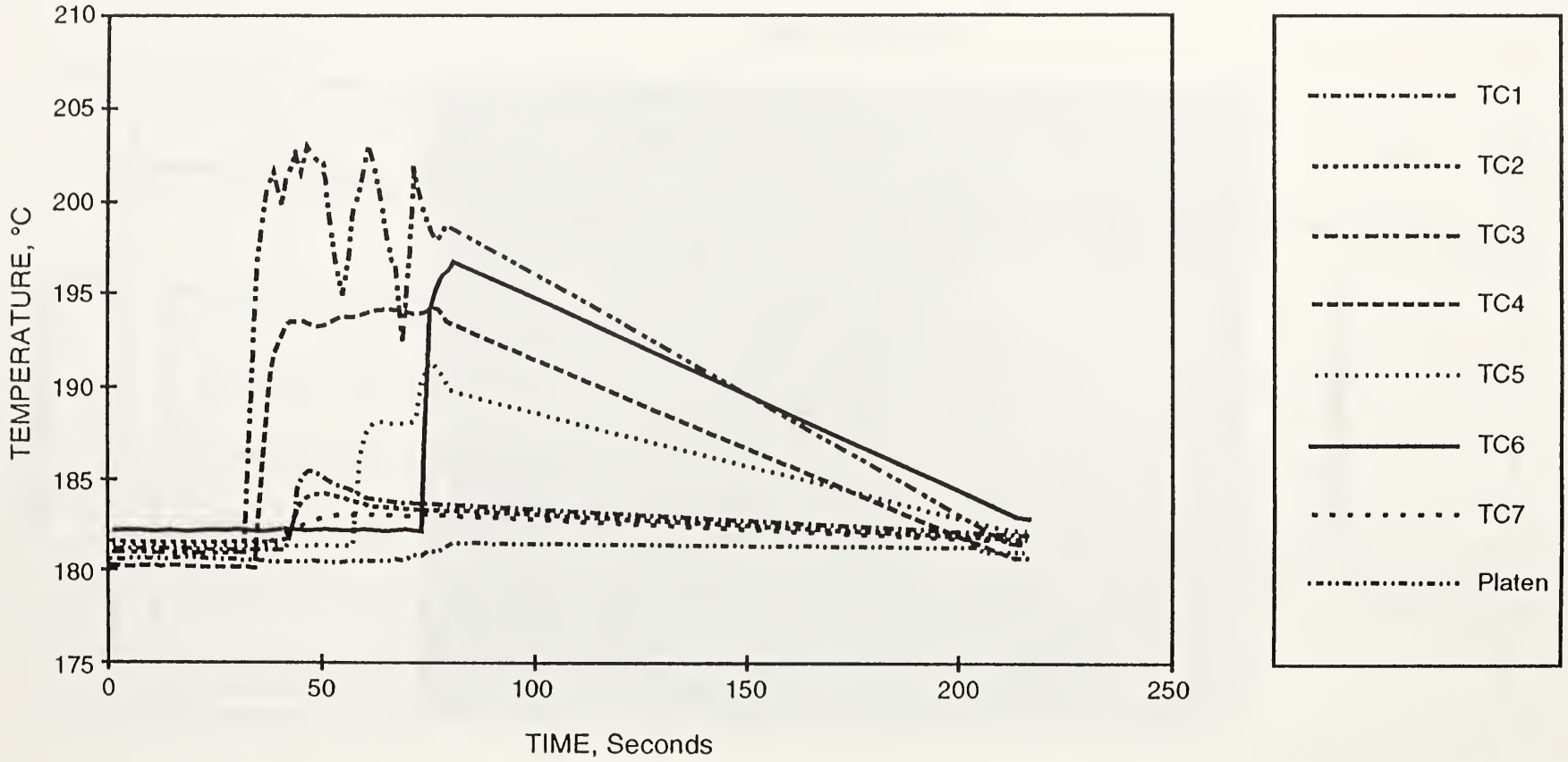
210
205
200
195
190
185
180
175
TEMPERATURE, °C
0
50
100
150
200
250
TIME, Seconds
TC1
TC2
TC3
TC4
TC5
TC6
TC7
Platen

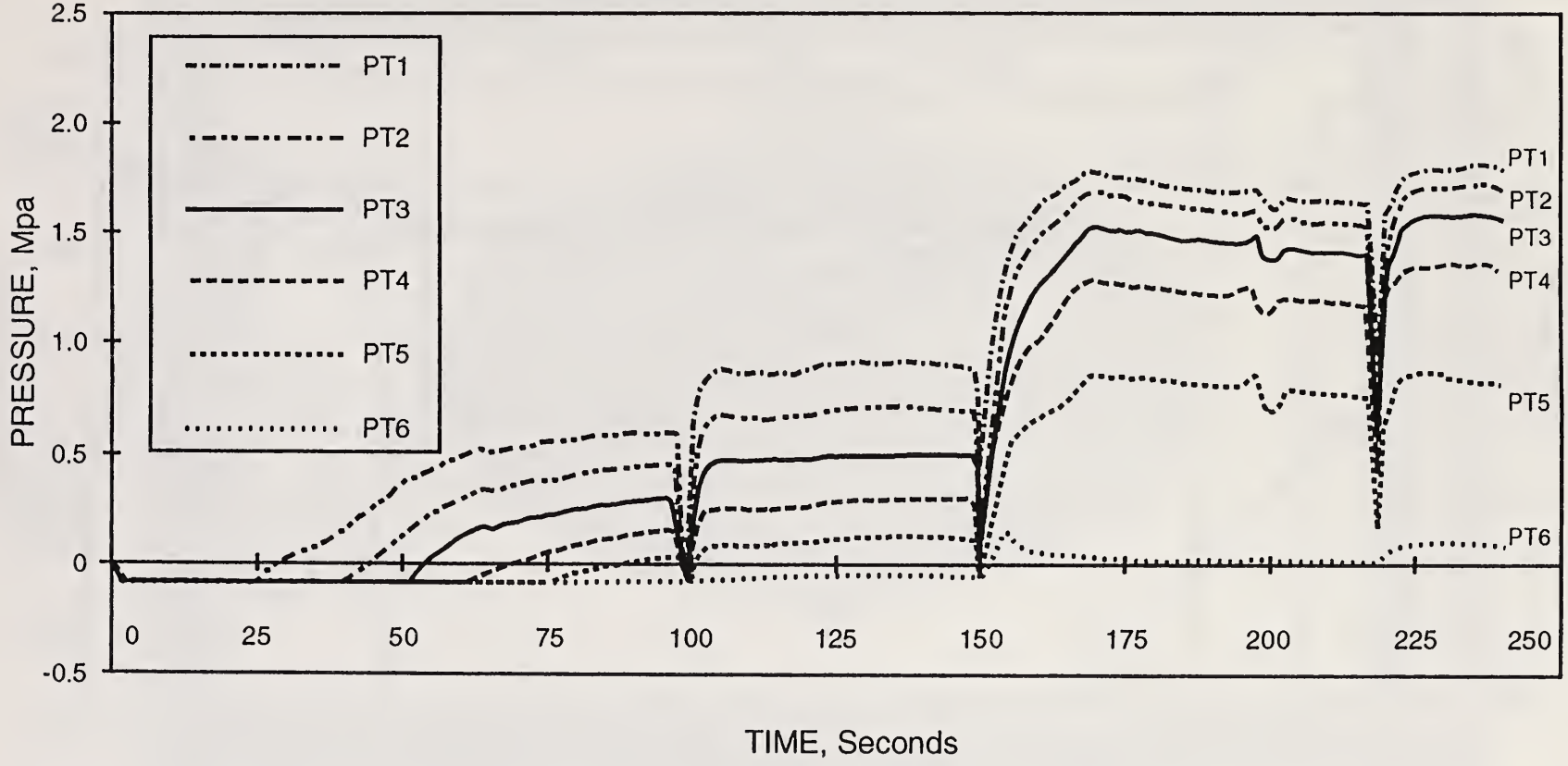
PT1
PT2
PT3
PT4
PT5
PT6
PRESSURE, Mpa
2.5
2.0
1.5
1.0
0.5
0
-0.5
0
25
50
75
100
125
150
175
200
225
250
TIME, Seconds

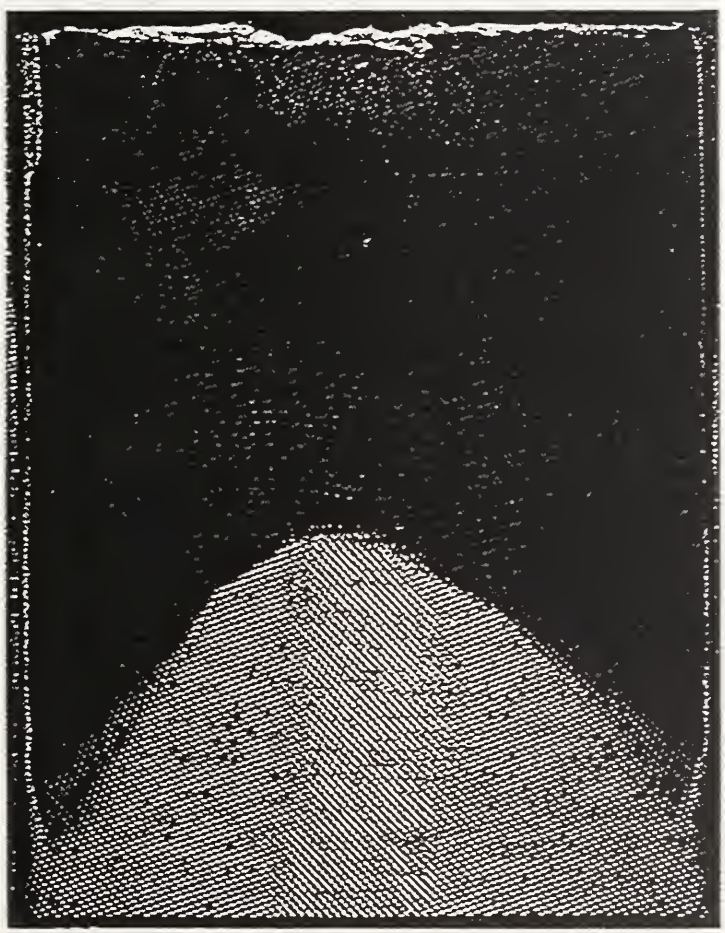

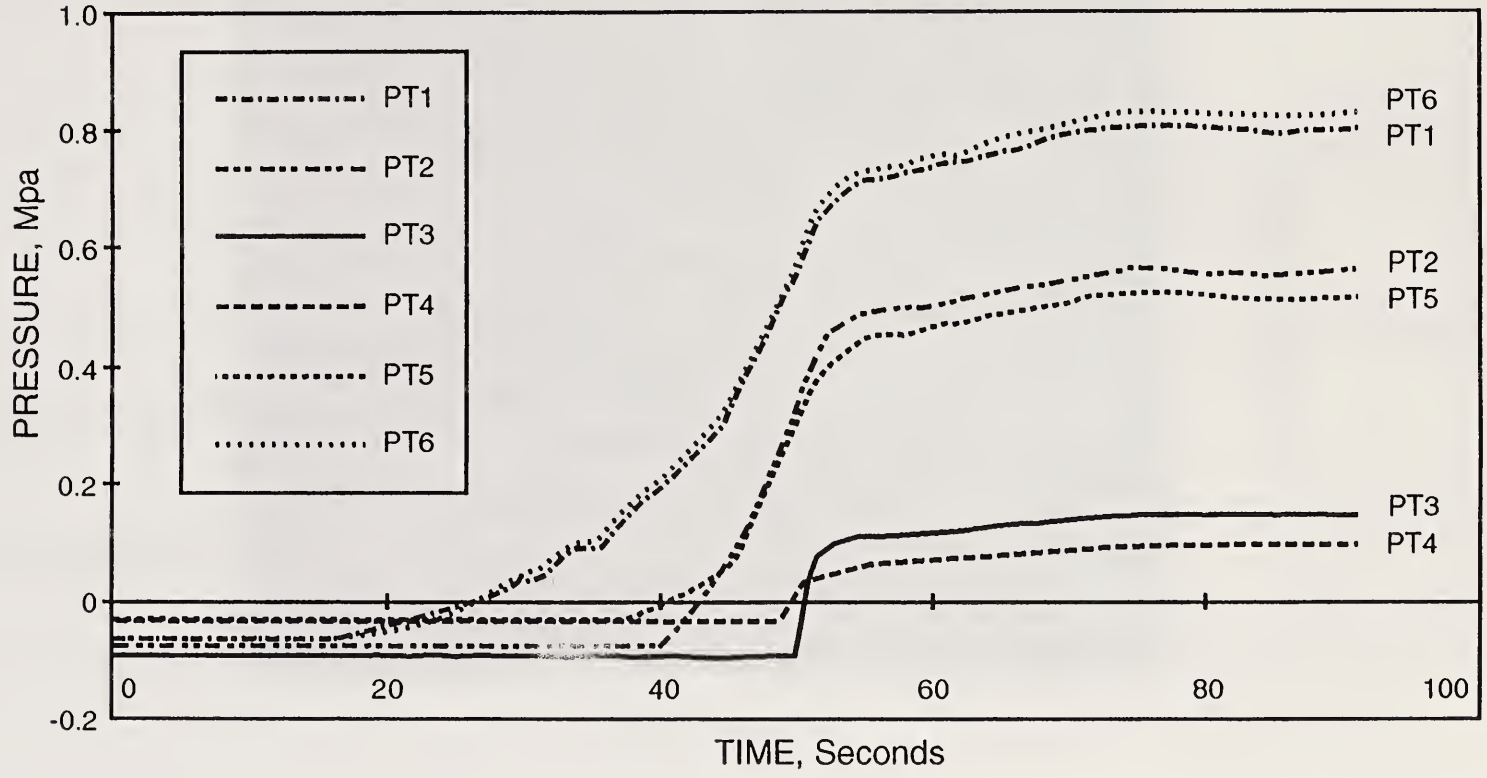
1.0
0.8
0.6
0.4
0.2
0
-0.2
PRESSURE, Mpa
PT1
PT2
PT3
PT4
PT5
PT6
PT6
PT1
PT2
PT5
PT3
PT4
0
20
40
60
80
100
TIME, Seconds

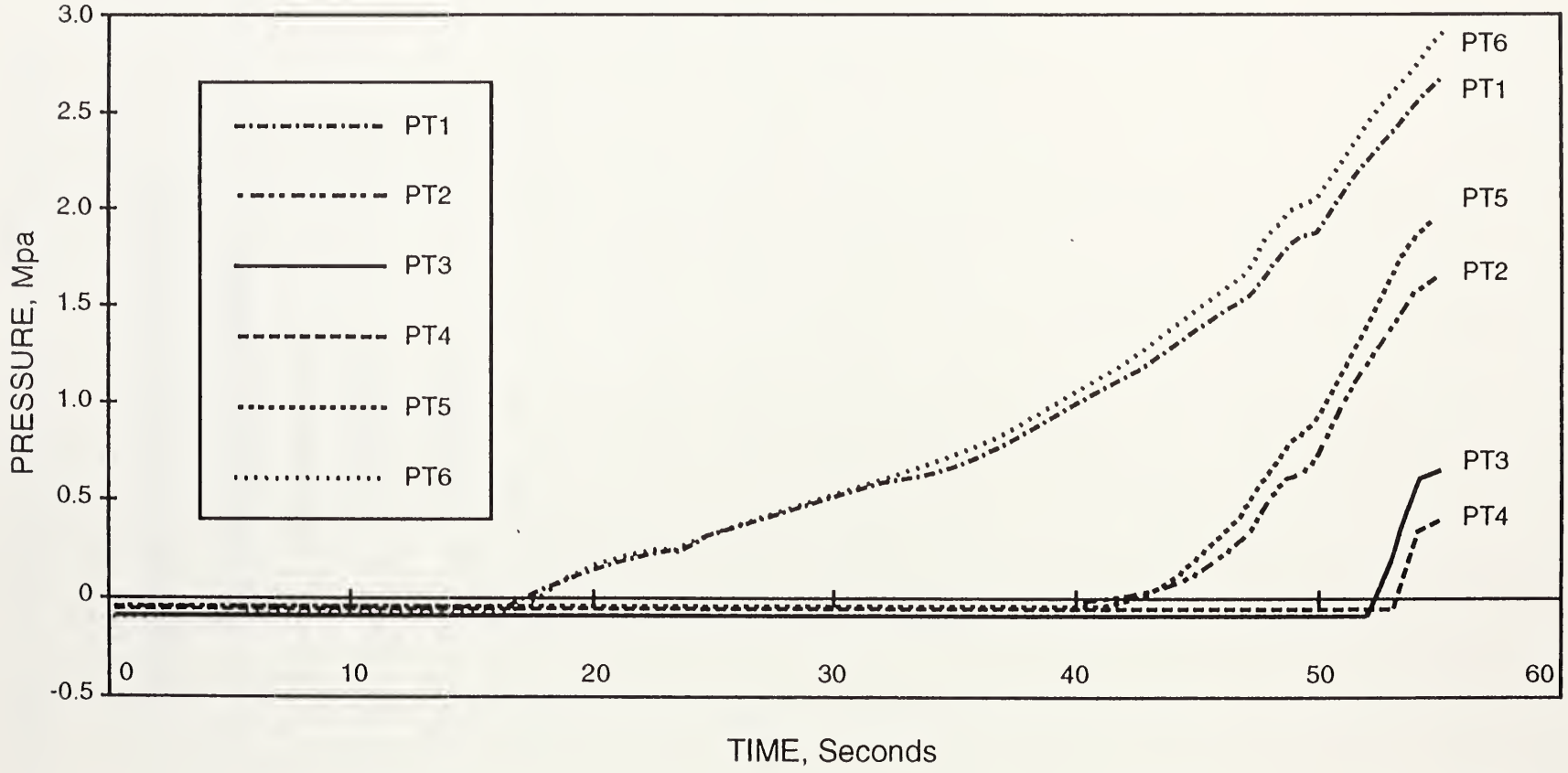
3.0
2.5
2.0
1.5
1.0
0.5
0
-0.5
PRESSURE, Mpa
0
10
20
30
40
50
60
TIME, Seconds
PT1
PT2
PT3
PT4
PT5
PT6
PT6
PT1
PT5
PT2
PT3
PT4

Liquid Composite Moulding - Design for Processing

C D Rudd, A C Long, P McGeehin, L J Bulmer, J R Lowe

Department of Mechanical Engineering

The University of Nottingham

University Park

Nottingham

NG7 2RD

Abstract

Liquid composite moulding strategies such as RTM and SRIM are becoming established for an increasing number of prototype and production parts. Coupled with this is a high level of interest in the development of mathematical models which describe different aspects of such processes. This paper reviews the stages of processing for RTM components including preform manufacture and identifies how processing science can become integrated within the overall design process. Detailed results are included for the prediction of fibre architecture in generally curved two dimensional preforms and the properties which arise from these.

Resin transfer moulding and structural reaction injection moulding are the focus of much attention at present from current and potential industrial users in addition to the academic community. Such processes provide manufacturing feasibility for a wide range of applications with obvious attraction to the transport industries. Due to the number of process variants(1) processes can be adapted for economic manufacture of both cosmetic and structural parts at low and high volumes.

RTM provides a convenient solution for applications at low to medium volumes and is particularly suited to large area components, providing significant parts integration which, when combined with the use of low investment shell moulds, offers potential for substantial reductions in tooling costs. SRIM in contrast offers reduced cycle times although generally higher pressures, with associated increases in tooling costs, restrict the process to high volumes. Hybrid processes exist involving the use of high pressure impingement mixed RTM resin systems which enable shorter impregnation and gel times than those in traditional RTM.

While the specification of composite components introduces degrees of freedom to the design process which are not generally present in metals, manufacture by LCM raises process issues which impinge upon component design as well as mould design and process control. Recent publications have addressed the impregnation phase including the effects of injection equipment(2), preform structure(3), mould wall effects(4) and injection gate geometry(5,6). Complementary studies have examined the deformation of fabrics such as those used in manufacture of fibre preforms(7). As yet there is little evidence of these techniques becoming

integrated with the component design process. It is clear that liquid moulding, like all manufacturing routes for composite materials involves a degree of interaction between the fundamental physics of the process, the performance of the composite part and the overall economics of manufacturing. At this relatively early stage of development, it is essential to gain an understanding of these interactions and their levels of significance. This involves satisfaction of the following conditions:

(a) Understanding fundamental physics

(b) Identifying processing/cost/performance relationships

(c) Development of models to describe (a) and (b)

(d) Incorporation within a design method

While activity is evident within each of the above phases, much effort is required at (a) to determine the level of processing science which is required to provide an adequate description of manufacturing processes and to identify appropriate methods and models which merit adoption on a significant scale.

The following sections consider aspects of liquid composite moulding, with special reference to RTM, which the authors have identified as having important consequences for design, performance or cost. In addition to the fundamental work which is described, where possible the route through (a)-(d) is defined for stages of liquid moulding from preform manufacture through impregnation and cure.

Mats and Fabrics

While manual assembly of reinforcements in the mould is feasible for low volume operations, preform manufacture is an essential element of most production processes. Preform design is traditionally based upon the structural requirements of the part with fibre orientation and volume fraction designed to meet specific load cases. However fabric specification including fibre orientation has major influences on processing properties including formability. Preform manufacture involves mapping a two-dimensional fabric onto a three-dimensional surface which is not generally developable, thus the transform must be accommodated by geometric changes within the fabric. Since composites rely generally upon high modulus fibres for reinforcement which can be considered as inextensible, the changes must be met by fabric shear or slip.

Characterisation of deformation mechanisms

In order to describe the deformation process, characteristic fabrics have been tested. Off-axis uniaxial tensile testing provides a useful characterisation method for flexible laminates and this has been used to study the behaviour of woven pre-pregs by Blanlot et al(8). The same technique has been used for dry, stitch bonded reinforcements to determine how reinforcement architecture modifies slip/shear characteristics. The degree of slip (departure from pure shear or "pin jointed" deformation) was estimated using:

$$S = \frac{W_{act} - W_{pin}}{W_{act}} \qquad (1)$$

The results shown in Figure 1 indicate that both 0°/90° and +/-45° fabrics exhibit significant

slip (up to 10%) while the quasi-unidirectional fabric behaves in an approximately pin-jointed fashion, demonstrating that reinforcement orientation has a major effect upon the deformation mechanism. The bi-directional reinforcements were shown to permit axial strains of up to 25% with less than 5% slip. This has important consequences for the prediction of reinforcement architecture and permits the scissor-drape approach to deformation modelling as described below.

Deformation modelling

As well as establishing feasibility for preform geometries, a modelling approach facilitates the prediction of generally curved two-dimensional preform structure. Knowledge of fibre orientations offers a route to improved structural design in addition to the processing considerations discussed later. A full description of the deformation mechanics involves consideration of large deformations and non-linear properties. A limited degree of success is possible by restricting fabric deformation to those possible by in-plane shear which involves the solution of a "scissor-draping" algorithm which is described in detail elsewhere(7). The method of solution involves calculation of the points of intersection of fibre crossover points with the draped surface. This approach enables fibre geometry to be estimated and potential problem areas such as wrinkles or high degrees of re-orientation to be designed out. An example of such a prediction is shown in Figure 2(a). This shows an area from a prototype automotive undershield. It is clear that the greatest fibre re-orientation occurs in areas of high draw and double curvature. Such an approach enables defect occurrence to be reduced as well as providing geometric information for lay-planning etc.. Local fibre orientations can also be used to estimate the variation in elastic properties over the part geometry. Currently this is done using the well known Krenchel expression(7) to

calculate reinforcement efficiency factors and thus the stiffness terms on any arbitrary axes. An example of the predicted variation in stiffness arising from fibre re-orientation is shown in Figure 2(b).

While the above approach provides a useful solution for fabric reinforcements, random materials such as continuous filament or swirl mats find many applications in LCM. Due to the structure of this class of materials, their deformation is better described by a modified plasticity, or strain hardening theory, eg:

$$\sigma = B\varepsilon^{n} \tag{2}$$

Where B is a stiffness factor and n is a strain hardening or fibre straightening index. Strains can also be used to estimate the modified reinforcement structure, the degree of anisotropy induced and thus the elastic properties of the final laminate. This has been confirmed in experiments by moulding continuous filament random mat laminates from pre-stretched reinforcements. Typical results from mechanical testing of the laminates is included in Figure 3 and a supporting analysis is presented elsewhere(7). It is clear from the results that a high degree of anisotropy ($E_x/E_y > 2.0$) can be induced in this way, with important consequences for structural performance. This demonstrates the need to take into account fibre movement during forming for both aligned and random reinforcements.

3 Reinforcement In-plane Permeability

Following the preform manufacture stage it is logical to consider the problem of impregnation. LCM operations involve the impregnation of a wide range of reinforcements

in both monolithic and multi-axial stacks. Prediction of flow within these is dependent upon reliable permeability data. The problem of permeability determination is considered at three levels (Figure 4):

1. Microscopic (single tow)
2. Unidirectional lamina
3 General laminates

Due to the heterogeneous structure of the reinforcement medium it has been established(9) that both macroscopic and microscopic flow regimes exist. Only at creeping flow rates (<0.1mm/s) has capillary flow been shown to dominate(10), the majority of LCM operations fall well outside this range. The consequence of this is a transverse impregnation mechanism within fibre bundles with the attendant problem of void formation. While void contents may be minimised by evacuating the cavity prior to impregnation by raising supply pressures, the presence of film formers, such as that shown in Figure 5(a), within fibre bundles may inhibit complete impregnation in some reinforcements, resulting in the type of void formation shown in Figure 5(b). The problem is influenced by the reinforcement structure and the effects of this have been studied in a programme of in-plane permeability testing on commercial stitch bonded fabrics. While closed-packed structures provide a reasonably homogeneous medium for fluid flow, large inter-tow spacing can promote the two-phase flow identified above. An example of this is shown in Figure 6, where preferential inter-tow flow can be seen to dominate. The effect can be seen to reverse at low pressure gradients, when capillary pressure dominates with resulting flow leaders within the fibre bundles.

Notwithstanding the voidage problems which occur at microscopic level, a high level of interest is evident in the macroscopic flow which occurs at ply and laminate level. In-plane permeabilities are generally determined using one-dimensional (radial or rectilinear) flow tests, both of which can be automated. Rectilinear flow tests require individual measurements of the principal, in-plane values and require considerable attention to the problem of preform fit. Failure to take account of this results in bypass flow. The radial flow test(11) eliminates problems such as channelling or bypass flow and enables simultaneous measurement of the in-plane principal permeabilities. A separate test is required to determine the through thickness value.

Unidirectional laminae exhibit principal axes which coincide with the 0° axes of the fabric. Although true unidirectional reinforcement is difficult to achieve using current preform technology, this can be approximated with quasi-unidirectional fabrics produced by warp knitting or stitch bonding. Typical data obtained from radial flow tests are shown for a quasi-unidirectional stitch bonded fabric in Figure 7. The material exhibits a high degree of anisotropy ($K_1/K_2 > 10$) The in-plane permeability value can be approximated by a second order tensor relationship which demonstrates reasonable agreement with the experimental results.

Multi-axial stacks

Unidirectional and monolithic preforms exhibit no through-thickness variation of in-plane permeabilities and if mould wall effects can be neglected then plug flow can be assumed. In

multi-axial preforms however, the principal axes of the plies are not coincident which complicates the derivation of in-plane values for the overall stack. Previous studies(11) have shown that complex or multi-axial stacks exhibit a marked departure from plug flow behaviour. It can be deduced that any mismatch in permeabilities between adjacent plies will result in stratified flow, giving rise to a through thickness filling mechanism in low permeability regions. While three-dimensional flow solutions are possible for the prediction of these phenomena, practical considerations dictate that the majority of design analysis will be carried out for two-dimensional (in-plane) solutions in generally curved space. Therefore it is essential to take this effect into account in the approximation of in-plane permeability.

Preform Permeability

While the above discussion has focused on in-plane permeability effects in laminate stacks, permeability testing is generally confined to two dimensional structures. As pointed out in Section 2, some displacement from the original fabric specification is usually necessary in order to create the generally curved two-dimensional structure. Stretch forming of random reinforcements involves fibre straightening and has been shown to impart a degree of anisotropy to the preform. This can be approximated by Figure 8. The effect on in-plane permeability can be estimated by applying expressions for the longitudinal and transverse permeabilities of the fibre bundle, such as those proposed by Gebart(12). These are based upon the architecture of the tow and enable the preform permeabilities to be estimated by integrating along the flow path. The permeabilities of a stretched, initially random, reinforcement can thus be estimated by integrating along the axes of a fibre ellipse, giving

the following(7):

$$\frac{l}{K_{avg}} = \int_0^{\pi} \frac{d \sin(\psi)}{\sin(\beta+\psi)\,[K_1 \cos^2(\psi) + K_2 \sin^2(\psi)]}\,\delta\beta \qquad (3)$$

Initial predictions are given in Figure 9 and compared with test plaque data over the practical range of deformation values. The results show close agreement with the model and demonstrate the departures from test plaque data which are likely to be encountered in practical moulding situations.

A parallel situation occurs in the processing of aligned fibre preforms. In this case, given the type of prediction described in Section 2 for fibre distribution, a useful estimate of in-plane permeabilities can be made based upon plug flow considerations which can be used with confidence for low ply group thicknesses. Correlations such as that shown in Figure 7 can be combined with the prediction of fibre orientation to yield the distribution of permeabilities over the area of the part. The fibre orientations are examined in each bi-linear patch and ply permeabilities are estimated using the second order tensor relationship described earlier. This is combined with the addition rule to give the following expression for a multi-axial stack of similar reinforcements:

$$K_{avg} = \frac{1}{h} \sum_{i=1}^{i=n} (K_1 \cos^2\theta_i + K_2 \sin^2\theta_i)\, t_i \qquad (4)$$

An example of this technique is shown in Figure 10. The output from such a model can be used as input data for flow predictions such as those described below.

4 Impregnation

Finite element/control volume based solutions to Darcy's law provide useful tools for prediction of pressure distribution and flow front advancement for impregnation during LCM(eg 14,15). Solutions can be formulated for constant flow rate, constant pressure pre-programmed supply conditions. In practical mould design situations, study of flow front advancement permits optimal siting of injection and vent ports, taking into account potential air entrapment and reduction of impregnation times. The same methods permit parametric studies which enable sensitivity analyses to be carried out, examining for example the effect of process variables such as fibre volume fraction, reinforcement type, preform fit etc. on flow characteristics. Given falling hardware costs and increasingly sophisticated flow models, the largest problem facing designers remains access to reliable characterisation data for the materials under consideration.

Mould design in a CAE environment is especially useful for low stiffness tooling systems based upon nickel electroform shell moulds. Pressure loading arising from the flow analysis can be transferred to structural models in order to predict deflections, thus aiding sizing calculations. This also enables the use of both transient pressure loadings and hydrostatic cases to be applied. An example of such predictions, taken from earlier work(14), is included in Figure 11, showing front positions (isochrones) arising from a single point injection gate up to the point of mould fill.

5 Cure

While the reduction of impregnation times via careful mould design is a useful feature of high

speed processing the major limitation on processing speed remains lengthy heating and curing times which characterise RTM operations. This is demonstrated in Figure 12 for a plaque moulding and the same effects are evident for all such processes based upon the injection of relatively cold, hot setting resins into a hot mould. Although the problem can be eliminated under some circumstances by reactive processing, a class of RTM applications has emerged, generally based upon polyester resins, where RTM cycle time reduction remains a key issue. The problem can be addressed by a combination of strategies among which mould thermal design is of great importance.

The interaction of mould thermal design with flow considerations further highlights the need for an integrated approach in design for RTM. Prediction of heating and curing times cannot be performed in isolation but requires a knowledge of the thermal history of the resin, reinforcement and mould walls. Under normal circumstances, mould quench is highly significant during impregnation. This can be predicted by coupled flow and heat transfer solutions(5). While non-isothermal flow modelling provides an important link to the cure cycle, the extent of this effect can be estimated by subjecting a though thickness heat transfer model of the mould wall to a boundary condition approximating the passage of resin at ambient temperature for the estimated duration of the impregnation phase. The effect of this on gate heating time is shown in Figure 13 which also demonstrates the benefit of incorporating local heating adjacent to the gate. A through-thickness heat conduction model using a finite difference solution was used to compare the heat-up rates within the injection gallery for a conventional mould wall, the same mould wall with an embedded resistance heating element for the 'heater on' and 'heater off' cases. The results suggest that local heating can be used to bring about significant reductions in gate reheat and thereby overall

cycle times.

While consideration is often given to the thermal-chemical aspects of cure, experimental work(2,13) has also demonstrated the existence and some consequences of cavity pressure during the cure phase. Major local changes in cavity pressure have been shown to occur in both RTM and SRIM which arise from the interaction of thermal expansion, volumetric and rheological changes within the matrix. This can represent a significant loading in the design of RTM shell moulds due to the relatively large temperature changes which occur prior to gel. The effect is illustrated in Figure 14 for a small plaque mould where the cure pressure activity is seen to exceed the impregnation pressure at the injection gate by greater than 1 bar. The same effect has been shown to be less marked in SRIM since the temperature change prior to gelation is generally much lower(13).

6 Summary

It has been shown that LCM processing affects part quality, performance and manufacturing economics. Preform manufacture will cause departure from flat test plaque properties and these will affect both structural and processing properties, although both of these factors can be taken into account during design. Reliable materials characterisation data, including permeability data is essential to support modelling and design work and new models for the description of multi-axial preforms remain a key issue. Macroscopic flow models are increasingly evident and these are becoming central to mould design studies. Non-isothermal solutions are particularly useful and the extension of these systems to address the thermo-chemical and rheological aspects of the cure phase is seen as an important step. The key to

success in economic manufacture is seen as the integration of the above stages with the component design process.

Acknowledgements

The authors are grateful to the following organisations for their continued support:

Ford Motor Company, Dowty Aerospace, DSM Resins, The Department of Trade and Industry, ICI Chemicals, PPG Glass Fibres, Science and Engineering Research Council, Shell Chemicals (all UK) and Ford Research Laboratory.

References

1 C.D. Rudd, and K.N. Kendall, *Proc. Instn Mech Engrs J. Manuf. Eng.*, 206 77 (1992).

2 K.N. Kendall, C.D. Rudd, M.J. Owen and V. Middleton, *Compos. Manuf.*, 3, 235 (1992).

3 Bruschke, M V, Luce, T L and Advani, S G. "Effective permeability of multi-layered RTM preforms" *Proc Am. Soc. for Composites 7th Technical Conf.*, University Park, Pa. 11pp.

4 Gibson, A G. *Compos Manuf* 3, 2 1992.

5 C.D. Rudd, and K.N. Kendall, *Proc. 3rd PRI Int. Conf on Automated Composites*, 30/1 (1991).

6 Han, K, Trevino, L, Lee, J and Liou, M. *Polym Compos* 14, 2 (1993)

7 C D Rudd, V Middleton, M J Owen, A C Long & P McGeehin "Design, Processing and Performance of Structural Preforms" *Proc. CANCOM '93, 2nd International Conference on Composite Structures and Materials*, Ottawa, 27-29 September 1993

8 R Blanlot, J-L Billoet, and H Gachon, H. *Proc ICCM 9*, Madrid (1993), pp 576-583.

9 Parnas, R and Phelan, F. *SAMPE Quart.* Jan 1991, pp 53-60.

10 R.J. Morgan, D.E. Larive, H. Yung, Huang, Z. Yuan, and K.P. Battjes, *Proc. ASM/ESD*, 229 (1990).

11 C D Rudd, E V Rice, L J Bulmer and A C Longbottom. *Plastics, Rubber and Composites Processing and Applications* 20, 2 (1993)

12 Gebart B R. *J Comp Mat* 26, 8, (1992)

13 Kendall, K N and Rudd, C D. "Flow and Cure Phenomena in Liquid Composite Moulding" Submitted to Polymer Composites (June 1993).

14 M.J. Owen, E.V. Rice, C.D. Rudd, and V. Middleton, *Proc. CADCOMP 92*, (1992). Also in *Computer Aided Design in Composite Material Technology III*, S. G. Advani et al, Computational Mechanics Publications, Southampton and Elsevier Applied Science, London and New York (1992).

15 F. Trochu, R. Gauvin, and Z. Zhang, *Proc. CADCOMP 92*, (1992). Also in *Computer Aided Design in Composite Material Technology III*, S. G. Advani et al, Computational Mechanics Publications, Southampton and Elsevier Applied Science, London and New York (1992).

Nomenclature

B	stiffness factor in random reinforcement constitutive law
d	radius of elliptical fibre swirl at angle β
h	total thickness of reinforcement stack
$\mathbf{K_1}$, $\mathbf{K_2}$	principal permeabilities of unidirectional fibres
$\mathbf{K_{avg}}$	average permeability of reinforcement stack in reference direction
l	major diameter of elliptical fibre swirl
n	strain-hardening index in random reinforcement constitutive law
S	proportion of reinforcement specimen contraction due to inter-fibre slip
$\mathbf{t_i}$	thickness of reinforcement layer
$\mathbf{W_{act}}$	actual width of reinforcement specimen under uniaxial stretching
$\mathbf{W_{pin}}$	predicted pin-jointed specimen width
ε	equivalent strain
θ_i	orientation of reinforcement layer
ψ	tangent to elliptical fibre swirl
σ	stress
$\mathbf{y}\sigma$	von Mises yield stress

Figure Captions

Figure 1 Uniaxial Force/displacement relationship for stitch bonded fabric reinforcements.

Figure 2(a) Drape model for prototype automotive undershield

Figure 2(b) Stiffness variation arising from draped undershield

Figure 3 Tensile modulus versus degree of pre-stretch for continuous filament random mat

Figure 4 Liquid composite moulding flow schematic

Figure 5(a) SEM of fibre bundle showing presence of film former.

Figure 5(b) Micro-voidage within fibre bundle

Figure 6 Off axis rectilinear permeability test showing two-phase flow.

Figure 7 Permeability vs fibre orientation for quasi-unidirectional reinforcement.

Figure 8 Stretch forming model for CFRM

Figure 9 Stretch forming effects on permeability for CFRM

Figure 10 Permeability mapping for prototype undershield

Figure 11 Flow front predictions for prototype undershield

Figure 12 Thermal history for plaque mould

Figure 13(a) Effect of gate heating on though-thickness temperature distribution

Figure 13(b) Effect of gate heating on injection gallery mid-plane thermal history

Figure 14 RTM cure pressure activity for small plaque mould.

Figure 1.

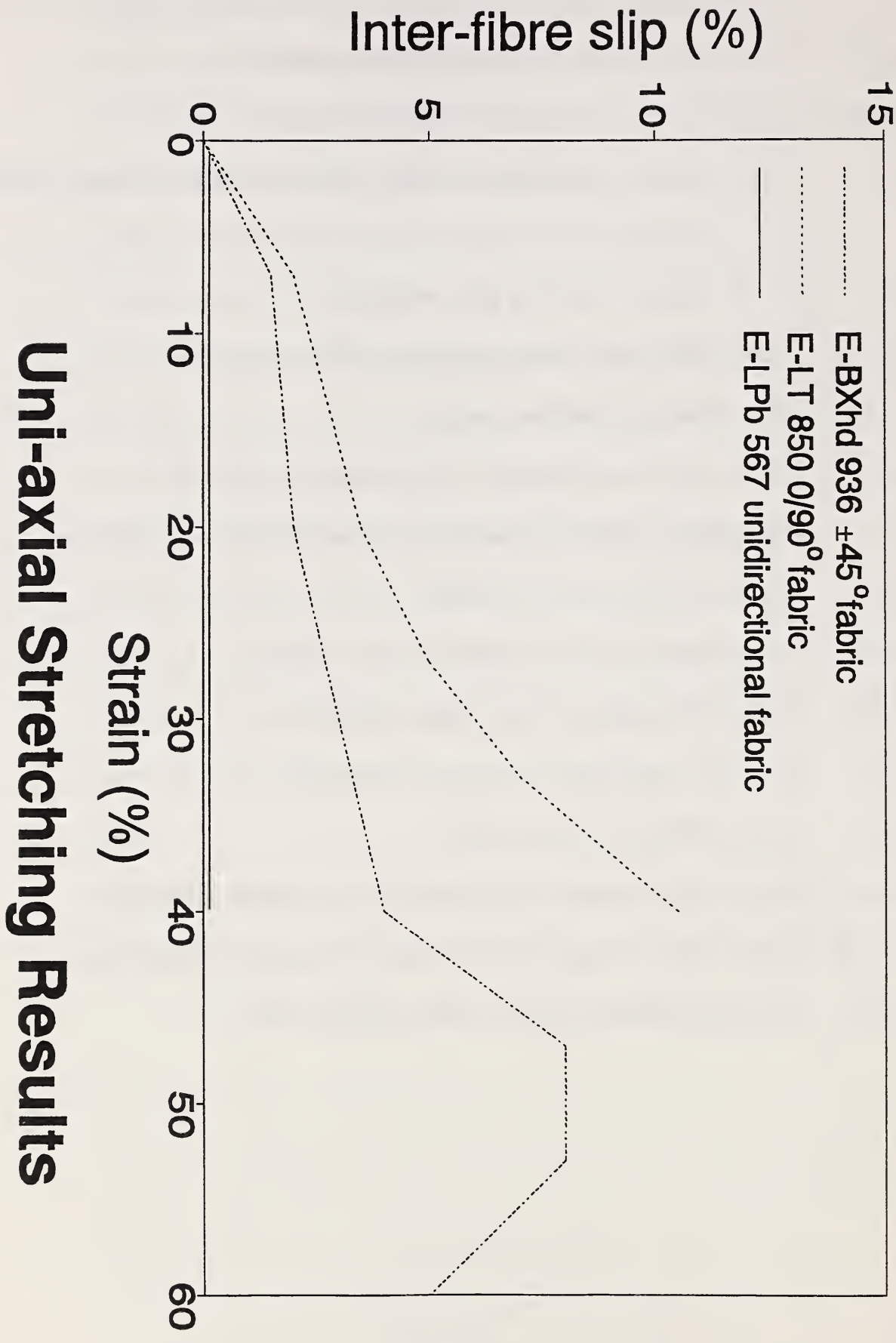
Uni-axial Stretching Results
Inter-fibre slip (%)
0
5
10
15
0
10
20
30
40
50
60
Strain (%)
E-BXhd 936 ±45°fabric
E-LT 850 0/90° fabric
E-LPb 567 unidirectional fabric

Figure 2a.

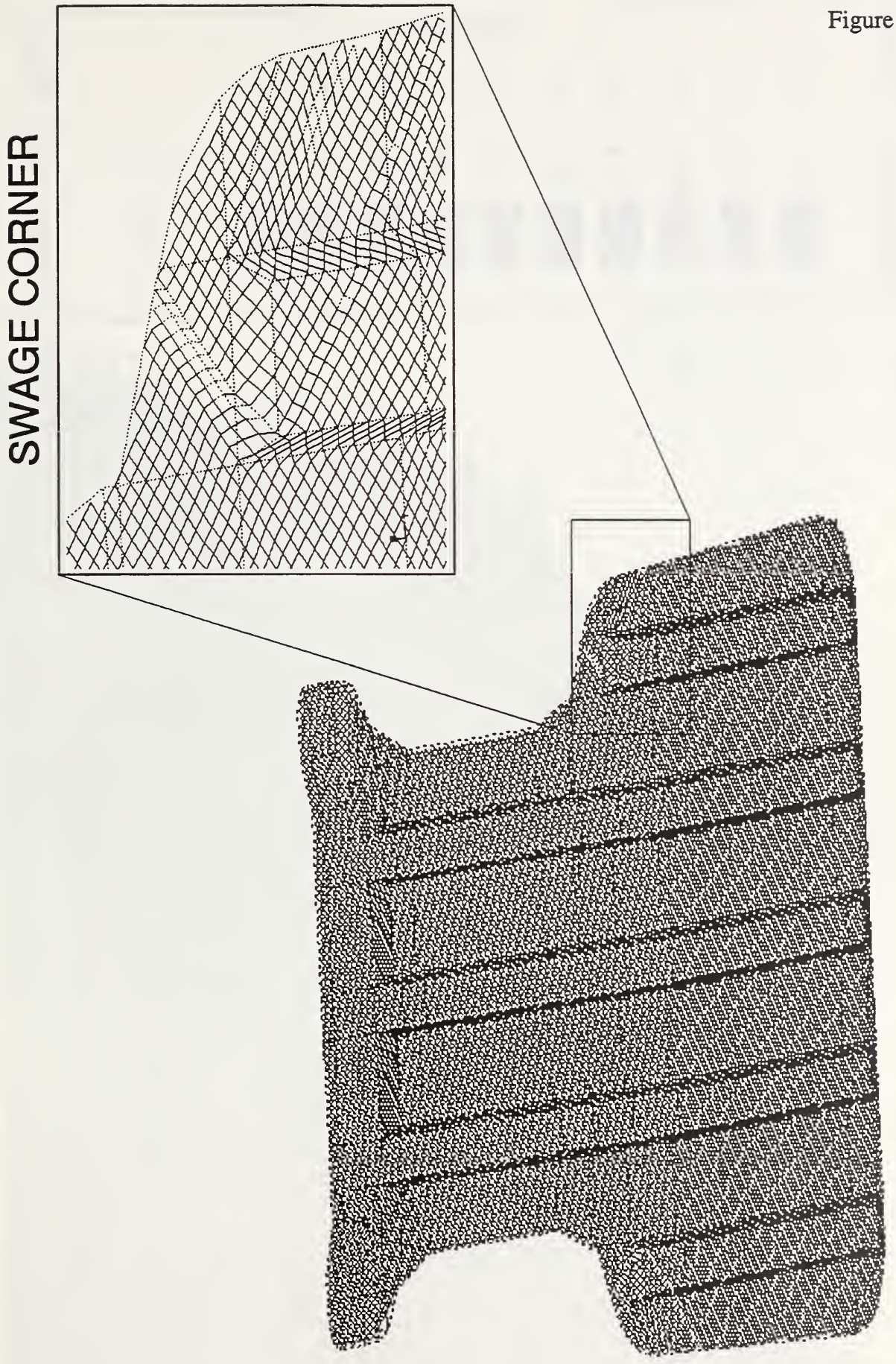

X direction
x
y
Modulus (GPa)
27.1 - 30.0
24.2 - 27.1
21.4 - 24.2
18.5 - 21.4
15.6 - 18.5
12.7 - 15.6
9.8 - 12.7
7.0 - 9.8
4.1 - 7.0
1.2 - 4.1
Press Any Key

Figure 2b.

Figure 3.

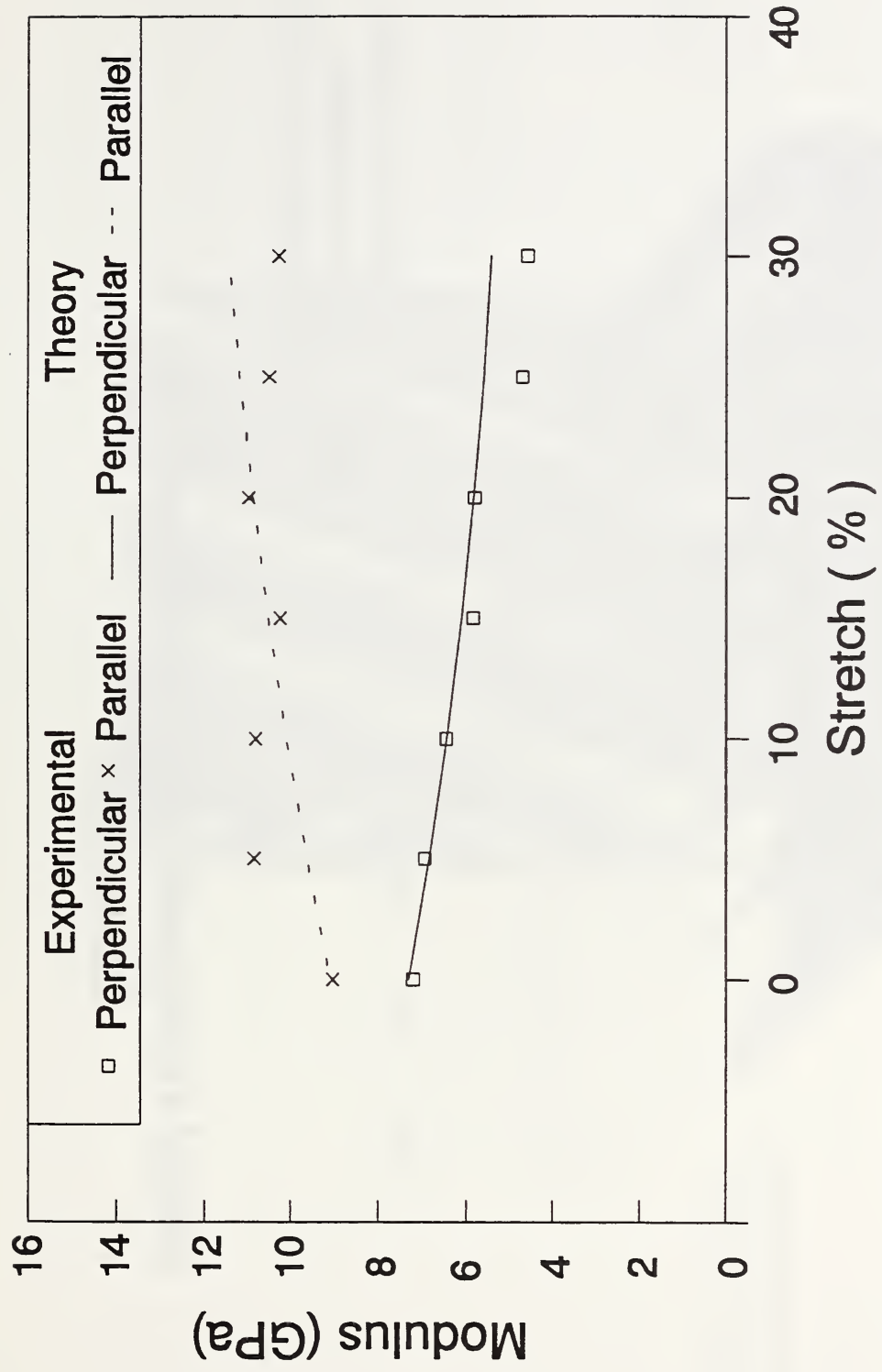
Experimental
Perpendicular
Parallel
Theory
Perpendicular
Parallel
Modulus (GPa)
Stretch (%)
0
2
4
6
8
10
12
14
16
0
10
20
30
40

Figure 4.

Liquid Composite Moulding Flow
Schematic
through-thickness variation
of in-plane permeability
leading to non-uniform flow front
heterogeneous ply structure
leads to in-plane fingering
effects

Figure 5a.

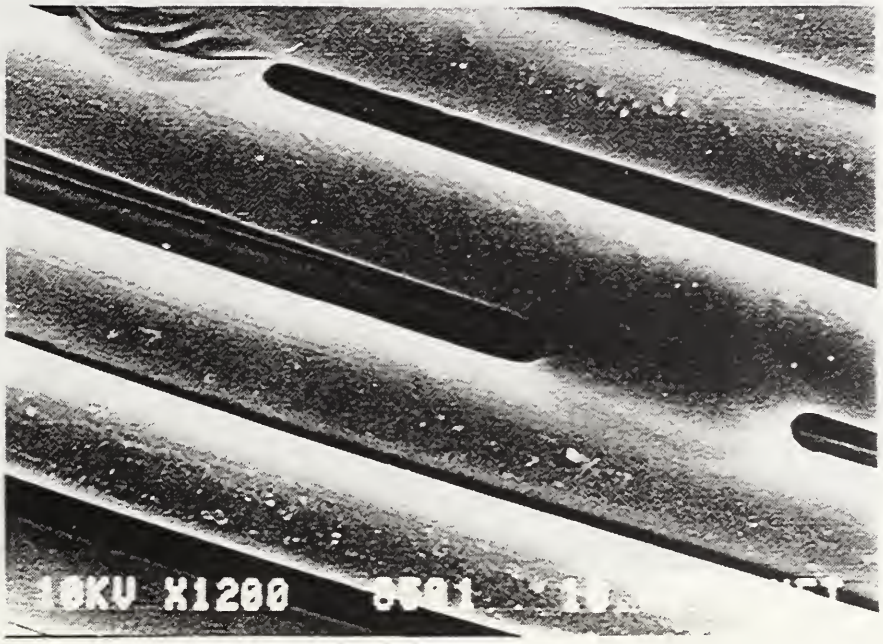

Figure 5b.

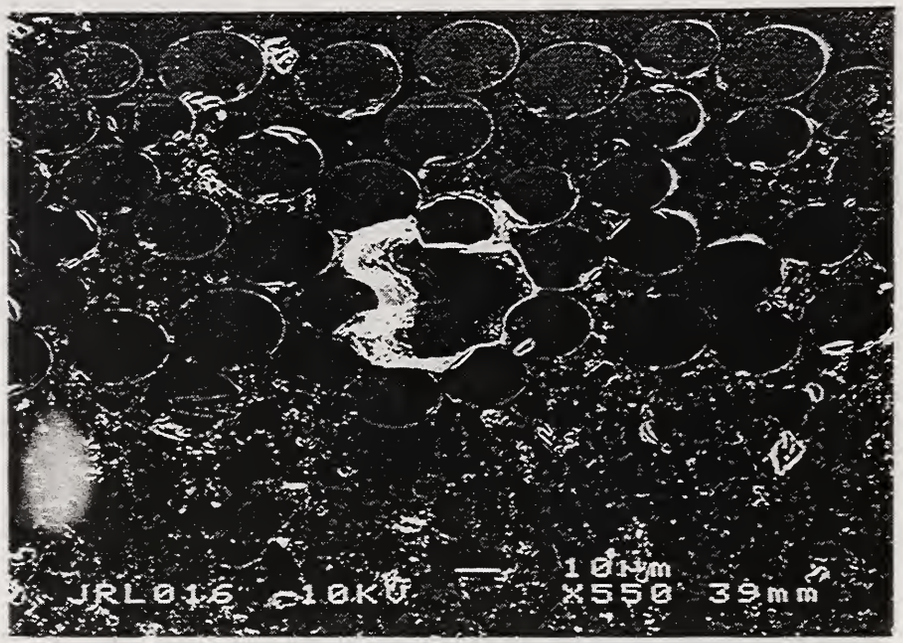

Figure 6.

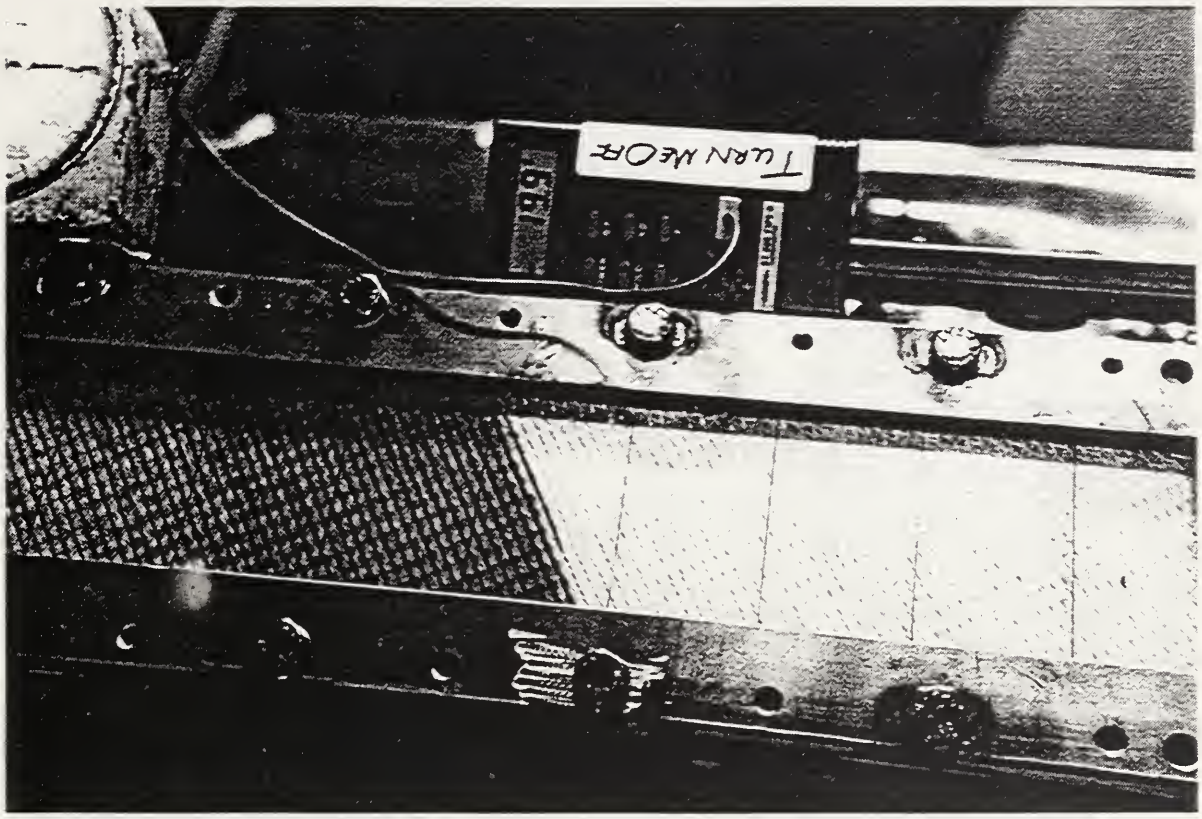

Figure 7.

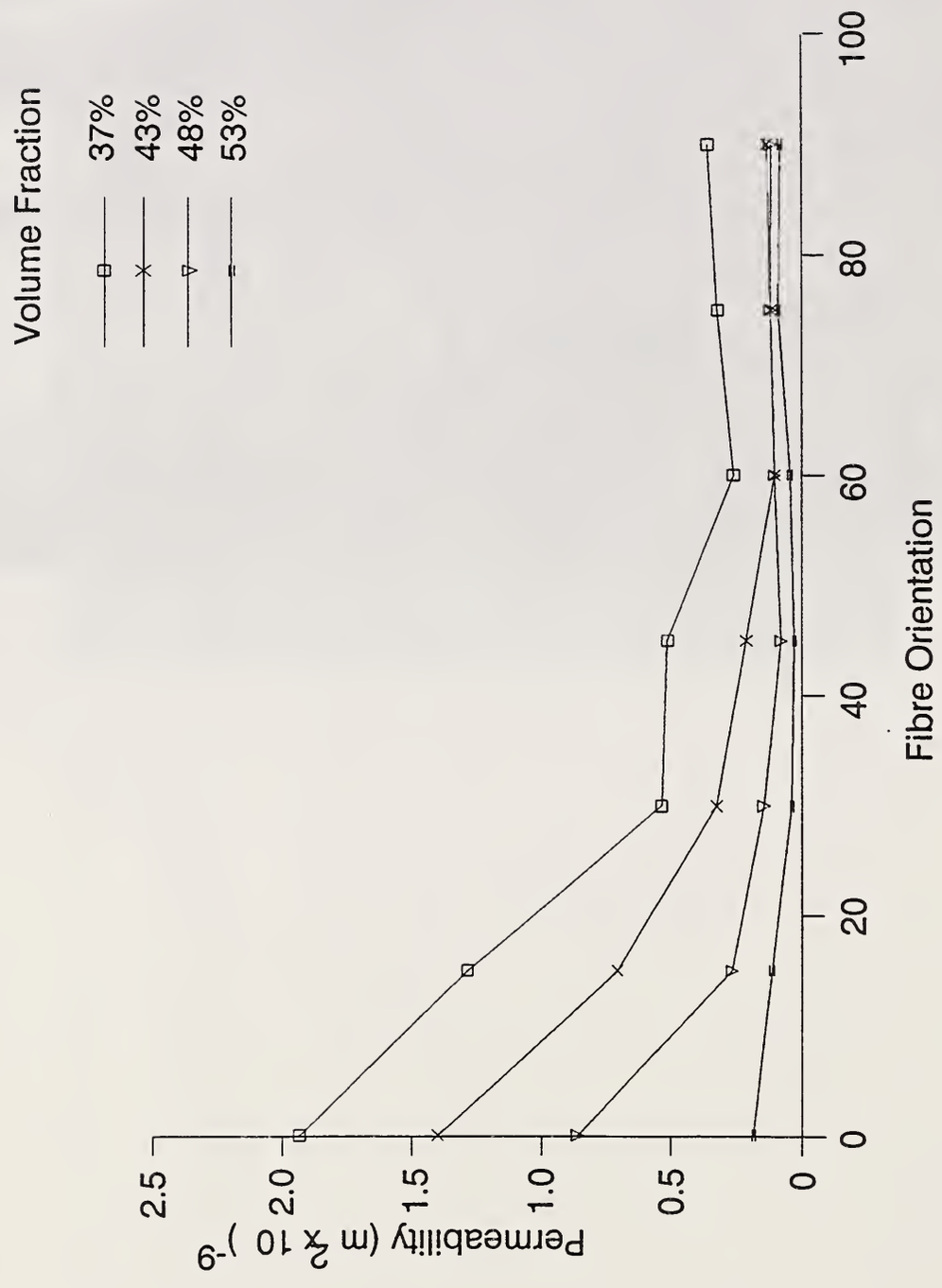
Volume Fraction
37%
43%
48%
53%
Permeability (m x 10)-9
2.5
2.0
1.5
1.0
0.5
0
0
20
40
60
80
100
Fibre Orientation

Figure 8.

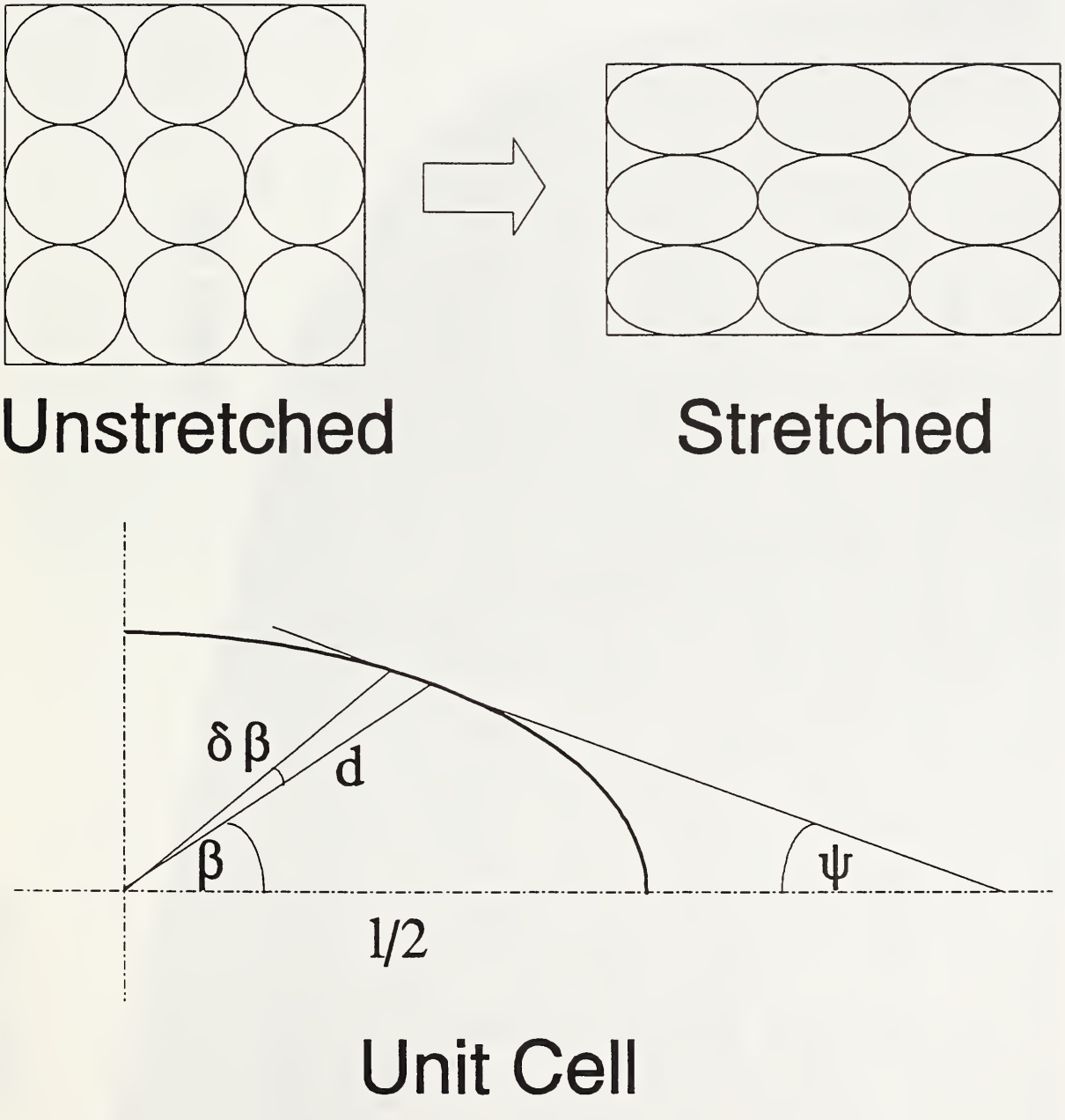

Figure 9.

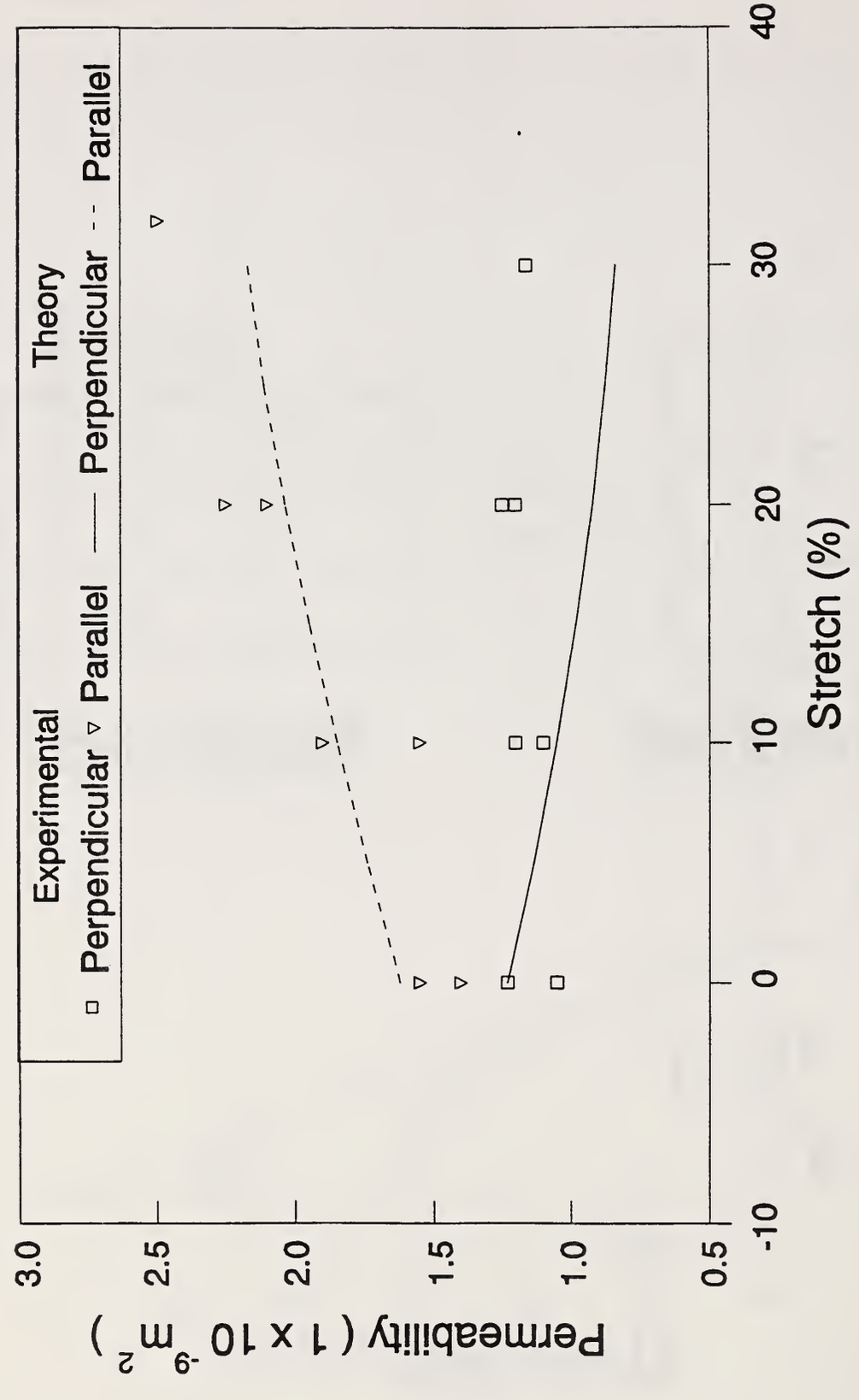
Experimental
Perpendicular
Parallel
Theory
Perpendicular
Parallel
Permeability (1 x 10 -9 m 2)
3.0
2.5
2.0
1.5
1.0
0.5
-10
0
10
20
30
40
Stretch (%)

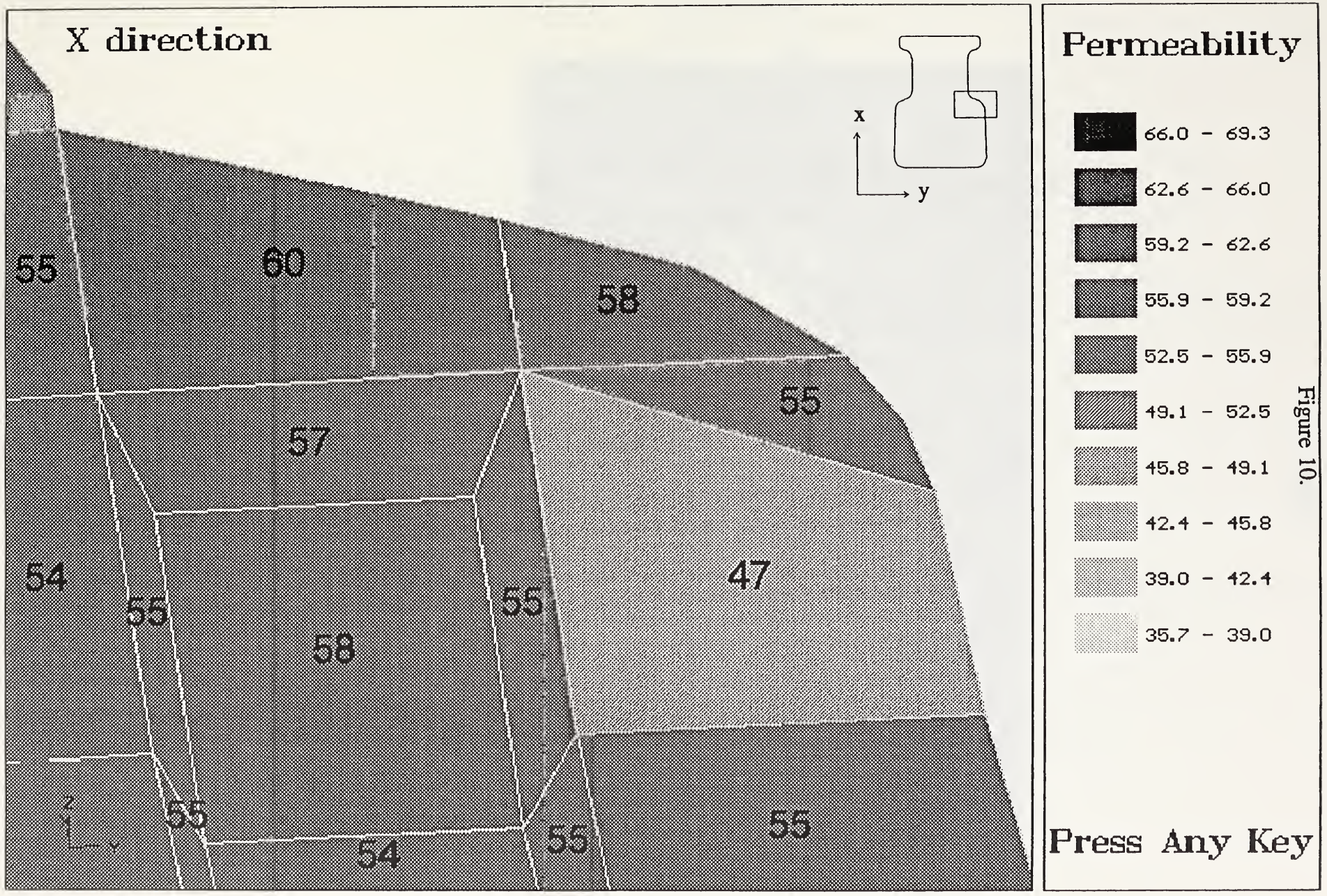
X direction
x
y
55
60
58
55
57
54
55
58
55
47
55
55
54
55
Permeability
66.0 - 69.3
62.6 - 66.0
59.2 - 62.6
55.9 - 59.2
52.5 - 55.9
49.1 - 52.5
45.8 - 49.1
42.4 - 45.8
39.0 - 42.4
35.7 - 39.0
Press Any Key

Figure 10.

Figure 11.

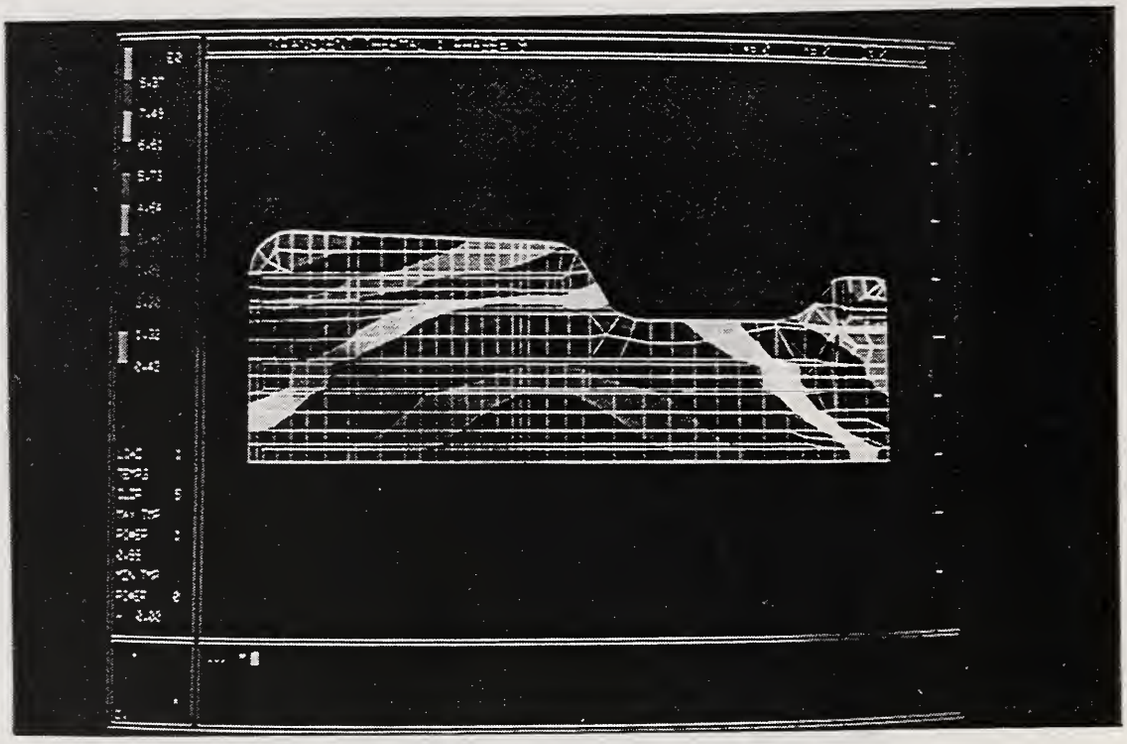

Figure 12.

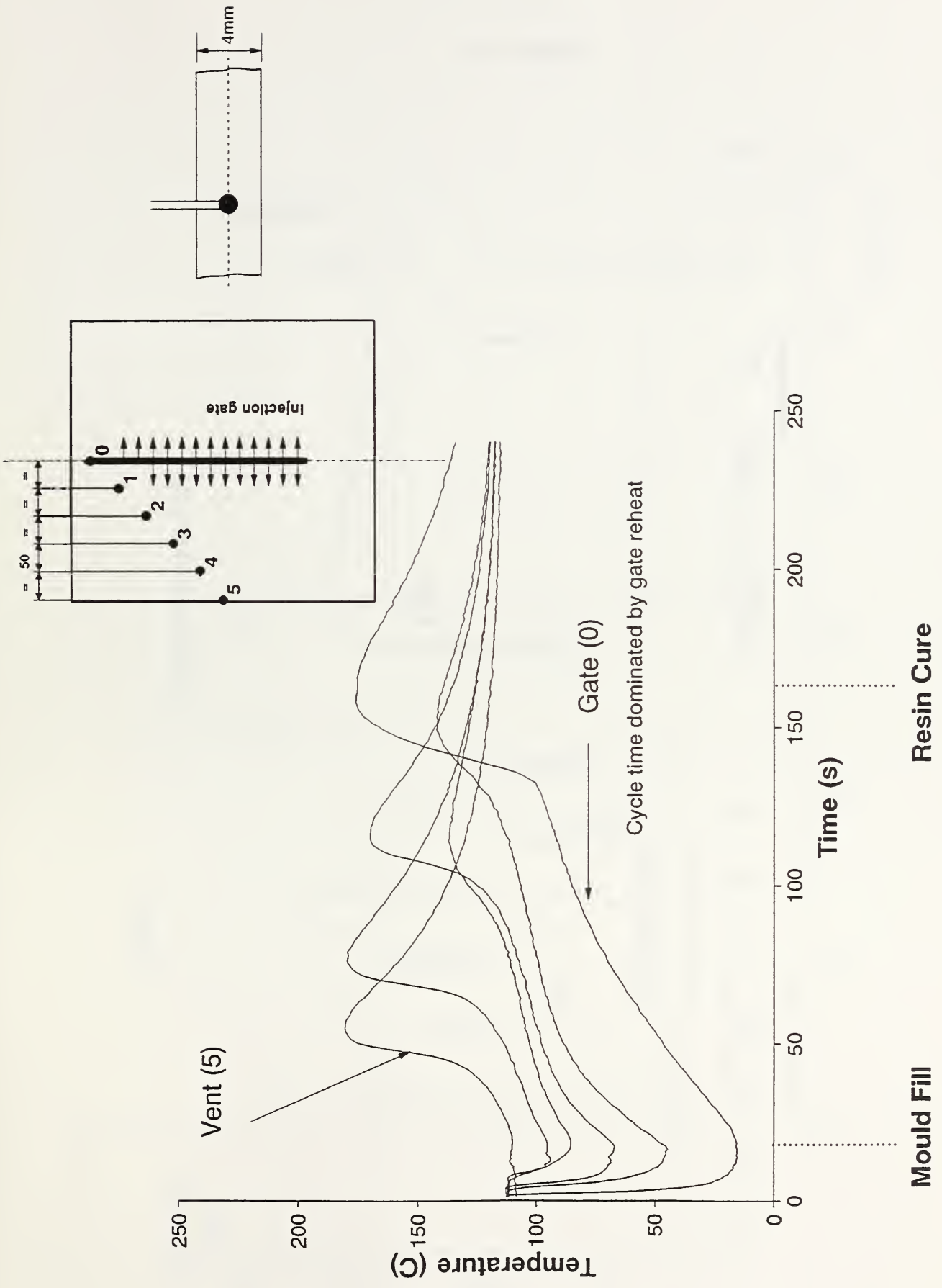
4mm
Injection gate
0
1
2
3
4
5
50
Vent (5)
Gate (0)
Cycle time dominated by gate reheat
Temperature (C)
Time (s)
Mould Fill
Resin Cure
0
50
100
150
200
250

Figure 13a.

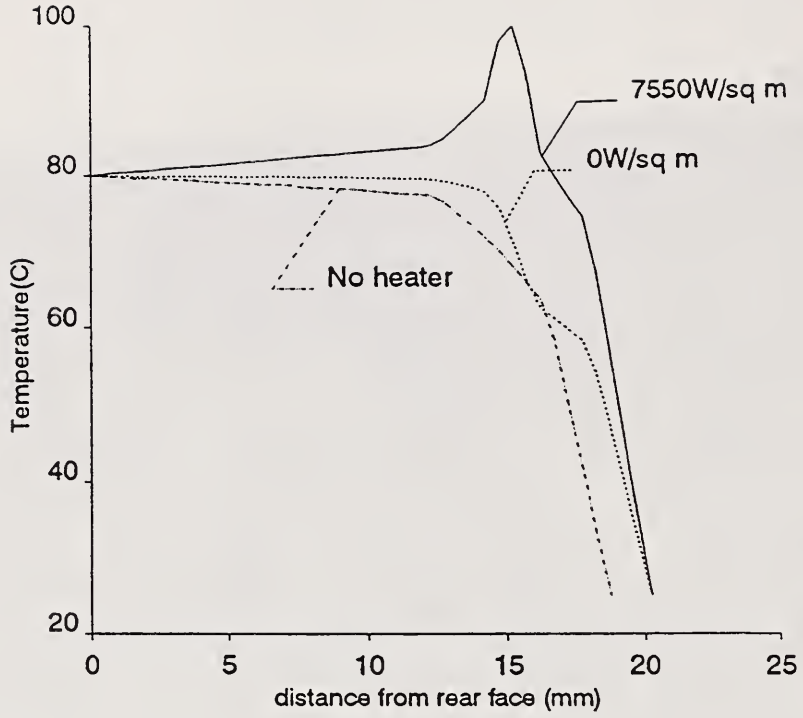

Figure 13b.

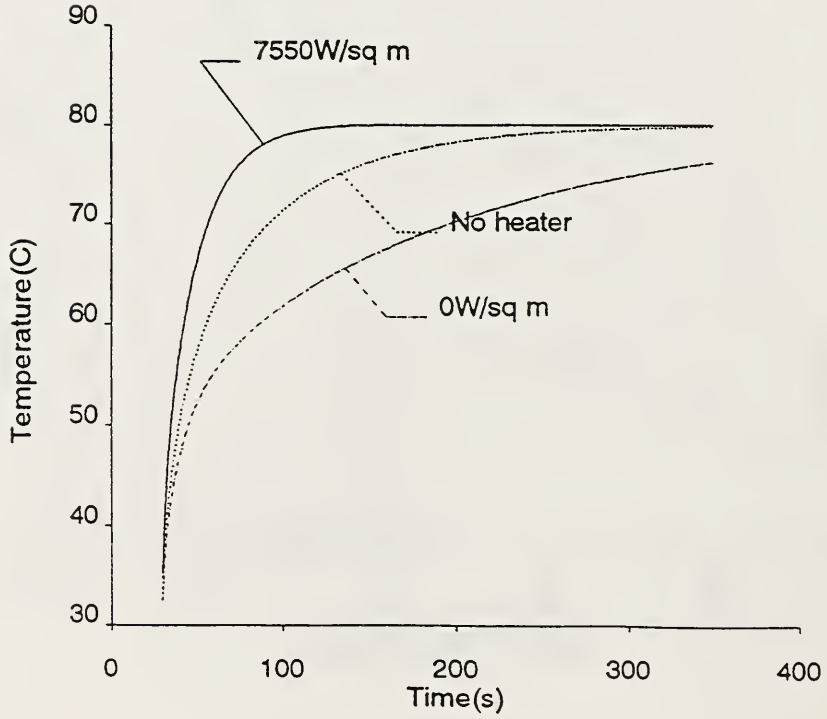

Figure 14.

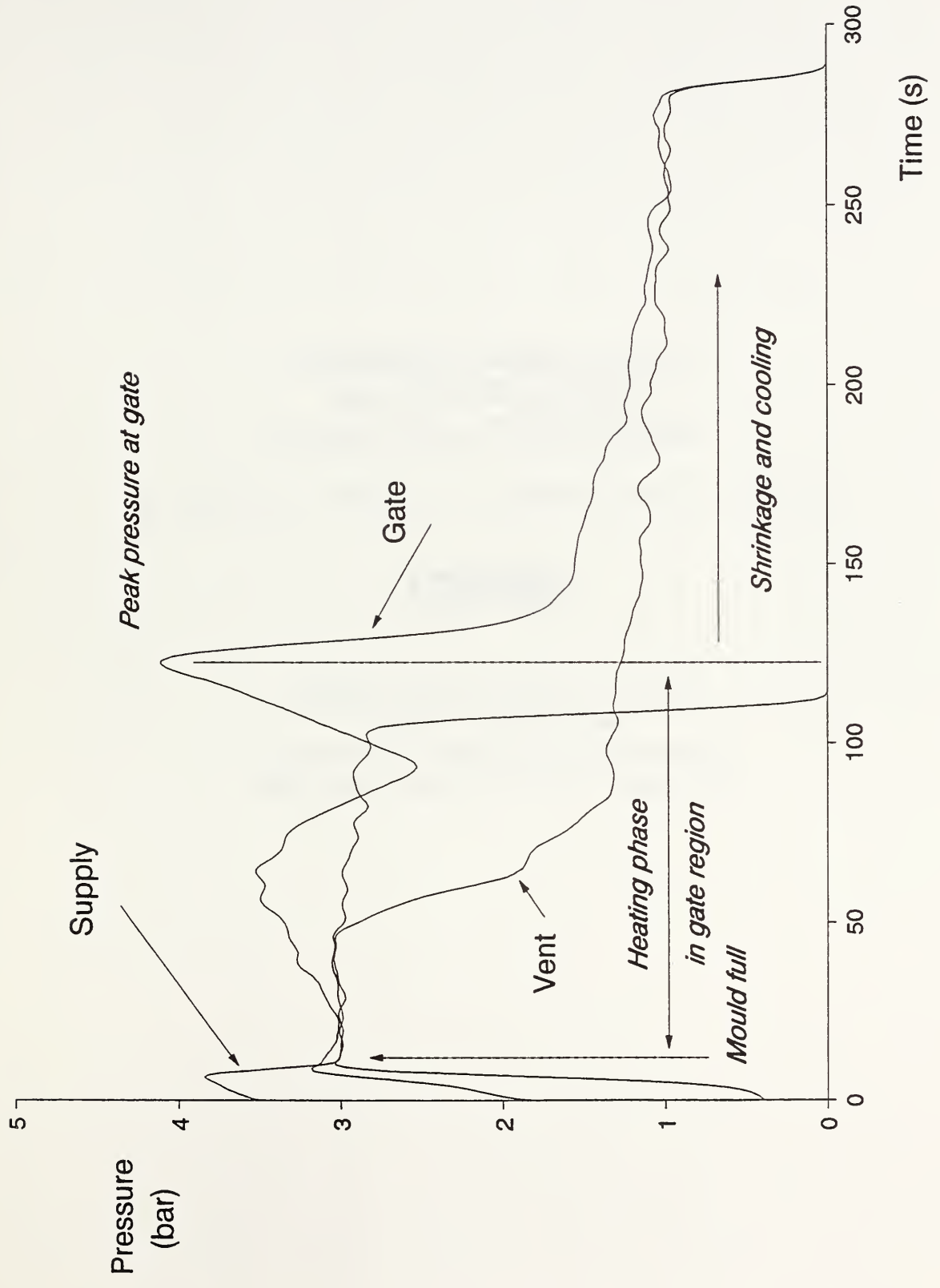
Pressure (bar)
5
4
3
2
1
0
0
50
100
150
200
250
300
Time (s)
Supply
Peak pressure at gate
Gate
Vent
Heating phase
in gate region
Mould full
Shrinkage and cooling

Permeability Measurement and Flow Simulation through Fiber Reinforcement

R. GAUVIN, F. TROCHU, Y. LEMENN and M. L. DIALLO

Applied Polymer Research Centre
École Polytechnique
Mechanical Engineering Department
Montréal, Québec H3C 3A7 (Canada)

ABSTRACT

Continuous fiber reinforced polymer composites can be produced by the injection of a reactive fluid into a mold with preplaced reinforcement. Mold filling modelling software such as our RTMFLOT software are being developed to help the design and production engineers meet their requirements. In these models, the utilisation of accurate permeability values is an absolute necessity for their usefulness. This paper presents permeability results for several reinforcements. Also, experimental techniques being used to measure the permeability are discussed. Several points are highlighted and suggestions are made to help the investigator in its search for reliable permeability data.

INTRODUCTION

Continuous fiber reinforced thermoset composites can be produces by injecting reactive liquid resins into a mold with preplaced reinforcement. The two major processes for doing that are the Structural Reaction Injection Molding process (SRIM) and the Resin Transfer Molding (RTM). Typically in SRIM, the viscosity is low while the injection rate and reaction time are high. In RTM, usually the viscosity is higher in the range of 200 to 1000 centipoise while the filling rate and the reaction kinetic are slow. In the RTM, the injection pressure is anywhere between 100 to 1000 KPa which allows low cost fiberglass-polyester type molds to be used.

Process optimisation and proper mold design require the development of a reliable mold filling model with an accurate description of resin flow through the reinforcement. In RTM, the reinforcement could take many forms, for instance, it could be a chop strand preform, a stitched preform, a continuous strand mat, a woven roving, a no-crimp fabric, or a combination of two or more of these reinforcements. A sound mold filling model requires an accurate description of resin flow through porous media of variable complexity. It is generally accepted to use the Darcy's law to describe the impregnation process of fibrous media. The law states that the flow rate through a unit area is proportional to the pressure gradient. The factor of proportionality being the permeability of the reinforcement. Over the years, several authors have studied various aspects of the RTM process. Some of them have also developed computer package similar to one we are developing (RTMFLOT) to simulate the mold filling phase and the reaction kinetic.

One of the key issue in the quality of the flow prediction of these softwares is how well does the permeability values being used to describe the reinforcement correspond to the actual value of the permeability, once the reinforcement has been place into the cavity. Various aspect such as surface density variation, fiber orientation, stacking sequence, compaction behavior and edge effects are elements which can provoke

discrepancies between flow prediction results and actual flow behavior.

In this paper, flow simulation and experimental results are compared on a subway seat to illustrate some of the issues mentioned earlier. Then permeability measurement techniques are discussed and permeability data are presented for several continuous fiber reinforcements. The surface density variation of three continuous strand mat is also given and its influence on permeability data is discussed.

FLOW SIMULATION

Darcy's law is the most commonly used model for flows through porous media. Despite its limitations for large velocities due to inertia, it was found satisfactory to simulate mold filling for the RTM process. Darcy's law states that the macroscopic velocity of the flow is proportional to the pressure gradient through the following equation:

$$V = \frac{[K]}{\mu} \nabla P \qquad (1)$$

where [K] is the permeability tensor (m^2) and μ denotes the resin viscosity (Pa.s). For incompressible fluids the continuity equation reduces to:

$$\nabla \cdot V = 0 \qquad (2)$$

Substituting (1) in (2) gives:

$$\nabla \cdot \left[\frac{[K]}{\mu} \nabla P \right] = 0 \qquad (3)$$

The first simulations of the RTM process were based on curvilinear finite differences [1-3]. Then models incorporating finite elements with the control volume method appeared [4-7]. A numerical procedure using only finite elements was developed

earlier [8]. The equations for our approach are based on linear non-conforming finite elements.

This method respects integrally the important physical condition of mass conservation across the inter-element boundaries. In the finite element model, the mold is decomposed into a set of elementary prismatic elements of triangular base. The pressure field is approximated on each elementary volume. The pressure varies on the element boundaries but is assumed constant through the thickness of the part. This reduces the problem inside a complex three-dimensional part to a two-dimensional analysis.

The RTMFLOT software is a complete environment with currently four modules, they are MESHFLOT, FLOT, VISUFLOT, HEATFLOT and DATAFLOT [9]. MESHFLOT is a finite element generation module based on dual kriging. With this technique, a triangular mesh is generated by mapping the mesh of a unit square onto the surface of the mold. The FLOT module uses Darcy's law as the governing equation to model the flow of resin through the reinforcement. Successive positions of the flow front as well as the pressure field are computed with that module. HEATFLOW is used when non-isothermal filling must be considered. Finally, DATAFLOT is the data bank where resin and reinforcement properties are stored.

Figure 1,2 and 3 respectively show the finite element mesh, the successive positions of the flow front and the pressure field at the end of filling for an isothermal mold filling simulation conducted for a subway seat with RTMFLOT. Figure 4 shows two successive short shots for the same parts. The part has a nominal thickness of 3.8 mm, is gel coated on one side and uses one layer of continuous strand mat OCF8610 from Owens Corning. The gelcoat thickness is about 0.6 mm. The polyester resin used was filled with 50% by weight of calcium carbonate and has a viscosity at room temperature of 1200 centipoises. The maximum pressure at the end of filling, closed to the injection port, was in the vicinity of 400 KPa.

When comparing figure 1 and 2, one can see that their are discrepancies between the simulation and the actual flow front positions. The flow model cannot be blamed for these differences but local variations of permeability are more likely responsible for it. This illustrates why, permeability data are a key issue for occurate and relevant flow prediction by any software.

PERMEABILITY MEASUREMENT

As mentioned earlier, any flow simulation is only as good as the permeability data it uses. There have been a number of theoretical and experimental investigations of the flow behavior in porous media of the types used in RTM. Some are listed here [10-20].

The general case of in-plane flow of an incompressible fluid through an anisotropic homogeneous uniform fiber reinforcement is shown in Figure 5. At time t = 0, the fluid covers the injection inlet radius R_0. Lather on, because of the anisotropic nature of the reinforcement, the flow front will take an elliptical shape as shown. For the general case, in the reference system 1 and 2 shown in figure 5, the permeability matrix of equation 1 takes the following form:

$$[K] = \begin{bmatrix} k_{11} & k_{12} \\ k_{21} & k_{22} \end{bmatrix} \quad (4)$$

The k_{11}, k_{12}, k_{21} and k_{22} are related to the permeability in the principal flow directions x and y through the following equations:

$$k_{11} = \frac{k_x + k_y}{2} + \frac{K_x - K_y}{2} \cos 2\theta \quad (5)$$

$$k_{12} = k_{21} = \frac{k_x - k_y}{2} \sin 2\theta \quad (6)$$

$$k_{22} = \frac{k_x + k_y}{2} - \frac{k_x - k_y}{2} \cos 2\theta \qquad (7)$$

When Θ equal zero, which means that the principal flow directions correspond to the material principal axis (machine direction 1 and cross direction 2), the permeability matrix becomes a diagonal matrix and takes the following form:

$$K = \begin{bmatrix} k_x & 0 \\ 0 & k_Y \end{bmatrix} \qquad (8)$$

Equation 8 represents the most commonly used case for unidirectional reinforcement and various 0^0 - 90^0 construction such as woven roving, and several type of fabrics. To measure k_x and k_y, researchers have basically used two techniques: unidirectional flow and bidirectional flow measurement.

Unidirectional flow measurement

Figure 6 shows a typical experimental set-up for unidirectional flow measurement. In this case, it has 87 cm long by 14.5 cm wide and cavity thickness can be varied. The cavity is transparent and photo cells are used to record the flow front positions. Either constant flow or constant pressure experiment can be run depending on the supply system used. Both types of experiments are rather simple to run and permeability is obtained using equation 1 for unidirectional flow.

With this set-up one should be very careful to prevent any edge flow racing effect. Also, precautions should be taken to assure a constant cavity thickness. This type of installation is generally used for continuous strand mats for which it is rather easy to avoid edge effects since their permeability leads to a low pressure experiment.

For continuous strand mats, the main difficulty in obtaining a reliable permeability value comes from their lack of homogeneity. To illustrate that, figure 7 shows the variation of surface density of 14.5 cm x 76 cm samples cut side by side in the roll

direction for three commercially available mats. They are the OCF8610 from Ovens Corning, the NICO-758 from Nico Fiber and the U-816 from Vetrotex CertainTeed. Such surface density variation translates into volume fraction variation and consequently into permeability variations from one area to another in a part. This becomes a real problem for accurate modelling, especially for parts molded with one or two layers of mats for which permeability could vary by a factor of almost 100% depending on the material used.

Even for thicker parts, it is a real difficulty. To illustrate that, figure 8 shows the permeability value computed using the nominal surface density for the mat OCF8610 as a function of fiber volume fraction V_f. These measures were obtained with a 4.35 mm thick cavity. For instance in that cavity, a nominal volume fraction of 0.20 is obtained with seven layers of mat which is much larger than the number used in most of the industrial parts. For this case of seven layers, a typical flow front speed was 11 mm/s and the inlet pressure at the end of the 76 cm filling was 155 KPa. In this figure:

$$1 \text{ DARCY} = 9.8697 \times 10^{-9} \text{ cm}^2 \quad (9)$$

If each sample is weighted before the experiment, smooth curves are obtained for the permeability versus fiber volume fraction for continuous strand mats. Figure 9 presents such results for five commercially available mats. Of course, these values represents the real permeability of the tested samples. However accurate flow prediction using these specific values remains difficult because the permeability will vary in different area of the mat. Instead, it would be advisable to use a spectrum of permeability values in designing a part using continuous strand mat.

BIDIRECTIONAL FLOW MEASUREMENT

For low permeability reinforcements such as fabrics, it becomes extremely difficult to avoid edge effects in a unidirectional flow measurement set-up described in figure 6. Instead, researchers have used experimental installations similar to the one built in our

laboratory and schematically described in figure 10. Figure 11 is a picture of the transparent cavity and a closed-up of a partly wetted sample. If one looks carefully on the picture, an array of small 63 mm bolts positioned every 11 cm can be seen. They prevent any undesirable deformation of the 2.5 cm thick plexiglass cover. A digital camera is used to record the flow front shape and successive positions. With such an installation, two experimental approaches can be used. The most popular one is a constant inlet pressure experiment because it corresponds to several industrial installations. The other one is a constant inlet flow experiment.

Constant pressure experiment

Adams & al [10,11,12] have used this technique for permeability measurement. Based on the continuity equation for incompressible fluid and Darcy's law, they have developed the equations for isotropic and anisotropic reinforcements.

For the isotropic case, the flow front should be of a circular shape and they gave the following solution:

$$\left(\frac{R_f}{R_0}\right)^2 \left[2\ln\left(\frac{R_f}{R_0}\right) - 1\right] + 1 = \frac{4k\Delta Pt}{\Phi\mu R_0^2} \qquad (10)$$

where:

R_f	=	Flow front radius at time t
R_0	=	Inlet radius, which is the radius of the hole cut through the reinforcement stack at the injection point
ΔP	=	Pressure gradient
t	=	Elapse time
μ	=	Fluid viscosity
Φ	=	Porosity
k	=	Permeability, here $k = k_x = k_y$

If F_i is defined as being the left side of equation 10, it can be plot as a function of time. It gives a straight line passing through the origin. From the slope of that line,

the permeability can be calculated.

For the anisotropic case, $k_x \neq k_y$ and the flow front has an elliptical shape. Using some simplifications and elliptical coordinates, Adams & al [11] have proposed an analytical solution rather complex since an iterative calculation is needed to obtain the permeability. Instead, following Chan and Hwang method [13], the orthotropic form of equation 3 can be transformed into an equivalent isotropic system where it takes on the form of the Laplace equation. In that method, a point (x,y) of the original domain is related to its transformed coordinates (x_e, y_e) by the relations:

$$x_e = \left[\frac{k_y}{k_x}\right]^{1/4} x \quad \text{and} \quad y_e = \left[\frac{k_x}{k_y}\right]^{1/4} y \tag{11}$$

The above relationship is equivalent to a length expansion or contraction along the given coordinate direction. Since in the equivalent isotropic system the flow front will become a circle and $R_{xe} = R_{ye}$, the relationship between x and y in the original system is:

$$y = \left[\frac{k_y}{k_x}\right]^{1/2} x \tag{12}$$

Then from a plot of flow front positions R_y versus R_x corresponding to the same time, a straight line through the origin is obtained. The slope m_1 of the line is:

$$m_1 = \left[\frac{k_y}{k_x}\right]^{1/2} \tag{13}$$

the equivalent form of equation 10 in the equivalent system becomes:

$$\left[\frac{R_x}{R_0}\right]^2 \left[2\ln\left[\frac{R_x}{R_0}\right] - 1\right] + 1 = \frac{4k_e \Delta P t}{\Phi \mu R_{x0,e}^2} \tag{14}$$

where the equivalent permeability k_e is given by:

$$k_e = \sqrt{k_x k_y} \tag{15}$$

and the equivalent inlet radius on the x axis is given by:

$$R_{x0,e} = \left[\frac{k_y}{k_x}\right]^{1/4} R_0 \tag{16}$$

We can rewrite equation 14 in the following manner:

$$F_a = \frac{4 k_e \Delta P t}{\Phi \mu} \tag{17}$$

where

$$F_a = R_{x0,e}^2 \left\{ \left[\frac{R_x}{R_0}\right]^2 \left[2 \ln \left[\frac{R_x}{R_0}\right] - 1\right] + 1 \right\} \tag{18}$$

If we plot F_a from equations 17 and 18 as a function of time we should get straight lines through the origin for any value of inlet radius R_0. To illustrate that, figure 12 shows a plot of F_a from equation 17 and 18 as a function of time. It represents three experiments with respective inlet diameters of 1.3 cm, 2.5 cm and 5 cm. For these experiments, 10 layers of NCS82675 fabric from J.B. Martin were used which gave a fiber volume fraction $V_f = 0.52$. The permeability is obtain from the slope of these lines. Figure 13 shows the permeability values in the machine and cross directions as computed for the same three experiments. We can clearly see that a small inlet radius may provoke a significant overestimation of the permeability. In some cases, underestimation may possibly occur. There are several reasons that could explain these variations. For instance, the location of the pressure transducer, the precision of the flow front position recording system, the inlet diameter and cavity thickness ratio, the quality of the cut, etc... In light of these results, we strongly suggest that

every experimental installation be checked for its sensitivity to the inlet boundary conditions. From figure 13, one can see that for our experimental set-up, an inlet diameter of 2.5 cm and larger give a rather constant permeability.

With these considerations in mind, permeability measurements were conducted on two non-crimp stitch (NCS) glass fabrics form J.B. Martin. They are commercialised for polyester and vinylester applications. Their structure is described in figure 14 and some of their physical characteristics are given in table 1. Figure 15 shows the permeability of these fabrics as a function of fiber volume fraction. Measurements were carried out with silicone oil of 100 centipoises supplied at a constant pressure in the range of 50 to 70 KPa. the inlet hole diameter was 2.5 cm to avoid disturbing effects discussed earlier. The sample size was 30 cm x 30 cm.

From figure 15, we can see that in both cases, the cross direction is more permeable than the machine direction. Since the rovings are the same in both directions, it is believed that the stitch polyester thread that runs on the top of the roving in the cross direction is responsible for that higher permeability. The NCS81053 has rovings roughly twice as large at the ones in the NCS82675. That induces larger space between the rovings of the NCS81053 which explaines why it has a larger permeability.

CONSTANT FLOW MEASUREMENT

The work of Adam & al [10-11-12] has been pursue by Greve an Soh [14]. They suggest that at each time step, the solution of the differential equations for the flow between parallel plates for the isotropic case is given by:

$$P_0 = \frac{Q\mu}{2\pi h k} \ln\left(\frac{R_f}{R_0}\right) \qquad (19)$$

where P_0 = Inlet pressure at time t

h = Cavity thickness

For the anisotropic case, if the same transformation of coordinates given in equation 11 is used, the solution for each time step then becomes [20]:

$$P_0 = \frac{Q\mu}{2\pi h\, k_e} \ln (R_{xe}) + b \qquad (20)$$

A plot of P_0 versus ln (R_{xe}) will yield a line with a slope m_2 and an intercept b. k_e is obtained from:

$$k_e = \frac{Q\mu}{2\pi h m_2} \qquad (21)$$

From the transformation of coordinates given in equation 11, the values of k_x and k_y are then calculated from equations 13 and 14 where m_1 is in fact the ratio between the ellipse axes. Usually, starting with a circular inlet, the flow front elleptical shape stabilises very rapidly and then the ratio m_1 from equation 13 remains constant.

CONCLUSION

Flow simulation softwares are extremely useful tools for the proper design of liquid molded composite parts. Production engineers can also use them for the optimisation of the production cycle of an existing part. For all these softwares, the exactness of the physical parameter they used is a key issue in their usefulness.

Permeability is probably the physical parameter which represents the largest difficulties. Its definition is simple and it seems very easy to measure. However, if we look at published data, we often observe significant differences between reported permeabilities for the same material. In our laboratory, we had difficulties to obtain consistent results from one set-up to another, from one researcher to another and even more so, from one batch to another for the same material. Several examples of such material variation were presented here.

Among others, Kaviany [21] in a numerical analysis of incompressible fluid flow through porous media based on continuity, momentum and energy equations, reported that the pressure drop across a porous medium is affected by four terms: the Darcy's factor, an entry shape factor, a wall friction factor and an inertia effect. As far as we know, in RTM and SRIM related literature, investigators have used only the Darcy term and neglected the others. Results presented here show that in some cases, the entry term is not negligible and that special care should be taken. For instance in the case reported here, an inlet hole diameter of 2.5 cm was necessary to reduce considerably the influence of that term as seen in figure 13. However, it has to be noted that the value of the inlet diameter for stable results might be different for an other installation of for significant change in flow speed and cavity thickness for the same installation.

To evaluate the importance of the wall friction effect, a porous media shape parameter γ is proposed by Kaviany [21]. It is defined by the following equation:

$$\gamma = \left(\frac{h^2 \Phi}{k} \right)^{1/2} \qquad (22)$$

where h is the cavity thickness, Φ the porosity and k the permeability. It is generally accepted to say that for the wall effect to be negligible, the constant γ must be greater than 100. In that case, the flow is closed to a plug flow while the flow front profile through the thickness is parabolic when $\gamma = 0$.

Inertia is also generally neglected but for high speed injection such as in SRIM and fast RTM it might not be the case. Further investigation is needed to study the influence of all these factors and others such as the nature of the fluid and the number of layers to name a few.

ACKNOWLEDGEMENTS

The authors would like to acknowledge the financial support of the National Science and Engineering Research Council of Canada, the Fonds concerté d'aide à la recherche du Québec, l'Institut de recherche en santé et sécurité du travail and the technical support of companies like Fibrex, Armkem, J.B. Martin, Vetrotex CertainTeed and Owens Corning.

REFERENCES

1. J.P. Coulter and S.I. Güçeri, Jour. Reinf. & Comp., 7(3), pp. 200-219, 1988.

2. S. Li and R. Gauvin, Jour. of Reinf. Plast. and Comp., 10(3), pp. 314-327, 1990.

3. F. Trochu and R. Gauvin, Jour. of Reinf. Plast. and Comp., 11(7), pp. 772-786, 1992.

4. C.A. Fraccia, J. Castro and C.L. Tucker, 4th Tech. Conf. of the Amer. Soc. for Composites, Technomics Publishing Co., p. 157, 1989.

5. M. V. Bruschke and S.G. Advani, Polymer Comp., 11(6), 1990.

6. W.B. Young, K. Rupel, K. Han and M.J. Liou, Polym Comp., 12(1), pp. 30-38, February 1991.

7. W.B. Young, K. Han, L.H. Fang, L.J. Lee and M.J. Liou, Polym Comp., 12(6), pp. 391-403, 1991.

8. F. Trochu and R. Gauvin, Adv. Comp. Let., 1(1), pp. 41-43, 1992.

9. F. Trochu, R. Gauvin and D.M. Gao, Advances in Polymer Technology, 12(4), 1993.

10. K.L. Adams, B. Miller and L. Rebenfeld, Polymer Eng. and Sci., 26(10), pp. 1434-1441, 1986.

11. K.L. Adams, W.B. Russel and L. Rebenfeld, Int. Jour. of Multiphase Flow, 14(2), pp. 203-215, 1988.

12. K.L. Adams and L. Rebenfeld, Textile Research Journal, 57, p. 647, 1987.

13. A.W. Chan and S.T. Hwang, Polymer Eng. Sci., 31, p. 1233, 1991.

14. B.N. Greve and S.K. Soh, SAE Transaction, 99(5), pp. 331-343, 1990.

15. B.R. Gebart, Journal of Composite Materials, 26(8), pp. 1100-1133, 1992.

16. L. Trevino, L.J. Lee, K., Rupel and M.J. Liou, 45th Ann. Conf., Composites Institute, Soc. of the Plastics Industry, Session 9-E, February 12-15, 1990.

17. R.C. Lam and J.L. Kardos, Polymer Eng. and Sci., 31(14), pp. 1064-1070, 1991.

18. R.S. Parnas and F.R. Phelan, SAMPE Quaterly, pp. 53-60, Janvier 1991.

19. B.T. Aström, R.B. Pipes and S.G. Advani, Journal of Comp. Mater., 26(9), pp. 1351-1373, 1992.

20. A.W. Chan, D.E. Larive and R.J. Morgan, Jour. of Comp. Mat., 27(10), 1993.

21. M. Kaviany, Int. Journ. of Heat Mass. Transfer., 28(4), pp. 851-858, 1985.

Table 1 Caracteristics of the NCS fabrics tested

		Glass Rovings		Polyester stitch wire	
	A real weight gr/m^2	Weight % MACHIHNE	Weight % CROSS	Weight % MACHINE	Weight % CROSS
NCS82675	320	48.5	44.3	4.9	2.3
NCS81053A	302	48.9	48.9	1.5	0.7

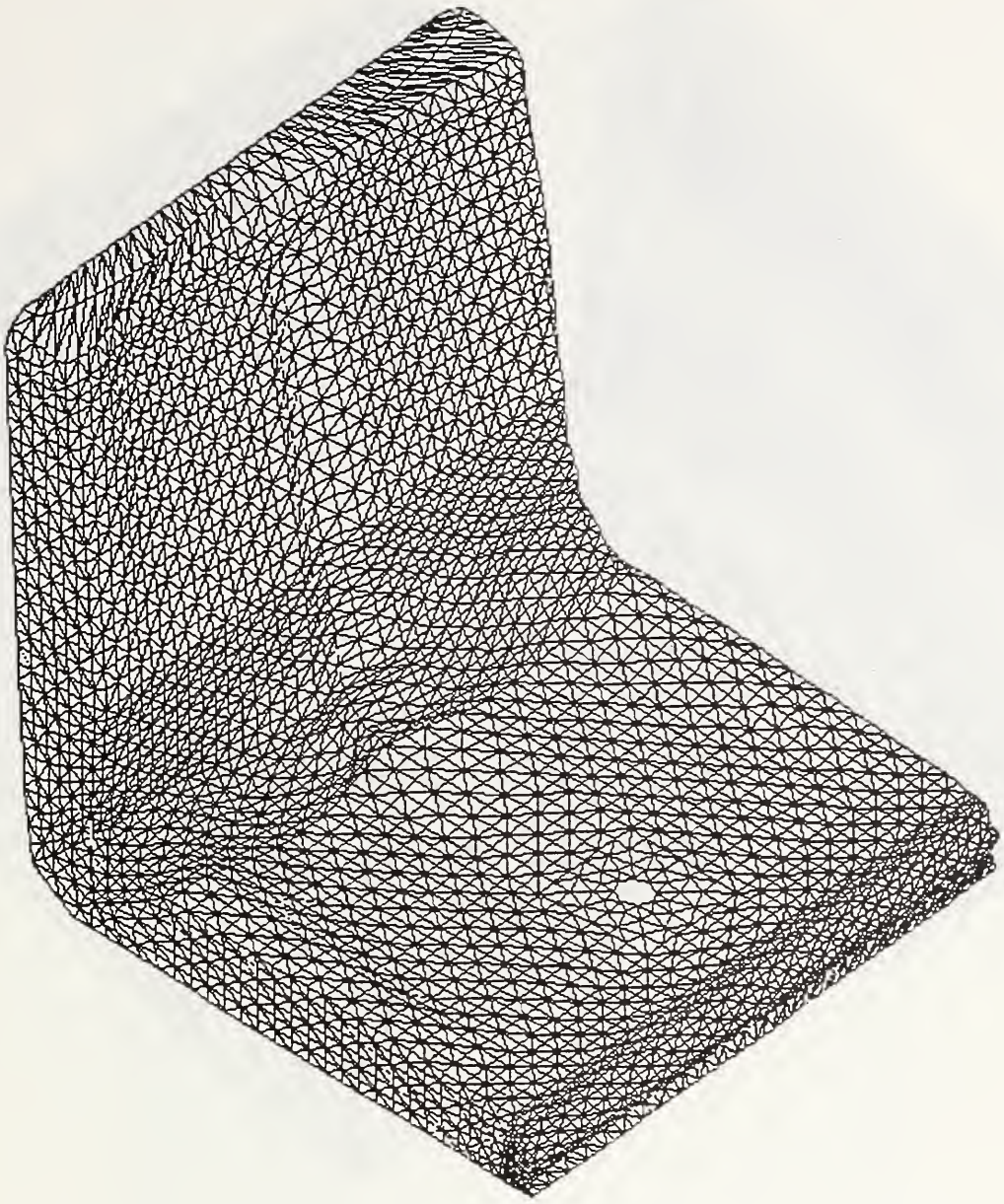

Figure 1 Finite element mesh for a subway seat

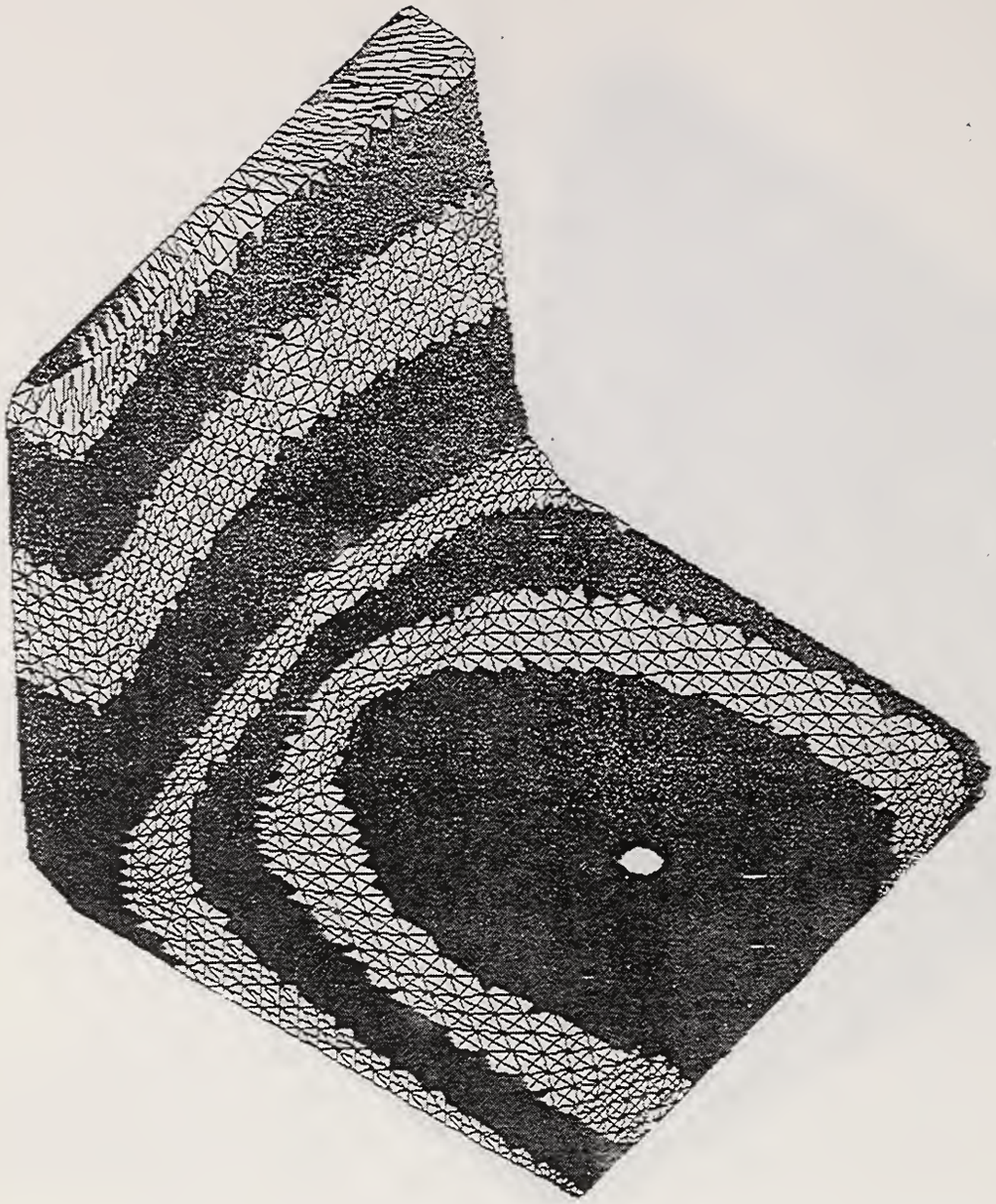

Figure 2 Successive flow front position

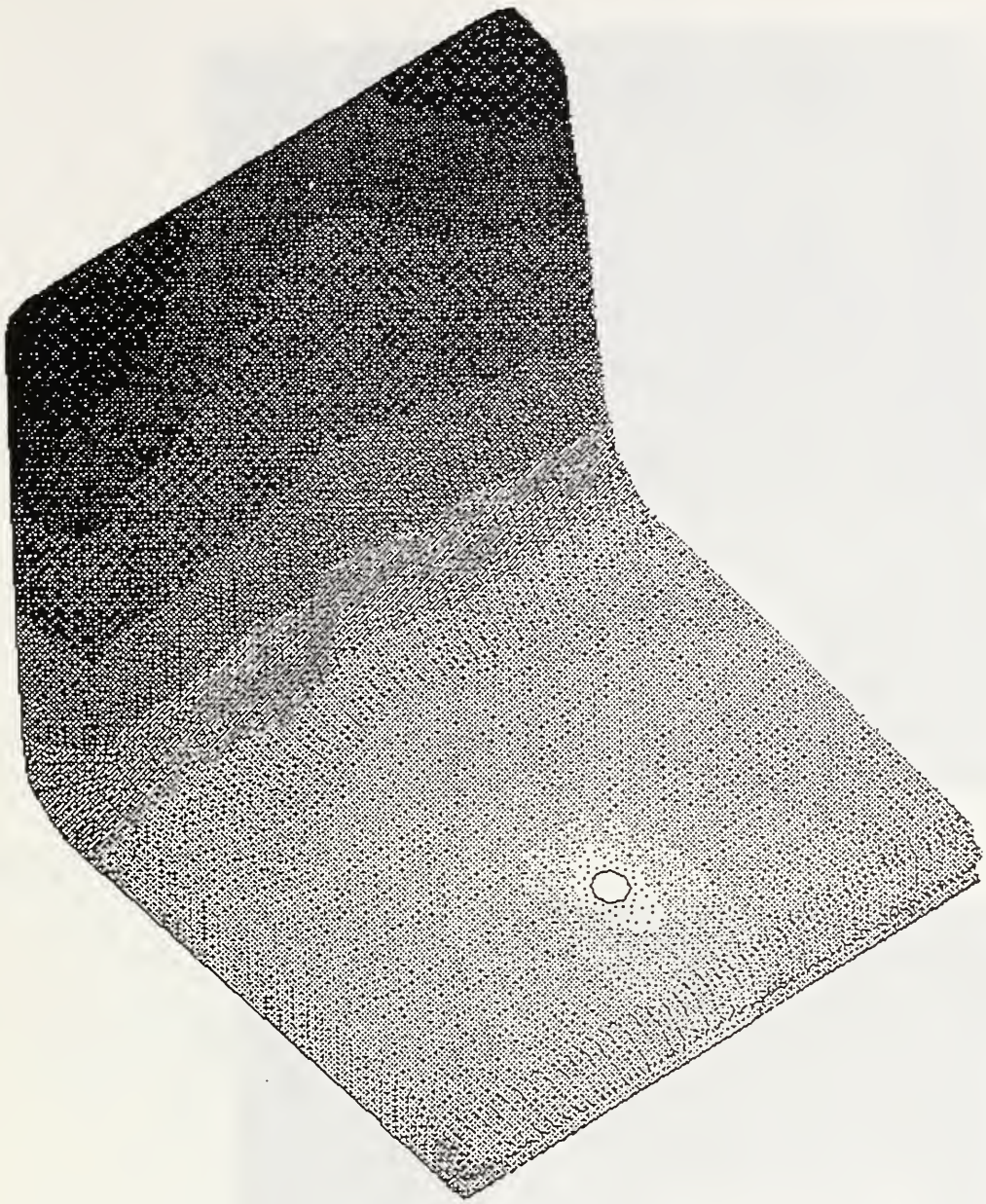

Figure 3 Pressure field at the end of filling

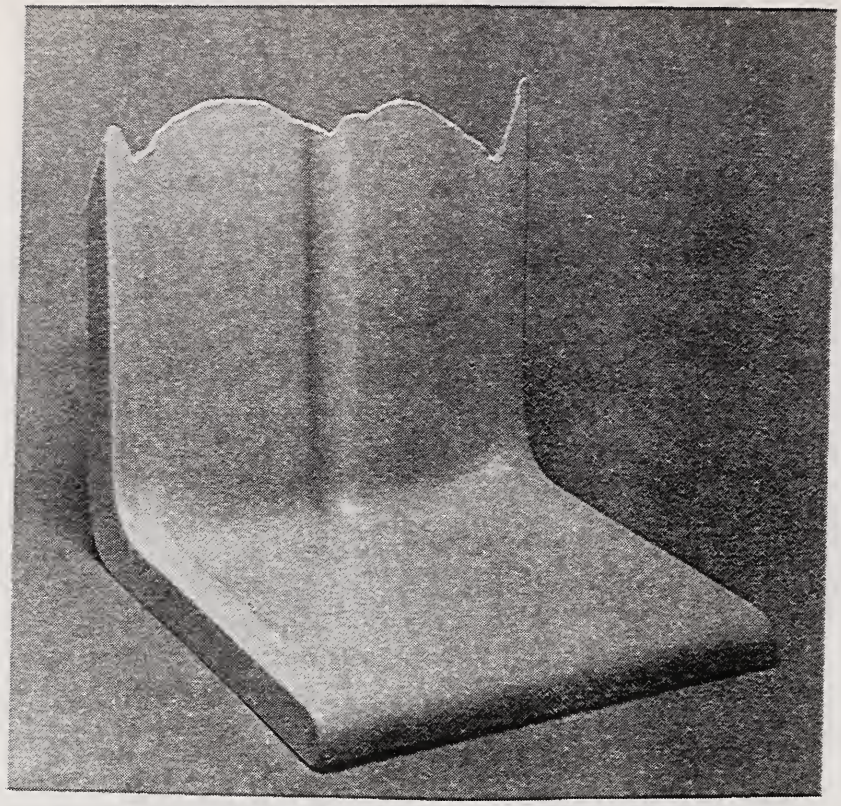

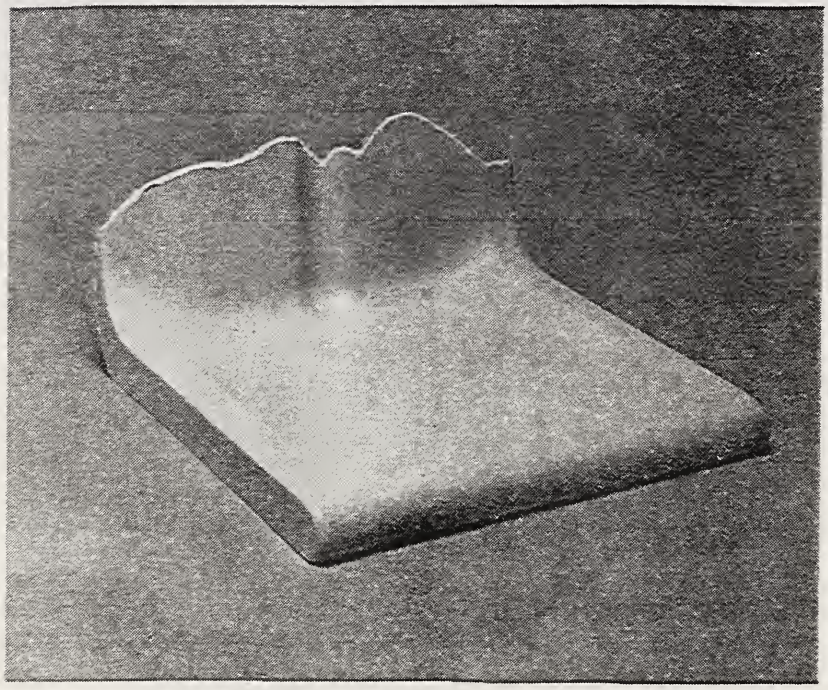

Figure 4 Short shots at two different time steps for the subway seat

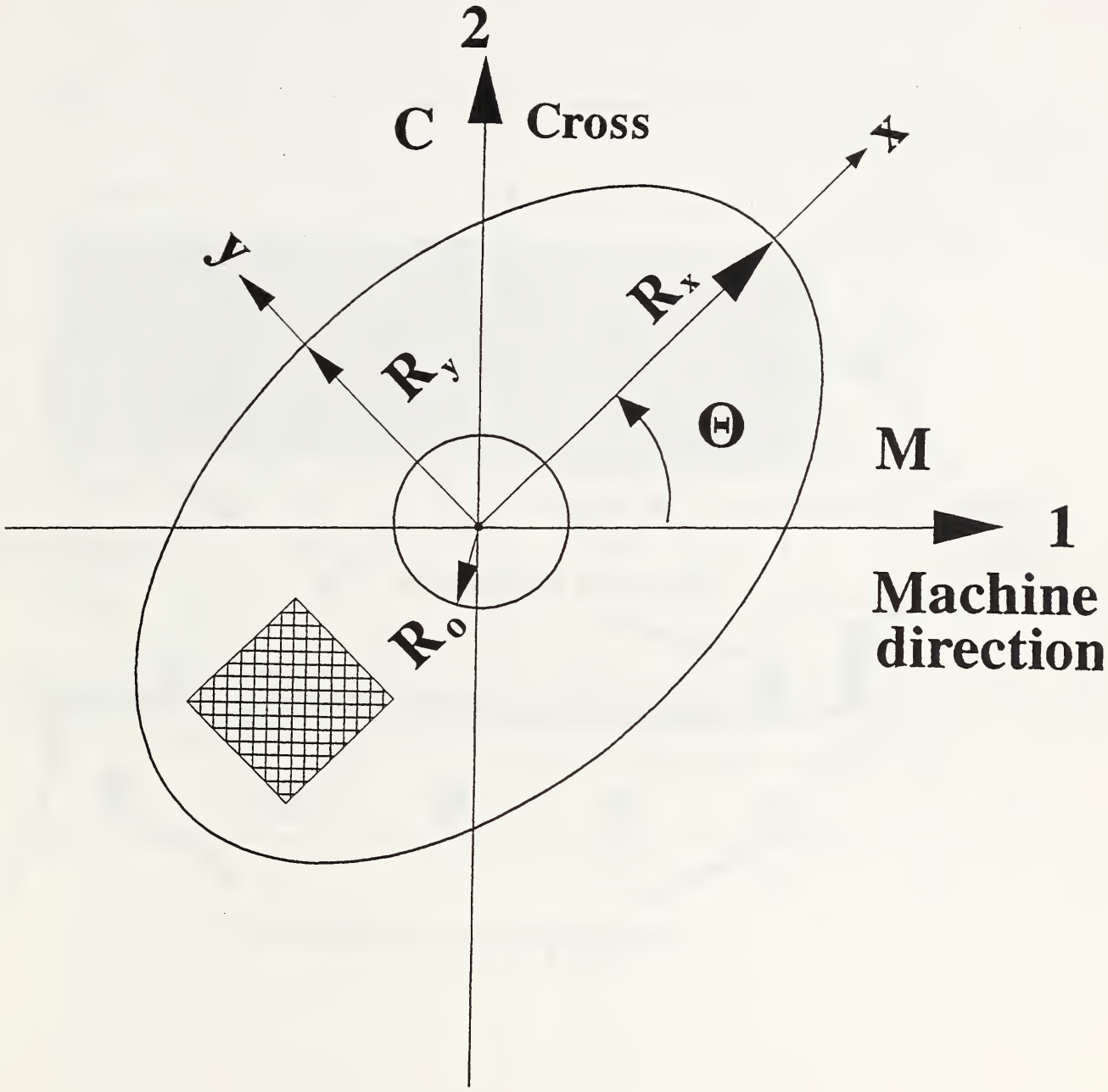

Figure 5 Schematic of the in-plane flow through an anisotropic homogenius uniform fiber reinforcement

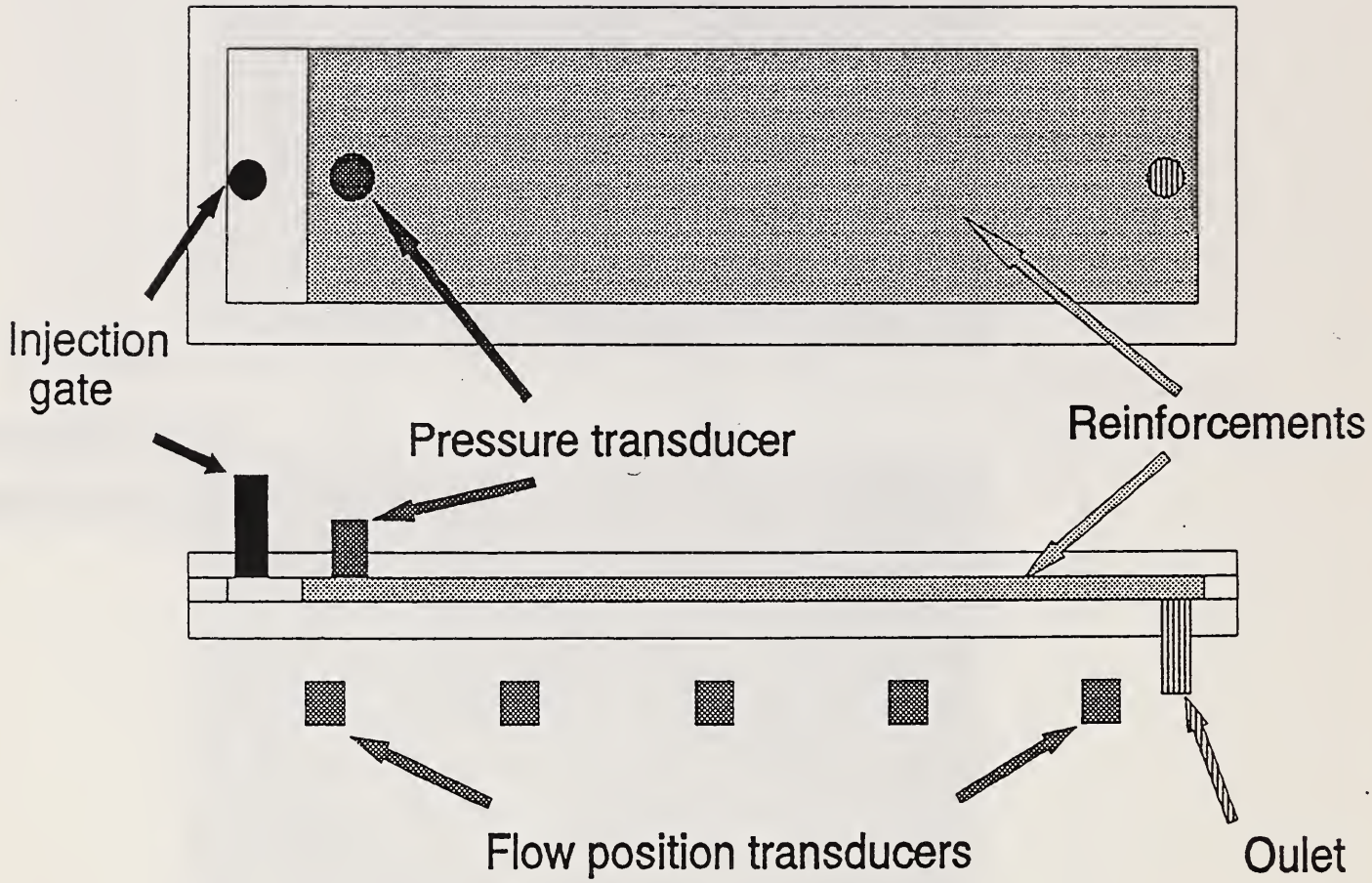

Figure 6 Schematic of an unidirectional flow set-up for permeability measurements.

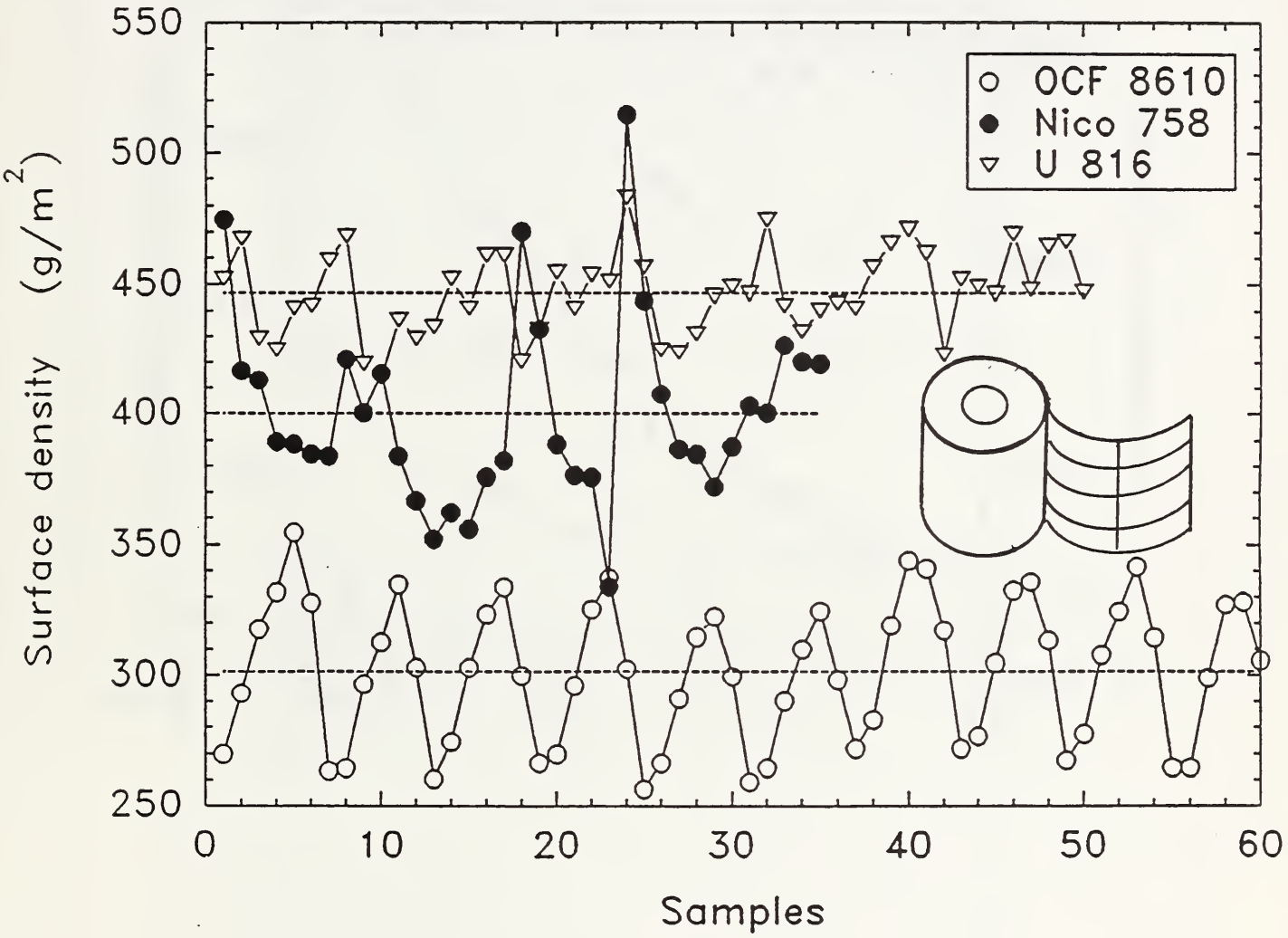

Figure 7 Variations of surface density for OCF8610, Nico758 and U816

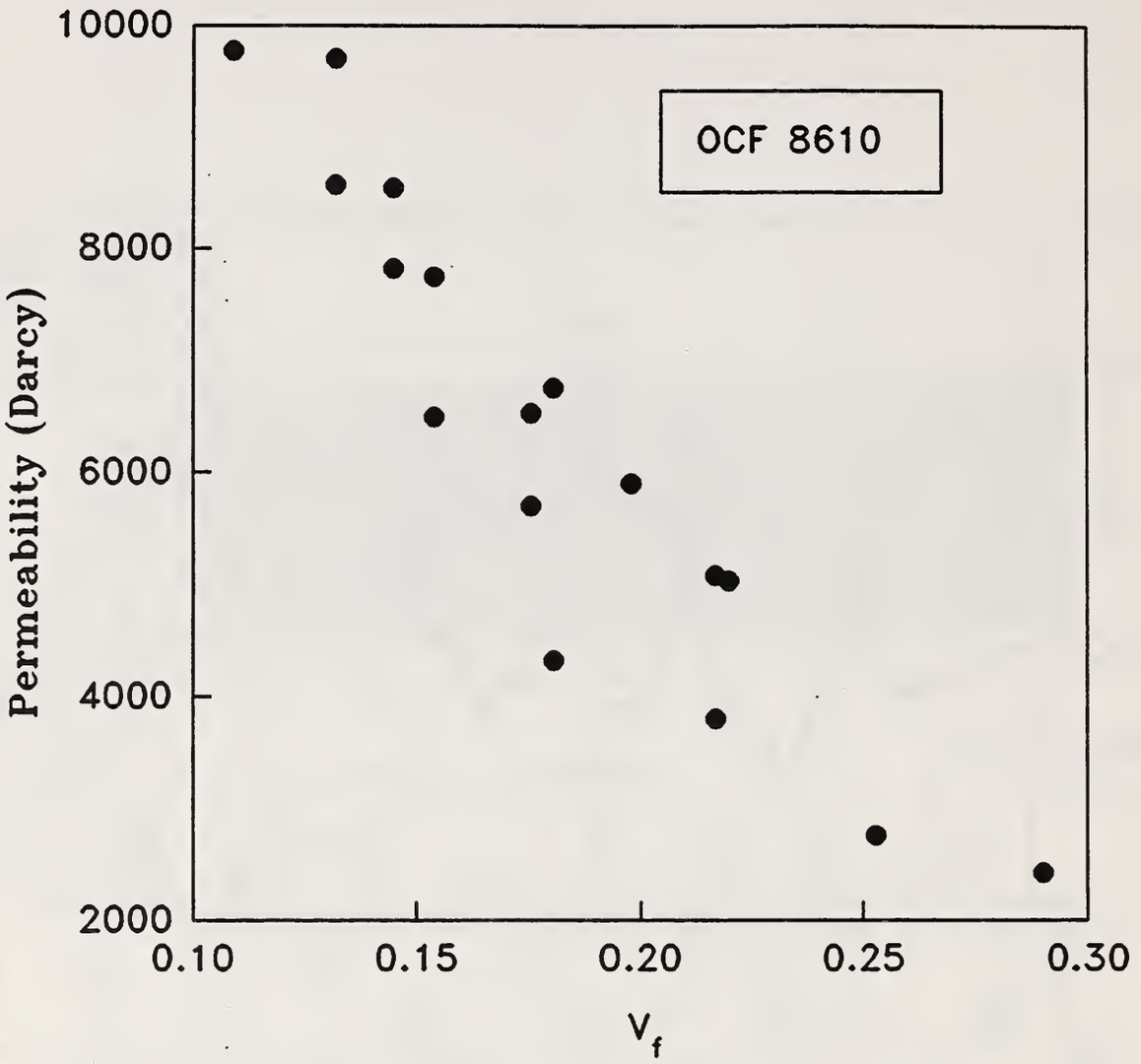

Figure 8 Permeability when computed with the nominal Mat surface density

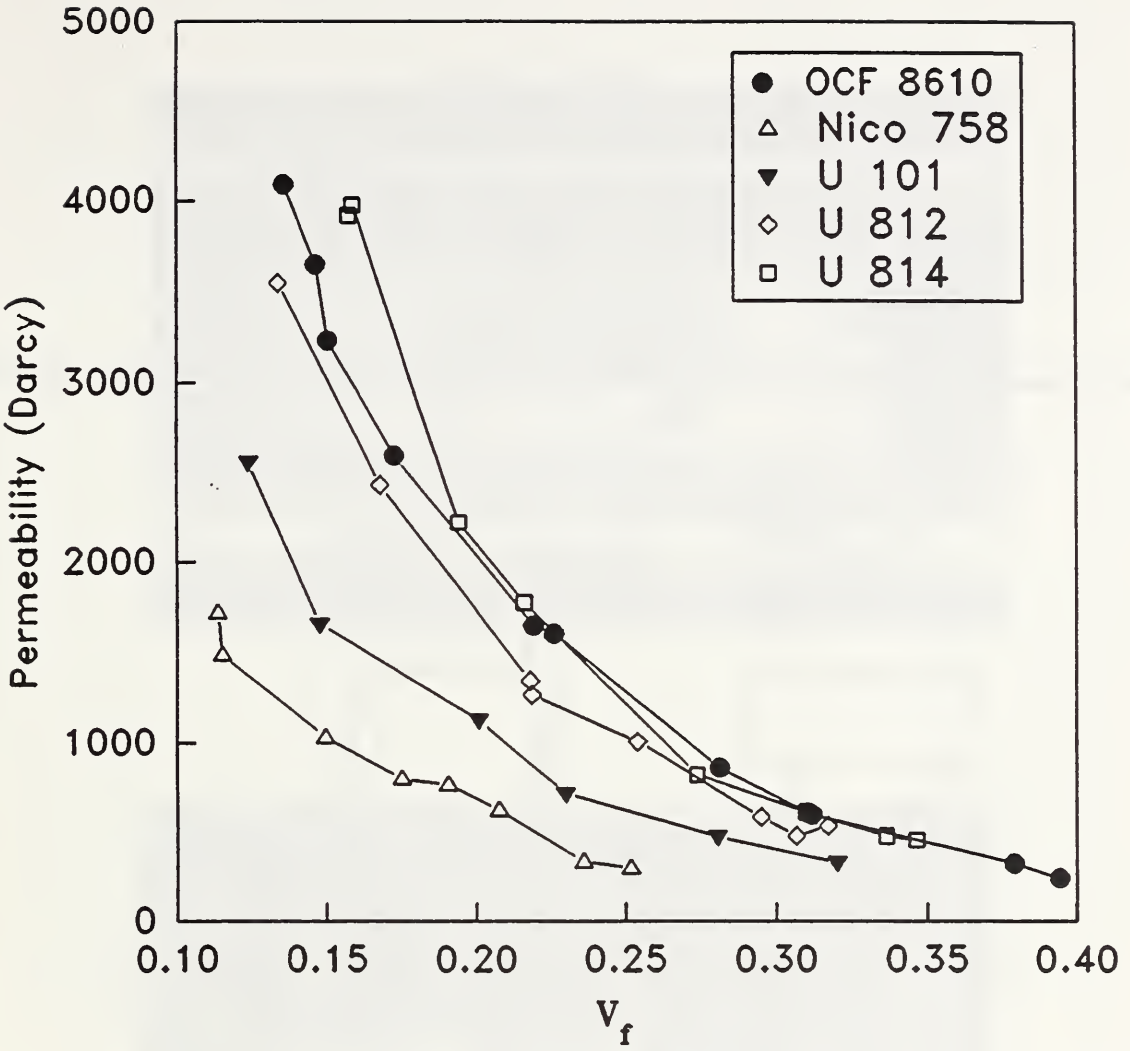

Figure 9 Permeability as a function of fiber volume content for individually weighted samples

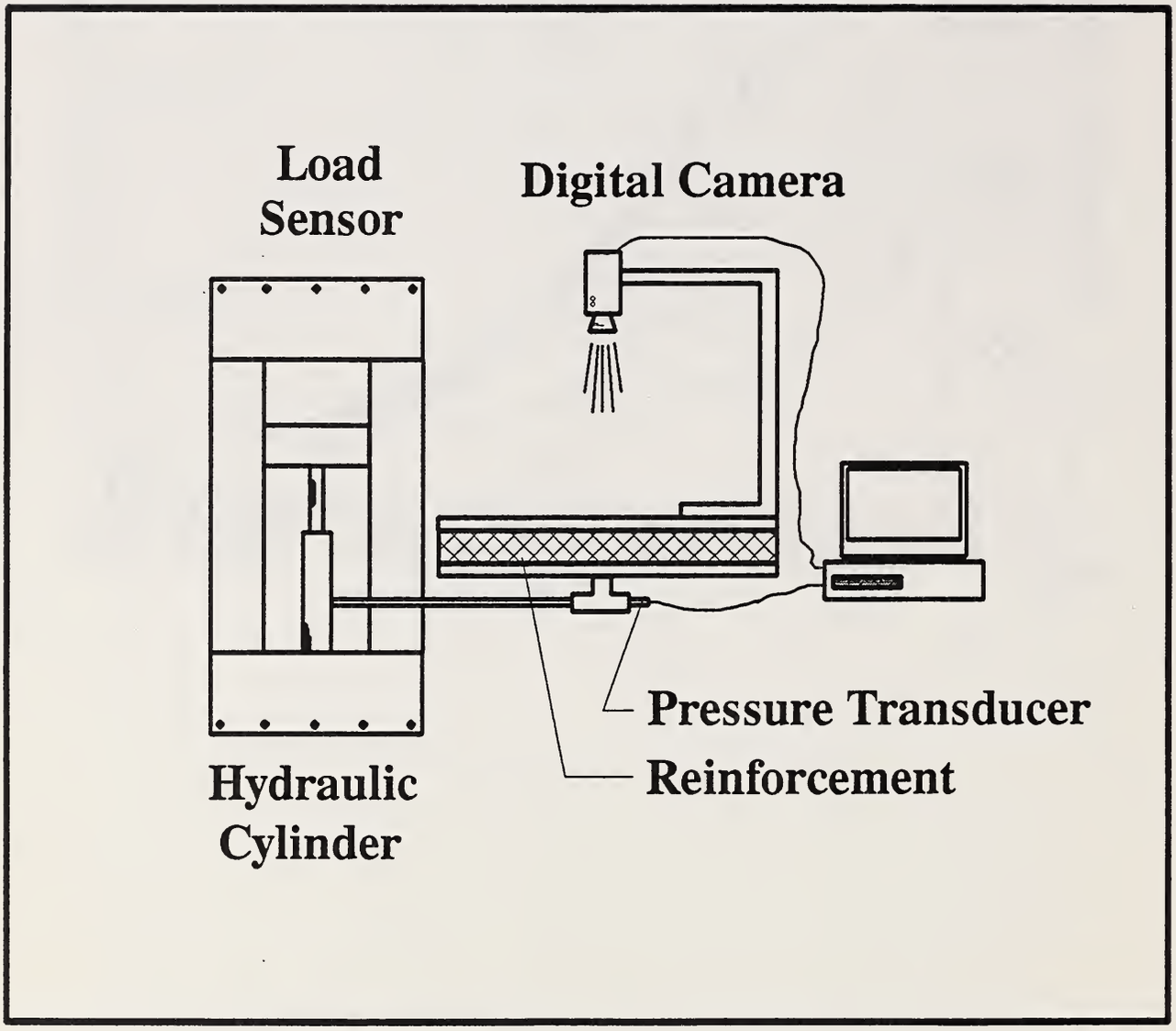

Figure 10 Schematic of the bidirectional flow measurement set-up

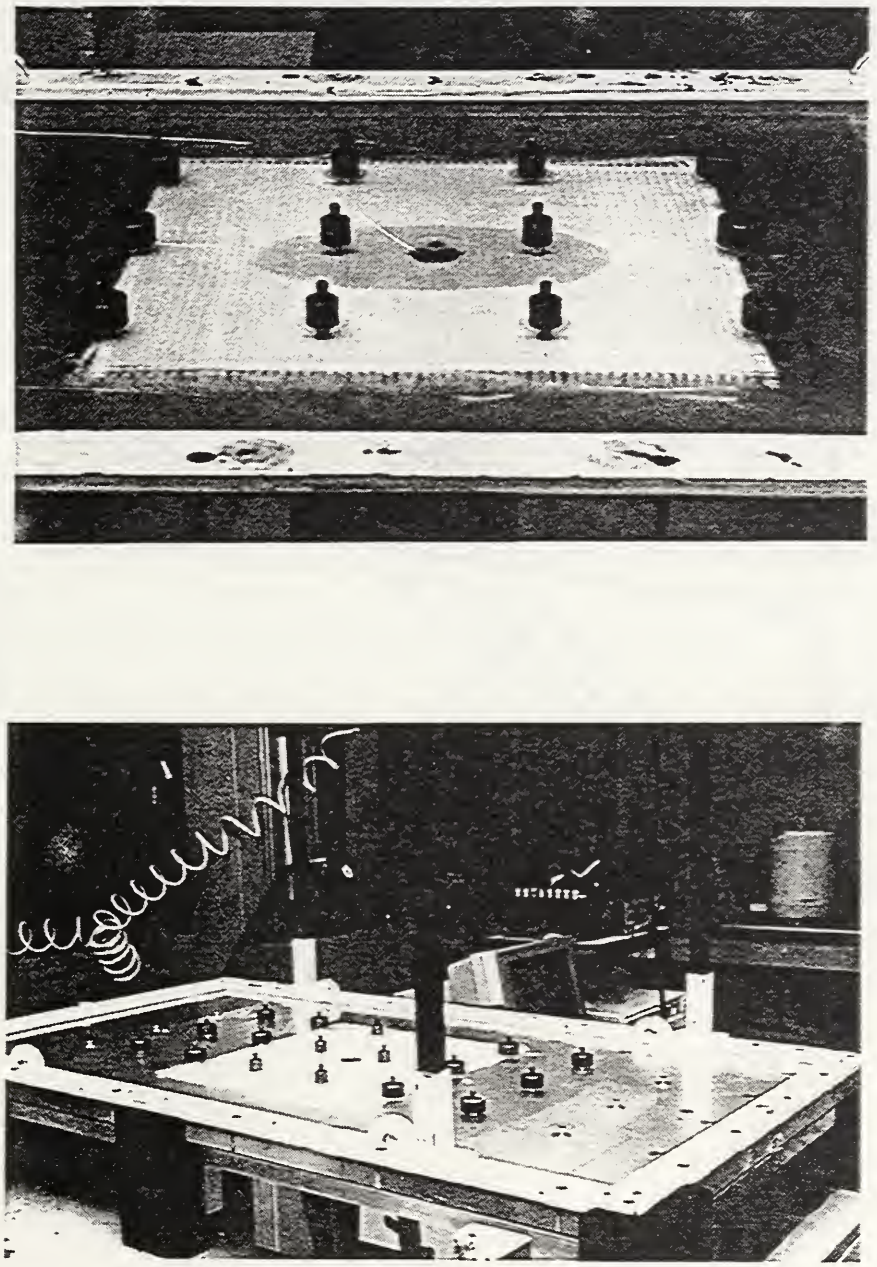

Figure 11 Bidirectional flow measurement facility

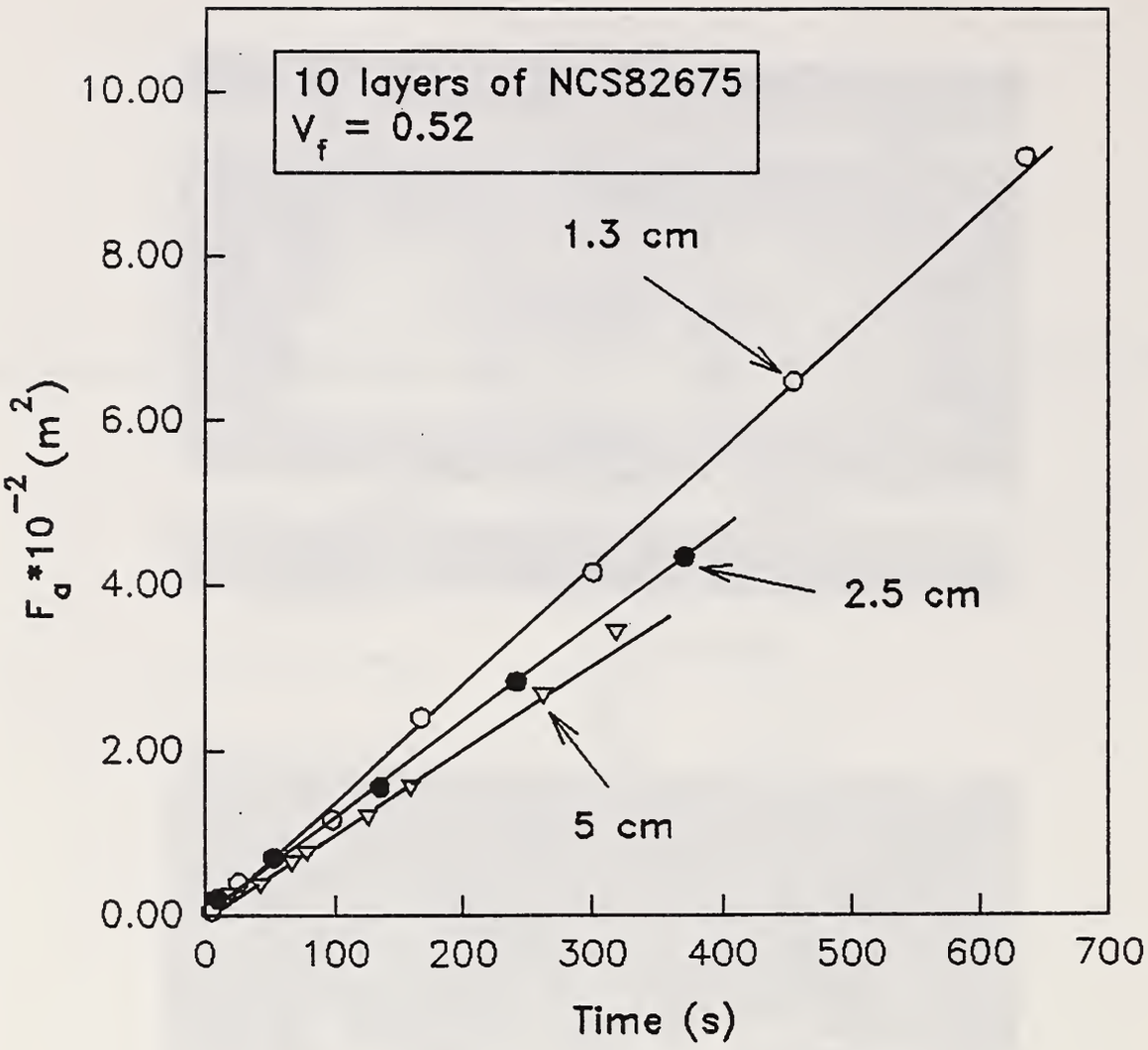

Figure 12 Plot of F_a from equations 17 and 18 as a function of time for three experiments using respectively 1.3 cm, 2.5 cm and 5 cm inlet diameters

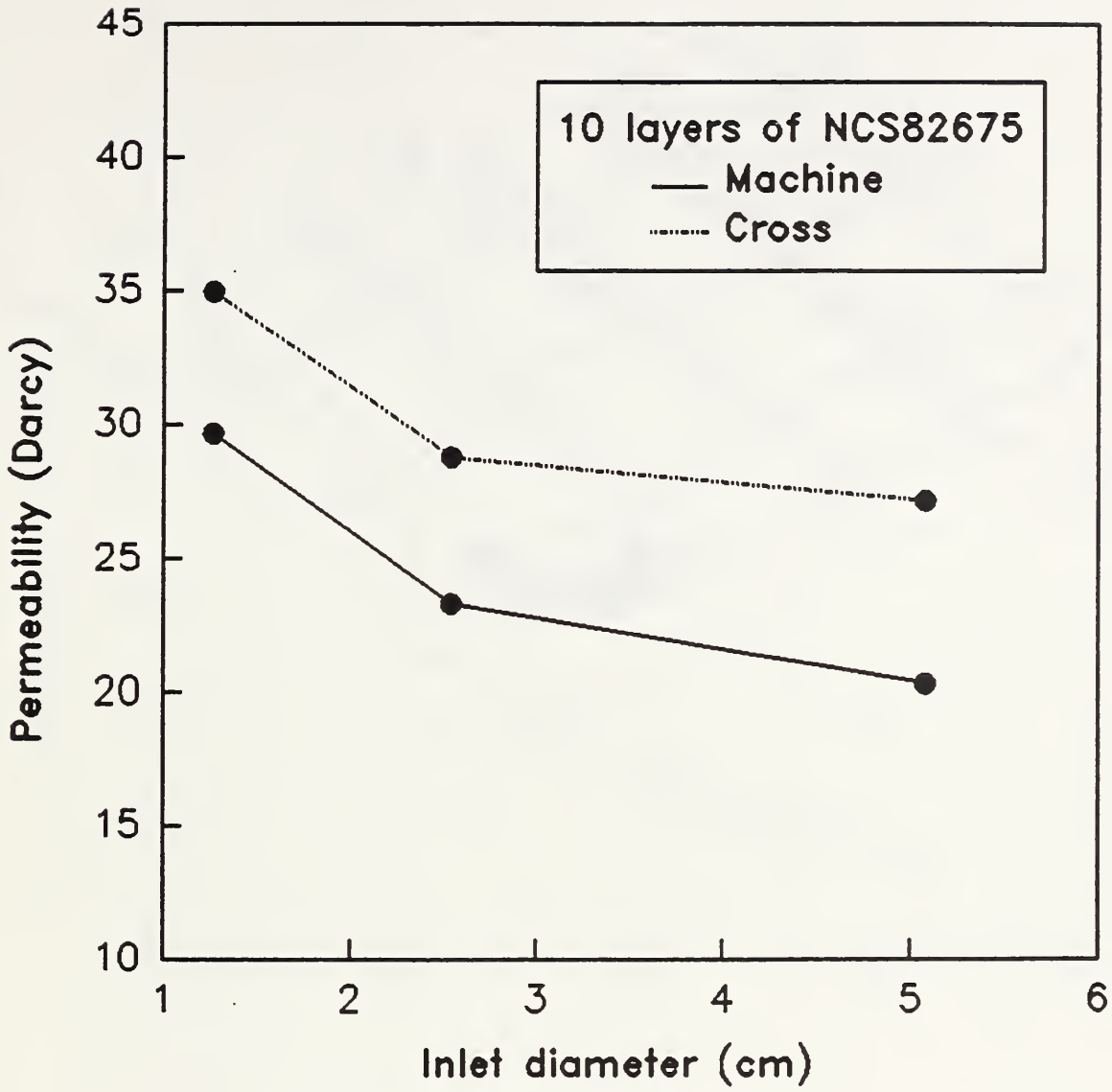

Figure 13 Permeability as a function of the inlet diameter for 10 layers of NCS82675 which gives a V_f = 0.52 in a 2.36 mm cavity

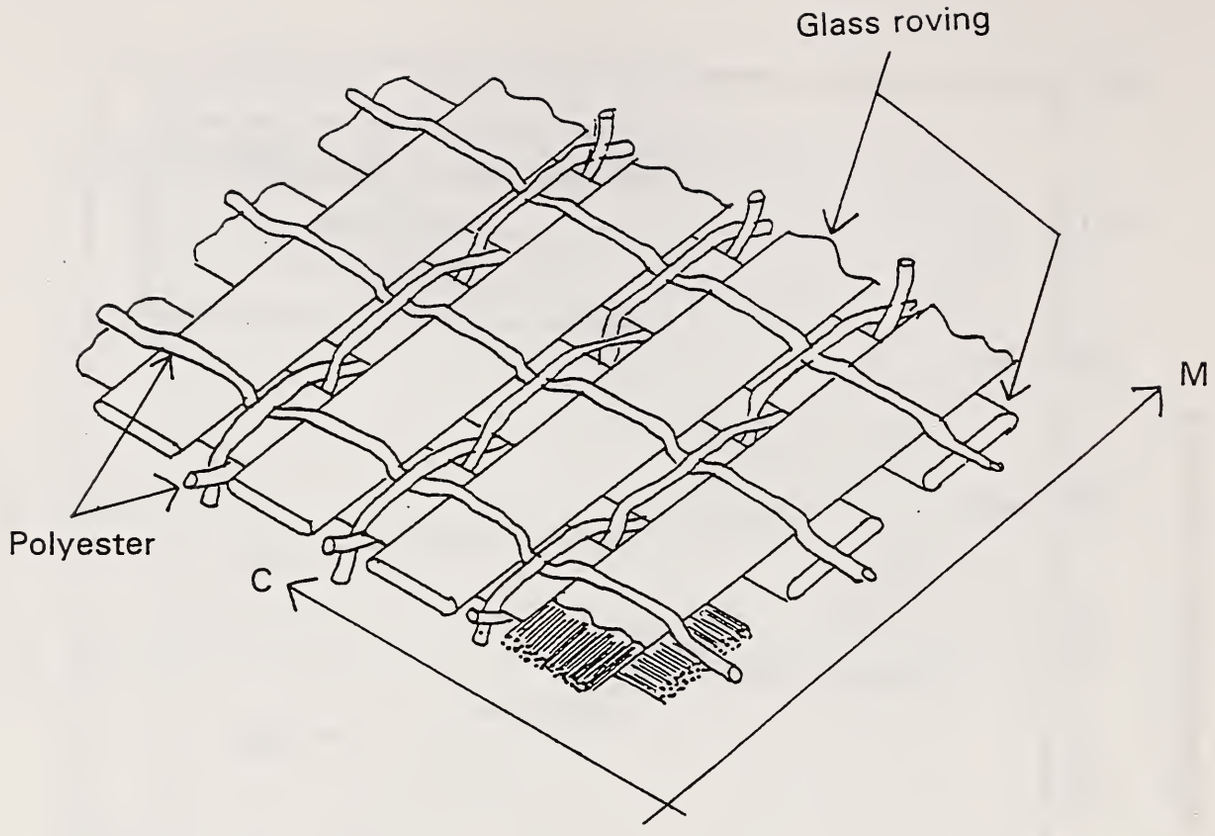

Figure 14 Fiber arrangement for the two NCS fabrics tested

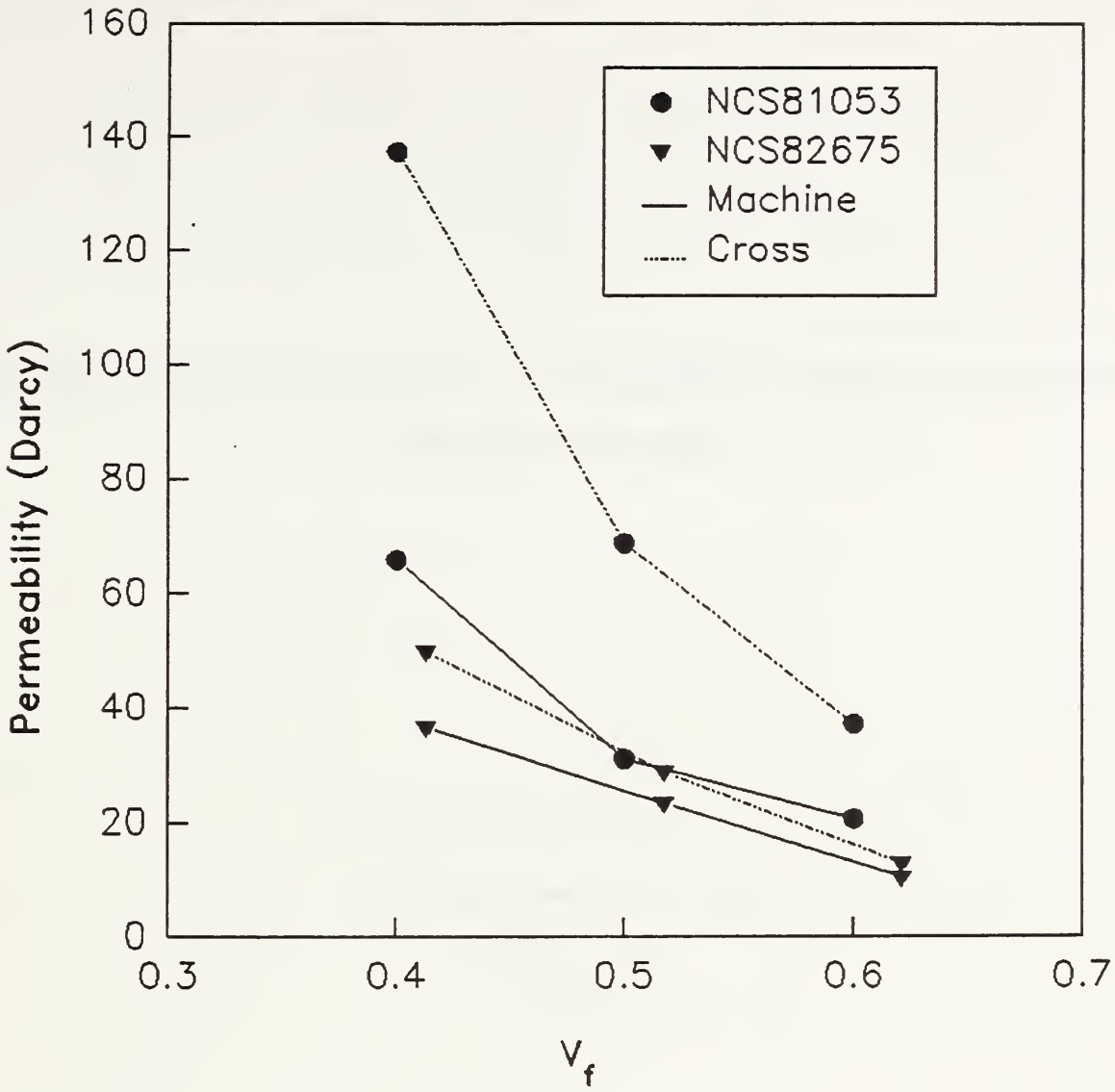

Figure 15 Permeability as a function of fiber volume fraction for two fabrics in the machine and cross direction

Measurement of in-plane permeability of anisotropic fibre reinforcements

B. Rikard Gebart and Peder Lidström

Swedish Institute of Composites
Box 271
S-941 26 Piteå
Sweden

Abstract

The permeability of fibre reinforcements for polymer composites is a crucial parameter for the impregnation of the reinforcement in most processing methods. Three of the most common methods (two with parallel flow and one with radial flow) for determination of the in-plane permeability tensor are studied both theoretically with an error propagation analysis and experimentally. A convenient method to determine both the principal directions and the principal values of the permeability tensor from measurements in three different directions is described.

The comparison of the methods shows that the parallel flow method gives a more accurate measurement in practice since the radial flow method suffers from a larger mould deflection due to the larger surface area of the mould. Experiments with radial flow in a stiffer mould shows that both the parallel flow and the radial flow method give the same result if the mould deflection is kept under control.

To overcome the disadvantage with a larger number of independent measurements in the parallel flow methods an alternative multi-cavity parallel flow method is suggested. A preliminary test with a double-cavity mould shows that the method works as expected. An advantage with the new method is that only the weight of fluid that flows out of the different cavities in a given time interval is necessary for determination of the ratio of the permeabilities. This makes it possible to relate the permeability tensor components to a reference porous medium with well defined permeability.

1. Introduction

Most processing methods for polymeric fibre composites involve steps with flow of a viscous fluid through a porous medium. Examples of such processes are resin transfer moulding (RTM), autoclave curing of prepregs and filament winding. The porous medium consist of a network of connected pores formed by the fibres in the reinforcement. The flow in this type of medium is well described by Darcy's law if the length scale of the part to be made is sufficiently large compared to the typical pore size [1]. Darcy's law in one dimensional flow is given by:

$$\frac{Q}{A} = \frac{K}{\mu}\frac{\Delta p}{L} \tag{1}$$

where Q [m^3/s] is the volumetric flow rate, A [m^2] is the area of the cross section of the test specimen and μ [Pas] is the viscosity. The pressure drop over the test specimen with length L [m] is Δp [Pa]. The constant of proportionality K [m^2] is usually called the permeability of the medium and is, according to the theory, only dependent on the geometry of the porous medium. The dimension of the various quantities is indicated within square brackets.
Darcy's law can be generalised to three spatial dimensions [1-3] by introduction of a tensor permeability K_{ij} [m^2]

$$u_i = \frac{K_{ij}}{\mu}\frac{\partial p}{\partial x_j} \tag{2}$$

The quantity u_i has often been called superficial velocity but a more fitting name would be volumetric flux density.
Both the one-dimensional and the multi-dimensional version of Darcy's law have been shown to agree excellently with experiment [4-7].
The crucial parameter in Darcy's law is the permeability which is a characteristic of the porous medium. It is often implicitly assumed that the permeability is a unique function of

the type of reinforcement fabric and the orientation of the individual layers in the stack. However, there will always be some degree of randomness between different mouldings due to misalignment of the layers and imperfections in the reinforcement layers (e.g. perturbations of the weaving pattern or surface weight variations).

Another common assumption is that the permeability is a unique function of the fibre volume fraction. Several models have been proposed for this function and used with relative success [8-10]. At a given fibre volume fraction it is generally believed that the permeability tensor is a constant regardless of the type of flow or actual value of the flow parameters as long as the pore Reynolds number is sufficiently low. However, it has been reported [4] that it is difficult to get the same value of the tensor components in different types of experiments even if care is taken in the experiments to minimise the errors so that they should give the same result. The experiments in [4] were done in thin moulds (3 mm) with radial flow and with parallel flow. Both experiments agreed excellently with Darcy's law but both the anisotropy and the magnitude of the permeability tensor components differed significantly. It was suggested by Gebart et al. [4] that the differences were due to experimental errors in the radial flow experiment.

The purpose of the present investigation is to investigate this problem in more detail and to try to find an objective and reliable method that can be used to determine the in-plane permeability of fibrous reinforcements. In the theory section an error propagation analysis is made for the different types of experiments that can be done to determine the permeability. This is followed by a section with experimental results from two types of experiments with two different types of reinforcements (Brochier Injectex 21091 and Vetrotex Unifilo U-812). In view of the experimental and theoretical results a new method with several attractive features is developed and presented in a separate section. Finally, the implication of the results for process simulations and industrial processing of composites is discussed.

2. Theory for permeability measurements

The generalised form of Darcy's law in eq.(2) defines the tensor permeability K_{ij}. The permeability tensor has, under relatively general conditions, been shown to be symmetric and positive definite [11]. A general proof of this property of the permeability tensor is possible with reciprocity techniques of the same type as in linear elasticity. The only assumption that is necessary for this proof is that the flow in the pores is governed by the lubrication approximation of the Navier-Stokes equations [12]. Hence, it will be assumed that the permeability tensor is symmetric and positive definite in the following.

The problem of mould filling is not fully stated without a continuity equation, an equation of state for the fluid and boundary conditions. The continuity equation in terms of flux density u_i is [2]:

$$u_{i,i} = 0 \tag{3}$$

in the case without sinks within the reinforcement. However, the case with sinks within the medium cannot be completely ruled out. One example where sinks could appear is the case with a fabric woven from fibre bundles that are nearly impermeable. In that case the space between the fibre bundles would be completely filled while there would still be voids inside the bundles. To a macroscopic observer it would appear as if there was a mass sink in the wetted part of the porous medium since some of the flow entering the mould would go into the fibre bundles and some of the flow would advance the flow front. However, under normal conditions it is likely that the impregnation of the fibre bundles will take place very soon after the flow front has passed. In other words the "sink effect" is a local effect close to the flow front. Hence, it will be assumed in this paper that the continuity equation is given by eq.(3).

The principal directions of the permeability tensor are not necessarily aligned with the "laboratory" coordinate system. Quantities evaluated in the laboratory coordinate system are indicated with primes (') while quantities evaluated in the coordinate system defined by the principal directions (the principal system) of the permeability tensor are without primes.

Moreover, it is assumed that one of the principal directions is out of the plane of the fabric to be tested.

2.1 Possible methods for permeability measurements

Any method to be used for permeability measurements must be relatively simple to perform and to evaluate. For this reason most of the methods reported in the literature has been either of radial flow type or of parallel flow type. A number of variations can be done on these methods. Examples of such variations are the use of either a stationary flow or a moving flow front.

Three different methods are commonly used to determine the effective permeability K_{eff}^{θ} in a given direction with angle θ to the laboratory coordinate system. The first two methods are done with unidirectional flow in a rectangular mould, the difference then lies in whether the flow is transient with moving flow front or stationary with saturated reinforcement.

The third method is to inject liquid through a hole in the reinforcement at the center of a flat mould. The shape of the flow front will then gradually go from a circle to an ellipse. The directions of the axes of the ellipse coincides with the principal directions of the permeability tensor. The radial position along the two principal directions of the moving flow front is registered as a function of time and the two principal values of the permeability tensor can be deduced from the results. In the two methods with unidirectional flow a total of three independent experiments have to be done for a completely unknown reinforcement while for the radial flow only one experiment is necessary. The formulas for computation of the effective permeability with the different methods are summarised in table 1.

Table 1: Theoretical formulas for computation of effective permeability

Method	K_{eff}^{θ}
Unidirectional flow, saturated reinforcement	$\frac{Q \mu L}{A \Delta p}$
Unidirectional flow, moving flow front	$\frac{\mu (1 - V_f)}{2 \Delta p} B_1$
Radial flow	$\frac{\mu (1 - V_f)}{\Delta p} \frac{1 - \alpha}{\alpha} R_0^2 B_2$

The constants B_1 and B_2 are slopes in least squares fits of functions of flow front position versus time. The curve fits that define the B_i's are the theoretical solution derived from Darcy's law and they have the form:

$$f_i (x_f, y_f) = B_i t \tag{4}$$

where (x_f, y_f) denotes the coordinates of the flow front at time t. In the case with unidirectional flow the solution is [9]:

$$f_u (x_f, y_f) = x_f^2 \tag{5}$$

The solution for radial flow is much more complicated but takes the general form of eq.4 [6]. The fibre volume fraction (V_f) used in the formulas has to be computed from the weight (m) of the reinforcement stack, the height of the cavity (h), the surface area of the reinforcement (width W and length L) and the density of the fibres (ρ). The α in the formula for radial flow denotes the ratio of the permeabilities in the principal directions and it has to be found through an iterative procedure. The formula for the radial flow permeability in Table 1 is the formula for the permeability in the x-direction, K_{xx}, and this is sufficient to determine K_{yy} if α is known. The whole procedure for the radial flow experiment has been described by

Adams et al. [6] while the unidirectional flow procedure with moving flow front has been described by Gebart [9] among others.

The basic equation for parallel flow is the one-dimensional version of Darcy's law in eq.(1) where the permeability K must be interpreted as an effective permeability defined by [7]

$$K_{eff}^{\theta} = K_{xx}\cos^2\theta\left(\left(1+\frac{K_{yy}}{K_{xx}}\tan^2\theta\right)-\frac{\left(\frac{K_{yy}}{K_{xx}}-1\right)^2}{\frac{K_{yy}}{K_{xx}\tan^2\theta}+1}\right) \qquad (6)$$

where θ is the angle between the laboratory coordinate system and the principal system.

In practice it is cumbersome to work with eq.(6) to evaluate the components of the in-plane permeability tensor. A more convenient way is to use the inverse of the permeability which in the following will be called the flow resistance. The flow resistance tensor and the permeability tensor has the same principal directions (if the permeability tensor is symmetric and positive definite). This makes it possible to find the principal directions of the permeability tensor by diagonalisation of the flow resistance tensor. After diagonalisation the components of the permeability tensor are found by inverting the components of the flow resistance tensor (this procedure is described in detail below).

The flow resistance is defined in the laboratory coordinate system as

$$R'_{ij}=\begin{bmatrix} R'_{xx} & R'_{xy} \\ R'_{xy} & R'_{yy} \end{bmatrix}=\frac{1}{K'_{xx}\cdot K'_{yy}-K'^{2}_{xy}}\begin{bmatrix} K'_{yy} & -K'_{xy} \\ -K'_{xy} & K'_{xx} \end{bmatrix} \qquad (7)$$

The components of the flow resistance tensor can be expressed in terms of the measured effective permeability (computed from one of the formulas for unidirectional flow in table 1)

$$R'_{xx}=\frac{1}{K_{eff}^{0^\circ}} \quad (8) \qquad R'_{yy}=\frac{1}{K_{eff}^{90^\circ}} \quad (9) \qquad R'_{xy}=\frac{1}{K_{eff}^{45^\circ}}-\frac{1}{2\cdot K_{eff}^{0^\circ}}-\frac{1}{2\cdot K_{eff}^{90^\circ}} \quad (10)$$

The angle between the laboratory co-ordinate system and the principal system is given by (cf. Mohr's circle in stress analysis)

$$\theta = \frac{1}{2}\arctan\left(\frac{2 \cdot R'_{xy}}{R'_{xx} - R'_{yy}}\right) \tag{11}$$

The principal values of the resistance tensor can be computed from

$$R_{xx} = \frac{1}{2}\left(R'_{xx} + R'_{yy}\right) + R \tag{12}$$

$$R_{yy} = \frac{1}{2}\left(R'_{xx} + R'_{yy}\right) - R \tag{13}$$

where

$$R = \sqrt{\frac{\left(\frac{1}{K_{eff}^{0^\circ}} - \frac{1}{K_{eff}^{90^\circ}}\right)^2}{4} + R_{xy}^2} \tag{14}$$

Finally, the inverse to the resistance tensor is the permeability tensor and it has the components

$$K_{xx} = \frac{1}{R_{yy}} \tag{15}$$

$$K_{yy} = \frac{1}{R_{xx}} \tag{16}$$

where K_{xx} is the largest principal value of the permeability tensor.

2.2 Error analysis

The three different methods can be compared from a theoretical point of view to see if either of the methods has some theoretical advantage over the others in terms of sensitivity to errors. The total error from each method is determined from the standard error formula [13]:

$$e_{tot} \approx \sqrt{\sum_{i=1}^{n}\left(\frac{\partial K}{\partial x_i}\right)^2 e_i^2} \tag{17}$$

Notice, that the error in the slope of a least square fit (the B_i:s) can be determined explicitly if the error in the values on which the fit is based is known [14]. To investigate the accuracy of the three different methods a comparison is made in Table 2. All measured values are assumed to have a relative error of 2% and the actual values are chosen close to typical experimental values. The computed permeability is in all cases $5.13 \cdot 10^{-10}$ m^2. Four of the parameters (W, h, m and ρ) in the table are the physical parameters needed to compute fibre volume fraction.

Table 2: Contribution to total error from different parameters

Parameter	Unidirectional flow, saturated reinforcement	Unidirectional flow, moving flow front	Radial flow
Q	16.7 %	-	-
μ	16.7 %	24.4 %	28.9 %
L	16.7 %	5.3 %	2.6 %
W	16.7 %	5.3 %	2.6 %
h	16.7 %	5.3 %	2.6 %
Δp	16.7 %	24.4 %	28.9 %
m	-	5.3 %	2.6 %
ρ	-	5.3 %	2.6 %
B_i	-	24.4 %	28.9 %
Total error	$2.51 \cdot 10^{-11}$ m^2	$2.07 \cdot 10^{-11}$ m^2	$1.91 \cdot 10^{-11}$ m^2
Relative error	4.9 %	4.0 %	3.7 %

The conclusion to be drawn from the comparison between the different methods is that although there is some difference between the three methods there is no theoretical reason to believe that anyone of the methods should be superior to the others. However, if a particular parameter should be difficult to determine with sufficient accuracy it would be advantageous to choose a method where the relative influence of this variable is small. As an example,

assume that the pressure is particularly difficult to measure. The radial flow method would then be the least suitable method because of its large sensitivity to errors in the pressure.

3. Experiments

The experiments were aimed at determining if the different methods can give consistent values for the permeability tensor. Two different moulds were used, one quadratic mould with a cavity dimension of 800x800x3 mm and one rectangular mould with a cavity dimension of 800x200x3 mm (see figures 1 and 2). The thickness of the mould cavities was checked over the whole surface by putting small pieces of modelling clay inside the mould before closing and by measuring the thickness of the pieces after opening. The mould thickness was found to be 3.1 and 3.0 mm respectively with a standard deviation of about 0.05 mm.

The mould surface deflection by an applied internal over pressure was also measured for both moulds and it was found that the deflection in the larger mould was more than five times larger than in the rectangular mould. The deflection was very close to linearly proportional to the over pressure in both cases. At 3 bars the deflection at the center of the large (quadratic) mould was close to 1 mm, i.e. about 30% of the cavity thickness (see figure 3).

An overview of the auxiliary equipment in the experimental set-up is shown in Figure 4.

Two different types of reinforcements were used in the experiments, one highly anisotropic fabric (Brochier Injectex 21091) and one almost isotropic continuous strand mat (Vetrotex Unifilo U-812). The experimental liquids were a commercial vinylester (BASF A-430) and a normal vegetable oil for cooking purposes (Melba 2042). Rheological measurements at different temperatures, different shear rates and with curing resin did not show any significant non-Newtonian behaviour. The rheological measurements also made it possible to determine the actual viscosity at the experimental temperature.

3.1 Results with traditional methods for permeability measurements

The experimental results agreed excellently with the theoretical solution for all three methods (see Figures 5-7). In the experiment with continuous flow in a saturated reinforcement a small deviation could be seen at the highest pressures (fig. 5) but this can be explained by the

significant deflection of the upper mould surface (app. 10% of the cavity thickness at the highest pressure).

For the two experiments with moving flow front (unidirectional and radial flow) an almost perfect agreement with the theory was obtained (figs. 6 and 7). However, the absolute value of the measured permeability computed from the experimental values differed between the two types of experiment by about 25% for the continuous strand mat and by even more for the Injectex fabric. The discrepancy between the two different methods (unidirectional and radial flow) can be explained by the much larger deflection of the point injection mould. To reduce the deflection with radial flow a new measurement on the Injectex fabric was made in the small mould. This was possible because the anisotropy of this fabric is so large that it will take a long time for the flow front to reach the mould wall if it is oriented appropriately in the mould. The resulting ratio between K_{xx} and K_{yy} was very close to the value obtained with unidirectional flow and saturated reinforcement. Moreover, the absolute value for the components of the permeability tensor only differed by about 3% (see table 3). Hence, it appears that the two methods (radial and unidirectional) can indeed give the same result if only the experimental parameters are under control.

The experiments with vegetable oil and either saturated flow or moving flow front show that these two methods give the same result within the experimental uncertainty (see Table 3). However, the numerical values are consistently on the high side in the moving flow front experiment compared to the saturated flow case and this can be a result of a slower impregnation inside the fibre bundles than outside them.

The two experiments with moving flow front and different experimental liquids show that the experimental liquid has no significant effect on the result as long as the viscosity is known.

Table 3: Summary of all permeability experiments.

Method	Exp. liquid	Reinf. type	K^0	K^{45}	K^{90}	K^0/K^{90}
Moving front, uni.	Vegetable oil	Unifilo U-812	$3.81 \cdot 10^{-10}$	$3.98 \cdot 10^{-10}$	$5.12 \cdot 10^{-10}$	0.74
Saturated, uni.	- " -	- " -	$3.67 \cdot 10^{-10}$	$3.85 \cdot 10^{-10}$	$4.72 \cdot 10^{-10}$	0.78
Moving front, uni.	Vinyl ester	- " -	-	-	$4.84 \cdot 10^{-10}$	-
Moving front, rad.	- " -	- " -	$4.87 \cdot 10^{-10}$	-	$6.38 \cdot 10^{-10}$	0.76
Moving front, uni.	Vegetable oil	Injectex 21091	$8.71 \cdot 10^{-10}$	-	$0.47 \cdot 10^{-10}$	18
Saturated, uni.	- " -	- " -	$8.54 \cdot 10^{-10}$	$0.80 \cdot 10^{-10}$	$0.37 \cdot 10^{-10}$	23
Moving front, rad.	Vinyl ester	- " -	$7.61 \cdot 10^{-10}$	-	$0.67 \cdot 10^{-10}$	11
Moving front, rad. in small mould	- " -	- " -	$8.36 \cdot 10^{-10}$	-	$0.38 \cdot 10^{-10}$	22

4. New method for measurement of in-plane permeability tensor

The experiments with the different methods showed that it is very important to avoid deflection of the mould by the injection pressure. In a mould for radial flow measurement of permeability of a practically useful size, there will always be some deflection. This is true even if the injection pressure is very low since the reinforcements used for composites act like a non-linear spring and a significant compaction pressure is needed to close the mould. This is a very unfortunate fact since the radial flow experiment is very attractive because of its simplicity (only one experiment needed). The uni-directional flow experiments on the other hand can be made in a smaller width mould and hence with a smaller deflection for a given internal (compaction + injection) pressure. The disadvantage with this type of experiment is that three independent measurements are needed before the full in-plane permeability tensor can be computed.

To eliminate the disadvantage of the unidirectional flow method while maintaining its advantages we suggest to make the permeability measurement in a specially constructed mould (fig. 8) with multiple cavities. The width of the cavities is kept relatively small and the

mould is closed with screws both around the outer circumference and between the parallel cavities to minimise the mould deflection from the injection pressure and the compaction pressure from the reinforcement. The cavities are all connected to a "plenum chamber" which will serve to provide a common injection pressure for all four cavities. One of the cavities can be loaded with a reference porous medium of well defined permeability while the other three cavities are loaded with the test reinforcement oriented in the 0°, 45° and 90° directions respectively.

The experiment is very simple, all that is needed is to measure the flow rate out of all four cavities at a constant inlet pressure and at a constant temperature. The ratio of the effective permeabilities is then (cf. eq.1) equal to the ratio of the flow rates (or the weight of the fluid that comes out of each cavity over a given interval in time). An additional advantage of the method is that the viscosity of the test fluid (if Newtonian), the temperature (if isothermal) and the injection pressure can be unknown if a suitable reference porous material is available to put in the fourth cavity. The known permeability can then be used to compute the numerical values of the other effective permeabilities.

The idea was tested in an experiment in the unidirectional flow mould. In this experiment resin was injected at the center of the mould with Injectex fabric oriented in the 0° and 45° direction on both sides of the injection hole so that a two-cavity mould was achieved (fig. 9). The measured ratio of the weight of resin that came out of each side agreed excellently with the ratio between the previously measured permeabilities.

5. Discussion

Three different methods for permeability measurements have been investigated. A theoretical error analysis shows that there is no obvious advantage with each method. However, an experimental investigation of two different reinforcements show that the different methods give values that differ more than could be expected from the error analysis assuming equal errors of 2%. The main error source is identified as the larger deflection of the mould in the radial flow experiment. A renewed experiment with radial flow in the smaller (stiffer) mould resulted in identical results within the experimental uncertainty for all three methods.

An alternative method with a multi cavity mould is proposed as a compromise between the simplicity of the radial flow and the smaller errors (in practice) with the unidirectional flow method. Initial tests with this method show that it gives results very close to those with the other methods.

The excercise presented in this paper shows that even a seemingly simple experiment can be very difficult to predict (predicting the outcome of the radial flow experiment based on the results from the unidirectional experiment or v.v.). In a more complex situation this will be even more difficult. This is a thought provoking fact for anyone considering large scale mould filling simulations in RTM. Probably the most important factors for a successful mould filling simulation are the deflection of the mould by the injection pressure and the resulting change in permeability. In order to include these effects in a simulation both the elastic behaviour of the mould and the permeability of the reinforcement at different fibre volume fractions has to be known.

6. Acknowledgements

We would like to thank Professor Peter Gudmundson for many fruitful discussions during the work with this paper.

7. Nomenclature

Q = Volumetric flow rate [m^3/s]

A = Cross section area of cavity in unidirectional flow [m^3/s]

K = Permeability [m^2]

μ = Viscosity [Pas]

Δp = Pressure difference driving the flow [Pa]

L = Length of the reinforcement [m]

K_{ij} = Permeability tensor [m^2]

u_i = Volumetric flux density [m/s]

B_i = Slope in least-squares fit of experimental values to theoretical line

V_f = Fibre volume fraction

α = Ratio of permeability components K_{yy}/K_{xx}

R_0 = Central hole radius in reinforcement for radial flow [m]

θ = Angle between laboratory coordinate system and principal system

R_{ij} = Flow resistance tensor [m^{-2}]

e_{tot} = Total error in measurement

ρ = Density of rerinforcement [kg/m^3]

m = Mass of reinforcement stack to be loaded in cavity [kg]

W = Width of mould cavity [m]

h = Thickness of mould cavity [m]

$K_{eff}^{0°}$ = Effective permeability in 0° direction [m^2]

8. References

1 Kaviany, M., *Principles of heat transfer in porous media*, Springer Verlag, New York, 1991

2 Collins, R.E., *Flow of fluids through porous materials*, Reinhold Publishing Co., New York, 1961

3 Whittaker, S., "Flow in porous media I: A theoretical derivation of Darcy's law", *Transport in Porous Media*, **1**, pp3-25, 1986

4 Gebart, B.R., P. Gudmundson, L.A. Strömbeck & C.Y. Lundemo, "Analysis of the permeability in RTM reinforcements", *Proc. ICCM/8*, Honolulu, 1991

5 Fracchia, C.A., "Numerical simulation of resin transfer molding", M.Sc. Thesis, University of Illinois, 1990

6 Adams, K.L., W.B. Russel & L. Rebenfeld, "Radial penetration of a viscous liquid into a planar anisotropic medium", *Int. J. Multiphase Flow*, **14**, pp203-215, 1988

7 Salem, A.J. & R.S. Parnas, "The unidirectional and radial in-plane flow of fluids through woven composite reinforcements", *Proc. 6th Technical Conference, American Society for Composites*, Albany, New York, 1991

8 Carman, P.C., "Fluid flow through granular beds", *Trans. Int. Chem. Eng.*, **15**, pp150-166, 1937

9 Gebart, B.R., "Permeability of unidirectional reinforcements for RTM", *J. Composite Materials*, **26**, pp100-1133, 1992

10 Gutowski, T.G., Z. Cai, S. Bauer, D. Boucher, J. Kingery & S. Wineman, "Consolidation experiments for laminate composites", *J. Composite Materials*, **21**, pp650-669, 1987

11 Sanchez-Palencia, E., *Non-homogeneous media and vibration theory*, Springer Verlag, Berlin, 1980

12 Gudmundson, P., Personal communication, 1992

13 Scarborough, J.B., *Numerical mathematical analysis*, Johns Hopkins, Baltimore, 1955

14 Press, W.H., B.P. Flannery, S.A. Teukolsky & W.T. Vetterling, *Numerical recipes. The art of scientific computing*, Cambridge University Press, Cambridge, 1989

Captions

Figure 1: Dimensions of mould and stiffening beams for parallel flow experiments.

Figure 2: Dimensions of mould and stiffening beams for point injection experiment.

Figure 3: Measured cavity deflection with internal over pressure. Mould 1 is the unidirectional flow mould and mould 2 is the mould for radial flow.

Figure 4: Experimental set-up for permeability measurements.

Figure 5: Comparison of Darcy's law (solid line) to experiments (symbols) for unidirectional flow through a saturated reinforcement. Notice the deviation at high injection pressure.

Figure 6: Comparison of theoretical solution (solid line) to experiments (symbols) for unidirectional flow with moving flow front.

Figure 7: Comparison of theoretical solution (solid line) to experiments (symbols) for radial flow with moving flow front.

Figure 8: Definition sketch for the multi-parallel flow method for permeability measurements.

Figure 9: Definition sketch for the double-parallel flow method for permeability measurements.

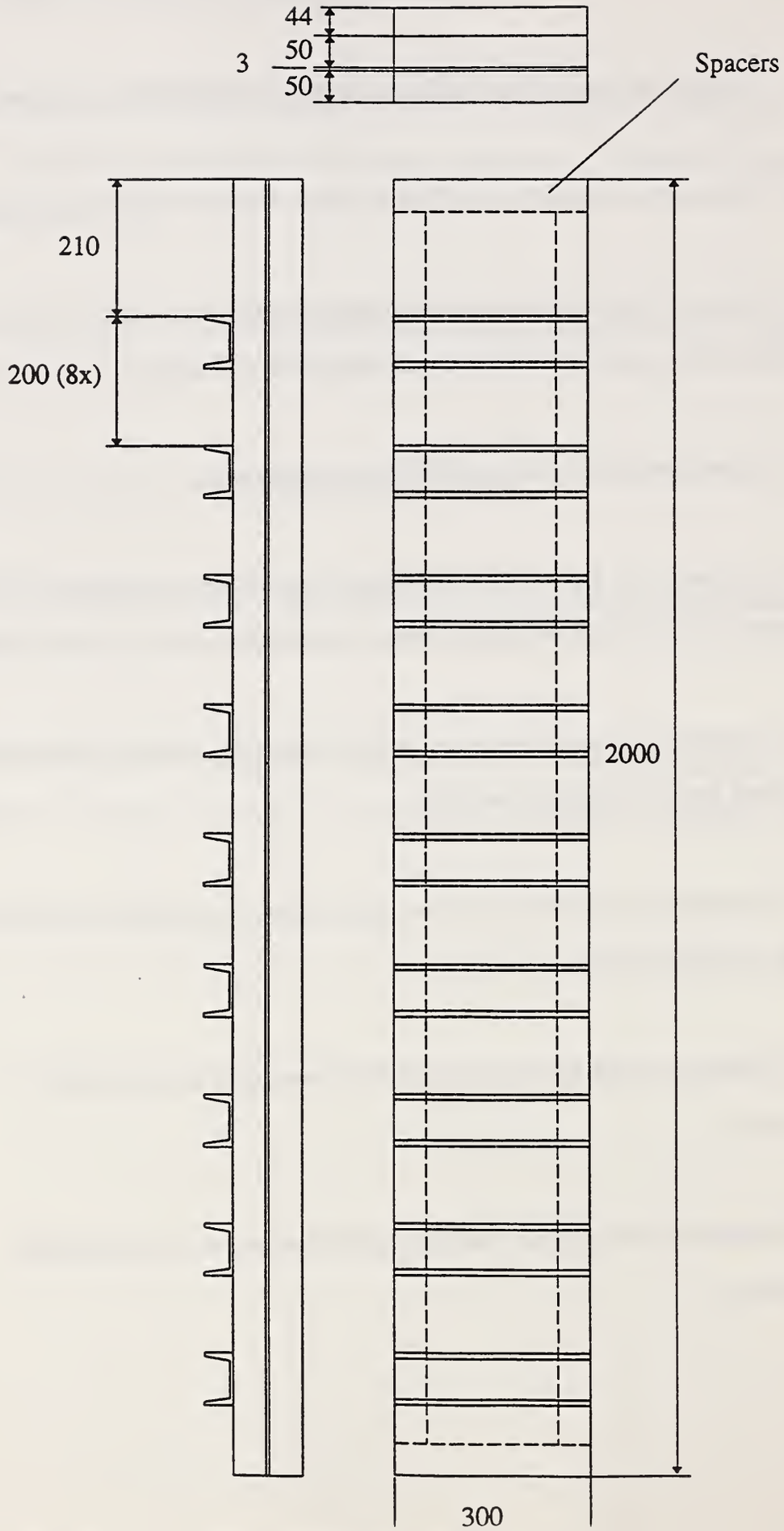
44
3
50
50
Spacers
210
200 (8x)
2000
300

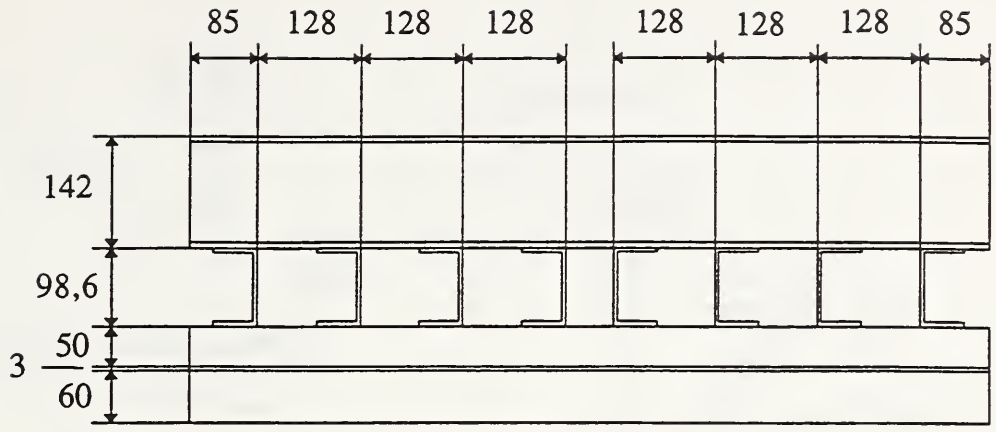
85
128
128
128
128
128
128
85
142
98,6
3
50
60

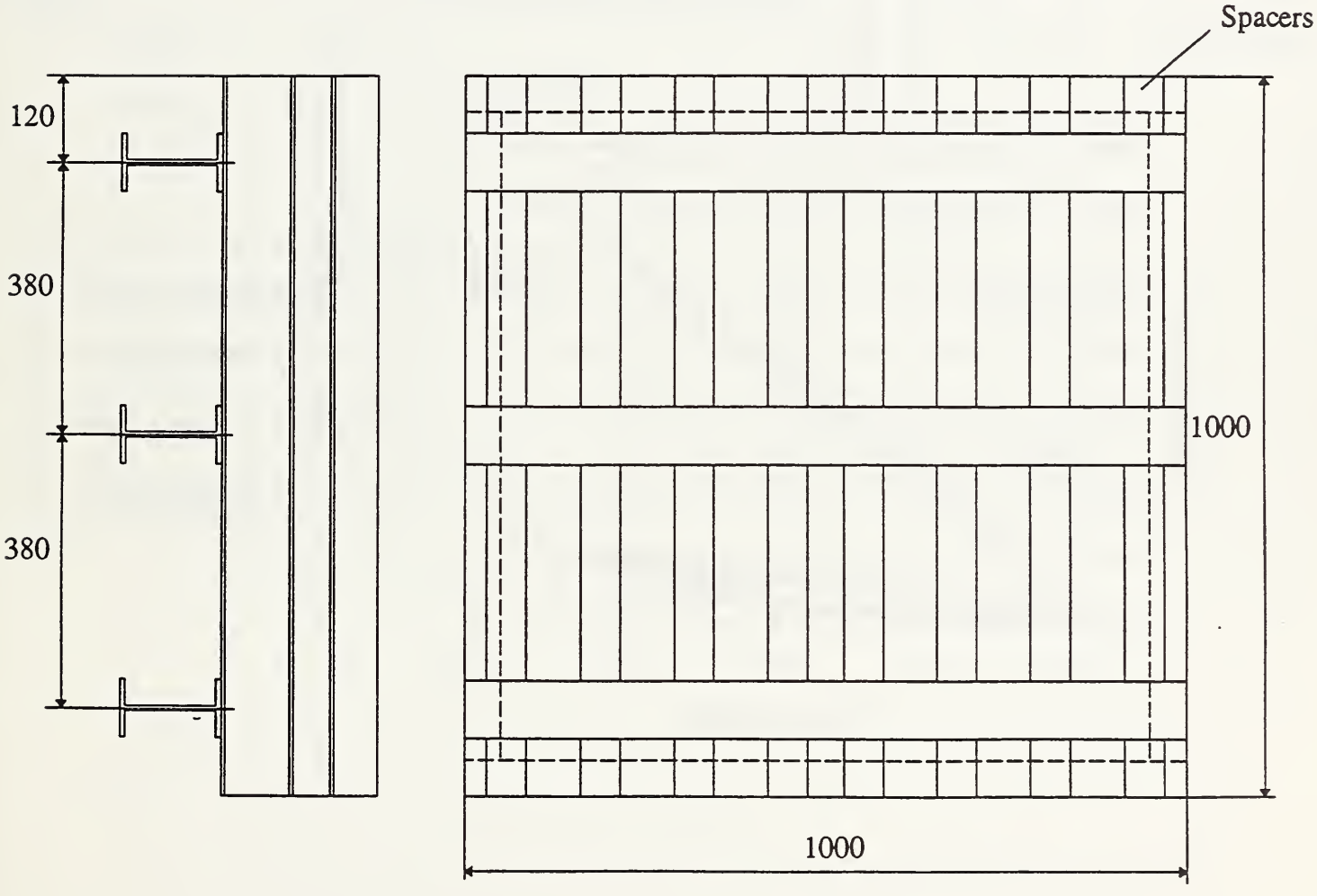
Spacers
120
380
380
1000
1000

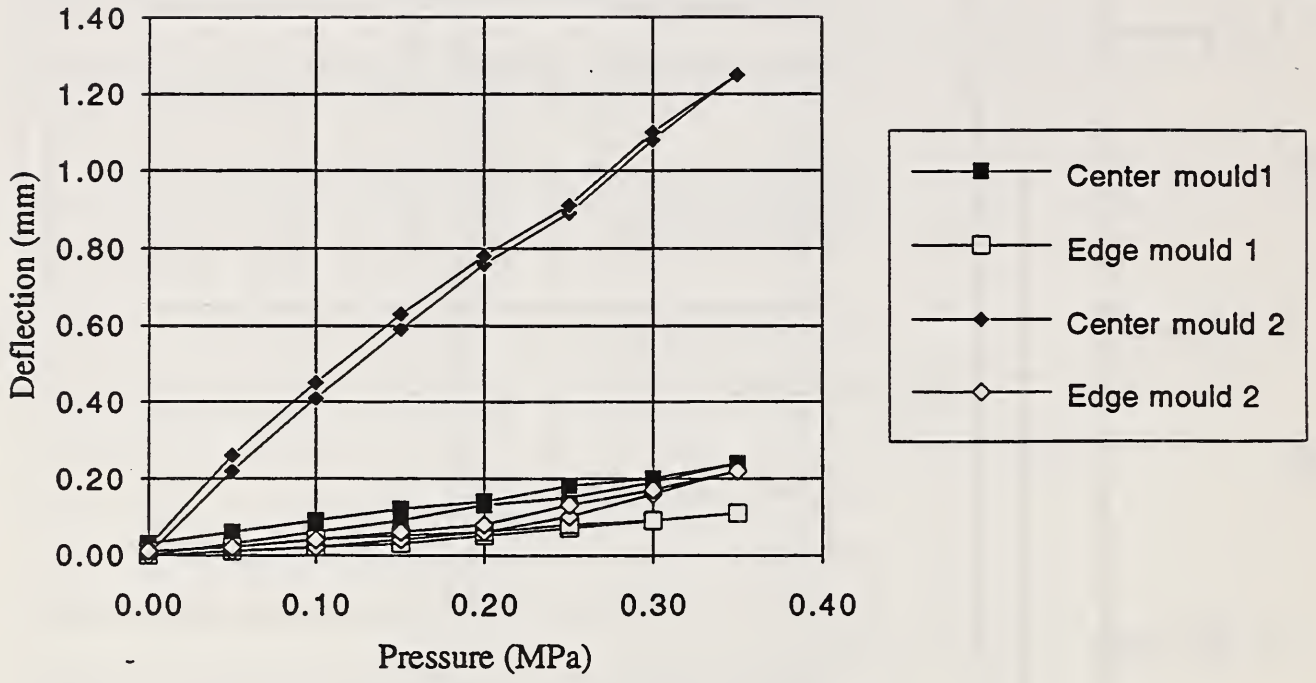
1.40
1.20
1.00
0.80
0.60
0.40
0.20
0.00
Deflection (mm)
0.00
0.10
0.20
0.30
0.40
Pressure (MPa)
Center mould1
Edge mould 1
Center mould 2
Edge mould 2

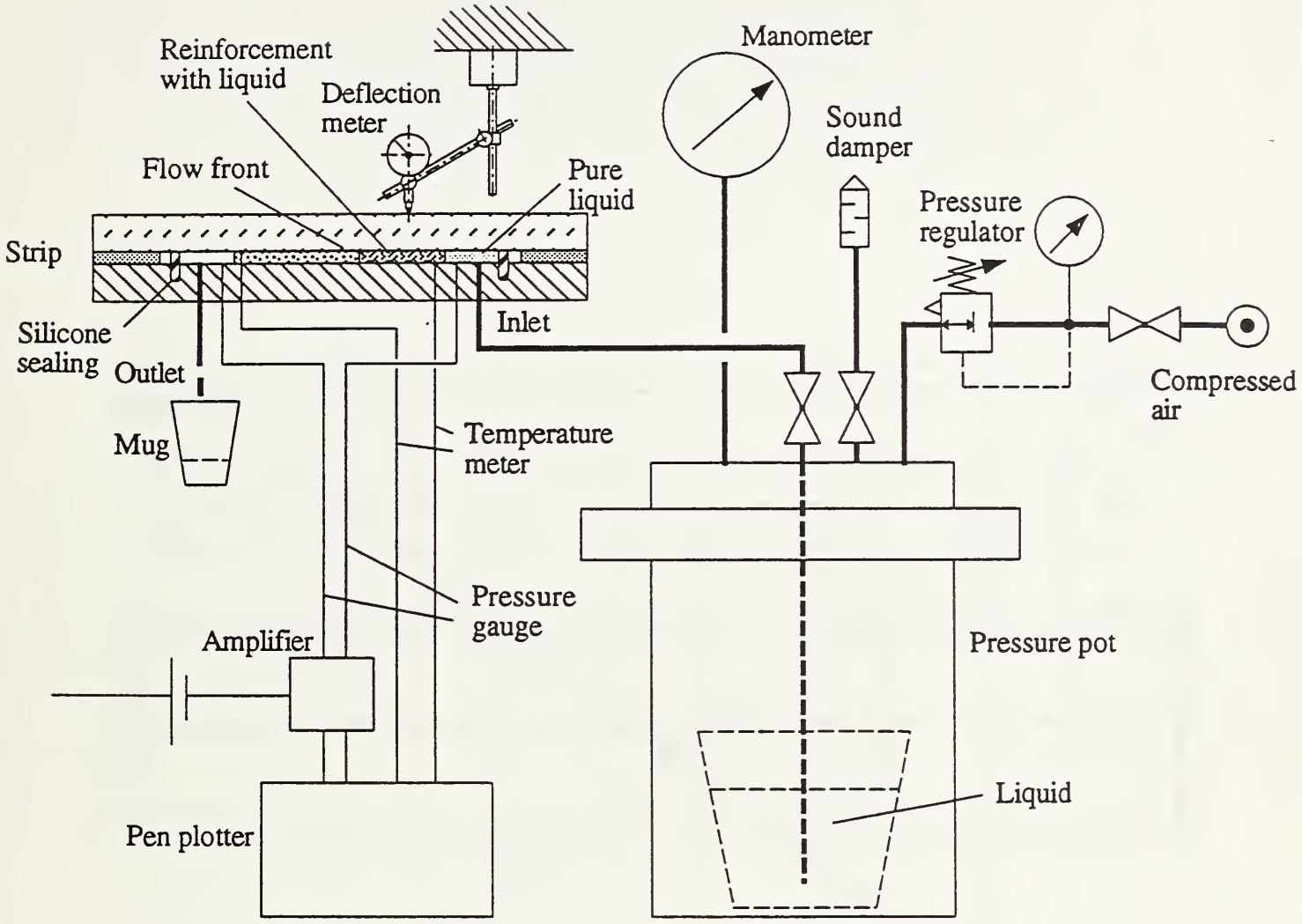
Reinforcement with liquid
Deflection meter
Manometer
Sound damper
Flow front
Pure liquid
Pressure regulator
Strip
Silicone sealing
Outlet
Inlet
Compressed air
Mug
Temperature meter
Pressure gauge
Amplifier
Pressure pot
Liquid
Pen plotter

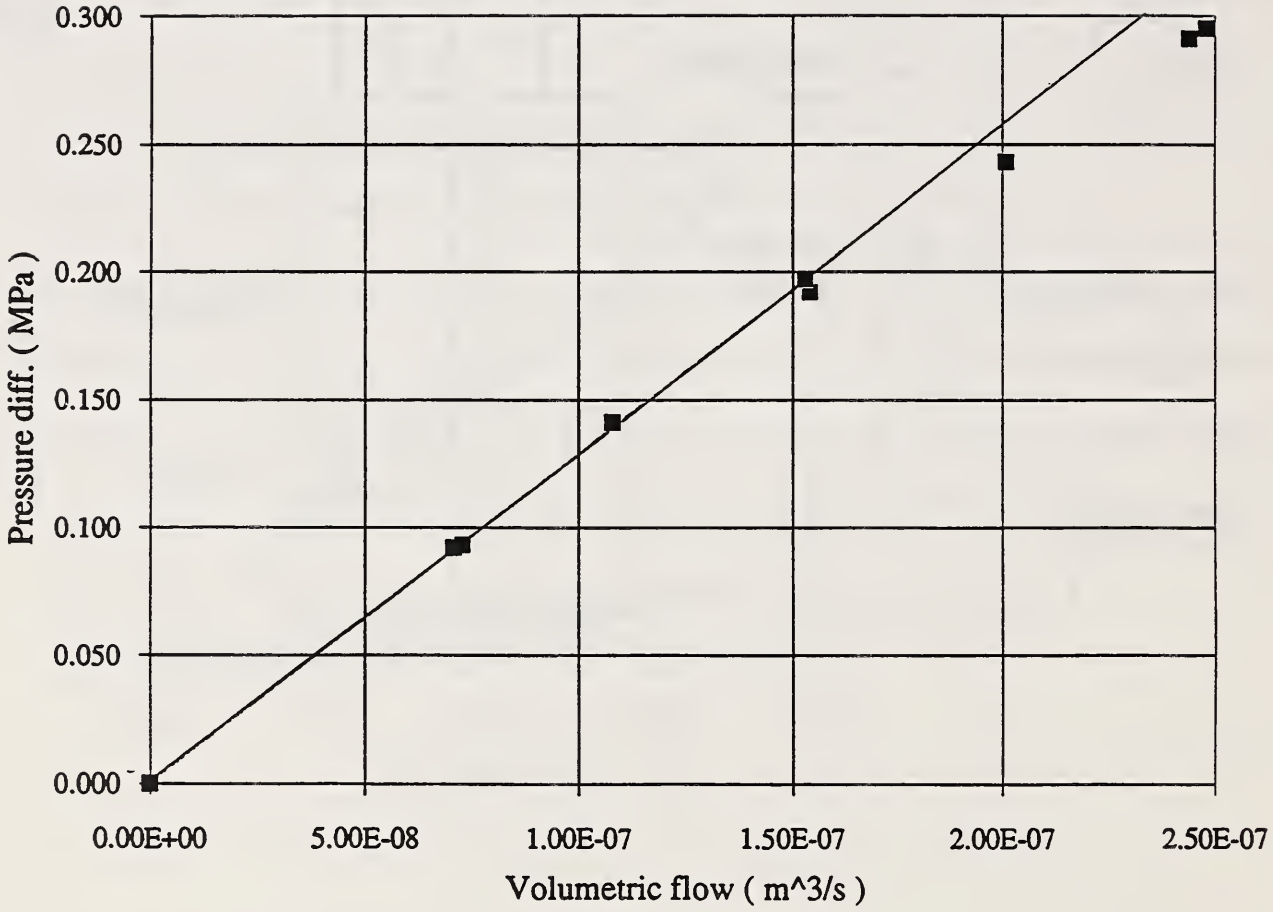
0.300
0.250
0.200
0.150
0.100
0.050
0.000
Pressure diff. (MPa)
0.00E+00
5.00E-08
1.00E-07
1.50E-07
2.00E-07
2.50E-07
Volumetric flow (m^3/s)

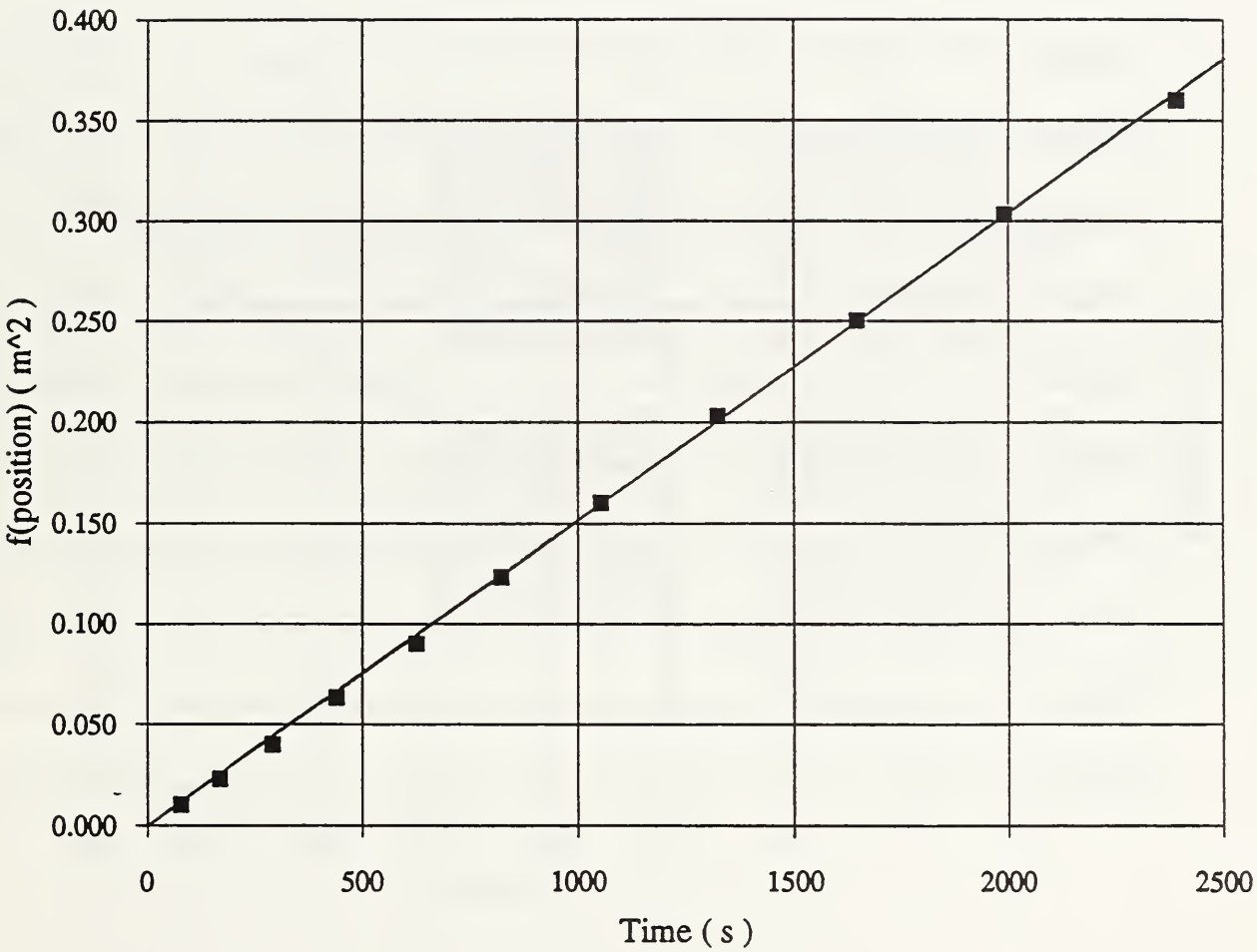
0.400
0.350
0.300
0.250
0.200
0.150
0.100
0.050
0.000
f(position) (m^2)
0
500
1000
1500
2000
2500
Time (s)

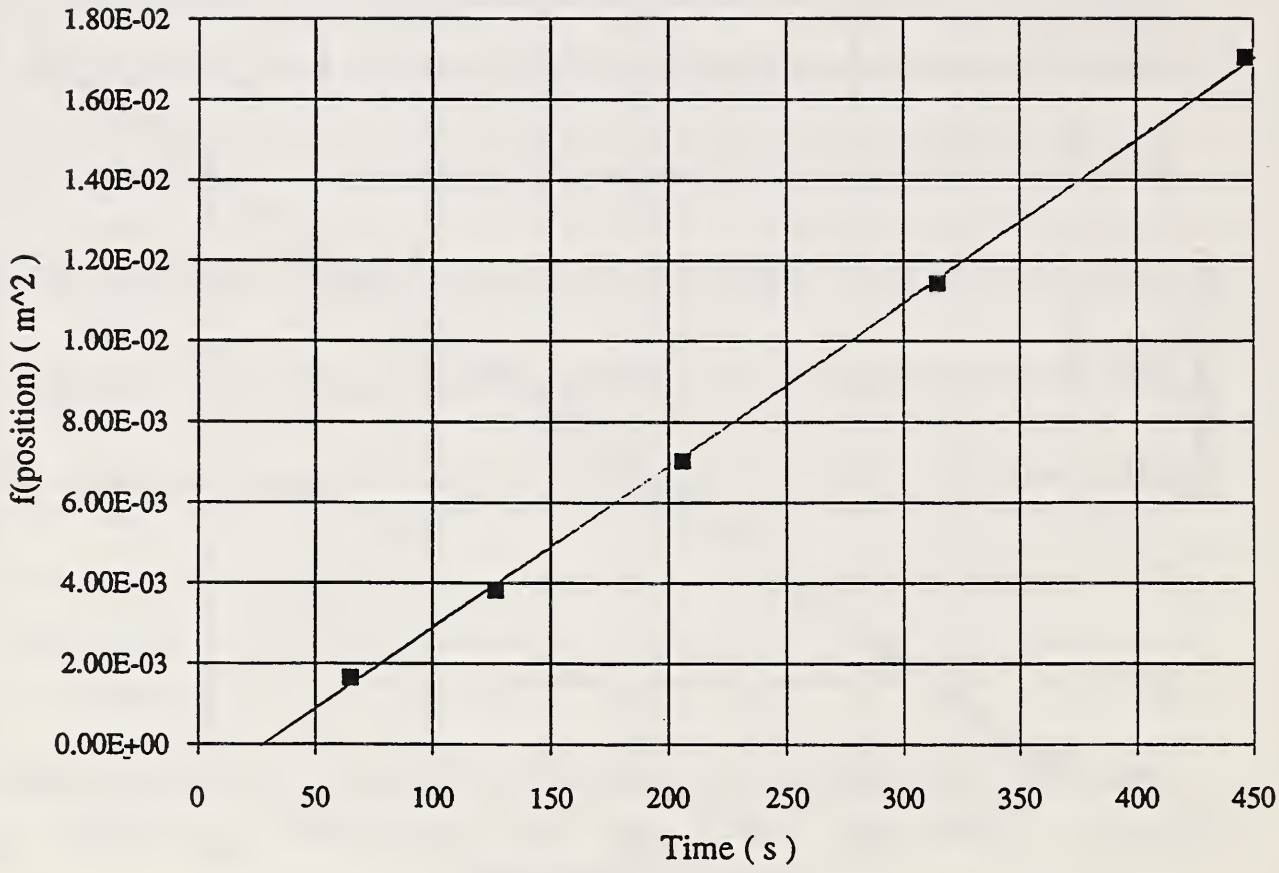
1.80E-02
1.60E-02
1.40E-02
1.20E-02
1.00E-02
8.00E-03
6.00E-03
4.00E-03
2.00E-03
0.00E+00
f(position) (m^2)
0
50
100
150
200
250
300
350
400
450
Time (s)

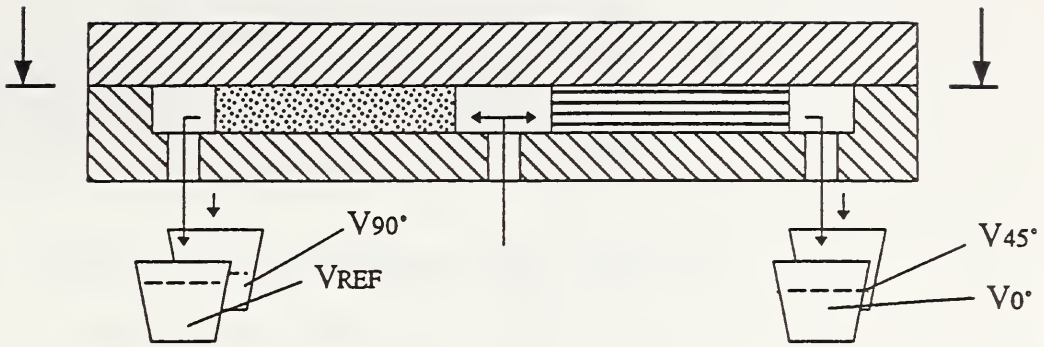
V90°
VREF
V45°
V0°

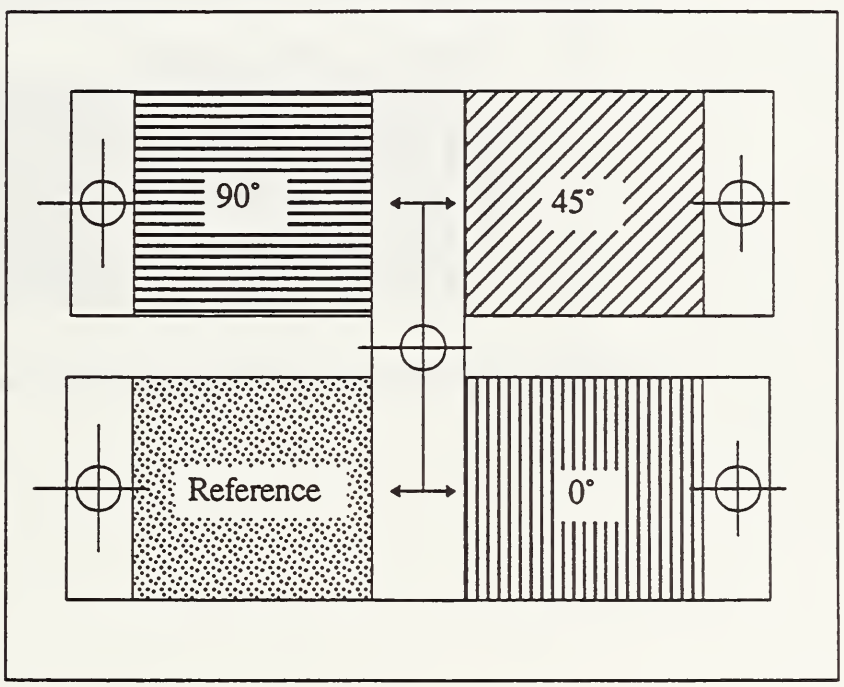
90°
45°
Reference
0°

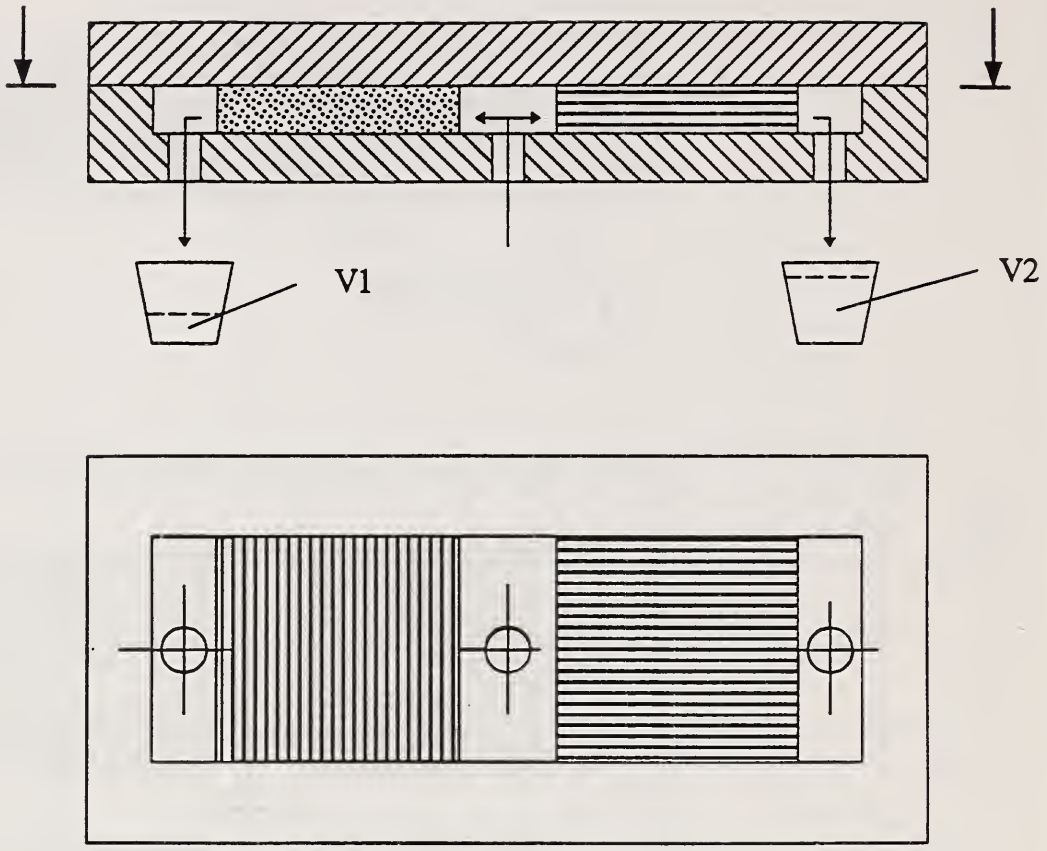
V1
V2

DYNAMICS OF BINDER DISPLACEMENT IN LIQUID MOLDING

by

Jinglei Chen, Douglas Backes and K. Jayaraman*

Department of Chemical Engineering and

Composite Materials and Structures Center

Michigan State University

East Lansing, Michigan 48824

* To whom correspondence should be addressed

Manuscript submitted to

Polymer Composites

based on presentation at the NIST Workshop on Manufacturing Polymer Composites by Liquid Molding, Gaithersburg, September 1993

ABSTRACT

This paper provides experimental data and an analytical description for mass transfer of soluble thermoplastic binder from a fiber preform to the resin during nonisothermal filling in liquid molding processes. Experimental washout curves for binder from a preform of random continuous glass mat into a vinyl ester resin during mold filling indicate binder concentrations varying from 1 to 5 wt. percent in the resin after fill. An experimental method has been developed for estimating binder concentration profiles within resin during fill from washout curves obtained with preforms of different lengths. The binder concentration profile and the viscosity profile must be determined and controlled because of the consequences for wet-out, preform deformation, development of "fingering" flow patterns and non-uniformities in molded parts. A model has been developed and tested for the resin viscosity during nonisothermal filling that takes into account three factors -- binder dissolution, temperature variations and a small amount of cure. The process model is confined to one-dimensional flow with negligible heat conduction and dispersion; yet it provides good estimates of temperature profiles during filling. The model predictions on binder dissolution match with experimental data to within 10 % under varying mold wall heating conditions. Hence the model describes the interaction between non-isothermal effects and binder dissolution effects well. Calculations with this model thus provide quick estimates of viscosity variation under various process conditions. Design guidelines based on the predicted viscosity variation have also been developed for operating conditions in resin transfer molding.

INTRODUCTION

The liquid molding process involves injection of reactive resin into a mold cavity with pre-placed fiber preforms. The preforms are commonly made with directional, woven glass fabric or random, non-woven, continuous strand, glass mats. When woven fabric alone is used in the preforms, stacked layers need to be precisely aligned to allow resin permeation and wet-out. This requires large amounts of time to prepare the preforms which results in decreased production rate and increased labor costs [1]. An alternative method is to use non-woven continuous strand mats either by themselves or as interspersed layers [2]. Plies of the random mat do not need to be precisely aligned on top of one another, thus greatly reducing the production time involved. Non-woven mats need to be held together while they are being shaped in the mold and most manufacturers have solved this problem by spraying the mats with a chemical binder. Because of the spraying method used, the binder is present in small pockets on the fiber bundles rather then being evenly spread across the fibers. The binder is usually a thermoplastic polymer which allows thermoforming of glass fiber mats into preforms. The binder is different from sizing that is applied on glass fiber to protect the fiber itself from damage and to improve adhesion between the fiber and the resin.

A typical binder used in thermoformable glass mats is a thermoplastic polyester of low molecular weight. Such binders are soluble in unsaturated polyester resin or vinyl ester resin formulations. A binder that dissolves in resin allows faster wet out of the preform. Dissolved binder in the resin also leads to reduced shrinkage -- see Owen et al. [3]. The solubility of the binder in resin is varied for different applications; thermo-formable glass fiber mats contain 4 to 10 weight percent of a thermoplastic polyester binder. Uneven dissolution of binder in resin within the filled mold may occur with the lowest concentration near the inlet and the highest near the other end. This will cause a distribution of properties such as stiffness in the molded part [3]. It may also lead to uneven shrinkage that generates large thermal stresses in the part. Also, the reaction rate and exotherm may be decreased by the presence of the thermoplastic binder as indicated by the work of Lee and coworkers [4] on low profile additives. Hence, it is important to predict the distribution of binder within the resin during the filling process.

Another consequence of binder dissolution is an increase in the resin viscosity. Backes et al. [5] have reported that the viscosity of a vinyl ester resin increases nearly two fold when the binder concentration in the resin reaches about 5 wt%, as shown in Figure 1 here. Also the dissolution time is found to be much less than the gel time of RTM resins, so that binder dissolution will have significant effects on the viscosity profile during mold filling. The resin pressure distribution is governed by both preform architecture and resin viscosity as seen in Darcy's law written for one-dimensional flow.

$$-\frac{dP}{dx} = \frac{\mu}{K}\left(\frac{Q}{A}\right) = \frac{u}{m} \tag{1}$$

where P denotes resin pressure, x denotes the coordinate along the flow direction, Q is the

volumetric flow rate, A is the area of cross section for flow, K is the permeability determined by preform architecture, μ is the resin viscosity, m is the mobility and u the superficial velocity. As can be seen from Eq. (1) increased resin viscosity will require a higher injection pressure for the same injection rate. This may give rise to preform compaction effects during mold filling -- see Han et al. [6] and Mishra and Jayaraman [7] -- which will hinder wet-out and generate inhomogeneities. Finally, increasing viscosity or decreasing mobility along the injection flow direction favors the development of "fingering" flow instabilities (see e.g. Tan and Homsy [8]), which give rise to inhomogeneities in the molded part [9]. The interlinked causes of non-uniformities developed during mold filling are displayed in the schematic of Figure 2. This figure displays three causes of viscosity variation -- binder dissolution, mold wall heating, and cure exotherm during reactive filling. Hence, it is important to predict variations in mobility during mold filling.

The object of this paper is first to report experimental results on the rate of binder dissolution and the binder concentration profile obtained in the filled mold under a variety of conditions. Binder washout curves from glass mats are obtained in the absence of initiator, to obtain data [10] on the mass transfer process. Next, a mathematical model is developed with the help of this data, for the mass transfer of binder from the preform to the resin. Finally, the mass transfer model is combined with a viscosity model and other conservation equations to predict the resin viscosity variation in the mold. This model is evaluated in comparison with other reported simulations [11-14] without the binder/resin interactions. Finally, this model is used to develop predictions related to combining mold wall heating with binder dissolution.

EXPERIMENTAL

Materials

The resin used in the experimental study is Derakane 411-C50 from Dow Chemical Corporation. The Derakane resin consists of 50 wt% vinyl ester and 50 wt% styrene. The catalyst is benzoyl peroxide (BPO). The brand of BPO used in the experiments is Cadox 40E supplied by the Akzo Chemical Company, which is an emulsion made up of 40 wt% BPO, 40 wt% diisobutyl pthalate, 7 wt% silica as filler, 3 wt% surfactant, and 10 wt% water. The materials other than BPO in the emulsion will have no effect on the curing process. The accelerator used is N,N-Dimethylaniline (DMA) from Aldrich Chemical. The glass mat used is Unifilo U-750 provided by Verotex / Certainteed Inc. The binder is a thermoplastic powdered polyester that is spray coated onto the mat and is 8% of the total mass of the mat. The binder was obtained separately for viscosity studies.

Apparatus

The mold filling experiments were conducted with 0.3175 cm thick preforms of random continuous glass mat placed in a rectangular mold with a transparent top. The bottom plate is made of aluminum, while the top plate is made of plexiglass; both have dimensions of 22.86 cm x 66.04 cm x 2.54 cm. The circular inlet gate is located at one end of the bottom plate and leads to a well from which the resin flows uni-directionally into the preform. The bottom plate

has several outlet port locations so that filling experiments could be conducted with preforms of different lengths. The middle ring is 0.3175 cm thick with an inside dimension of 19.05 cm x 62.23 cm. After allowing for the well near the inlet and the sealing ring, the area available for the fiber preform is 15.56 cm x 56.52 cm. The edges of the preform were glued to the mold and C-clamps were used to hold the mold together with a sealing ring. The mold wall temperature was recorded with a thermocouple (Omega CF-000-J-2-60-1). A temperature controller (Omega CN911A) and five 2.54 cm x 50.8 cm etched foil heater strips were used to control the mold wall heating. A Multiflow Model 5515 Resin Transfer Machine (Liquid Controls) was used to inject the two-part resin through a static mixer into the mold. The resin viscosity was measured by a Brookfield model LVF-DVIII viscometer. A Nikon F3 camera with an automatic advance was used to take photographs of the flow patterns.

Procedures

The time scale of binder dissolution in the absence of flow was determined as follows with styrene alone. Pre-weighed samples of fiber mat held in a wire mesh into styrene for a predetermined length of time and then reweighing the sample. The difference in the fiber weights before and after the submerging is the amount of binder dissolved. This process was continued until the weight of the fiber stabilizes signifying that all of the binder has been dissolved off.

Binder washout curves in flow were obtained with the vinyl ester resin flowing through preforms with 15 vol % and 40 vol % of fibers placed in the mold. Resin without initiator was injected by the Resin Transfer machine with a fixed shot size of 10 ml under different machine pressures. The mold was heated to different temperatures but the resin inlet temperature was 23 C in all cases. Resin samples were collected at the mold outlet over regular time intervals. Since resin viscosity increases monotonically with the binder concentration, the amount of binder in a resin sample can be determined by measuring its viscosity at a reference temperature and looking up a curve of binder concentration vs resin viscosity at the reference temperature -- see Figure 1. This curve was determined by using powdered binder obtained from Vetrotex/Certainteed. Various amounts of the powdered binder were mixed into a series of resin samples and their viscosities were measured with a Brookfield viscometer.

A profile of binder concentration in resin along the flow length in the filled mold, was pieced together from a series of washout curves with preforms of several different lengths (in increments of 7.6 cm). The mold outlet port was located at the end of the preform in each case. The use of these washout curves to obtain the required spatial profile is described in the next section. In order to observe the flow pattern within the filled section, first clear resin was injected some distance into the mold; this was followed by mixing a tracer dye in-line into the resin through the static mixer. The progress of the dyed resin through the clear resin was photographed with a camera positioned overhead.

Experimental Results and Discussion

The time taken for binder dissolution without flow is shown in Fig. 3 for several

temperatures. At a typical mold fill time of 1 minute, 45% of the binder from the glass fiber mat is dissolved at 23°C, 83% at 40°C, and 93% at 60°C. After 1.5 minutes, nearly 100% of the binder is dissolved at 40°C and at 60°C. Figure 4 shows the progress of the resin during fill at the conditions of the washout experiments. The time at which resin advances to different positions in the mold is plotted against position in this figure. The time needed to fill the mold with 3 plies was 226 seconds at a machine pressure of 25 psi while at 60 psi it was 41 seconds. A drop in resin velocity during the fill is noticeable only at the lower machine pressures.

The binder washout curves obtained with 3 plies at several mold temperatures are shown on Figure 5. The void volume to be filled was 230 ml with 3 plies or 15 volume % of fibers. So, the resin volume collected for the washout curves was the same order of magnitude as the void volume in the preform. In all the cases, the binder concentration in the resin decreases as resin is flushed through the preform and levels out after a volume equal to the void volume is flushed out. Comparison of the washout curves shows that higher mold wall temperatures result in steeper concentration profiles. Over 250 ml of resin flushed, the binder concentration drops from 7.5% to 1% for 60°C, 7.2% to 0.5% for 40°C and 6.5% to 2% for 23°C). Several effects are involved: the higher rate of binder dissolution at higher temperatures and the competing effects of increasing temperature and binder dissolution on resin viscosity. A binder washout curve is shown in Fig. 6 for a preform with 40 fiber volume %. This preform was prepared in a Wabash press and is *only half as long* as the other preforms. The binder concentration starts at a fairly low value -- 1 wt%, increases to a maximum of 4.8% and decreases gradually. This is quite different from the curves in Figure 5 where the maximum concentration is attained near the beginning of the washout.

The profiles of binder concentration in resin and of the resin viscosity within the mold at the time of fill can be constructed from washout curves obtained with several preform lengths. An example of this construction may be seen on Figure 7 where the viscosity curves obtained with different lengths of the 3-ply preform (with a machine pressure of 30 psi) are presented. One starts with the first point on the viscosity curve of the longest preform. This is the resin viscosity at the mold outlet. From the washout curve for the second longest preform, one would read the concentration at a flushed volume equal to the volume difference between the second longest preform and the longest preform. This process is continued to the shortest preform and these points are used to construct the spatial profiles. The resulting viscosity profile is shown in Fig. 8 with the viscosity increasing from 118 cps to 167 cps across the length of the mold. Since the mold wall temperature is only 28°C which is very close to resin inlet temperature (23°C) and reaction is inhibited (no catalyst in these runs), the viscosity is affected predominantly by the binder concentration. Fig. 8 shows that the resin viscosity (and the binder concentration) increases along the resin flow direction. This would be expected since the fibers closer to the inlet end of the mold have been exposed to resin longer and hence become progressively depleted of binder. The viscosity gradient is also greater for lower operating pressures (fill rates): the viscosity increases by 105 cps across the length of the mold at 20 psi as opposed to 49 cps at 30 psi. For lower flow rates, the resin is in contact with the fiber for a longer time and therefore will absorb more binder. With a

binder concentration gradient resulting in the mold after filling, the part will experience greater shrinkage near the inlet of the mold than at the outlet which could result in decreased part strength.

The effect of binder dissolution on the flow pattern *within* the filled region has been viewed under different fill rates with the help of a tracer dye. The mold wall temperature was 28 C and the resin inlet temperature was 23 C. Photographed flow patterns presented in Figures 9a and 9b for two different machine pressures of 20 psi and 30 psi respectively show both the clear resin front and the dyed resin front; the corresponding rates of front advancement (see Figure 4) are 0.61 cm/s and 1.58 cm/s respectively. Both photos were taken after the first, clear resin had advanced the same distance into the mold; the clear resin front is nearly flat over the width but the second, dyed resin front is marked by the presence of fingers. The fingers in Figure 9a have grown less than the fingers in Figure 9b. The adverse viscosity gradient arising from progressive binder dissolution has led to these fingers. The growth rate is critically affected by the flow rate with higher flow rates leading to longer fingers -- cf. [8].

A PROCESS MODEL

In the following sections, a mathematical model is developed to describe the mass transfer of binder from the fiber preform to the resin during mold filling and in the washout experiments described above. This model is combined with a viscosity model and other conservation equations to estimate the variation of resin viscosity during the filling process. The resin viscosity is an important intermediate variable to control the flow patterns within the filled region and the development of inhomogeneities in the molded part.

Resin Viscosity Model

In order to take into account the three factors that affect the resin viscosity, the first step is to describe the resin viscosity as a function of binder concentration, temperature, and conversion for mold filling processes coupled with binder dissolution. For the Derakane vinyl ester resin used in the experiments, the viscosity is expressed as a product of three separable factors,

$$\mu(T,\alpha,c_b) = \mu(T) \times f_1(c_b) \times f_2(\alpha) \tag{2}$$

where the effects of temperature, binder concentration, and conversion are fitted to the following expressions

$$\mu(T) = \exp(-15.3 + \frac{5981.5}{T}) \ (mPa\text{-}s) \tag{3}$$

$$f_1(c_b) = 1.0 + .1841\, c_b + .0083\, c_b^2 + .0014\, c_b^3 \tag{4}$$

$$f_2(\alpha) = (1 - \frac{\alpha}{\alpha_g})^{(-3.32 \times \frac{\alpha}{\alpha_g} - 0.66)} \tag{5}$$

where μ denotes resin viscosity, T, temperature, c_b, binder concentration in resin in wt%, α, conversion, and α_g, gel conversion which is 0.015. The experimental viscosity data in the absence of reaction, compared with the predicted viscosity from Eq. (4) in Fig. 10, demonstrate the success of the factor method.

Binder Dissolution Model

The rate of binder dissolution, R_b is described by the following relation,

$$R_b = K_m a_m (b w_b - \frac{\phi}{1-\phi} c_b) \tag{6}$$

where K_m is the mass transfer coefficient, a_m is the surface area per unit volume, b is a solubility coefficient, w_b is binder concentration on fiber (g/cm^3 fiber volume), c_b is binder concentration in resin (g/cm^3 resin volume), and ϕ is porosity. The dissolution data for flow through a rectangular mold from Backes [10] is fitted with the following correlation for mass transfer coefficient between fluid and porous media (see Smith [15]),

$$\frac{K_m \phi}{u} = \beta_1 (\frac{\mu}{\rho D})^{-2/3} (\frac{d_p \rho u}{\mu})^n \tag{7}$$

where u is superficial velocity, ρ is density, D is the molecular diffusivity of the binder in resin, AND d_p is the fiber bundle diameter. β_1 and n are constants to be determined through data fitting. The change of diffusivity with temperature can be found from the correlation given by Bird et al. [16].

$$D = \frac{\kappa T}{6\pi R_A \mu} \tag{8}$$

Here κ is the Boltzman constant, and R_A is the diffusive radius of binder particles. Finally, the mass transfer rate can be written as

$$R_b = \beta a_m \frac{u}{\phi} \left(\frac{\mu^2}{\rho T}\right)^{-2/3} \left(\frac{d_p \rho u}{\mu}\right)^n \left(b w_b - \frac{\phi}{(1-\phi)} c_b\right) \tag{9}$$

where

$$\beta = \beta_1 \left(\frac{\kappa}{6\pi R_A}\right)^{2/3} \tag{10}$$

Eq. (9) will then be used with the following component balance equations to predict binder dissolution during mold filling process.

$$\phi \frac{\partial c_b}{\partial t} + u \frac{\partial c_b}{\partial x} = \frac{1-\phi}{\phi} R_b \tag{11}$$

$$\frac{\partial w_b}{\partial t} = -R_b \tag{12}$$

Energy Balance

The resin temperature T and the preform temperature T_B are determined from the following pair of energy balances involving two source terms -- a wall heat flux Q^w, and the reaction exotherm. Variations transverse to the flow have been neglected in these equations. The effect of this simplification has been evaluated and is presented in the following section.

$$\rho C_p \phi \frac{\partial T}{\partial t} + \rho C_p u \frac{\partial T}{\partial x} = -\phi Q_B + \phi R_c (-\Delta H) + Q_w \tag{13}$$

$$(\rho C_p)_B (1-\phi) \frac{\partial T_B}{\partial t} = \phi Q_B \tag{14}$$

The heat flux Q_w from the mold wall to the resin and fiber bed is written as

$$Q_w = \frac{h_w}{l}(T_w - T) \tag{15}$$

where l is the preform thickness, T_w is the mold wall temperature, and h_w is the heat transfer coefficient between the filled fiber preform and the mold wall with flow through the preform. The following relation for h_w has been derived by Bejan [17] for boundary layer flow in porous media.

$$\frac{h_w}{\rho C_p} = 0.564\left(\frac{k}{\rho C_p}\ \frac{u}{x}\right)^{1/2} \tag{16}$$

The rate of heat exchange per unit volume between resin and fibers Q_B is defined by the relation

$$Q_B = h_v(T - T_B) \tag{17}$$

where T_B is the fiber temperature, and h_v is a volumetric heat transfer coefficient between fiber and resin, calculated from the following empirical correlation of Lin et al. [11]

$$\frac{h_v}{\rho C_p} = 0.0917 + 0.0195u(\times 10^{-2} m/\text{sec}) \tag{18}$$

Extent of Reaction

The mass balance accounting for conversion α is

$$\phi\frac{\partial \alpha}{\partial t} + u\frac{\partial \alpha}{\partial x} = \phi R_c \tag{19}$$

The reaction rate of the vinyl ester resin at low conversions has been fitted by Larson and Drzal [18] as follows.

$$R_c = \frac{k_i(1-\alpha)}{t_z - t} \tag{20}$$

where

$$k_i = 5.69\times10^{11}\exp\left(\frac{-10360}{T}\right) \tag{21}$$

$$t_z = 1.7\times10^{-11}\exp\left(\frac{8555}{T}\right) \tag{22}$$

Boundary Conditions and the Numerical Scheme

The method of characteristics was used to integrate the first order partial differential equations presented -- see Acrivos [19]. Eqs.(12) and (14) are numerically integrated along one set of characteristics,

$$t = constant \tag{23}$$

starting with the initial conditions imposed at the time when resin reaches the location

$$x = x_f\ ,\ w_b = w_{b0} \qquad T_B = T_{B0} \tag{24}$$

Eqs. (11), (13), and (19) are numerically integrated along the other set of characteristics,

$$x = \frac{u}{\phi}t + constant \tag{25}$$

starting with the boundary conditions at the inlet to the mold

$$x=0\ ,\ c_b=0$$
$$T=T_i \qquad (26)$$
$$\alpha=0$$

These characteristic lines are for one dimensional, rectilinear flow with constant u. If u is varying slowly with time, a step-wise u variation that is close to the real u variation could be used.

For radial flow with constant flow rate, the characteristics are given by,

$$t=constant$$
$$r=\int\frac{u}{\phi}dt+constant \qquad (27)$$

where r is radial distance from the center gate and u is a function of r.

COMPUTED RESULTS AND DISCUSSION

Model Validation

The present model is confined to one-dimensional flow with negligible heat conduction and dispersion; but it takes into account three factors that will affect resin viscosity. Calculations with this model thus provide quick estimates of viscosity variation under various process conditions. The following simulations are done to check the binder dissolution model and the effects of such simplifications. The preform dimensions for the rectangular mold are 15.56 cm x 56.52 cm x 0.3175 cm.

Three sets of experimental binder concentration data from isothermal and non-isothermal filling experiments with the rectangular mold [10] have been used to determine the mass transfer parameters. The isothermal filling was done at 23°C. For the non-isothermal filling experiments, the resin inlet temperature was 23°C, while the mold wall temperature was set at 40°C and 60°C, respectively. The variation of the flow rate during the filling experiments has also been taken into account by using flow velocities varying step-wise with time. The predicted change in outlet binder concentration with time is plotted in Fig. 11 with the experimental data from Backes [10] -- cf. Figure 5. The fitted constants used in Eq. (9) are as follows,

$$\beta=1.374\times10^{-10}$$
$$n=-0.95$$

It can be seen from Fig. 11 that the numerical results match well with the experimental measurements. The deviation from experimental data for the isothermal run is less than 5 %

and the deviation for the non-isothermal runs is less than 10 %. Hence the mass transfer model for binder dissolution in Eqs. (6) - (9) is valid.

In order to explore the effect of ignoring conduction in the energy balance, another simulation has been carried out for a case studied by Lin et al. [11] -- filling of a center-gated disk shaped mold with palatinol oil. The mold dimensions and process conditions are the same as those in [11]. Results of the present simulation are compared with those given in [11], where a two-dimensional model with heat conduction is used to generate numerical results. Fig. 12 shows the comparison of temperature transients at two different locations in the mold. The same trends are shown with an average difference less than 15%. This shows that despite the omission of heat conduction, the present one-dimensional model with mold wall heating as a source term provides good estimates of the temperature profiles.

Other Model Predictions

The predicted binder concentration profile for isothermal filling of the end gated rectangular mold with a 45 second fill time is presented in Fig. 13. Both the resin inlet temperature and the mold wall temperature are set at 23 °C. However, the experimental curves presented in Figure 8 were obtained with the mold wall temperature being 5 C higher than the inlet temperature. Nevertheless, the final binder concentration at the end of the mold compares well between Figure 13 and the curve for the corresponding flow rate in Figure 8.

Next, computational results for non-isothermal filling are presented to explore the effect of mold wall heating on binder distribution and viscosity variations with and without binder dissolution. To isolate the effects of mold wall heating, the simulations are first done for preforms without any soluble binder. The base case has the resin inlet temperature at 25°C and the mold wall temperature at 35°C. The mold wall temperature is raised to see its effects on resin viscosity profile. The filling time is 45 sec for all these simulations and is much less than the resin gel time. Fig. 14 shows the viscosity profiles for different mold wall temperatures. As can be seen, increased mold wall temperature will result in a larger decrease in viscosity along the mold filling direction. However, raising the mold wall temperature might also accelerate the reaction. At a mold wall temperature of 60°C there is a small increase in viscosity at the flow front as a result of the reaction. For the slow reacting RTM resins, the viscosity increase caused by reaction would be insignificant. When a fast reacting SRIM resin is used, the increase in the reaction rate due to higher mold temperatures could be important [19]. When the preforms have resin soluble binder, mold wall heating would accelerate binder dissolution and generate two competing effects on the viscosity. The calculated resin viscosity profiles with three uniform mold wall temperature levels and with a stepped wall temperature profile are shown in Fig. 15. It shows that for low mold wall temperature (35°C) profile, the resin viscosity will increase along the mold due to dissolved binder. Raising the mold wall temperature will lower the increase in viscosity (see 40°C and 50°C cases). Fig. 15 also shows that raising the wall temperature in the local region of viscosity increase (stepped T_w profile) could be more effective in terms of reducing viscosity gradient, than raising the mold wall temperature uniformly.

DESIGN GUIDELINES

If uneven binder distribution and increasing viscosity in the direction of flow are detrimental to the properties of the molded part, a threshold of gradient may be identified either in binder concentration or correspondingly in the viscosity. Then one may define a window of operating conditions for which the binder concentration gradient or the viscosity gradient will be below the agreed upon threshold. As an example, an important design parameter is the ratio of fill time t_{fill} to a characteristic dissolution time $t_{diss.}$. This ratio may be computed by the following relation,

$$\frac{t_{fill}}{t_{diss.}} = \int_0^L \frac{K_m a_m}{u} dx \tag{28}$$

where the front location is denoted by L and the mold fill time is given by

$$t_{fill} = \int_0^L \frac{dx}{u} \qquad (24) \tag{29}$$

A small ratio of fill time to the characteristic dissolution time means that there is not enough time for the binder to be dissolved. If the ratio is large, the binder concentration dissolved in resin will be high.

The logarithmic viscosity gradient at the flow front is plotted against the ratio of the fill time to the dissolution time in Fig. 16 for two cases with different mold wall temperatures. Fig. 16 shows that the viscosity gradient increases with increasing ratio of fill time to the characteristic dissolution time. The gradient increases more rapidly at low values of this ratio then levels off as the resin nears its solubility limit. Increases in the mold wall temperature will result in a smaller viscosity gradient at low fill times because more heat has been transferred resulting in a higher resin temperature. Then as the ratio of fill time to dissolution time increases (front moving forward), the viscosity gradient eventually becomes larger for the higher mold wall temperature than for lower mold wall temperature since the higher temperature resin will dissolve more binder. If for example, a viscosity gradient of zero is used as a threshold, the fill time should be less than 5 percent of the dissolution time scale at a mold wall temperature of 35 C.

CONCLUSIONS

Experimental washout curves for binder from a preform of random continuous glass mat

into a vinyl ester resin during mold filling indicate widely varying binder concentration in the resin after fill. A method has been developed for estimating concentration profiles within the filled mold from washout curves with different preform lengths. Uneven binder dissolution contributes to increases in viscosity and to a drop in mobility along the fill direction by a factor of 2 to 3. The binder concentration profile and the viscosity profile must be determined and controlled because of the consequences for wet-out, preform deformation and development of "fingering" flow patterns. A model has been developed and tested for the resin viscosity during nonisothermal filling that takes into account three factors -- binder dissolution, temperature variations and a small amount of cure. An easily solved process model has been developed for mass transfer of binder from fibers to resin during nonisothermal filling and validated with the experimental data. This model is confined to one-dimensional flow with negligible heat conduction and dispersion; yet it provides good estimates of temperature profiles during filling. The model predictions on binder dissolution match with experimental data to within 10 % under varying mold wall heating conditions. Hence the model describes the interaction between non-isothermal effects and binder dissolution effects well. Calculations with this model thus provide quick estimates of viscosity variation under various process conditions. Design guidelines based on the predicted viscosity variation have also been developed for operating conditions in resin transfer molding.

Acknowledgements

This research was supported by the NSF Center for Low-Cost, High-Speed Polymer Composites Processing at Michigan State University. Partial support was also provided by the State of Michigan through an REF grant administered by the Composite Materials and Structures Center at Michigan State University. The Liquid Controls Resin Transfer machine was made available to us by the Tank Automotive Research and Development Center in Warren, Michigan under a CRDA. The authors appreciate the assistance of John Knight with the preform preparation.

NOMENCLATURE

A	=	Area of cross section for flow
a_m	=	Surface area of preform per unit mold volume
b	=	Solubility constant
C_p	=	Specific heat
c_b	=	Binder concentration in resin
D	=	Molecular diffusivity of binder in resin
d_p	=	Fiber bundle diameter
h_w	=	Heat transfer coefficient between fluid and mold wall
h_v	=	Volumetric heat transfer coefficient between fiber and resin
K	=	Permeability
K_m	=	Mass transfer coefficient
k	=	Heat conductivity

k_i = Rate constant
l = Thickness of the mold
n = Empirical constant
P = Pressure
Q = Volumetric flow rate
Q_B = Volumetric heat flux between fiber and resin
Q_w = Heat flux from mold wall to resin
R_A = Diffusive radius
R_b = Rate of binder dissolution
R_c = Reaction rate
r = Radial position in the mold
T = Resin temperature
T_B = Fiber temperature
T_{B0} = Initial fiber temperature
T_i = Inlet resin temperature
T_w = Mold wall temperature
t = Time
$t_{diss.}$ = Characteristic dissolution time
t_{fill} = Filling time
t_z = Characteristic time for reaction
u = Superficial velocity
V_f = Volume fraction of fiber preforms in mold
w_b = Binder concentration on fiber
w_{b0} = Initial binder content on fiber
x = Coordinate in injection direction
x_f = Flow front position

Greek Symbols

α = Extent of cure
α_g = Gel conversion
β = Empirical constant
ϕ = Porosity
ρ = Density
κ = Boltzman constant
μ = Viscosity

REFERENCES

1. S.W. Horn, Advanced Composite Materials: New Developments and Applications Conference Proceedings, Detroit (1991).

2. C.T. Morse, O.O. Ochoa, J.H. Barron, and D.L. Barron, Advanced Composites: Design,

Materials and Processing Technologies, Proceedings of the 8th Annual ASM?ESD Advanced Composites Conference, Chicago (1992).

3. M.J. Owen, Middleton, V., C.D. Rudd, and I.D. Revill, *Interfacial Phenomena in Composite Materials, Conference 1989*, University of Sheffield, (1989).

4. C.P. Hsu, M. Kinkelaar, P. Hu, and L. J. Lee, *Polymer Engineering and Science*, 31, 1450 (1991).

5. D. Backes, K. Jayaraman, and C.A. Petty, "The Effects of Resin Soluble Binder on Flow through Continuous Strand Glass Mats", SAE Technical Paper Series no. 930175, Dearborn, (1993).

6. K. Han, L. Trevino, L.J. Lee, and Ming Liou, *Polymer Composites*, 14, 144 (1993).

7. S. Mishra, and K. Jayaraman, *Proc. 9th Annual ASM/ESD Advanced Composites Conference*, Dearborn, (1993).

8. C.T. Tan and G.M. Homsy, *Physics Fluids*, 3549 (1986).

9. N.S. Losure, C.A. Petty, and K. Jayaraman, manuscript in preparation.

10. D. Backes, M.S. thesis, Chemical Engineering Dept., Michigan State University, East Lansing (1993).

11. R.J. Lin, L.J. Lee, and M.J. Liou, *Polymer Composites*, 14, 71 (1993).

12. M.J. Owen, C.D. Rudd, and K. N. Kandall, *Proc. 7th Annual ASM/ESD Advanced Composites Conference*, Detroit (1991).

13. J.P. Coulter, and S.I. Guceri, *Proc. Manufacturing International'88*, ed. T.G. Gutowski, ASME, NY, (1988).

14. A.G. Loos, and J. Weideman, Advanced Composite Materials: New Developments and Applications Conference Proceedings, Detroit (1991).

15. J.M. Smith, *Chemical Engineering Kinetics*, MeGraw-Hill (1981).

16. R.B. Bird, W.E. Stewart, and E. N. Lightfoot, *Transport Phenomena*, John Wiley & Sons (1960).

17. A.B. Bejan, *Convection Heat Transfer*, MeGraw-Hill (1984).

18. B. Larson, and L..T. Drzal, "Resin Spreading & Fiber Wetting in a Liquid Composite Molding Environment", submitted for publication.

19. A. Acrivos, *I.E.C. Process Design and Development*, 703 (1956).

20. J. Chen, K. Jayaraman, and C.A. Petty, *Proceedings of ASM/ESD 9th Annual ACCE meeting* (1993).

FIGURE CAPTIONS

Figure 1 Measured viscosity variation of a vinyl ester resin with % weight binder in the resin at 23 °C

Figure 2 Causes of non-uniformity during mold filling

Figure 3 Dissolution of binder in styrene over time at different temperatures

Figure 4 Resin front position in the mold vs time for filling through 3 ply random glass fiber mats ($V_f = 0.15$) at different machine pressures

Figure 5 Binder washout curves: binder concentration in resin at mold outlet with volume of resin flushed through 3-ply fiber preforms under different operating conditions. Note: resin volume in mold = 230 cm^3.

Figure 6 Binder washout curve: variation of binder concentration in resin at mold outlet with volume of resin flushed through fiber preforms ($V_f = 0.4$), $T_w = 28$ °C and $t_{fill} = 38$ seconds, resin volume in mold = 80 cm^3.

Figure 7 Variation of resin viscosity at mold outlet with volume of resin flushed through fiber preforms of different lengths

Figure 8 Binder concentration profiles within the filled preform (with 3 plies) for two different machine pressures

Figure 9 Comparison of flow patterns within the filled region at the same front location with $T_w = 28$ °C for two different machine pressures. a: 20 psi; b: 30 psi.

Figure 10 Test of binder contribution in viscosity model at different temperatures

Figure 11 Comparison of predicted and experimental binder washout curves at $T_i = 23$ °C. experimental data: +, $T_w = 23$ °C; *, $T_w = 40$ °C; o, $T_w = 60$ °C; ____ model prediction

Figure 12 Resin temperature transients for non-isothermal radial filling simulation, ____ prediction of the model in this paper, ---- Lin's numerical solution

Figure 13 Predicted binder concentration profile after mold filling, $T_i = T_w = 23$ °C

Figure 14 Resin viscosity variation through preforms without soluble binder at different mold wall temperatures ($T_i = 25$ °C). ____ $T_w = 35$ °C; ---- $T_w = 50$ °C; -.-. $T_w = 60$ °C

Figure 15 Resin viscosity variation through preforms with soluble binder at different mold wall temperatures (T_i = 23 °C). .... T_w = 35 °C; ____ T_w = 40 °C; -.-. T_w = 50 °C; ---- stepped T_w = 40 °C from 0 to 20 cm, 50 °C from 20 to 45 cm, 40 °C from 45 to 52 cm

Figure 16 Variation of logarithmic viscosity gradient at front with increasing ratio of fill time to the characteristic dissolution time

Figure 1

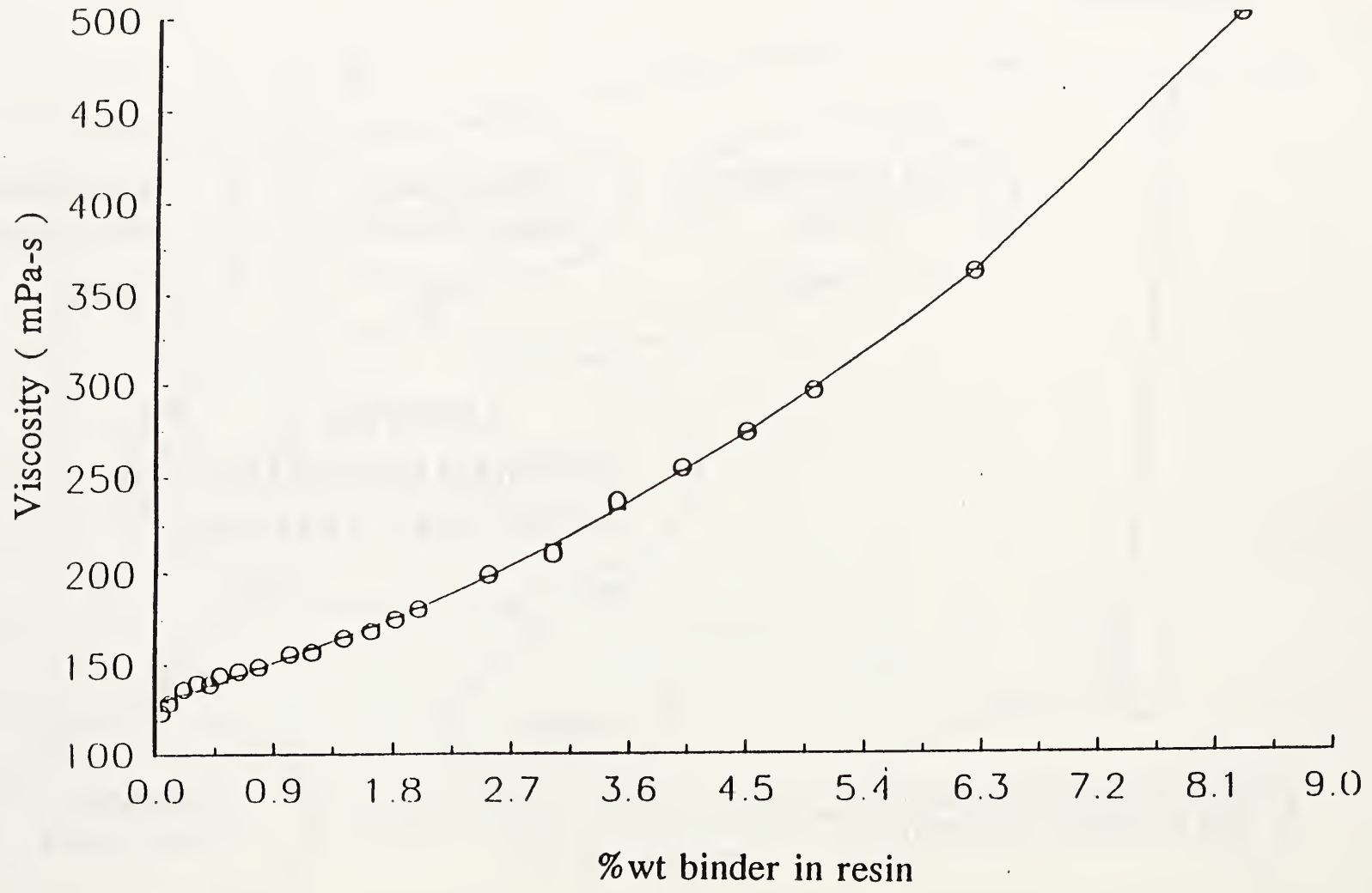
500
450
400
350
300
250
200
150
100
Viscosity (mPa-s)
0.0
0.9
1.8
2.7
3.6
4.5
5.4
6.3
7.2
8.1
9.0
%wt binder in resin

NON-UNIFORMITY IN MOLD FILLING

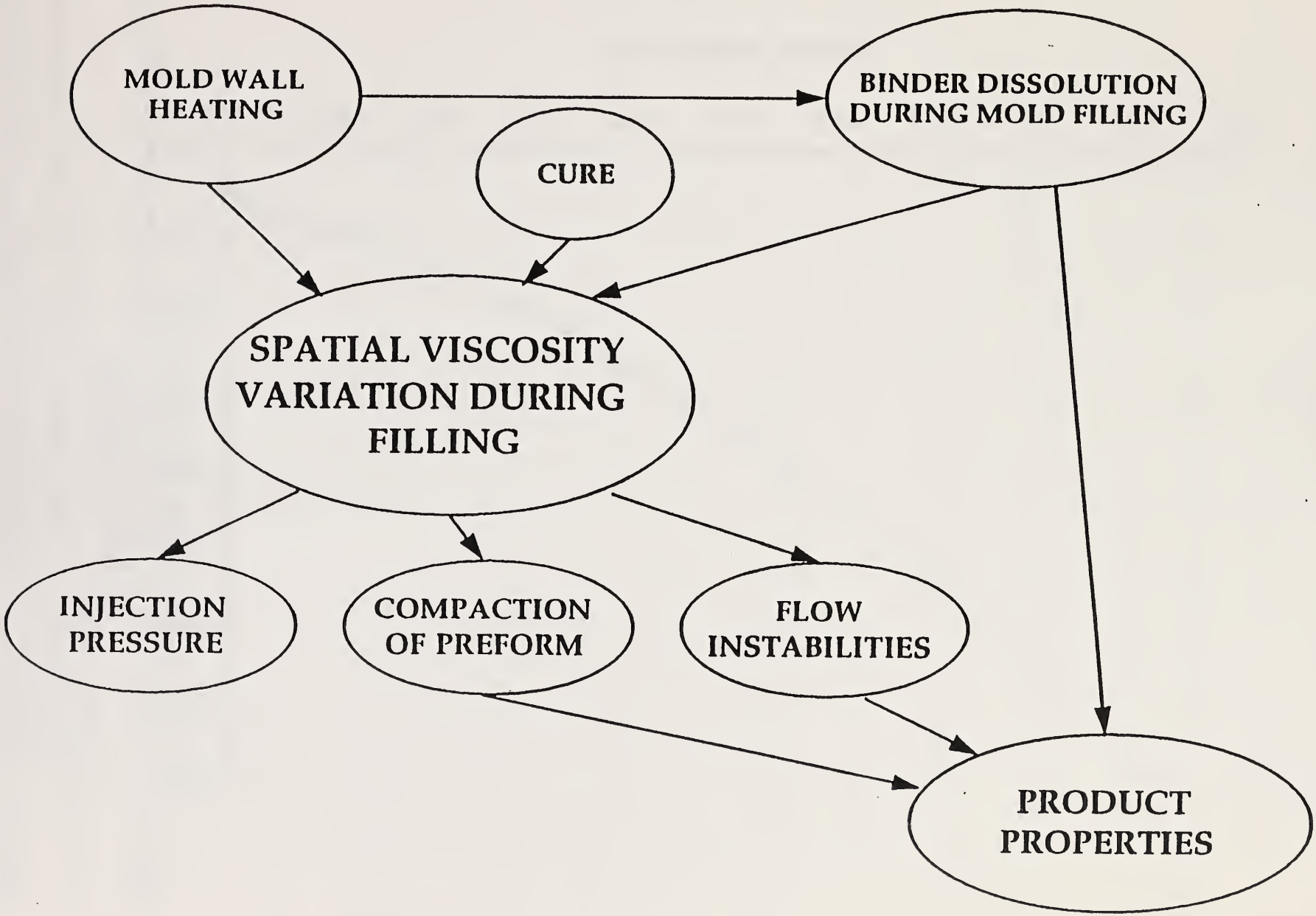

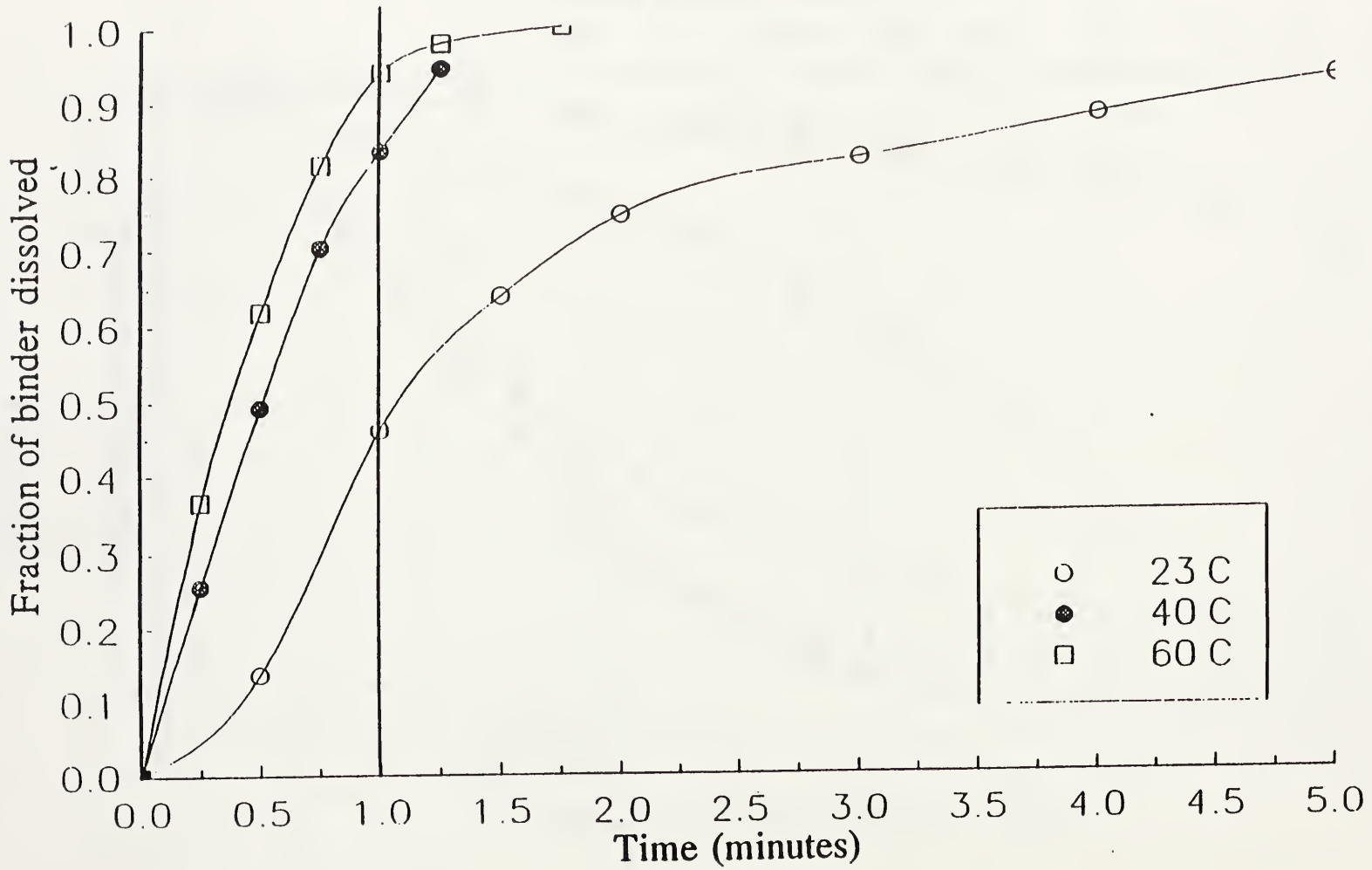
Fraction of binder dissolved
1.0
0.9
0.8
0.7
0.6
0.5
0.4
0.3
0.2
0.1
0.0
0.0
0.5
1.0
1.5
2.0
2.5
3.0
3.5
4.0
4.5
5.0
Time (minutes)
23 C
40 C
60 C

Figure 4

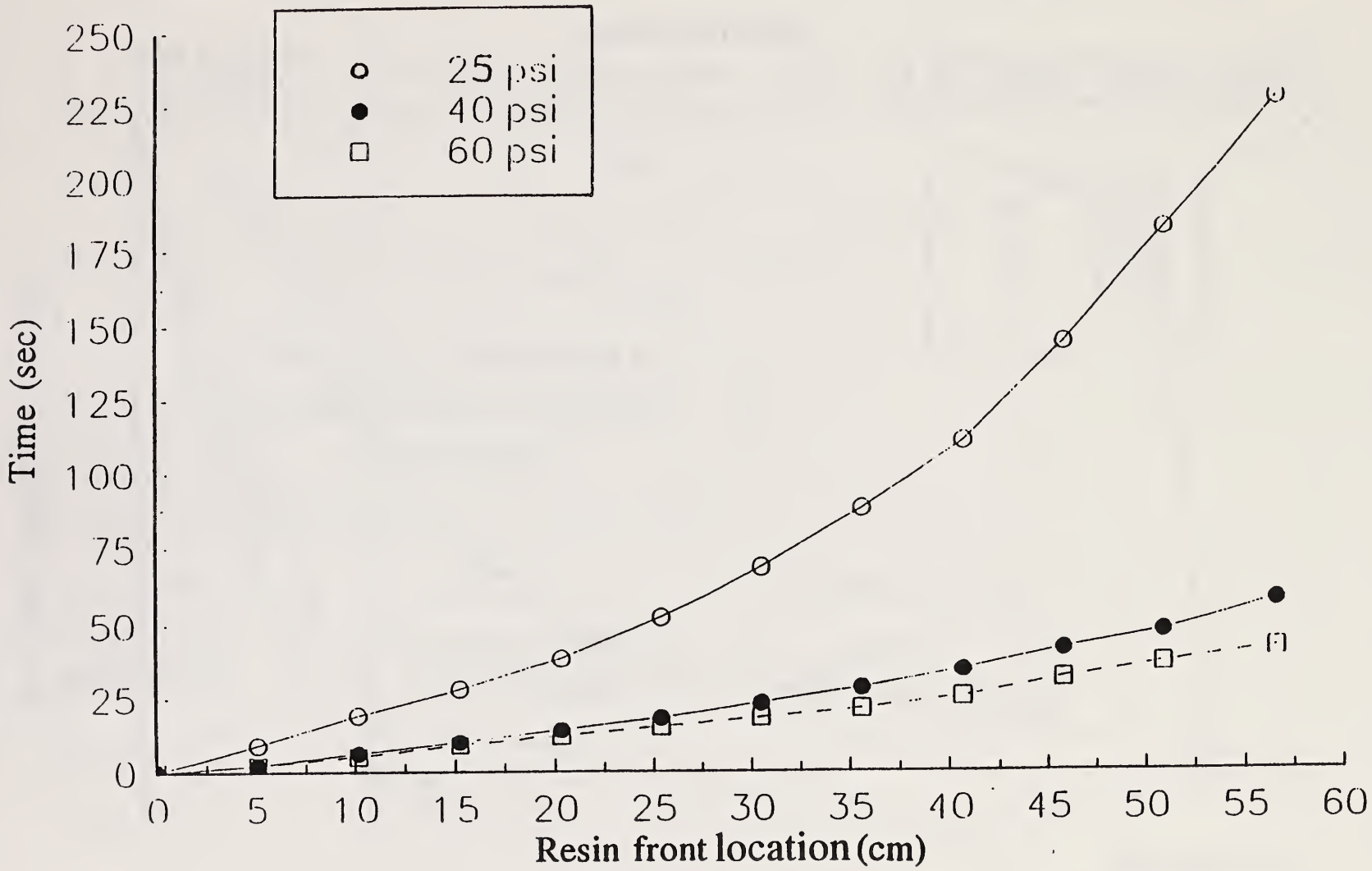
25 psi
40 psi
60 psi
Time (sec)
250
225
200
175
150
125
100
75
50
25
0
0
5
10
15
20
25
30
35
40
45
50
55
60
Resin front location (cm)

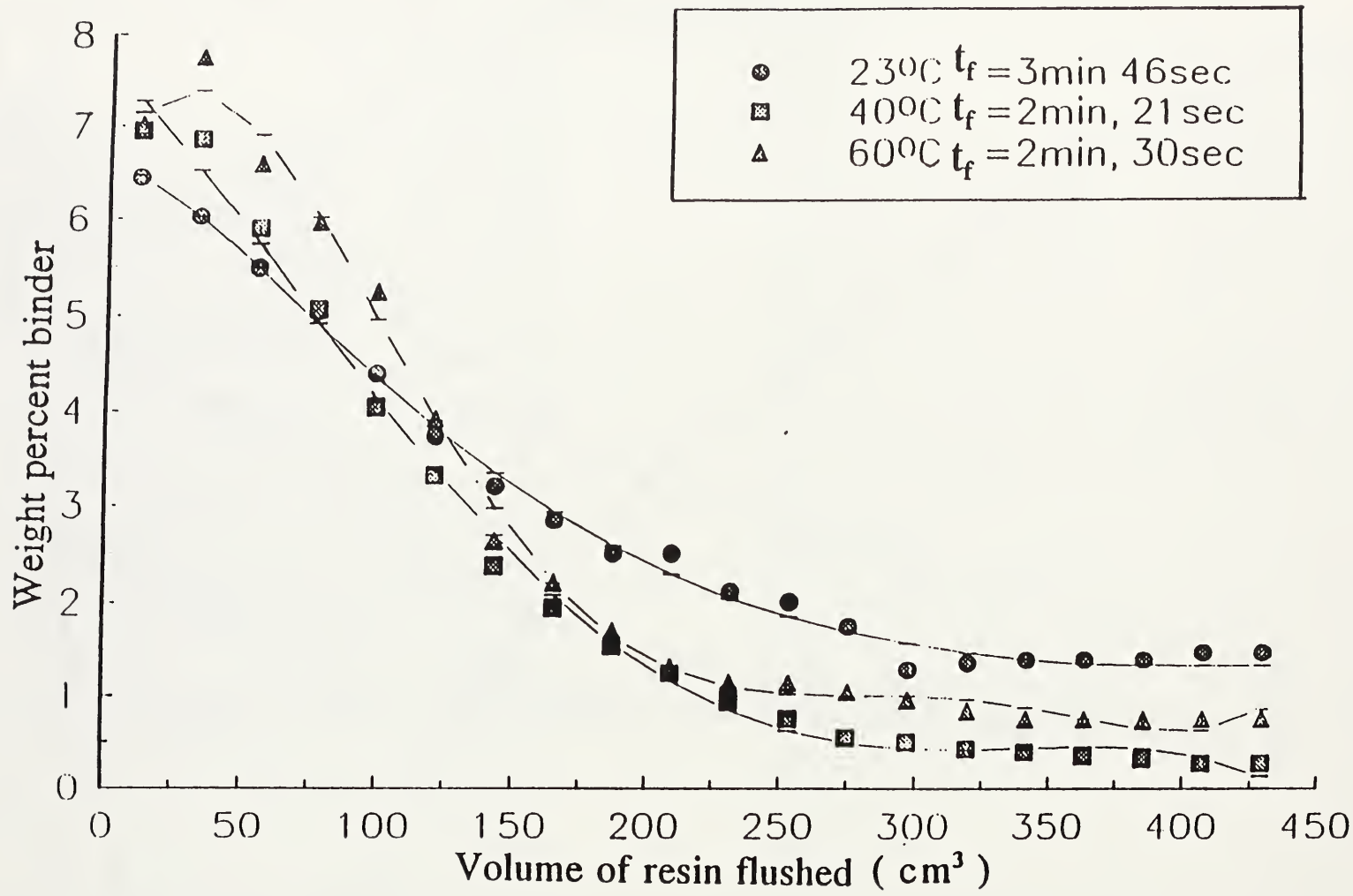
230C t_f = 3min 46sec
40°C t_f = 2min, 21 sec
60°C t_f = 2min, 30sec
Weight percent binder
0
1
2
3
4
5
6
7
8
0
50
100
150
200
250
300
350
400
450
Volume of resin flushed (cm³)

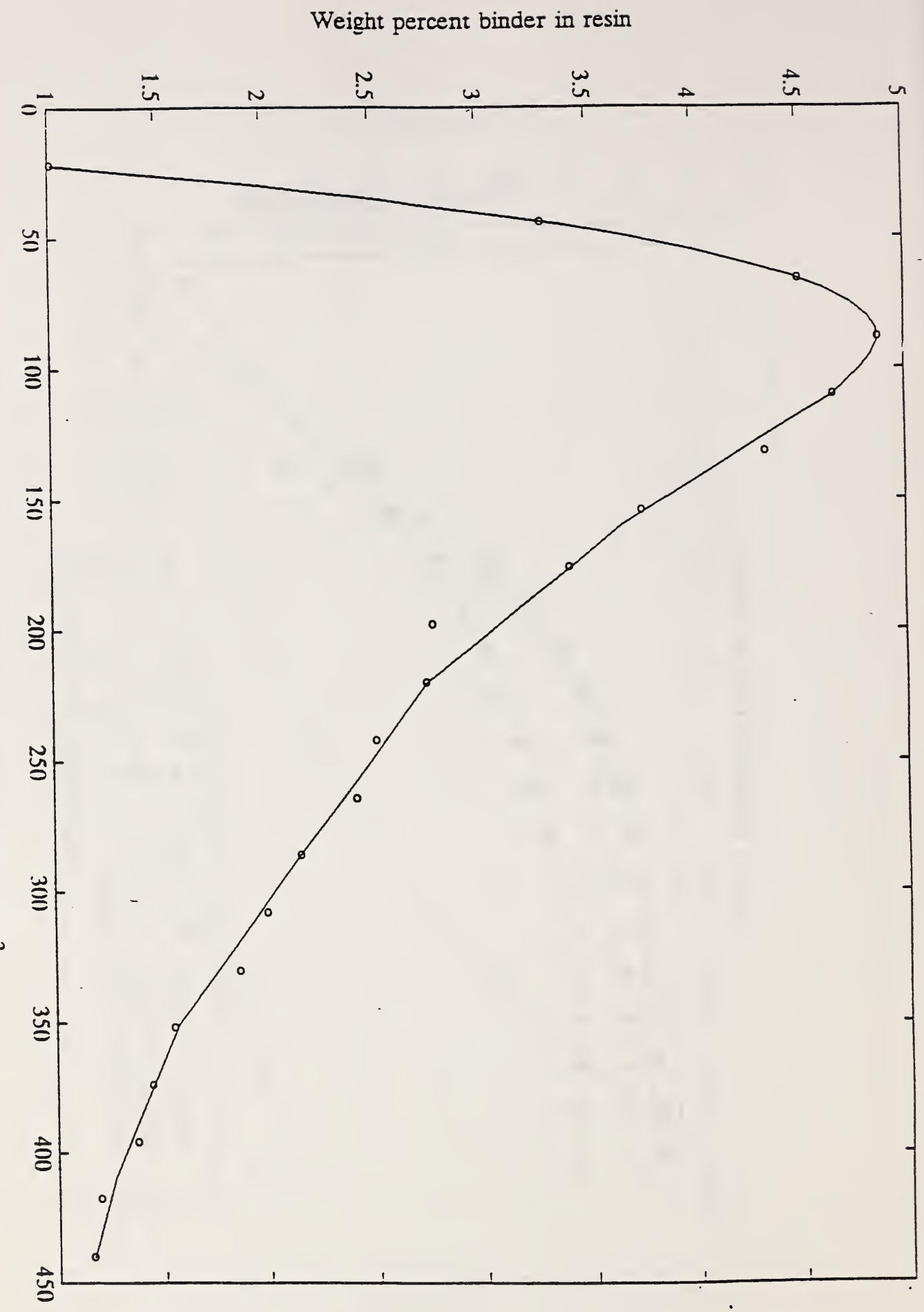
Weight percent binder in resin
1
1.5
2
2.5
3
3.5
4
4.5
5
0
50
100
150
200
250
300
350
400
450
Volume of resin flushed through preform, cm^3

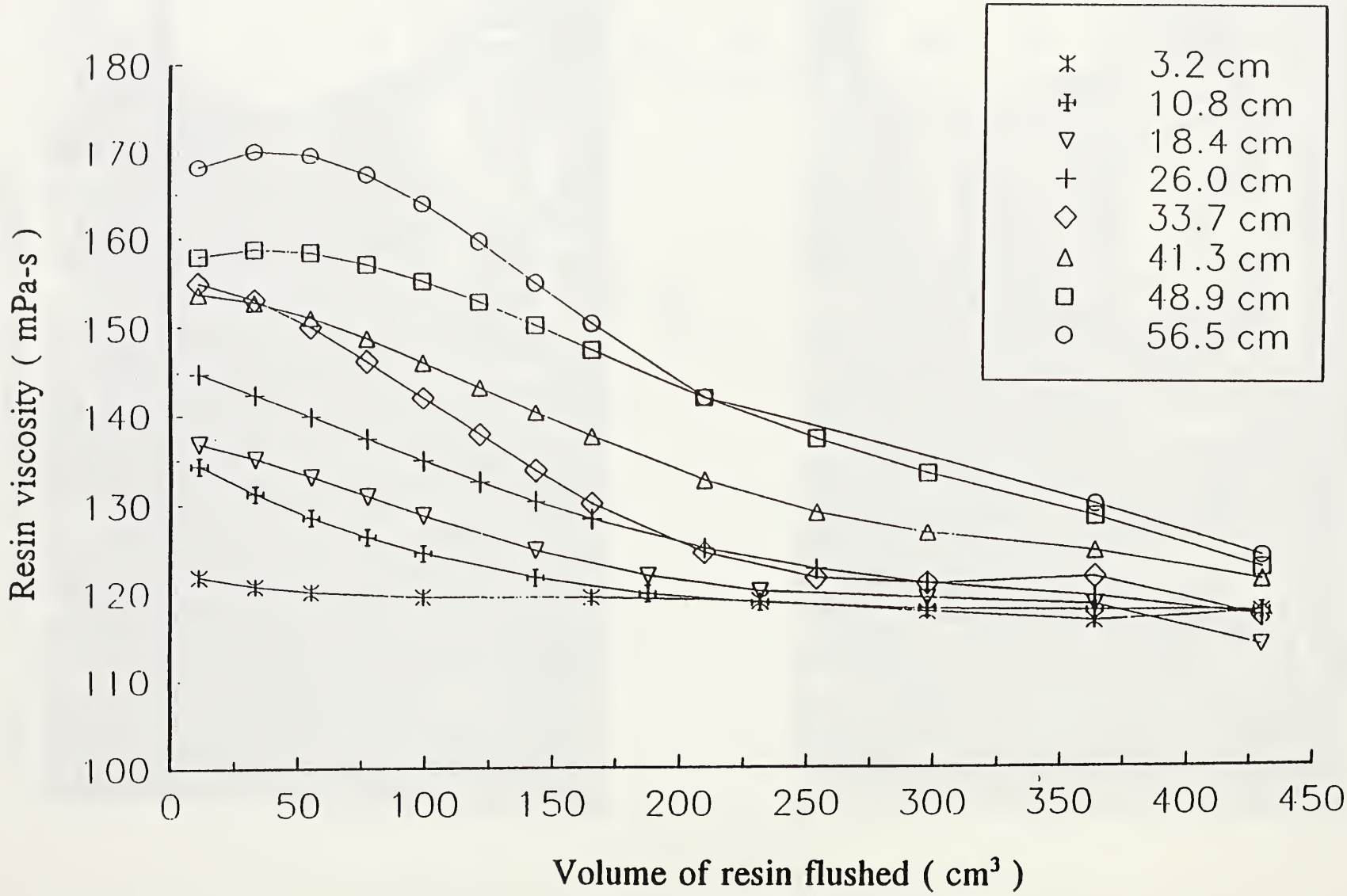
3.2 cm
10.8 cm
18.4 cm
26.0 cm
33.7 cm
41.3 cm
48.9 cm
56.5 cm
Resin viscosity (mPa-s)
180
170
160
150
140
130
120
110
100
0
50
100
150
200
250
300
350
400
450
Volume of resin flushed (cm³)

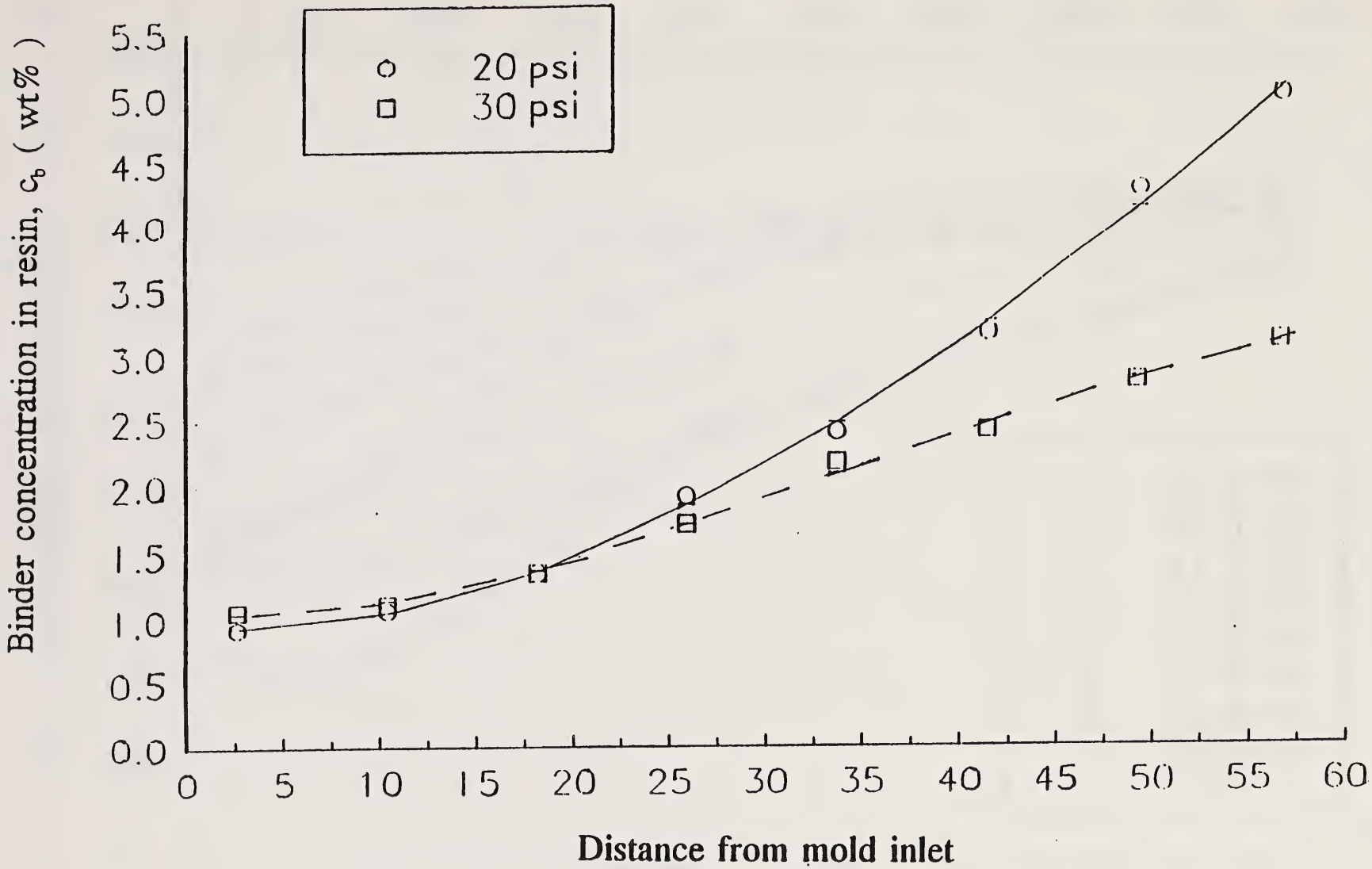
20 psi
30 psi
Binder concentration in resin, c_b (wt%)
5.5
5.0
4.5
4.0
3.5
3.0
2.5
2.0
1.5
1.0
0.5
0.0
0
5
10
15
20
25
30
35
40
45
50
55
60
Distance from mold inlet

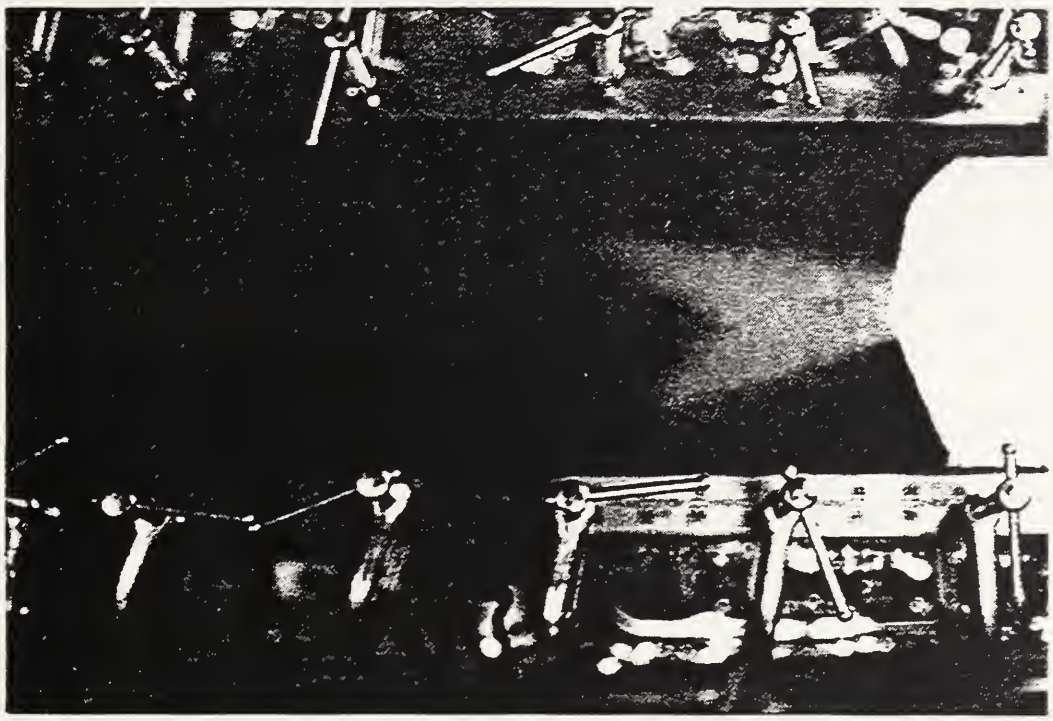

(a)

(b)

Figure 10

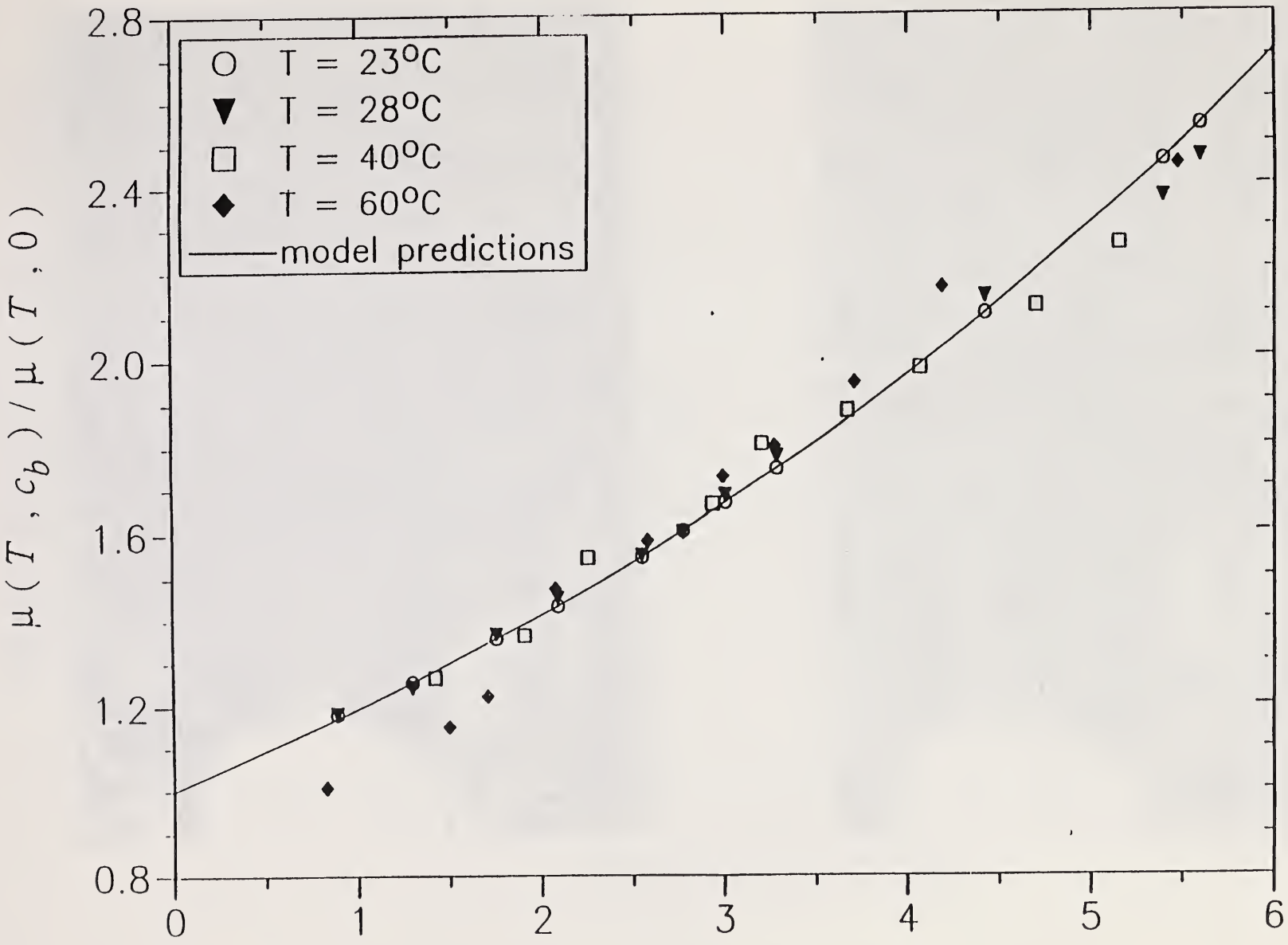
O T = 23°C
▼ T = 28°C
□ T = 40°C
◆ T = 60°C
——model predictions
$\mu(T, c_b) / \mu(T, 0)$
2.8
2.4
2.0
1.6
1.2
0.8
0
1
2
3
4
5
6
Binder concentration in resin, c_b (wt%)

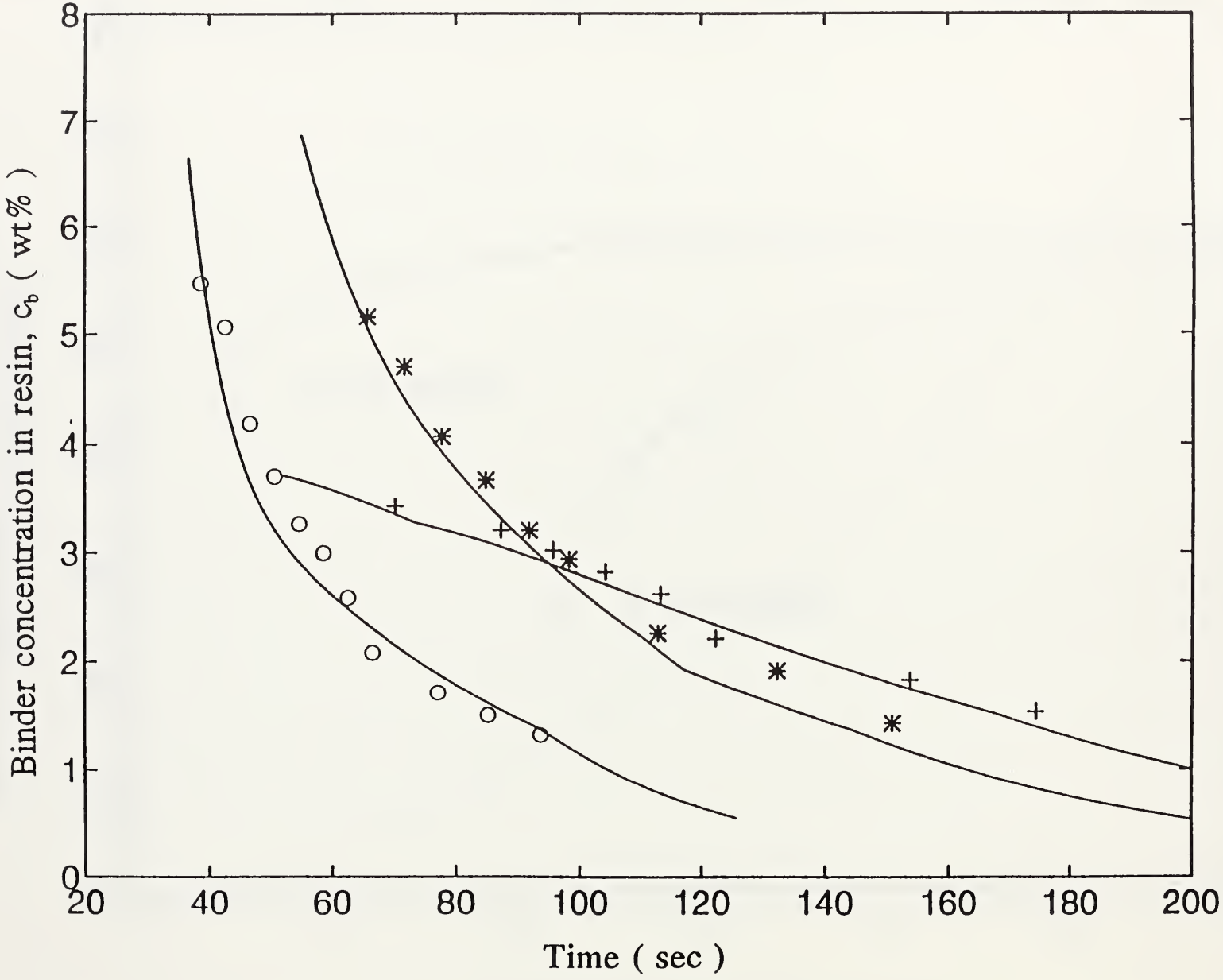
Binder concentration in resin, c_b (wt%)
Time (sec)
0
1
2
3
4
5
6
7
8
20
40
60
80
100
120
140
160
180
200

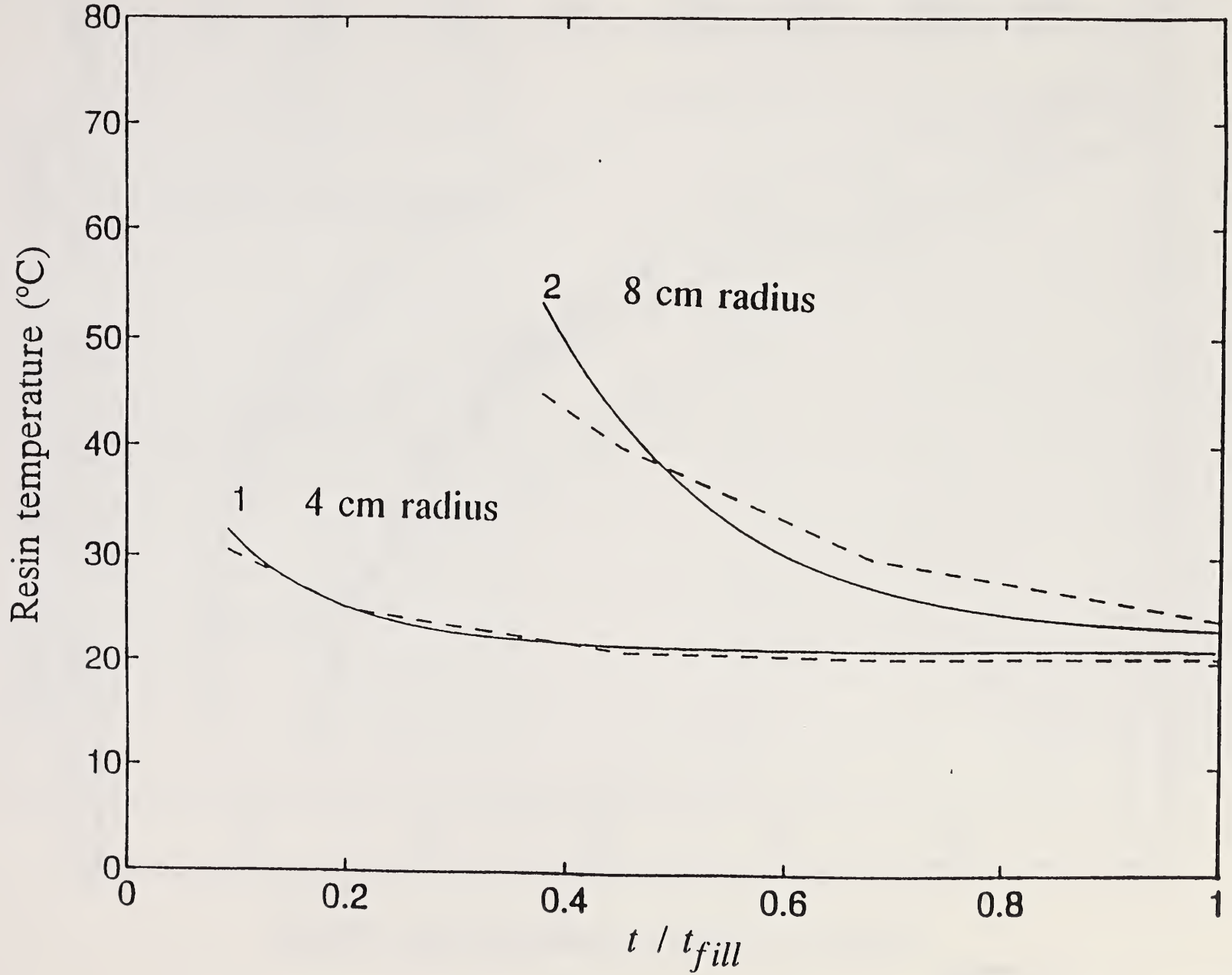
Resin temperature (°C)
80
70
60
50
40
30
20
10
0
0
0.2
0.4
0.6
0.8
1
t / t_{fill}
1 4 cm radius
2 8 cm radius

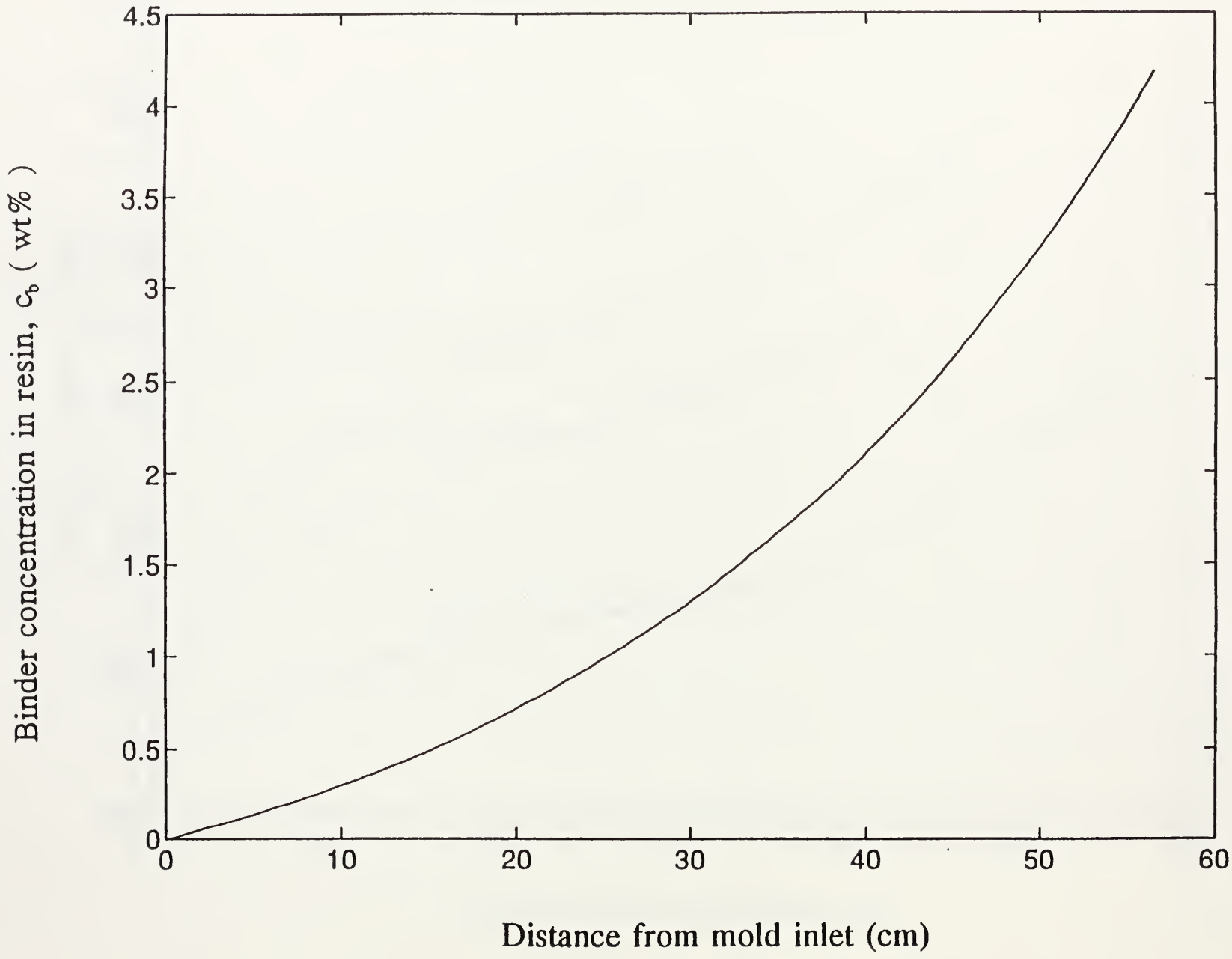
Binder concentration in resin, c_b (wt%)
4.5
4
3.5
3
2.5
2
1.5
1
0.5
0
0
10
20
30
40
50
60
Distance from mold inlet (cm)

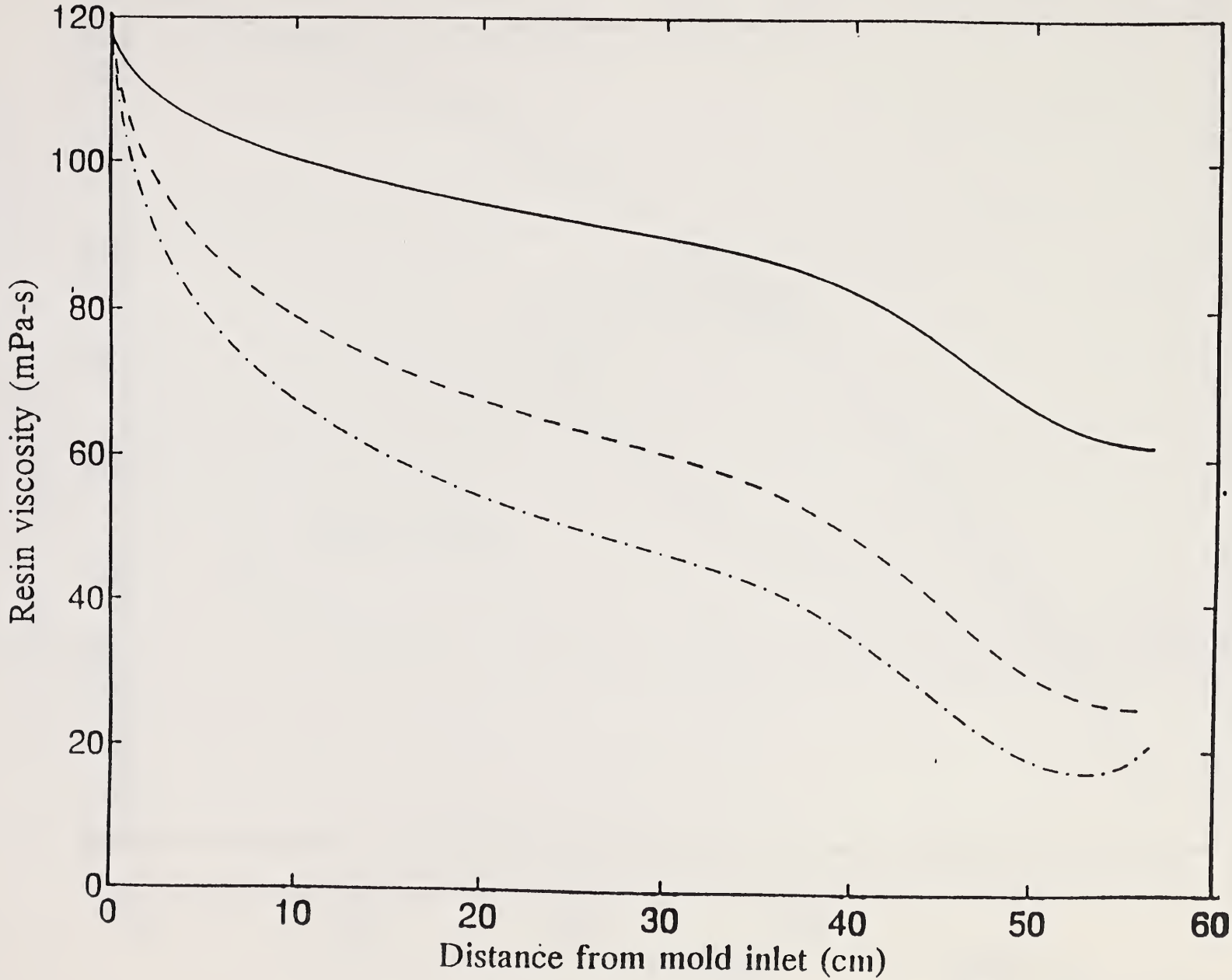
120
100
80
60
40
20
0
Resin viscosity (mPa-s)
0
10
20
30
40
50
60
Distance from mold inlet (cm)

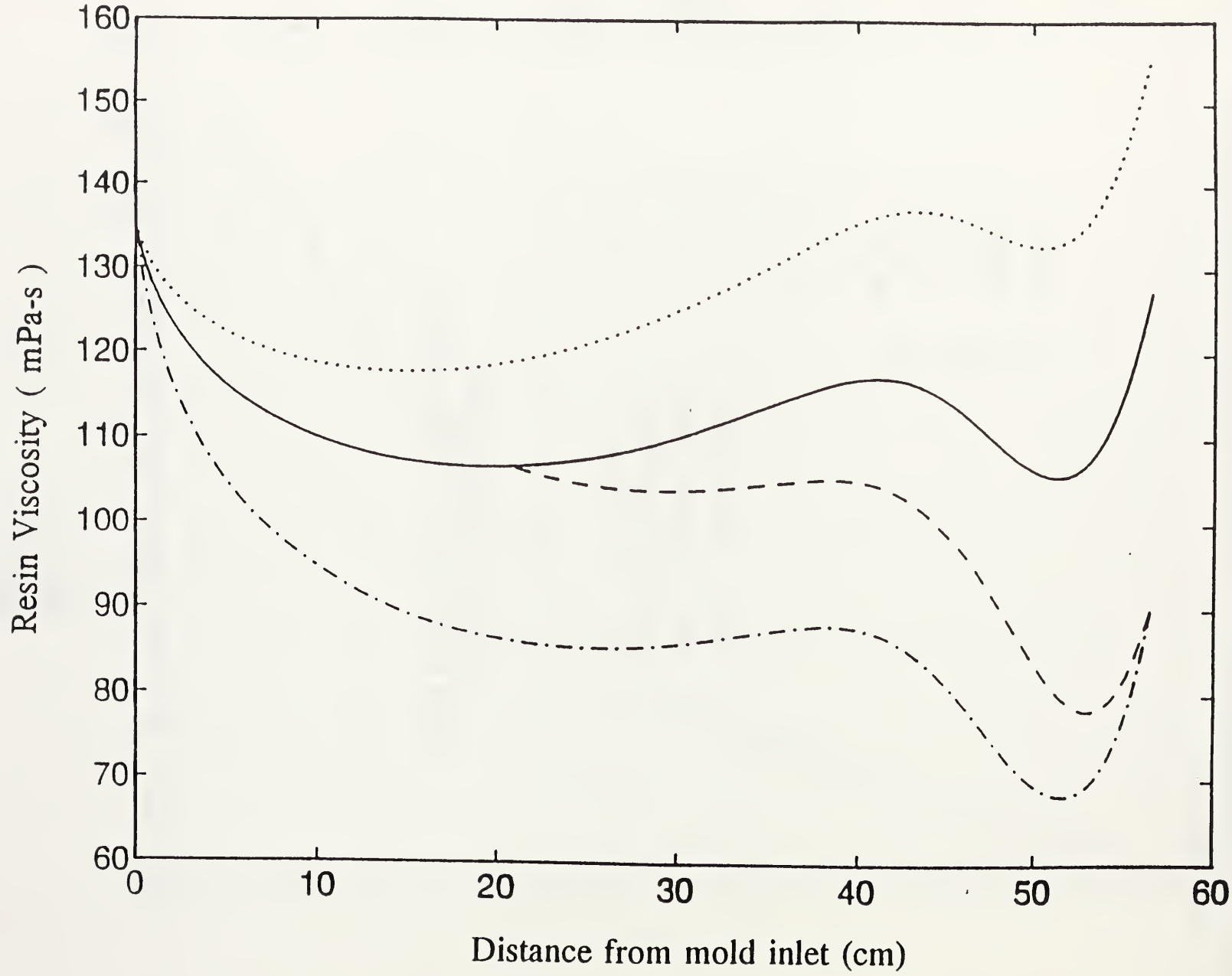
160
150
140
130
120
110
100
90
80
70
60
Resin Viscosity (mPa-s)
0
10
20
30
40
50
60
Distance from mold inlet (cm)

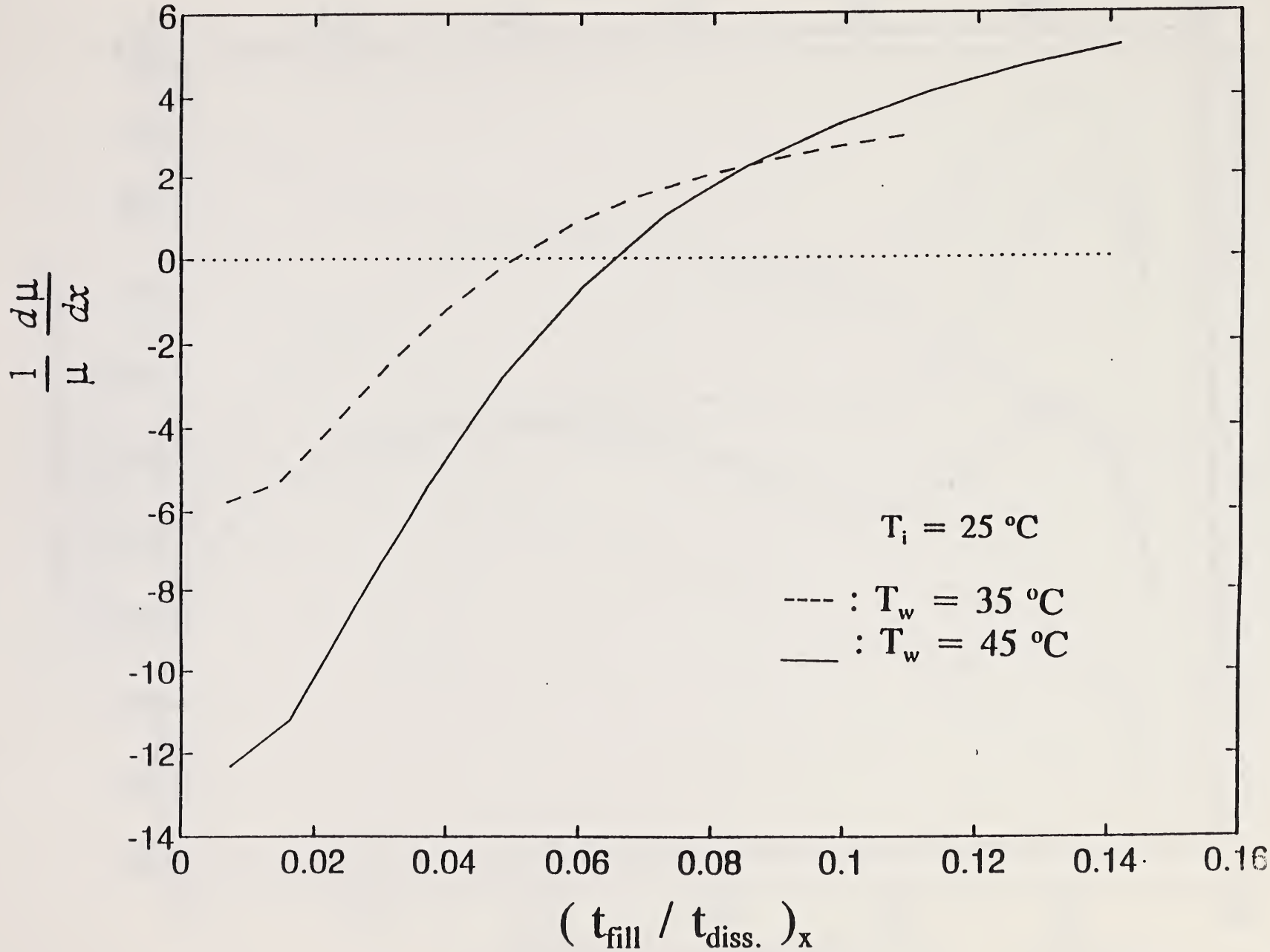
6
4
2
0
-2
-4
-6
-8
-10
-12
-14
0
0.02
0.04
0.06
0.08
0.1
0.12
0.14
0.16
$\frac{1}{\mu}\frac{d\mu}{dx}$
T_i = 25 °C
---- : T_w = 35 °C
___ : T_w = 45 °C
(t_{fill} / $t_{diss.}$)$_x$

Mold Filling Issues in High Speed Reactive Liquid Molding

by

J. M. Castro
GenCorp Research
2990 Gilchrist Road
Akron, Ohio 44305

To be presented at:
Workshop on Manufacturing Polymer Composites by Liquid Molding
September 20-24, 1993

ABSTRACT

Two forms of high speed reactive liquid molding are discussed, one that uses mixing activated chemical systems, commonly known as SRIM and the other which uses thermally activated systems, commonly referred to as high speed RTM. The key difference between both processes occurs in the mixing stage, which is critical and must occur on-line for SRIM, but not necessarily for RTM. Beyond mixing, both processes are similar. The chemorheological changes that occur during the filling stage as well as procedures to obtain viscosity rise equations to be used in process modelling are discussed. The filling stage is discussed and cases where simple models can be used to represent it are pointed out. Examples of the use of computer simulation for practical applications are given.

INTRODUCTION

Reactive Liquid Molding (RLM) can be defined as a process for producing fiber reinforced polymeric parts in final shape, directly from low viscosity monomers or prepolymers. It involves the injection of a reactive mixture into a closed mold where a dry preform of reinforced fibers and sometimes other elements such as foam cores and metal attachment pieces are pre-placed. The reactive mixture then fills the spaces between the fibers. The reactive mixture then cures, forming a stiff solid composite that can be removed from the mold. In its earliest version, also known as Resin Transfer Molding (RTM), it has been used in molding large fiber reinforced parts for a long time, mainly from polyester based resins and occasionally epoxy resins. The traditional RTM process is carried out with in-line pumping of two components through a static mixer about 50 psi injection pressure, no holding pressure, mold temperatures around 150°F, and a long mold filling time and total typical cycle time of 10-20 minutes. If the reactivity of the mixed resins is increased to shorten cycle time, the resin is apt to cure in the mixer and injection line.

Unless the long cycle times of the traditional RTM process can be reduced, the economic value of such process tends to be limited to jobs with production volume under 10,000 parts. Two modified processes which cut down the cycle time are the mixing activated high speed RLM (MA/HSRLM) and the thermally activated high speed RLM (TA/HSRLM)[1]. The basic principles of these processes are the same except for the mixing. In the mixing activated high speed RLM, also commonly known as SRIM, two or more highly reactive monomers or prepolymers, are brought into intimate molecular contact by impingement mixing. From the mixing head, they flow into the mold containing the preform and react rapidly to form a solid part. The impingement mixing chamber directly attaches to the mold and a piston empties mix from the chamber into the mold at the end of injection. A sketch of the process[2] is shown in Figure 1. The mold wall temperature (Tw) is not necessarily much different than the starting material temperatures (To), since the monomers are highly reactive at To.

In the thermally activated high speed RLM process, also commonly known as high speed RTM, the main change from usual RTM is to raise the mold temperature so the monomers, which do not react appreciably at To, cure more rapidly. Residence time in the mixer is therefore not too critical, and it may be carried out in a separate operation or equipment. The reaction starts after the materials come in contact with the hot mold. The mold temperature is much higher than the starting material temperature. A schematic diagram of the process[2] is shown in Figure 2. The main problem in accomplishing HSRTM is finding an inexpensive mold that can take the $\geq$ 200°F mold temperatures needed in practice.

After the mixing step, both processes are similar. There is a filling or shaping step and a curing step as shown schematically in Figure 3 which also shows a typical change of the viscosity and modulus as it occurs during the process[3]. As shown in Figure 3, the viscosity just after mixing is low. It remains low for the initial part of the reaction. The mold should be filled during this period. At the end of filling, the elastic modulus should quickly rise to a sufficiently high value to allow the fast removal of the part. The main difference between both processes during the curing stage is that for the mixing activated system, the reaction front moves in general from the inside to the outside[4]. For the thermally activated process, if the preform is not allowed to preheat, the reaction front moves from the wall to the center. As the preform is allowed to preheat, the last place to cure could move from the center to the wall.

CHEMO-RHEOLOGY

Viscosity is the most important material property in polymer processing operations involving flow. Thermoplastic melt viscosity is influenced primarily by temperature and shear rate. Reactive systems are complicated by the increase in viscosity due to chemical reaction[5]. In RLM, since flow is coupled with chemical reaction, we need to know the viscosity increase with reaction.

To model the filling stage, an expression relating explicitly the viscosity to temperature and the extent of reaction, is needed because temperature affects the viscosity rise in two opposing ways. Increasing the temperature will cause the viscosity (η) to decrease at a given extent of reaction (C*) but will also raise the reaction rate, producing an increase in C* and viscosity. In order to separate these effects, the kinetics must be measured independently. An η-C* correlation can be constructed by taking isochrones of viscosity and extent of reaction[5]. The procedure is shown schematically in Figure 4.

In order to measure the viscosity rise of thermally activated systems typical of those used in high speed RTM, in general, a standard rheometer with a good environmental chamber for temperature control can be used. The rheometer is preheated to the desired temperature and the material charged as quickly as possible. Isothermal viscosity rise measurements can then be made at several temperatures in general up to or close to the molding temperature.

For systems typical of the ones used in SRIM, since they are highly reactive once mixed, an on-line viscometer directly attached to the RIM machine needs to be used[6]. However, if the system can be slowed down by using less catalyst, the viscosity rise can be measured using a standard rheometer and then extrapolated to higher catalyst levels using kinetic data if one can assume that the shape of the viscosity rise remains the same[7].

For process modelling, we need an expression to relate the viscosity to the chemical state of the reactants. It has been found that typical SRIM system, can be treated as Newtonian fluids[7], thus the viscosity is a function only of the temperature and the extent of reaction. The following equation, proposed by Castro and Macosko[7,8] has been found useful by several investigators in process modelling[8,9,10,11]:

$$\eta = A\eta e^{\frac{E\eta}{RT}}\left(\frac{Cg^*}{Cg^* - C^*}\right)^{A+BC^*} \qquad (1)$$

where Cg* is the gel conversion, Eη is the activation energy and A and B are constants.

FILLING STAGE

In general, to analyze the filling or shaping stage during the RLM process, one needs to consider the coupling between chemical reaction, flow and heat transfer[11,13,14]. This coupling comes through the viscosity, thus, it one could assume that the viscosity remains nearly constant during filling, the reaction and heat transfer effects can be neglected. When this is the case, the filling stage can be assumed isothermal and the chemical reaction neglected during filling; which decreases the computation time required to analyze it enormously. Thus, it is of interest to discuss this aspect further.

In general, there is very little time for a preform to heat after placing it in the mold since injection starts soon after. Furthermore, for the cases of traditional RTM and SRIM, the mold wall temperature is not much higher than the initial material temperature. Thus neglecting the heat transfer during flow is a good first approximation. As far as reaction effects for typical RTM, where polyester type materials are used, we could neglect them if the fill time is much shorter than the inhibition time. As for SRIM materials, where polyurethane type systems are used, chemical reaction effects can be neglected if the fill time is much smaller than the time to reach the gel point evaluated at the average temperature between the initial material temperature and the mold wall temperature. This criteria has been found very useful by Castro and Macosko[8], which defined this ratio as the gelling number (G).

For high speed RTM where the mold wall temperature is much higher than the initial material temperature and where it may be desired to preheat the preform to decrease the cycle time, more work is needed to see how far one can push an isothermal simulation in analyzing the filling stage. The key is how sensitive is the viscosity to temperature and chemical reaction.

Most parts of commercial interest are fairly thin. Thus, 2D flow simulation can be used most of the time. For thicker parts where the 3D effects are important, one would need to use a more computer time intensive 3D simulation. For thin parts, if chemical reaction and heat transfer effects can also be neglected, it can be shown that a Generalized Hele-Shaw model such as the ones developed for injection molding can, in some cases, be used to analyze the filling stage during RLM[12]. To better understand this, Table 1 summarizes the thickness averaged equations for both RLM and the Generalized Hele-Shaw model. Where the viscosity used in the RLM equations is the fluid velocity within the pores, the so called intrinsic velocity which is the one needed to obtain the filling pattern.

From Table 1, one can conclude that to predict RLM flow, with a flow simulation program based on the Hele-Shaw model, Equation A-1 must be made equivalent to A-2, B-1 to B-2 and C-1 to C-2. This will occur when the following conditions are met:

$$\frac{h^2_{HS}}{12\eta_{HS}} = \frac{K}{\eta\phi} \qquad (2)$$

and

$$h_{HS} = h\phi \qquad (3)$$

Substitution of Equation (3) in Equation (2) gives:

$$\eta_{HS} = \frac{\eta}{12K} h^2 \phi^3 \qquad (4)$$

Thus, for a given RTM flow condition, that is, given viscosity (η), permeability (K), part thickness (h), porosity (ϕ) and flow rate (Q) or injection pressure (Po), a Hele-Shaw based flow simulation program can be run with fictitious η and h as given by Equations (3) and (4). The predicted flow front positions; pressures and fill times will be those for the RLM case.

Two cases should be discussed. First, for the case when the permeability, porosity and mold thickness are uniform all through the part, one need only to calculate a pseudo-height and a pseudo-viscosity according to Equations (3) and (4), respectively. Secondly, for the case when the glass content or porosity are not uniform; only flows with combinations of variations in K, h and ϕ that give constant η_{HS} can be solved. On the other hand, if we can empirically fit K as a function of ϕ for a given mat in the range of interest with a truncated cubic equation

$$K = c_1 \phi^3 \qquad (5)$$

This simplifies Equation (4) to

$$\eta_{HS} = \frac{\eta_r}{12C_1} h^2 \qquad (6)$$

Thus, if the RLM mold thickness remains constant and Equation (5) applies, one can also simulate the case where the porosity and K are a function of position using (3) and (6).

APPLICATIONS

A flow simulation program to predict the position of the flow front during filling can be helpful to select injection locations which minimize the potential for gross trapping of air* or the locations where vents may be needed to allow the air to escape. *Trapping small bubble is almost inherent due to "micro fingering" of flow through mat at leading edge of fill. For example, Figures 6 and 8 show the fill pattern for a lift gate injecting in the locations shown in Figures 5 and 7, respectively. Figures 5 and 7 also show

the suggested location of air vents. For injection machines with limited injection pressure potential, or preforms that "wash" or compress with too high pressure, it will also be useful to predict the lowest fill time possible for a given injection pressure.

PRACTICAL CONCERNS

The value of the permeability plays a key role in predicting the flow during RLM. The permeability will be influenced by the preforming process and possibly varying compression of an imperfectly sized and shaped preform during mold closure prior to injection and may change during filling as well. In practice, permeabilities often vary greatly in an unknown fashion and are probably the biggest hindrance to accurate flow simulations.

Ideally, one would like to be able to predict what occurs during the preforming process and then use this prediction to obtain a permeability value. So far, at most flow simulation can be used as a guide. More work is needed on the effect of the local mat deformation during the preforming stage on the permeability[13].

Another important consideration is channeling, common when an imperfectly cut preform does not extend fully to the edge of the part. In practice, to avoid this, preforms often extend beyond the cavity thus also reducing leakage from the mold, and parts are later machined to size. Preform deformation during flow is also a major concern and would greatly affect the flow.

When deriving Darcy's law, the viscosity is assumed constant. More work is needed to determine how this should be modified for the cases where the viscosity changes appreciably during flow[14].

REFERENCES

1. Johnson, C. F., Chanka, N. G. and Jeryan, R. A., "Resin Transfer Molding of Complex Automotive Structures," Proceedings 41st Annual Conference SPI, Jan. 27-31, 1986, 12A.
2. Castro, J. M., "On the Mathematical Modelling of the Reaction Injection Molding (RIM) Process," Latin American Journal of Heat and Mass Transfer, 6, 67 (1982).
3. Broyer, E. and Macosko, C. W., "Heat Transfer and Curing in Polymer Reaction Molding," AIChE J., 22, 268 (1976).
4. Castro, J. M., Gonzalez, V. M. and Macosko, C. W., "Process Behavior Differences Between Thermally and Mixing Activated RIM Type Chemical Systems," Soc. Plast. Eng. Tech. Papers, 39, 363 (1981).
5. Castro, J. M., Macosko, C. W. and Perry, S. J., "Viscosity Changes During Urethane Polymerization with Phase Separation," Polymer Communications, 1984, Vol. 25, March 1982.
6. Perry, S, J., Castro, J. M., and Macosko, C. W., "A viscometer for Fast Polymerizing Systems," Journal of Rheology, 29 (1), 19-36 (1985).
7. Castro, J. M. and Macosko, C. W., "Kinetics and Rheology of Typical Polyurethane Injection Molding Systems," Soc. Plast. Eng. Tech. Papers, 38, 434 (1980).
8. Castro, J. M. and Macosko, C. W., "Studies of Mold Filling and Curing in the Reaction Injection Molding (RIM) Process, AIChE J., 28, 250 (1982).
9. S. Estevez and Castro, J. M., "Applications of a RIM process Model in the Analyses of Premature Gelling, Demold Time and Maximum Temperature Rise," Polym. Eng. Sci., 24, 428 (1984).
10. M. J. Schmidt and Castro, J. M., "Continuous Reactive Processing I: Reactive Coating," Polym. Eng. Sci., 25, 541 (1985).
11. Lin, R. J., Lee, James L. and Liou, Ming J., "Mold Filling and Curing Analysis in Liquid Composite Molding," Polym. Comp., Vol. 14, No. 1, 71 (1993).
12. Lee, Y. M., Castro, J. M., Tomlinson, G. and Straus E., "Analyses of Flow in the RTM Process," New Developments in Polymer Composites for Automotive

Applications, SAE 57-67 (1989).

13. Lee, L. James, "Liquid Composite Molding: A State of the Art Review," Report No. ERC/NSM-P-92-22, Ohio State University ERC for Net Shape Manufacturing, April 1992.
14. Tucker, C. L., and Dessenberger, "Governing Equations for Resin Transfer Molding," a chapter to be published in the book, Flow Phenomena in Polymeric Composites, S. Advani, Editor (1993).

Table I

Summary of Field Equations for Hele-Shaw and RLM

Hele-Shaw

$$(A\text{-}1)\quad \frac{\partial}{\partial x} v_{xHS}\, h_{HS} + \frac{\partial}{\partial y} v_{yHS}\, h_{HS} = 0$$

$$(B\text{-}1)\quad v_{xHS} = -\frac{h^2_{HS}}{12\eta_{HS}} \frac{\partial p}{\partial x}$$

$$(C\text{-}1)\quad v_{yHS} = -\frac{h^2_{HS}}{12\eta_{HS}} \frac{\partial p}{\partial y}$$

RLM

$$(A\text{-}2)\quad \frac{\partial}{\partial x} h\, v_{xr}\, \phi + \frac{\partial}{\partial y} h v_{yr}\, \phi = 0$$

$$(B\text{-}2)\quad v_{xr} = -\frac{K}{\eta\phi} \frac{\partial p}{\partial x}$$

$$(C\text{-}2)\quad v_{yr} = -\frac{K}{\eta\phi} \frac{\partial p}{\partial y}$$

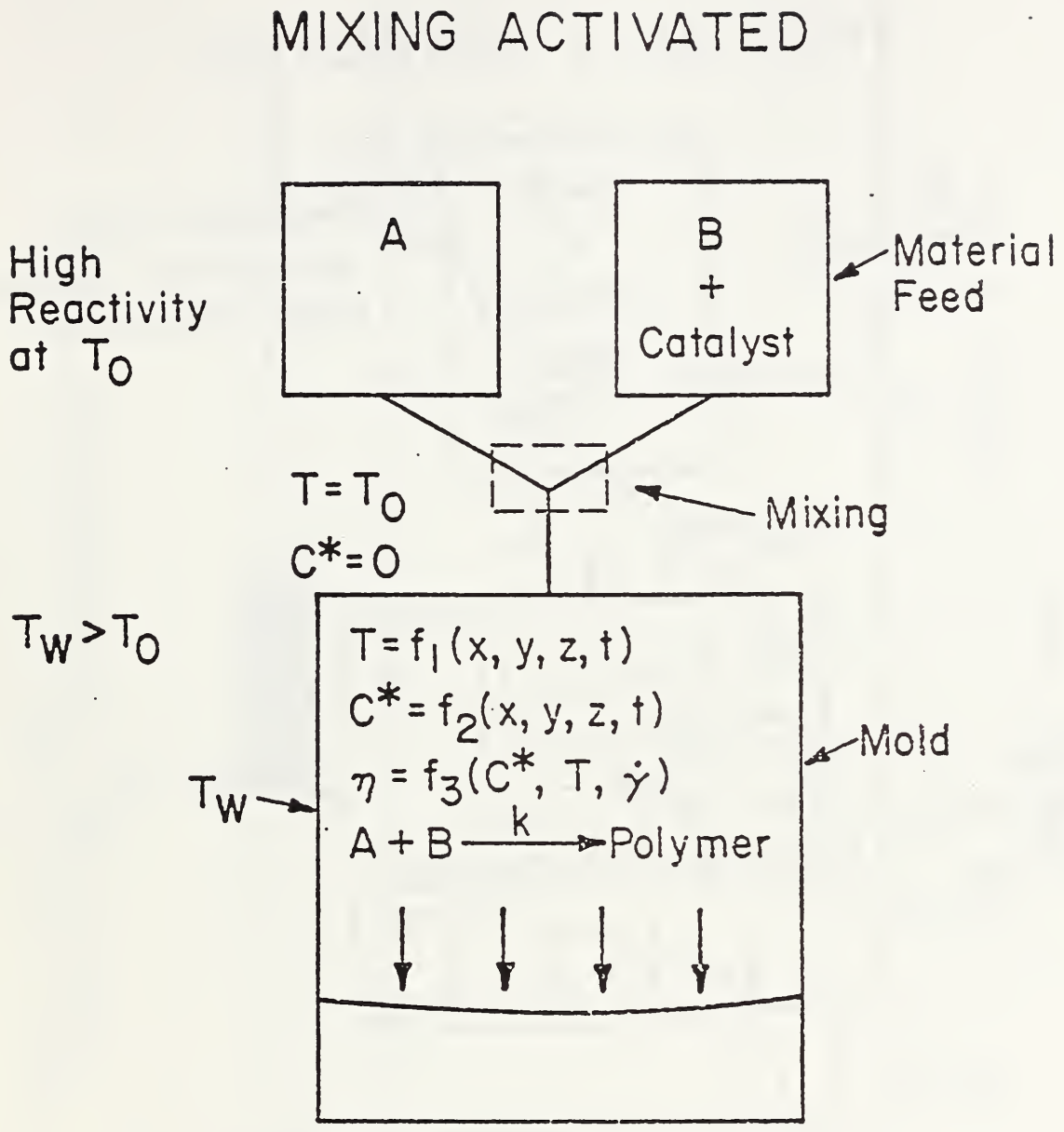

Figure 1. Schematic diagram of a mixing-activated HSRLM process. Temperature (T), extent of reaction (C*) and viscosity (η) are a function of position and time in the mold.

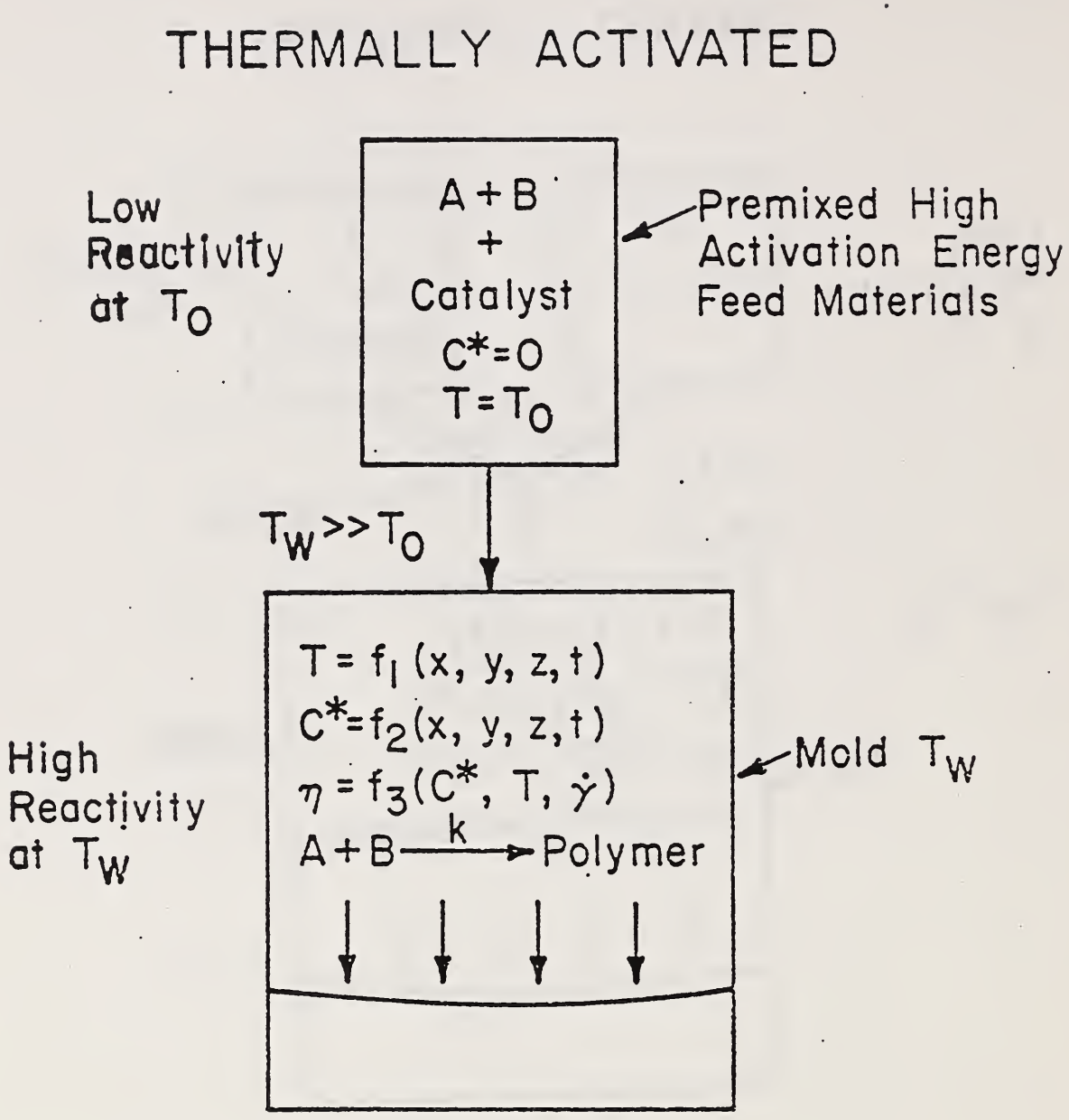

Figure 2. Schematic diagram of a thermally-activated HSRLM process. Temperature (T), extent of reaction (C*) and viscosity (η) are a function of position and time in the mold.

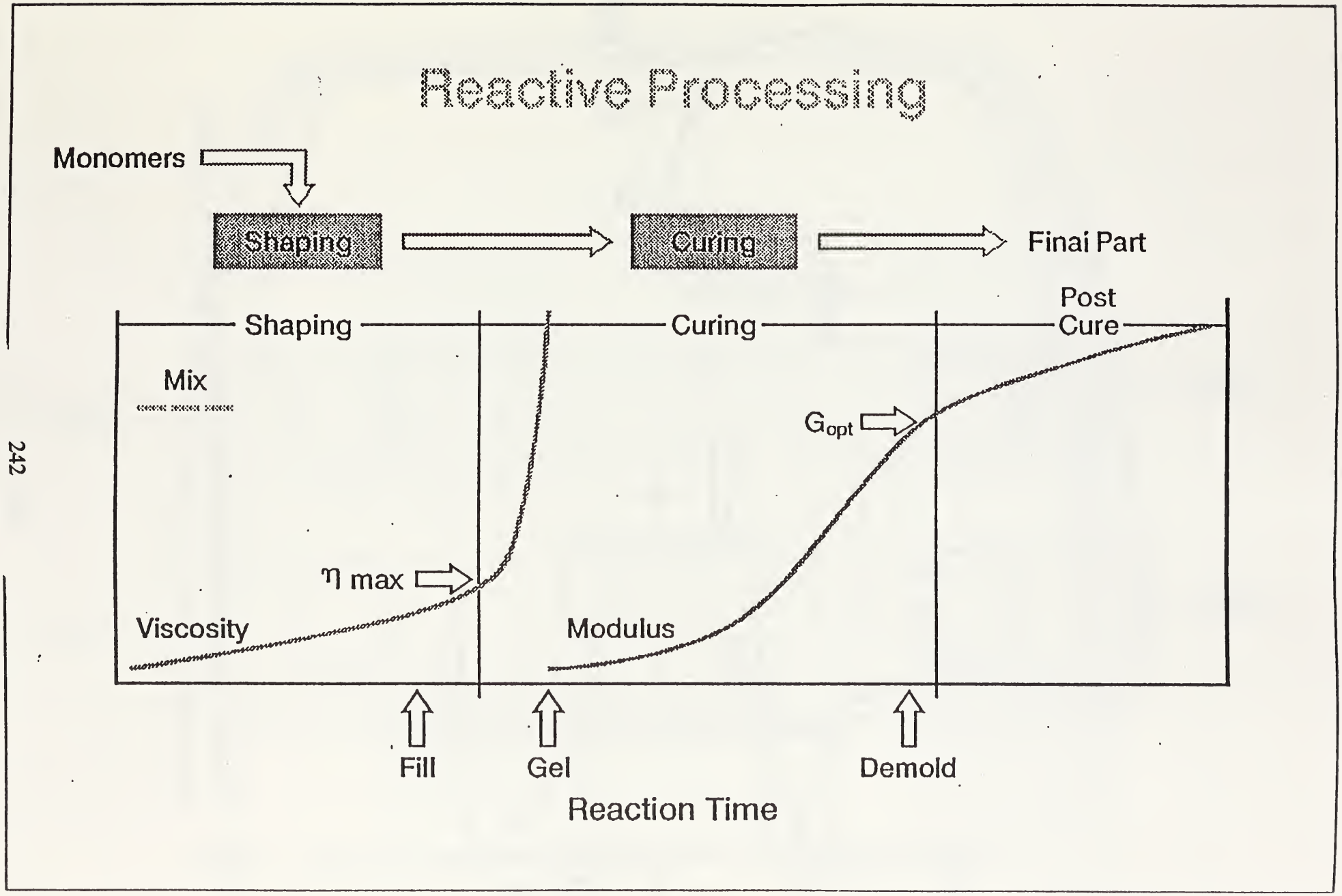

Figure 3. Rheological changes for typical RLM process.

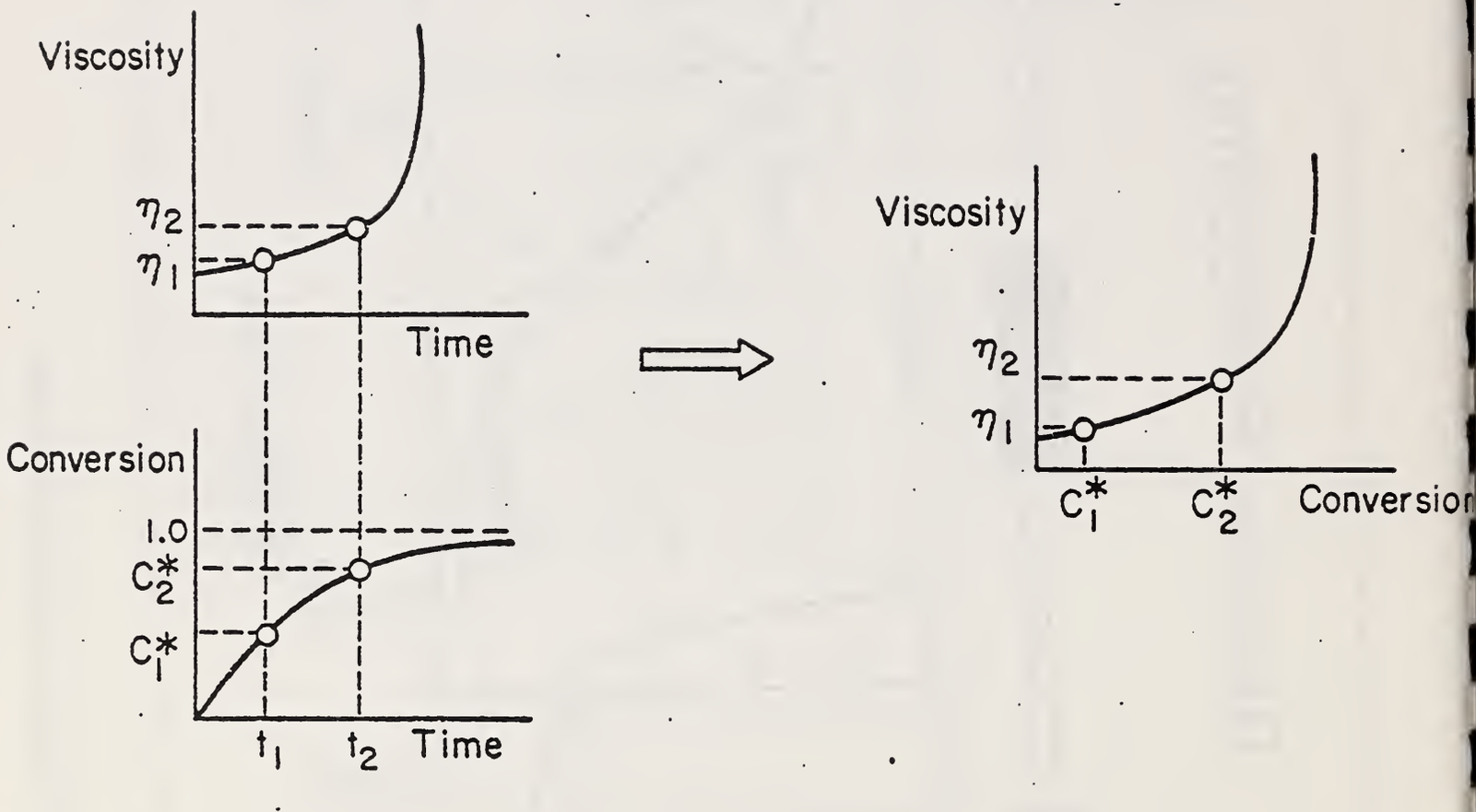

Figure 4. Mapping of a viscosity rise vs. time plot into a viscosity vs. extent of reaction plot.

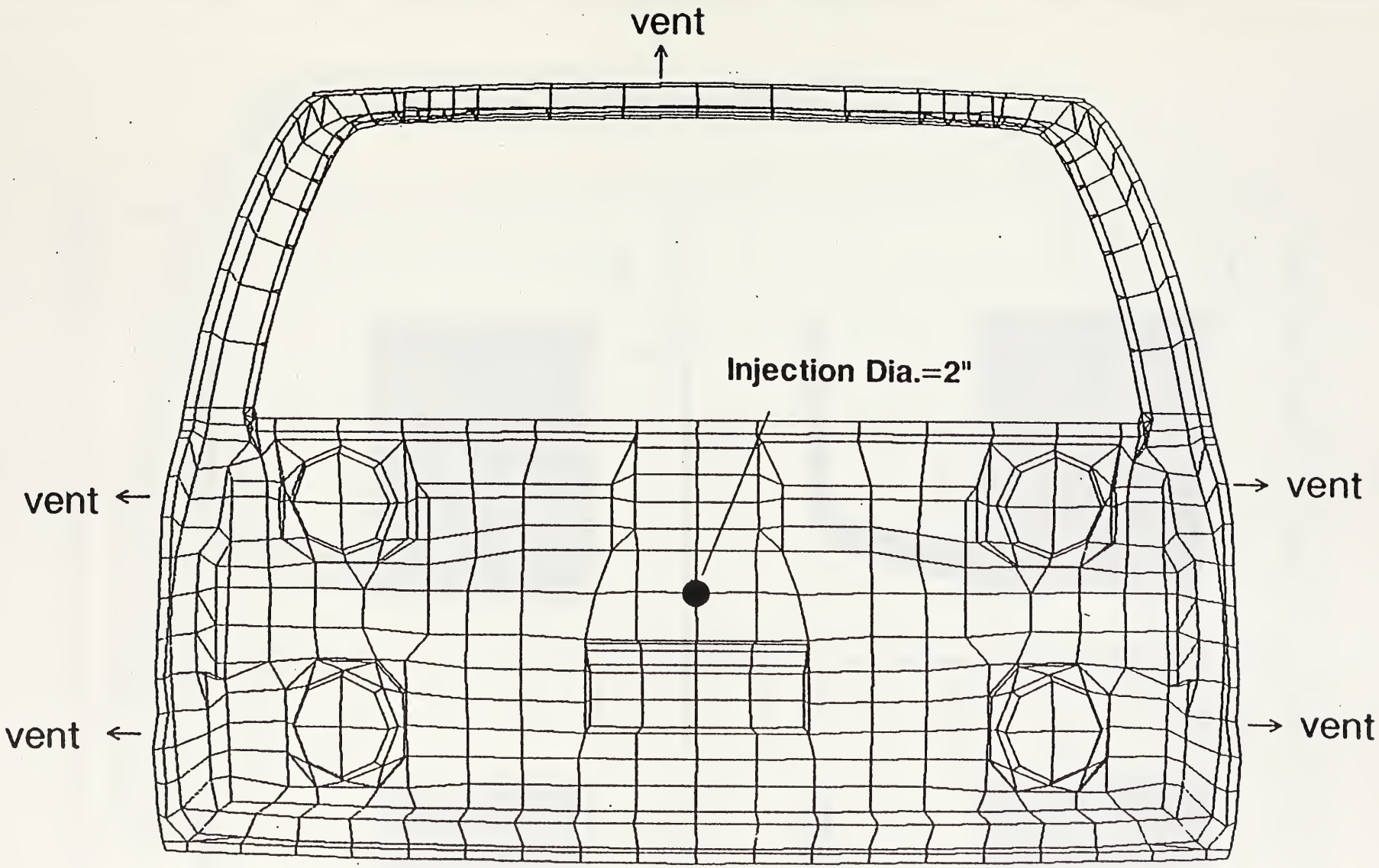

Figure 5. Automotive liftgate with point source gate under lock area (Case 1).

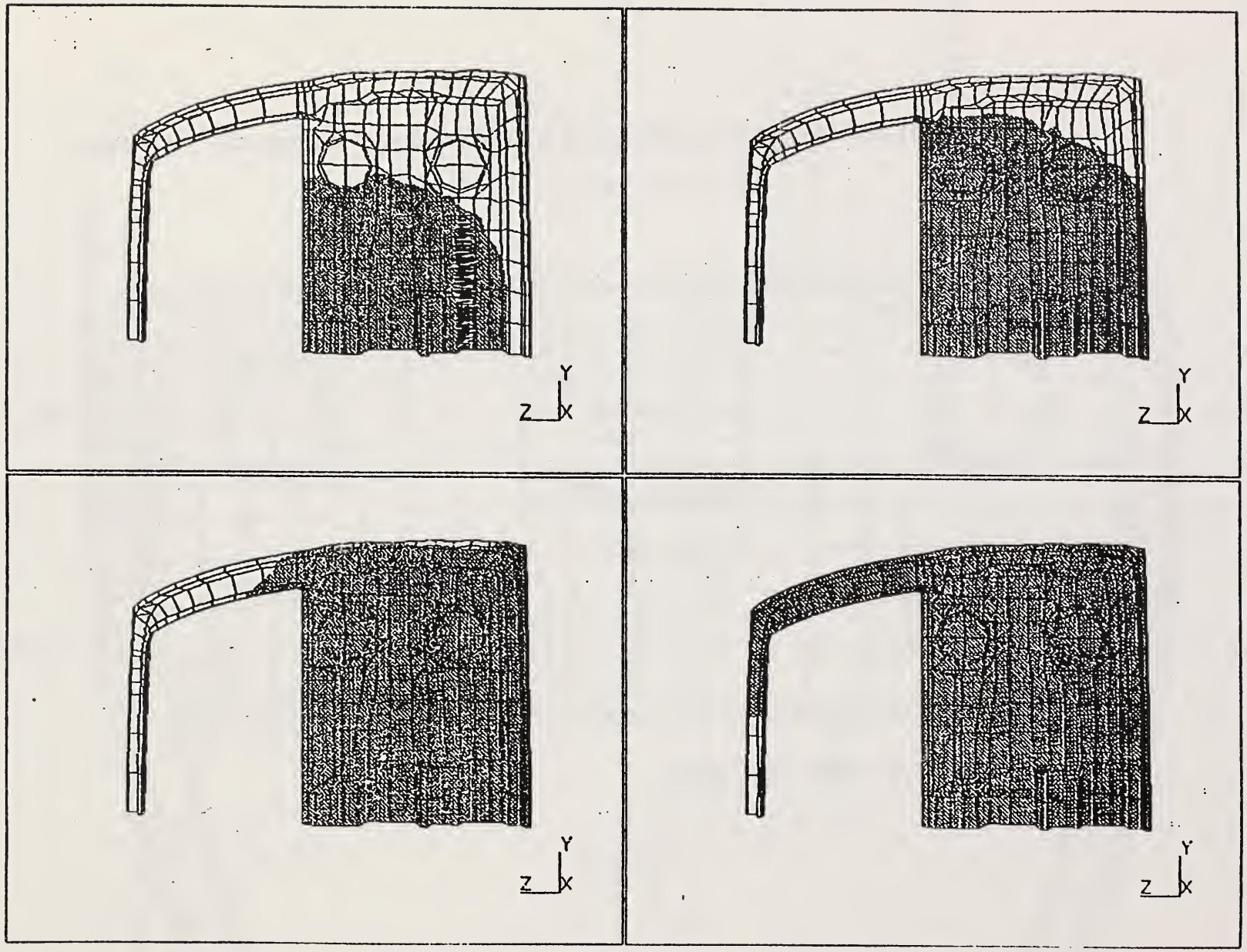

Figure 6. Flow patterns for injection (Case 1).

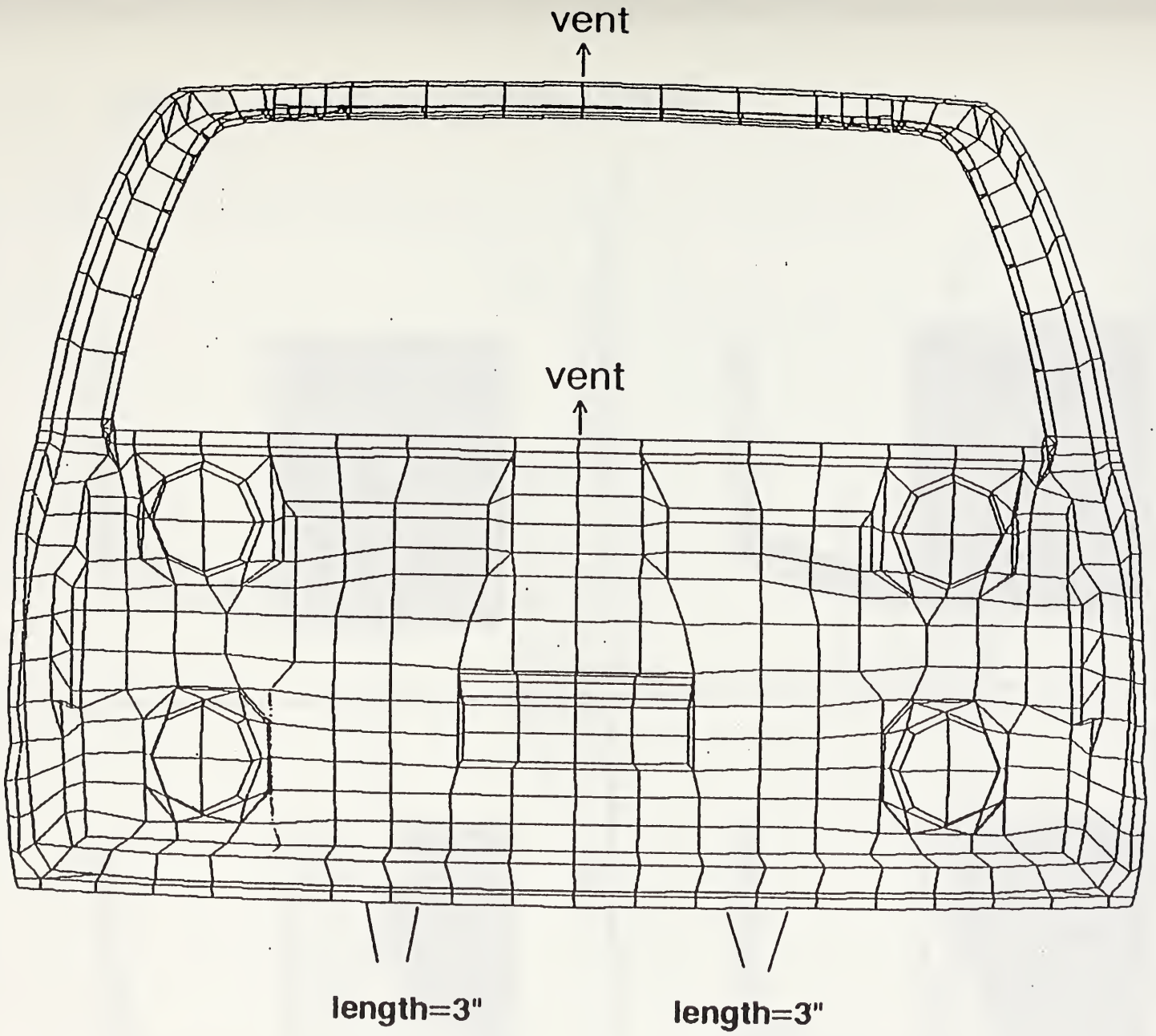

Figure 7. Automotive liftgate with two small fan gates (Case 2).

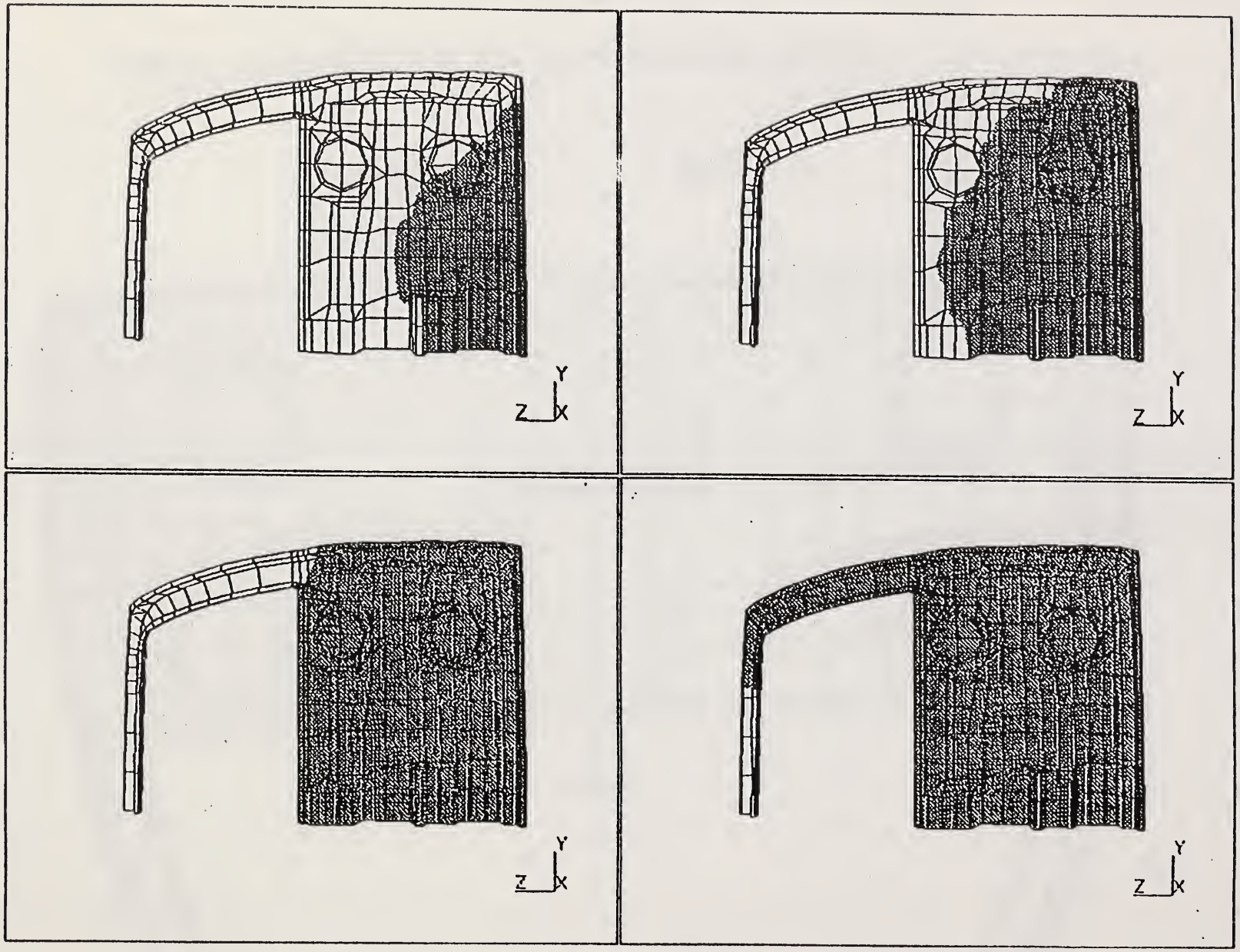

Figure 8. Flow patterns for injection (Case 2).

Heat Transfer and Reaction Issues in Liquid Composite Molding

Charles L. Tucker III
Department of Mechanical and Industrial Engineering
University of Illinois
Urbana, IL 61801

January 21, 1994

Presented at the
Workshop on Manufacturing Polymer Composites by Liquid Molding
National Institute of Standards and Technology
Gaithersburg, Maryland
September 20-22, 1993

Submitted to *Polymer Composites*

INTRODUCTION

In liquid composite molding a liquid polymer resin is injected into a mold that contains a fiber preform, undergoes a curing reaction, and hardens. The main examples are resin transfer molding (RTM) and structural reaction injection molding (S-RIM). Many practical issues in liquid composite molding are related to heat transfer and reaction. A short shot results from curing the resin too quickly compared to the injection speed. Total cycle times are determined by the curing rate, but curing the resin too fast will result in thermal spiking and degradation of the resin. Warping and residual stresses in a molded part are determined by the temperature and cure histories. Resin shrinkage during cure affects both large-scale dimensional stability and small-scale features such as surface finish.

The management of heat transfer and chemical reaction in liquid composite molding is complex because so many factors interact. These interactions are indicated schematically in Fig. 1. As the resin enters the mold it absorbs heat from the mold and from the preform by conduction, and transports that heat within the mold by convection. The resin flow pattern influences the temperature distribution by convection, and the flow pattern is in turn affected by temperature-dependent changes in resin viscosity. A curing reaction is initiated either by a rise in resin temperature (RTM) or by mixing two reactants just prior to injection (S-RIM). The reaction rate depends on temperature, and heat liberated from the exothermic reaction raises the temperature. There are also connections between the flow pattern and the reaction: degree of cure is convected with the resin, and resin viscosity is a function of the degree of cure.

The research community has responded to this complexity by building mathematical models and computer simulations of flow, heat transfer, and chemical reaction for RTM and S-RIM molding. Computer simulations and their underlying mathematical models can incorporate all of the physical phenomena indicated above. Solutions to the model can reveal how the various factors will interact for any given part geometry and processing conditions. Models and simulations are already proving to be useful guides for the design of parts and tooling, and aids to the selection of resins and fiber preforms. Models are particularly useful when one wishes to adapt the process to new materials, such as a resin with a unique curing behavior. They also provide guidance to researchers who wish to develop new materials with better processing characteristics.

For a model to be useful it must give accurate and reliable predictions. One must also know the limits of the model – the conditions when it will not be accurate. The basic steps in building a good model are always the same:

1. Incorporate the appropriate physical phenomena into a mathematical model.
2. Gather enough material property data to use the model.
3. Analyze the model to provide some understanding of the physical phenomena.
4. Solve the model accurately for relevant cases.

This paper discusses current issues in the modeling of heat transfer and chemical reaction in liquid composite molding processes. Though not a complete survey of the literature, it attempts to identify areas where progress has been made, and to point to areas that deserve further attention from the research community. The remainder of the paper is organized around the four topics listed above.

BUILDING THE MATHEMATICAL MODEL

A model for a manufacturing process is a collection of equations, data and correlations that represents important aspects of the process behavior. The pattern for constructing a physics-based process model is illustrated in Fig. 2. There are three types of ingredients. First are fundamental physical laws, such as the balance equations for mass, momentum, and energy. These apply to all materials and situations, though we often specialize the equations for the particular case of interest. Second are constitutive equations, which describe the behavior of a particular material. Rheological constitutive equations give stress as a function of strain or strain rate, but other material behaviors such as reaction kinetics also fall in this category. Third are the geometry and boundary conditions imposed by the particular process. Information such as mold cavity shape, mold temperatures, and resin injection rate appear in this category.

For most problems, writing the balance equations is one of the easiest steps in building the model. Surprisingly, this is *not* true for RTM and S-RIM models. The literature shows wide agreement on the mass balance equation, and virtually all models use Darcy's law for the momentum balance. However, the energy and species balance equations differ from model to model. This is a serious issue, for some of the equations that have been used are incompatible with others. In fact, some models have errors in their energy balance.

The source of the problem is the difficulty of writing energy and species balance equations for multi-phase systems. The balance equations for single-phase materials are uniformly accepted and agreed upon, and one can simply look them up in a standard text. Balance equations for multi-phase systems are less readily available, and even the research literature in multi-phase flow and heat transfer contains many different versions of the equations.

Tucker and Dessenberger (1994) review different methods for deriving the balance equations and provide a reliable set of balance equations on which models for RTM and S-RIM can be based. They derive their equations using the approach of local volume averaging, since this develops the multi-phase equations from the accepted single-phase equations by a rigorous procedure. Their development is compatible with a recent text of the subject (Kaviany, 1991), which is also recommended. We now summarize the key points of that development.

Local Volume Averaging

The local volume averaging approach begins by viewing the problem on a microscopic scale, where one can see the resin flowing around individual fibers. The problem on this scale is assumed to be governed by the usual balance equations for mass, momentum, and energy. One then chooses an averaging volume V, which is large enough to take in both the solid and liquid phases, but smaller than the macroscopic dimensions of the part. The average velocity and average temperature are then defined using averages over the volume V. These are the variables that actually appear in the final equations. One advantage of the local volume averaging method is that it defines these average variables precisely.

The averaging volume V can be partitioned into a volume V_f that contains only fluid, and a volume V_s that contains only solid (see Fig. 3). The fluid and solid volume fractions are then defined as

$$\varepsilon_f = \frac{V_f}{V} \tag{1}$$

$$\varepsilon_s = \frac{V_s}{V} \tag{2}$$

We will use a subscript f for the fluid phase (the resin) and a subscript s for the solid phase (the fibers); this is consistent with the majority of the literature on multiphase materials. If the solid is saturated with fluid then ε_f is the same as the porosity of the solid.

There are actually three different types of average variables, and it is important to distinguish between them. We illustrate here with temperature T, but any other variable can be averaged the same way. The *spatial average* is simply the average over the volume V of the properties of both the fluid and solid phases; this is denoted by angle brackets:

$$\langle T \rangle = \frac{1}{V} \int_V T \, dV \tag{3}$$

The *phase average* considers only the value associated with a given phase (fluid or solid), but still averages this property over the entire volume V. Points within V but lying in the other phase make no contribution to this average, so for a fluid property the integral is taken over V_f, defined as

those parts of V that contain fluid. A phase average is also denoted by angle brackets, but with a subscript on the variable indicating the phase that is averaged. The phase average temperature of the fluid is then defined as

$$\langle T_f \rangle = \frac{1}{V} \int_{V_f} T_f \, dV \tag{4}$$

The third type of average is the *intrinsic phase average*. This average is taken over only V_f for fluid properties, or V_s for solid properties. To denote an intrinsic phase average we use a subscript f or s within the angle brackets, plus the same letter as a superscript outside the brackets. The intrinsic phase average of fluid temperature is then given by

$$\langle T_f \rangle^f = \frac{1}{V_f} \int_{V_f} T_f \, dV \tag{5}$$

Figure 3 provides a pictorial interpretation of the different types of averages. All three types of averages appear in the balance equations. The volume-average heat capacity $\langle \rho C_p \rangle$ appears in the energy equation, Darcy's law is commonly written using the phase-average fluid velocity $\langle \mathbf{v}_f \rangle$, and $\langle T_f \rangle^f$ is a convenient measure of the fluid temperature. The different averages are inter-related, for example

$$\langle T_f \rangle = \varepsilon_f \langle T_f \rangle^f \tag{6}$$

$$\langle T \rangle = \langle T_f \rangle + \langle T_s \rangle = \varepsilon_f \langle T_f \rangle^f + \varepsilon_s \langle T_f \rangle^s \tag{7}$$

Many errors can result from confusing the different averages.

To derive balance equations for the average variables, one starts by writing the appropriate microscopic balance equation. As a simple example, the mass conservation equation for the fluid (assuming constant fluid density) is

$$\nabla \cdot \mathbf{v}_f = 0 \tag{8}$$

One takes the volume average of this equation, i.e.

$$\langle \nabla \cdot \mathbf{v}_f \rangle = \langle 0 \rangle \tag{9}$$

The right-hand side is zero, but the left-hand side must be treated carefully. Using the averaging theorem (Whitaker, 1967; Slattery, 1981) one finds (Tucker and Dessenberger, 1994)

$$\frac{\partial \varepsilon_f}{\partial t} + \nabla \cdot \langle \mathbf{v}_f \rangle = 0 \tag{10}$$

If we then assume that ε_f is constant, i.e. that the fiber bed is not being consolidated, then the expected form of the continuity equation results:

$$\nabla \cdot \langle \mathbf{v}_f \rangle = 0 \tag{11}$$

This is the continuity equation used by almost all RTM and S-RIM process models.

Tucker and Dessenberger show that the same procedure on the momentum balance equation, combined with certain assumptions and simplifications, produces Darcy's law:

$$\langle \mathbf{v}_f \rangle = -\frac{1}{\mu} \mathbf{S} \cdot \nabla \langle P_f \rangle^f \tag{12}$$

Here $\mathbf{S}$ is the permeability tensor, μ is the fluid viscosity, and $\langle P_f \rangle^f$ is the average fluid pressure.

The Energy Equation

The derivation of the volume-averaged energy equation is quite long and will not be reproduced here. The main assumptions are: the solid is stationary; both the solid and the fluid have constant density, conductivity and heat capacity; and the solid and fluid are in local thermal equilibrium. Mathematically this last assumption can be written as

$$\langle T_f \rangle^f = \langle T_s \rangle^s = \langle T \rangle \tag{13}$$

Physically this means that the time scale for microscopic heat conduction between the solid and fluid is much smaller than the time scale over which the average temperature changes. Thus, any small-scale temperature differences are quickly erased by local conduction, and within any averaging volume the solid and fluid have essentially the same temperature. This allows the average energy equations for the fluid and solid to be added together, producing a single equation for the average temperature.

$$\langle \rho C_p \rangle \frac{\partial \langle T \rangle}{\partial t} + (\rho C_p)_f \langle \mathbf{v}_f \rangle \cdot \nabla \langle T \rangle = \nabla \cdot \left\{ \left(\mathbf{k}_e + \mathbf{K}_D \right) \cdot \nabla \langle T \rangle \right\}$$
$$+ \varepsilon_f \rho_f H_R \langle r_f \rangle^f + \mu \langle \mathbf{v}_f \rangle \cdot \mathbf{S}^{-1} \cdot \langle \mathbf{v}_f \rangle \tag{14}$$

Equation (14) contains the expected terms: transient and convection terms on the left-hand side, and conduction, heat of reaction, and viscous dissipation terms on the right. $\mathbf{k}_e$ is the effective conductivity tensor for heat conduction through both the fluid and the solid; it represents the combined conductivities when the fluid is stationary in the solid. H_R is the heat of reaction per unit mass of the fluid, and c_f represents the chemical conversion (degree of cure) in the fluid. r_f is the reaction rate (time derivative of c_f), which depends on the degree of cure and the fluid temperature through a kinetic equation.

One unexpected factor in Eqn. (14) is $\mathbf{K}_D$, the thermal dispersion tensor. Thermal dispersion is the transport of heat by local fluctuations in the velocity. Most readers will be familiar with this phenomena in turbulent fluid flow, where it is often called eddy diffusivity. The convection of heat by the average velocity is represented by the second term on the right-hand side of Eqn. (14). However, the microscopic velocity differs from the average velocity, both in a turbulent flow and in any flow through porous media. If a temperature gradient is also present, then these fluctuations contribute to the energy transport. $\mathbf{K}_D$ models this transport.

The dispersion term is first derived in terms of local fluctuations in temperature and velocity, and them approximated using the dispersion tensor $\mathbf{K}_D$ and the gradient of the average temperature. (See Tucker and Dessenberger, 1994, for details). The rate of dispersion should increase as the velocity increases, and we expect that the dispersion will have different rates parallel and perpendicular to the flow. Theoretical modeling of dispersion in beds of spherical particles (Kaviany, 1991) suggests that the coefficients are approximately

$$K_{||} \approx 0.8\,(\rho C_p)_f\, v_f \sqrt{S} \tag{15}$$

$$K_{\perp} \approx 0.1\,(\rho C_p)_f\, v_f \sqrt{S} \tag{16}$$

Here $K_{||}$ and $K_{\perp}$ are the components of $\mathbf{K}_D$ parallel and perpendicular to the velocity, v_f is the magnitude of the fluid velocity, and S is a scalar permeability. Note that permeability has units of length squared, so $\sqrt{S}$ provides a convenient measure of the microscopic length scale of the porous medium.

The Cure Equation

The volume averaging procedure can also be used to derive a species balance, or cure, equation.

$$\varepsilon_f \frac{\partial \langle c_f \rangle^f}{\partial t} + \langle \mathbf{v}_f \rangle \cdot \nabla \langle c_f \rangle^f = \nabla \cdot \left\{ \varepsilon_f \left(\mathbf{D}_f + \mathbf{D}_D \right) \cdot \nabla \langle c_f \rangle^f \right\} + \varepsilon_f \, r_f \left\{ \langle c_f \rangle^f, \langle T_f \rangle^f \right\} \tag{17}$$

Another dispersion term arises, with a dispersive mass transport tensor $\mathbf{D}_D$ enhancing the effective molecular diffusivity $\mathbf{D}_f$. Dispersive mass transport is potentially more important than thermal dispersion. In the energy equation the thermal dispersion enhances an already significant thermal conductivity. But in the cure equation the molecular diffusivity $\mathbf{D}_f$ is so small that it is typically neglected. Dispersion can make the diffusion term in Eqn. (17) significant, greatly altering the character of the equation and its solutions.

One Temperature or Two?

Equation (14) relies on the assumption of local thermal equilibrium, Eqn. (13), so that only one energy equation is needed to solve for one average temperature. This is sometimes referred to as a one-temperature or lumped model. Some workers have used a two-temperature model instead. Here both the fluid and solid temperatures are averaged over the local volume V, but the two average temperatures are not necessarily equal at each place and time. Two energy equations are then required to solve for the two temperatures $\langle T_f \rangle^f$ and $\langle T_s \rangle^s$.

Clearly a two-temperature model will use more computer than a one-temperature model. However, two-temperature models are required when the temperature changes rapidly. This might be the case in some S-RIM moldings, where the reaction rate is extremely high or where fast filling makes convective heat transfer very rapid. Whitaker (1986, 1991) has given careful consideration to the conditions under which the assumption of local thermal equilibrium will break down, and has established a number of criteria for this in terms of dimensionless variables.

The necessary equations for a two-temperature model can be derived by separately averaging the energy balance equations for the fluid and the solid. When this is done rigorously (Kaviany 1991; Chapt 7) the fluid equation has the form

$$\varepsilon_f (\rho C_p)_f \left(\frac{\partial \langle T_f \rangle^f}{\partial t} + \underline{\mathbf{u}_{ff} \cdot \nabla \langle T_f \rangle^f + \mathbf{u}_{fs} \cdot \nabla \langle T_s \rangle^s} \right)$$

$$= \nabla \cdot \mathbf{K}_{ff} \cdot \nabla \langle T_f \rangle^f + \underline{\nabla \cdot \mathbf{K}_{fs} \cdot \nabla \langle T_s \rangle^s}$$

$$+ A_v h_c \left(\langle T_s \rangle^s - \langle T_f \rangle^f \right)$$

$$+ \varepsilon_f \rho_f H_R \langle r_f \rangle^f + \mu \langle \mathbf{v}_f \rangle \cdot \mathbf{S}^{-1} \cdot \langle \mathbf{v}_f \rangle \qquad (18)$$

and the solid equation is

$$\varepsilon_s (\rho C_p)_s \left(\frac{\partial \langle T_s \rangle^s}{\partial t} + \underline{\mathbf{u}_{sf} \cdot \nabla \langle T_f \rangle^f + \mathbf{u}_{ss} \cdot \nabla \langle T_s \rangle^s} \right)$$

$$= \underline{\nabla \cdot \mathbf{K}_{sf} \cdot \nabla \langle T_f \rangle^f} + \nabla \cdot \mathbf{K}_{ss} \cdot \nabla \langle T_s \rangle^s$$

$$+ A_v h_c \left(\langle T_f \rangle^f - \langle T_s \rangle^s \right) \qquad (19)$$

Equations (18) and (19) contain many unexpected terms. The velocities $\mathbf{u}_{ff}$, $\mathbf{u}_{fs}$, $\mathbf{u}_{sf}$ and $\mathbf{u}_{ss}$ are not physical velocities, but "convective velocities" that depend on the fluid velocity and other parameters of the system. The associated terms reflect the possibility that the convective velocity for the fluid is different from the fluid velocity, that temperature gradient in the

solid can influence the fluid convection, and that the solid can have a convection-type term even though it is stationary. On the right-hand sides the tensors $\mathbf{K}_{ff}$, $\mathbf{K}_{fs}$, $\mathbf{K}_{sf}$ and $\mathbf{K}_{ss}$ represent total effective conductivities, including both conduction and dispersion effects, so they should be functions of the fluid velocity. Again the conductive flux in the liquid can depend on the temperature gradient in the solid, and vice versa.

Both equations contain a term for interchange of heat between the phases, modeled using the interfacial area per unit volume A_v and an interphase heat transfer coefficient h_c. Note that these terms are complementary; the heat leaving the fluid equals the heat entering the solid. The coefficient h_c should be a function of fluid velocity.

Clearly the derivation of two-temperature models is a complicated problem, and the adoption of a complete two-temperature model requires the experimental evaluation of many coefficients. None of the underlined terms in Eqn. (18) and (19) have been used in any RTM models so far, and their importance has not been assessed. The two-temperature models in the literature do include the interphase term (Gonzales and Macosko, 1985; Lin, Lee and Liou, 1991, 1993; Aoyagi, Uenoyama and Güçeri, 1992; Chan and Hwang, 1992a, 1992b). Kaviany (1991) points out that including the h_c term and omitting the underlined terms is a common approach in the multi-phase flow literature, but he speculates that models using this approach are adjusting h_c empirically to compensate for terms that should not have been dropped from the equations.

MATERIAL PROPERTY DATA

An S-RIM or RTM model that includes heat transfer and chemical reaction requires a great amount of material property data. Some of these data are readily available, or can easily be measured by standard techniques. Included on this list are the intrinsic densities, heat capacities, and thermal conductivities of the fluid and solid; the porosity of the solid; and the reaction heat and reaction kinetics of the fluid.

Other properties are either less readily available or more difficult to measure. Resin viscosity vs. reaction rate can be obtained by making isothermal measurements of viscosity vs. time and cross-plotting the results with isothermal curing data (see the paper by Castro in this volume). The permeability of fiber preforms has proved surprisingly difficult to measure, and even the basic premise Darcy's law has been called into question (see the paper by Gauvin in this volume). However, as permeability experiments are refined, by identifying and eliminating sources of experimental artifacts, the data give closer and closer concurrence with Darcy's law (Heitzmann and Tucker, 1993). Another property in the "slightly more difficult" list is the effective thermal conductivity of the saturated fluid/solid mixture. In principle this can be estimated from the intrinsic conductivities, but such estimates have not been tested against experiments.

For other properties the measurements are either very difficult or have not even been attempted. On this list are the thermal dispersion tensor, the mass dispersion tensor, and the fluid/solid heat transfer coefficient (Gonzalez and Macosko, 1985; Lin, Lee and Liou, 1993).

It is important to remember that no matter how rigorous the derivation of the model equations, and no matter how elegant the numerical solution, a model cannot be used without reliable material property data.

ANALYSIS OF THE MODEL

Before choosing a numerical solution method and writing simulation software, one should spend some time working with the model in a more general context. Useful studies of the isothermal flow equations have been presented by Gebart, Gudmundson and Lundemo (1991) and Cai (1992). However, thermal aspects of liquid composite molding have received little attention, though the work or Richardson (1983, 1989) on thermoplastic injection molding provides an excellent pattern to follow. The following section demonstrates two related types of model analysis: scaling (which leads to dimensionless groups), and analytical solutions for special cases.

Scaling and Dimensionless Groups

When a model has many parameters, such as the equations we now have for RTM and S-RIM, there are many ways to combine the parameters to make dimensionless groups. Buckingham's Pi theorem tells us how many independent dimensionless groups may be formed from a given set of parameters, but it provides no guidance on how to form the groups. In such cases a very useful approach is scaling analysis. One casts the equations into dimensionless form, choosing characteristic values that give every dimensionless variable a magnitude close to unity. The dimensionless balance equations and boundary conditions then contain combinations of the problem parameters – dimensionless groups – that are physically meaningful for the model. That is, each dimensionless group then describes the relative importance of two competing physical effects.

These dimensionless groups can be used in a variety of ways. Computing the numerical values of the groups for any particular experiment will quickly show what physical effects are important in that case. This is an enormous help in interpreting experimental results. It is also useful when comparing different experiments. If two experiments are performed under conditions that produce similar values of the dimensionless groups, then they should give similar results.

Dimensionless groups are also an aid to modeling. A very small value of a dimensionless group indicates a physical effect that is unimportant in the case at hand. This information can be used to simplify the model by eliminating the corresponding terms in the governing equations.

Tucker and Dessenberger (1994) have performed a scaling analysis on the model equations that were presented above. The important dimensionless groups associated with the energy equation are summarized in Table 1. In this table t_r represents a characteristic time for the chemical reaction (computed from the kinetic equation). α_t is the total thermal diffusivity, defined as $(k_{zz}/(\rho C_p)_f)$, with k_{zz} representing the total effective conductivity in the thickness direction. L is a characteristic length of the mold cavity in the flow direction and the cavity thickness is $2H$. V represents a characteristic value of the fluid velocity $\langle \mathbf{v}_f \rangle$, and d_p is an average fiber or particle diameter. The physical meaning of some of these groups will be elaborated in the next sub-section.

Analytical Solutions for Special Cases

Analytical solutions for special cases provide benchmarks against which numerical solutions may be tested for accuracy. One gains confidence that a computer simulation is solving the equations correctly only by comparing its results with analytical solutions. An even more important benefit of analytical solutions is the insight they provide into the process and how it works. A good set of analytical solutions helps develop physical understanding about the process. We illustrate that potential here by showing two special-case solutions for heat transfer in liquid composite molding.

The following examples treat the case of small Gelling number, $G << 1$. This means that the mold filling time is much less that the time for chemical reaction. In such cases one can ignore all effects of the curing reaction during mold filling, including the heat-of-reaction term in the energy equation and the influence of reaction on viscosity. This assumption almost never holds for S-RIM, but it can occur in some practical RTM cases and it allows us to learn about heat transfer without the complications of the curing reaction.

We consider flow into a rectangular plaque that is gated along one edge. The porosity and permeability of the preform are assumed to be constant. Flow occurs only in the x direction, so the temperature can be a function of the flow direction x and the thickness direction z, but not of the transverse direction y. The resin is injected at a temperature T_{in} and the mold wall temperature and initial preform temperature are both T_0. Normally T_0 will be greater than T_{in}. We will assume that the thermal conductivity is not a function of temperature, and that x and z are principal axes for both the thermal conductivity and the permeability.

Initially we assume that the resin viscosity does not change substantially over the temperature range from T_{in} to T_0. Then the flow equations, (11) and (12), can be used to show that the fluid velocity $\langle v_x \rangle$ is uniform in x and z and that $\langle v_z \rangle$ is zero. We further assume that the resin is injected at a

constant flow rate, so that $\langle v_x \rangle$ is know and is constant in time, and that viscous dissipation is negligible (small Brinkman number, Br << 1).

For this situation the energy equation (14) reduces to

$$\langle \rho C_p \rangle \frac{\partial \langle T \rangle}{\partial t} + (\rho C_p)_f \langle v_x \rangle \frac{\partial \langle T \rangle}{\partial x} = k_{xx} \frac{\partial^2 \langle T \rangle}{\partial x^2} + k_{zz} \frac{\partial^2 \langle T \rangle}{\partial z^2} \quad (20)$$

where k_{xx} and k_{zz} are components of the total effective thermal conductivity tensor, $(\mathbf{k}_e + \mathbf{K}_D)$.

Heat Transfer – Effect of Filling Speed

If resin injection continues after the mold is full, with resin entering the gate and exiting at one or more vents, then the temperature distribution in the mold cavity will reach a steady state. Even if the mold is not flushed in this way, a substantial region near the gate will have the steady-state temperature distribution. To model this part of the cavity, the transient term $\langle \rho C_p \rangle (\partial \langle T \rangle / \partial t)$ can be dropped from Eqn. (20), and the temperature solution will depend only on the Graetz number (see Table 1). The Graetz number Gz can be thought of as a dimensionless filling speed.

A small Graetz number corresponds to a filling speed that is slow compared to heat conduction. The conduction terms are then large compared to the convection term, so they dominate the energy equation. At steady state the effect of the mold wall boundary condition (24) diffuses throughout the cavity, and the resin and preform are at the mold temperature.

$$\langle T \rangle \approx T_0 \quad \text{for} \quad \text{Gz} << 1 \quad (21)$$

The only exception is a small entrance region, of width about equal to H, where the temperature changes from T_{in} to T_0. This is sketched in Fig. 4a.

A large Graetz number indicates a filling speed much faster than heat conduction. Now the convection term dominates, carrying fluid from the inlet through the cavity with little change in temperature. The effects of heat conduction are confined to a thin boundary layer near the mold wall, and the isotherms are nearly parallel to the x axis. This means that the x-direction conduction term can also be ignored in Eqn. (20). The energy equation then reduces to

$$(\rho C_p)_f \langle v_x \rangle \frac{\partial \langle T \rangle}{\partial x} = k_{zz} \frac{\partial^2 \langle T \rangle}{\partial z^2} \quad (22)$$

with boundary conditions

$$\langle T \rangle = T_{in} \quad \text{at} \quad x = 0 \quad (23)$$

$$\langle T \rangle = T_0 \quad \text{at} \quad z = \pm H \quad (23)$$

Since the velocity $\langle v_x \rangle$ is constant, this equation is easily solved. Introducing the coordinate z' as the distance measured from the wall towards the center of the cavity (see Fig. 4c), the temperature near the wall is found to be

$$\frac{\langle T \rangle - T_{in}}{T_0 - T_{in}} = 1 - \text{erf}\left(\frac{z'}{2\sqrt{\alpha_t\, x/\langle v_x \rangle}}\right) \quad \text{for} \quad \text{Gz} >> 1 \tag{25}$$

Here erf represents the Gaussian error function.

For this high Graetz number case the thermal boundary layer increases in thickness with distance from the entrance. Equation (25) corresponds to a boundary layer whose thickness δ grows in proportion to the square root of distance from the mold entrance.

$$\delta = 4\sqrt{\frac{\alpha_t\, x}{\langle v_x \rangle}} \tag{26}$$

At high Graetz number the boundary layer thickness δ is always less than the cavity half-thickness H.

A third possibility for filling speed is that the Graetz number is of order one, Gz ~ 1. Then the thermal boundary layers from the two sides just about meet each other at the far end of the cavity. A schematic of the temperature distributions for these three cases is sketched in Fig. 4. All three cases can occur in practice.

Effect of Heated Mold and Preform

The preceding section considered steady-state temperature distributions. We can also learn something about the time-dependent distributions (Bakharev, 1993). Consider the case of large Graetz numbers, Gz >> 1, and examine only the core region, where conduction of heat from the wall is unimportant. In analyzing this region we can ignore the z-direction conduction term, but we now retain the transient term. The energy equation (20) then becomes

$$\langle \rho C_p \rangle \frac{\partial \langle T \rangle}{\partial t} + (\rho C_p)_f \langle v_x \rangle \frac{\partial \langle T \rangle}{\partial x} = 0 \tag{27}$$

This is a wave equation, with the wave speed given by

$$V_{wave} = \langle v_x \rangle \frac{(\rho C_p)_f}{\langle \rho C_p \rangle} = \frac{\langle v_x \rangle (\rho C_p)_f}{\varepsilon_f (\rho C_p)_f + \varepsilon_s (\rho C_p)_s} \tag{28}$$

Because the fluid only has to fill the pore space in the solid, the flow front advances faster than the average fluid velocity. Its speed is

$$V_{front} = \frac{\langle v_x \rangle}{\varepsilon_f} \tag{29}$$

Comparing Eqns. (28) and (29) shows that the ratio of the two speeds depends on the porosity and on the relative heat capacities of the fluid and the solid,

$$\frac{V_{wave}}{V_{front}} = \frac{\varepsilon_f (\rho C_p)_f}{\varepsilon_f (\rho C_p)_f + \varepsilon_s (\rho C_p)_s} \tag{30}$$

so the thermal wave is always slower than the flow front. The initial temperature distribution $\langle T \rangle(x, t=0)$ simply translates in the x direction at a speed V_{wave}. In our problem the fluid enters the gate at a constant temperature T_0, but the fluid absorbs heat from the preform, which starts out at T_1. The global energy balance is satisfied if the fluid ahead of the wavefront is at T_1 and the fluid behind the wavefront is at T_0. That is, for large Graetz numbers and outside the thermal boundary layer, the temperature distribution is

$$\frac{\langle T \rangle - T_0}{T_1 - T_0} = u_s (x - V_{wave}\, t) \qquad \text{for} \qquad Gz >> 1 \tag{31}$$

where u_s represents the unit step function. This temperature distribution is sketched in Fig. 5.

Physically this step in temperature is caused by transfer of heat from the preform to the resin. The resin entering the mold at T_0 absorbs heat from the preform, which is initially at T_1. Because our model assumes local thermal equilibrium, the fluid and solid must have the same average temperature at each point, so the transfer of heat between fluid and solid is, at least in the model, instantaneous. Near the gate the preform is cooled to the resin temperature T_0. The resin absorbs no heat as it flows through this initial, cool portion of the preform. Only when the resin reaches a place where the preform is still hot can it absorb any heat. This warm resin then moves on into the hot region, and the segment of the preform that gave up its heat to warm the resin becomes part of the cool region.

In practice, conduction and dispersion in the x direction will smear out the temperature step described in Eqn. (31). The resulting temperature profiles in the core will be like the ones sketched in Fig. 5b. If a two-temperature model is used, the fluid and solid will be seen to have slightly different temperatures in the vicinity of the step.

Regardless of the modeling details, this result explains why pre-heating the preform is not an effective way to warm up the resin and speed the curing process. The pre-heat does transfer from the preform to the resin, but in a non-uniform way. The first resin to enter the mold absorbs the heat from the preform near the gate, and carries that heat downstream to other parts of the cavity. This leaves a cool preform near the gate, so the preform is

unable to warm up the last resin to enter the mold. As a result, the temperature is always low near the gate. Experimental measurements on temperatures and cure histories support this conclusion (Gonzalez and Macosko, 1985; see also the paper by Rudd in this volume).

NUMERICAL SOLUTION METHODS

The final step in modeling is to obtain accurate solutions to the model equations for cases of practical interest. This requires one to treat realistic cavity geometries, represent anisotropic and layered performs, use realistic models for the rheological and kinetic behavior of the resin, and include all the terms in the governing equations. To handle these many factors we turn immediately to numerical methods.

The governing equations are partial differential equations, and both finite difference and finite element methods can be used to solve them (e.g., Güçeri, 1989; Pittman, 1989). Many complex factors are routinely treated by standard numerical methods. Included on the list of "easy" problems are: conduction, diffusion, and dispersion terms; time-dependent solutions; complicated reaction kinetics; viscous dissipation and heat of reaction in the energy equation; cure- and temperature-dependent viscosity; and anisotropic permeability and thermal conductivity. Two-temperature models for heat transfer also present no special numerical difficulties, other than the additional time needed to compute a solution. The two most difficult issues for standard numerical methods are moving the flow front and solving transport equations that are dominated by the convection terms.

Methods for Moving Boundary Problems

Many classical problems in computational fluid mechanics and heat transfer, such as flow in a duct or flow around an airfoil, have fixed boundaries. But mold filling involves a moving flow front, so it is always a moving boundary problem. The position and shape of the resin front is not known *a priori*, but must be calculated as part of the solution. Also, the front may divide or recombine as the resin fills into ribs and bosses or flows around inserts. Even molds with very simple geometries may have complex flow front shapes if the permeability of the preform varies from point to point.

Numerical techniques for free and moving boundary problems are surveyed in the context of polymer processing by Wang and Lee (1989). These authors explain the finite element/control volume (FE/CV) method at some length, and indeed this method has been used widely for RTM and S-RIM simulations (Fracchia, Castro and Tucker, 1989; Molnar, Trevino and Lee, 1989; Bruschke and Advani, 1990, 1991; Lin, Lee and Liou, 1991, 1993; Chen and Wang, 1993).

This method uses a mesh of two-dimensional finite elements to model the cavity geometry and represent the pressure distribution. The software automatically divides the mold into control volumes, associating a control volume with each node. The front motion is followed by tracking nodal fill factors, which equal the ratio of resin volume to pore space in each control volume. A fill factor of 1 means that the volume surrounding the node is saturated with resin, while a fill factor of zero means that the surrounding volume contains no resin. Nodes with fill factors between zero and one are close to the flow front. The front is advanced by calculating volume flow rates between nodes.

The FE/CV method can only locate the front approximately at any instant in time, but it maintains accurate global mass conservation and can handle any geometry that can be meshed. Several other methods have been used, including numerically-generated finite difference grids (Coulter and Güçeri, 1989; Trochu and Gauvin, 1992; Aoyagi, Uenoyama and Güçeri, 1992) and dynamically generated finite element meshes (Chan and Hwang, 1992a, 1992b). These schemes offer better accuracy near the flow front by having a smoother front representation, but they are usually limited to simple geometries. It is also very difficult for these methods to deal with spatially varying material properties (like a preform that has patches of different composition). The FE/CV method deals easily with such parts by simply assigning different material properties to each (stationary) element.

Methods for Hyperbolic Problems

A more difficult problem, and one that has received less attention from the RTM and S-RIM research community, is the treatment of hyperbolic and nearly-hyperbolic equations. Mathematically, the heat conduction equation is elliptic. Elliptic equations arise in problems that are dominated by diffusion-like phenomena. The solution to an elliptic equation at any interior point is influenced by the solution at nearby points in all direction. Hence, the interior solution is influenced by the boundary conditions on all sides.

In contrast, an energy equation with convection terms but no diffusion terms is mathematically hyperbolic. Hyperbolic equations arise when the solution propagates in specific directions. The solution to a hyperbolic problem depends only on the solution at points in a certain direction from the point of interest. In a convection-dominated energy equation the solution at any point depends only on the upstream temperatures, and not on the temperatures or the boundary conditions downstream or across the stream.

The relative importance of the convection and conduction terms in the energy equation for RTM and S-RIM models is described by the Graetz Number, defined in Table 1. For small Graetz number, $Gz << 1$, the conduction terms dominate the equation, while a large Graetz number, $Gz >> 1$, indicates that the convection terms dominate and the equation is more hyperbolic in character.

Conventional numerical methods, like the Galerkin finite element method or finite difference methods based on central differences, are excellent at solving elliptic equations, but are very poor at solving hyperbolic equations. If one of these methods is applied to solve the energy equation, the solutions will be accurate and smooth as long as the Graetz number is small, but as the Graetz number increases the temperature solution develops oscillations or "wiggles." For sufficiently large Graetz number the solution will become unstable, and the computed nodal temperatures will tend to positive or negative infinity.

Note that, without the dispersion term, the cure equation (17) is *always* convection-dominated, since the molecular diffusivity $\mathbf{D}_f$ is very small. In a sense the introduction of dispersion terms into the energy and cure equations makes the numerical solution process easier, by rendering the equations more diffusive.

The problem of convection-dominated equations is well known in computer modeling. Numerical solutions can be obtained by altering the numerical treatment of the governing equations. However, there are many ways to do this and not all methods are equally accurate.

To demonstrate this point, consider one-dimensional flow at a constant flow rate and assume that the temperature is held constant at T_0. This could be achieved in practice by making T_{in} equal to T_0 and choosing conditions that give $Da^{IV} << 1$. The cure equation is then

$$\frac{\partial \langle c_f \rangle^f}{\partial t} + \langle v_x \rangle \frac{\partial \langle c_f \rangle^f}{\partial x} = r_f(\langle c_f \rangle^f, T_0) \tag{32}$$

To solve this equation with the finite difference method one would introduce a grid with nodes at coordinates x_1, x_2, etc., with a spacing Δx between consecutive nodes. Let c_i be the value cure $\langle c_f \rangle^f$ at node x_i. Discrete equations are then developed by replacing the spatial derivative in Eqn. (32) with a finite difference formula. The centered difference version of (32) is

$$\frac{dc_i}{dt} + \langle v_x \rangle \frac{c_{i+1} - c_{i-1}}{2\Delta x} = r_f(c_i, T_0) \tag{33}$$

Unfortunately, software based on Eqn. (33) is unstable. After a few time steps the solutions will begin to oscillate, and soon the whole solution will blow up.

A popular fix is to base the finite difference approximation of $\partial \langle c_f \rangle^f / \partial x$ at node i on a first-order formula that involves only node i and the node immediately upwind. If the resin is flowing in the positive x direction, the finite difference equation is

$$\frac{dc_i}{dt} + \langle v_x \rangle \frac{c_i - c_{i-1}}{\Delta x} = r_f(c_i, T_0) \tag{34}$$

This approach is called *first-order upwinding*. Software based on Eqn. (34) produces stable, smooth solutions. However, the solutions are not always correct. If one writes out expressions for the finite difference derivative formulas in terms of Taylor series expansions and substitutes them into Eqn. (34) (e.g., Minkowycz et al, 1988, p. 470), one finds that the equation actually solved by (34) is

$$\frac{\partial \langle c_f \rangle^f}{\partial t} + \langle v_x \rangle \frac{\partial \langle c_f \rangle^f}{\partial x} = r_f(\langle c_f \rangle^f, T_0) + \alpha_{art} \frac{\partial^2 \langle c_f \rangle^f}{\partial x^2} + \text{higher-order terms} \quad (35)$$

Here α_{art} is an artificial, or numerical, diffusivity, given by

$$\alpha_{art} = \frac{\langle v_x \rangle \Delta x}{2} \quad (36)$$

Comparing (35) to (32) shows that the first-order upwinding method has introduced a diffusion or conduction-like term into the equation. This smoothes out any perturbations in the solution, so it makes the solution stable. However, it also changes both the nature of the governing equation and the solution. The magnitude of the artificial diffusivity depends on the grid spacing Δx. As the grid is made finer the artificial diffusion becomes smaller and the numerical solution approaches the exact solution.

Other numerical methods for solving convection-dominated equations also introduce artificial diffusion, but in a more limited and controlled way. The usual strategy is to add just enough diffusion to stabilize the numerical scheme, but not so much as to alter the solution. For finite element methods, the favored technique is called Streamline Upwind/Petrov-Galerkin, or SUPG (Brooks and Hughes, 1982; Hughes and Mallet, 1986). This scheme adds artificial diffusion only in the flow direction, by altering the weighting function used to derive the finite element equations. A variety of alternate finite difference schemes are also available (e.g., Minkowycz et al., 1988, Chapts. 9 and 12).

The difference between two numerical methods for solving hyperbolic problems is illustrated in Fig. 6. Presented here are solutions to Eqn. (32) with $\langle v_x \rangle = 10$ and cure kinetics described by

$$r_f = (0.001 + 5\langle c_f \rangle^f)(1 - \langle c_f \rangle^f)^2 \quad (37)$$

for a mold of length $L = 100$. Fig. 6a shows solutions at the instant of fill obtained using finite differences and first-order upwinding, while Fig. 6b shows solutions using one-dimensional linear finite elements and SUPG. Both schemes converge on the exact solution as the number of nodes is increased, but the SUPG solution is more accurate for any given mesh size and converges more rapidly as the mesh is refined.

The same types of numerical errors appear in two- and three-dimensional problems. The danger is that the users of simulation software may inadvertently obtain distorted, unrealistic solutions due to the limitations of

the numerical method. This problem deserves careful attention from the research community.

SUMMARY: RESEARCH ACHIEVEMENTS AND NEEDS

We can now summarize the achievements of recent research and identify some immediate needs. Again the discussion will be organized according to the four steps of modeling.

Building the Mathematical Model

We now have a complete mathematical model for flow, heat transfer and curing, at least when the assumption of local thermal equilibrium is accurate. Rigorous derivation of the governing equations by the local volume averaging method has cleared up ambiguities about how some terms should be handled, and has introduced the need for dispersion terms in the energy and cure equations. This part of the model seems to be well in hand.

Equally rigorous equations for the two-temperature model have been derived, but the few two-temperature treatments to date have ignored many terms in these equations. If two-temperature models are indeed important then further theoretical and experimental work is needed to sort out the best governing equations.

Other aspects of the RTM and S-RIM processes have not received as much attention from modelers, but they are equally as important as heat transfer and curing. The issue of void formation and transport during mold filling is critical. Trapped gas bubbles degrade both the appearance and the structural performance of a molded part, so they are important in both high-performance and high-volume applications. Void formation is related to non-uniform advancement of the flow front on the micro-scale. After a bubble forms it may change size due to pressure changes in the surrounding fluid, and may then move with the flow. Some early studies and modeling approaches have already appeared (Parnas and Phelan, 1991; Lundström, Gebart and Lundemo, 1991; Mahale, Prud'homme and Rebenfeld, 1992; Chan and Morgan, 1992).

Another area where modeling could help is preforming. Making basic reinforcement products (tows, mats, cloth) into a preform, especially for a complicated 3-D mold, represents a major cost for RTM or S-RIM parts. Preforming models are needed to determine what shapes can and cannot be formed. This information would be particularly helpful in the early stages of part design. Also, details of the preforming operation affect the resin flow during mold filling. By knowing the deformation of a mat or cloth at any point in the mold, one can anticipate changes in the local permeability and deal with this issue. Some preforming calculations have been made for biaxial woven fabrics (Mack and Taylor, 1965; Heisy and Haller, 1988; Robertson et al., 1981; 1984; Van West, Keefe and Pipes, 1989; Van der Weeën, 1991), but none are yet available for random fiber mats.

Obtaining Material Property Data

A complete simulation of RTM or S-RIM mold filling requires a great deal of material property data. We have well-established measurement methods and a reasonable amount of data for many properties, including reaction kinetics, resin rheology, and the permeability of preforms. Intrinsic thermal conductivities of the fiber and resin are also available, but there is little data on the effective conductivity of resin-saturated preforms. Even less data is available for dispersion in the energy and cure equations. Even the best models and numerical methods will be useless without complete and reliable materials property data. More experimental work is needed.

Analysis of the Model

We have a meaningful set of dimensionless parameters for the flow, heat transfer and cure models, and analytical solutions for a few special cases. However, the discussion of model analysis in this paper has only touched on the possibilities of this approach. Collecting or generating additional analytical solutions for heat transfer and cure for a variety of special cases would greatly enhance our understanding of the physical phenomena that occur in liquid composite molding. Analytical solutions also provide rigorous tests for the numerical solution methods that will be the everyday tools of design and process engineers.

Numerical Solution Methods

Currently, we have numerical methods that can automatically handle mold filling in parts with complex geometry, and can represent the interactions between flow, heat transfer, and the chemical and rheological behavior of the resin. The main question at this time is the accuracy of different numerical schemes for problems with fast filling and fast reactions. This issue has been thoroughly researched by other parts of the computational fluid dynamics and heat transfer community, so the main need is to test various methods and select an appropriate one.

Conclusion

Liquid composite molding is a complicated process with interactions between many physical phenomena. Modern modeling and numerical simulation techniques can represent these many interactions, and help engineers to select materials, shape molds, and design parts. However, the existence of a robust computer code with color graphics does not guarantee accurate results. Only by being careful about the mathematical model, material properties, and numerical solution methods can we develop useful engineering tools.

REFERENCES

Aoyagi, H., M. Uenoyama and S. I. Güçeri, "Analysis and Simulation of Structural Reaction Injection Molding (SRIM)", *International Polymer Processing, 7,* 71-83 (1992).

Bakharev, A. S., Department of Mechanical and Industrial Engineering, University of Illinois, personal communication (1993).

Brooks, A. N. and T. J. R. Hughes, "Streamline Upwind/Petrov-Galerkin Formulations for Convection Dominated Flows with Particular Emphasis on the Incompressible Navier-Stokes Equations," *Comp. Meth. Appl. Mech. Engng., 32,* 199-259 (1982).

Bruschke, M. V. and S. G. Advani, "A Finite Element/Control Volume Approach to Mold Filling in Anisotropic Porous Media," *Polymer Composites, 11*, 398-405 (1990).

Bruschke, M. V. and S. G. Advani, "RTM: Filling Simulation of Complex Three Dimensional Shell-Like Structures," *SAMPE Quarterly,* 2-11, October (1991).

Cai, Z., "Analysis of Mold Filling in the RTM Process," *J. Compos. Mater, 26,* 1310-1338 (1992).

Chan, A. W. and R. J. Morgan, "Modeling Preform Impregnation and Void Formation in Resin Transfer Molding of Unidirectional Composites," *SAMPE Quarterly, 23, No. 3*, 48-52 (1992).

Chan, A. W. and S.-T. Hwang, "Modeling Nonisothermal Impregnation of Fibrous Media With Reactive Polymer Resin," *Polymer Eng. Sci., 32*, 310-318 (1992a).

Chan, A. W. and S.-T. Hwang, "Modeling Resin Transfer Molding of Axisymmetric Composite Parts," *J. Matls. Proc. Mfg. Sci., 1*, 105-118 (1992b).

Chen, T.-Y. and V. W. Wang, "A Unified Simulation for Reactive Polymer Processing: RIM, SRIM and RTM," *SPE Tech. Papers, 39,* 2421-2425 (1993).

Coulter, J. P. and S. I. Güçeri, "Resin Impregnation During the Manufacturing of Composite Material Subject to Prescribed Injection Rate," *J. Reinf. Plast. Compos., 7*, 200-220 (1988).

Fracchia, C. A., J. Castro and C. L. Tucker, "A Finite Element/Control Volume Simulation of Resin Transfer Mold Filling ," Proceedings of the American Society for Composites Fourth Technical Conference, pp. 157-166, Technomic, Lancaster, PA (1989).

Gebart, B. R., P. Gudmundson and C. Y. Lundemo, "An evaluation of alternative injection strategies in RTM," Tech. Rep. 90-023, Swedish Institute of Composites, Box 271, S-941 26 PITEÅ, Sweden (1991).

Gonzalez-Romero, V. and C. W. Macosko, "Adiabatic Filling Through Packed Beds in Composite Reaction Injection Molding," *Polym. Process Eng., 3*, 173-184 (1985).

Güçeri, S. I., "Finite Difference Solution of Field Problems," *Fundamentals of Computer Modeling for Polymer Processing*, C. L. Tucker, ed., Hanser, Munich (1989).

Heisey, F. L. and K. D. Haller, "Fitting Woven Fabric to Surfaces in Three Dimensions," *J. Textile Inst., 79*, 250-263 (1988).

Heitzmann, K. F. and C. L. Tucker, "Permeability Measurement of Woven and Non-Woven Reinforcements," poster presented at the Workshop on Manufacturing Polymer Composites by Liquid Molding, National Institute of Standards and Technology, Gaithersburg, Maryland, September 20-22 (1993).

Hughes, T. J. R. and M. Mallet, "The Generalized Streamline Operator for Multidimensional Advective-Diffusive Systems," *Comp. Meth. Appl. Mech. Engng., 58*, 305-328 (1986).

Kaviany, M., *Principles of Heat Transfer in Porous Media*, Springer-Verlag, New York (1991).

Lin, R., L. J. Lee and M. J. Liou, "Non-isothermal Mold Filling and Curing Simulation in Thin Cavities with Preplaced Fiber Mats," *International Polymer Processing, 6,*, 356-369 (1991).

Lin, R., L. J. Lee and M. J. Liou, "Mold Filling and Curing Analysis in Liquid Composite Molding," *Polymer Composites, 14*, 71-81 (1993).

Lundström, T. S., B. R. Gebart and C. Y. Lundemo, "Void Formation in RTM," Technical Report 91-024, Swedish Institute of Composites, Piteå, Sweden (1991).

Mack, C. and H. M. Taylor, "The Fitting of Woven Cloth to Surfaces", *J. Textile Inst., 47*, T477-T488 (1956).

Mahale, A. D., R. K. Prud'homme and L. Rebenfeld, "Quantitative Measurement of Voids Formed During Liquid Impregnation of Nonwoven Multifilament Glass Networks Using an Optical Visualization Technique," *Polymer Eng. Sci., 32*, 319-326 (1992).

Minkowycz, W. J., E. M. Sparrow, G. E. Schneider, and R. H. Pletcher, *Handbook of Numerical Heat Transfer*, Wiley, New York (1988).

Molnar, J. A., L. Trevino and L. J. Lee, "Liquid Flow in Molds with Prelocated Fiber Mats," *Polymer Composites, 10*, 414-423 (1989).

Parnas, R. S. and F. R. Phelan Jr., "The Effects of Heterogeneous Porous Media on Mold Filling in Resin Transfer Molding," *SAMPE Quarterly,* 53-60 (1991).

Richardson, S. M., "Moulding." in *Computational Analysis of Polymer Processing*, J. R. A. Pearson and S. M. Richardson, eds., Applied Science, London (1983).

Richardson, S. M., "Simplified Geometry Models," *Fundamentals of Computer Modeling for Polymer Processing*, C. L. Tucker, ed., Hanser, Munich (1989).

Robertson, R. E., E. S. Hsiue, E. N. Sickafus and G. S. Y. Yeh, "Fiber Rearrangements During the Molding of Continuous Fiber Composites. I. Flat Cloth to a Hemisphere," *Polymer Composites, 2*, 126-131 (1981).

Robertson, R. E., E. S. Hsiue and G. S. Y. Yeh, "Fiber Rearrangements During the Molding of Continuous Fiber Composites. II. Flat Cloth to a Rounded Cone," *Polymer Composites, 5*, 191-197 (1984).

Slattery, J. C., *Momentum, Energy and Mass Transfer in Continua,* Second Edition, Krieger Publishing Co., Huntington, New York, (1981).

Trochu, F. and R. Gauvin, "Limitations of a Boundary-Fitted Finite Difference Method for the Simulation of the Resin Transfer Molding Process," *J. Reinf. Plast. Compos., 11,* 772-786 (1992).

Tucker, C. L. and R. B. Dessenberger, "Governing Equations for Flow and Heat Transfer in Stationary Fiber Beds," *Flow and Rheology in Polymer Composites Manufacturing,* S. G. Advani, ed., Elsevier, Amsterdam (1994).

Van der Weeën, F., "Algorithms for Draping Fabrics on Doubly-Curved Surfaces," *Int. J. for Numerical Methods in Engineering, 31*, 1415-1426 (1991).

Van West, B. P., M. Keefe and R. B. Pipes, "The Draping of Bidirectional Fabric Over Three-Dimensional Surfaces," *Proceedings of the American Society for Composites Fourth Technical Conference*, Technomic, Lancaster, Pa., 463-472 (1989).

Wang, H. P. and H. S. Lee, "Numerical Techniques for Free and Moving Boundary Problems," *Fundamentals of Computer Modeling for Polymer Processing*, C. L. Tucker, ed., Hanser, Munich (1989).

Whitaker, S., "Diffusion and Dispersion in Porous Media," *AIChE J., 13,* 420-427 (1967).

Whitaker, S., "Local Thermal Equilibrium: An Application to Packed Bed Catalytic Reactor Design," *Chemical Engineering Science, 41*, 2029-2039 (1986).

Whitaker, S., "Improved Constraints for the Principle of Local Thermal Equilibrium," *Ind. Eng. Chem. Res., 30*, 983-997 (1991).

Table 1. Dimensionless groups in the energy equation.

Name	Symbol	Definition	Interpretation
Gelling No.	G	$\frac{\varepsilon_f L}{t_r V}$	$\frac{\text{fill time}}{\text{reaction time}}$
Graetz No.	Gz	$\frac{V H^2}{\alpha_t L}$	$\frac{\text{flow-direction convection}}{\text{transverse conduction}}$
Damköhler No., Group IV	Da^{IV}	$\frac{\varepsilon_f \rho_f H_R H^2}{\langle k \rangle \Delta T t_r}$	$\frac{(\partial T/\partial t) \text{ from reaction}}{(\partial T/\partial t) \text{ from conduction}}$
Microscopic Thermal Peclet No.	Pe_{tp}	$\frac{V d_p}{\alpha_t}$	$\frac{\text{dispersion}}{\text{conduction}}$
Brinkman No.	Br	$\frac{\mu V^2 H^2}{S \Delta T \langle k \rangle}$	$\frac{\text{viscous dissipation}}{\text{conduction}}$

LIST OF FIGURES

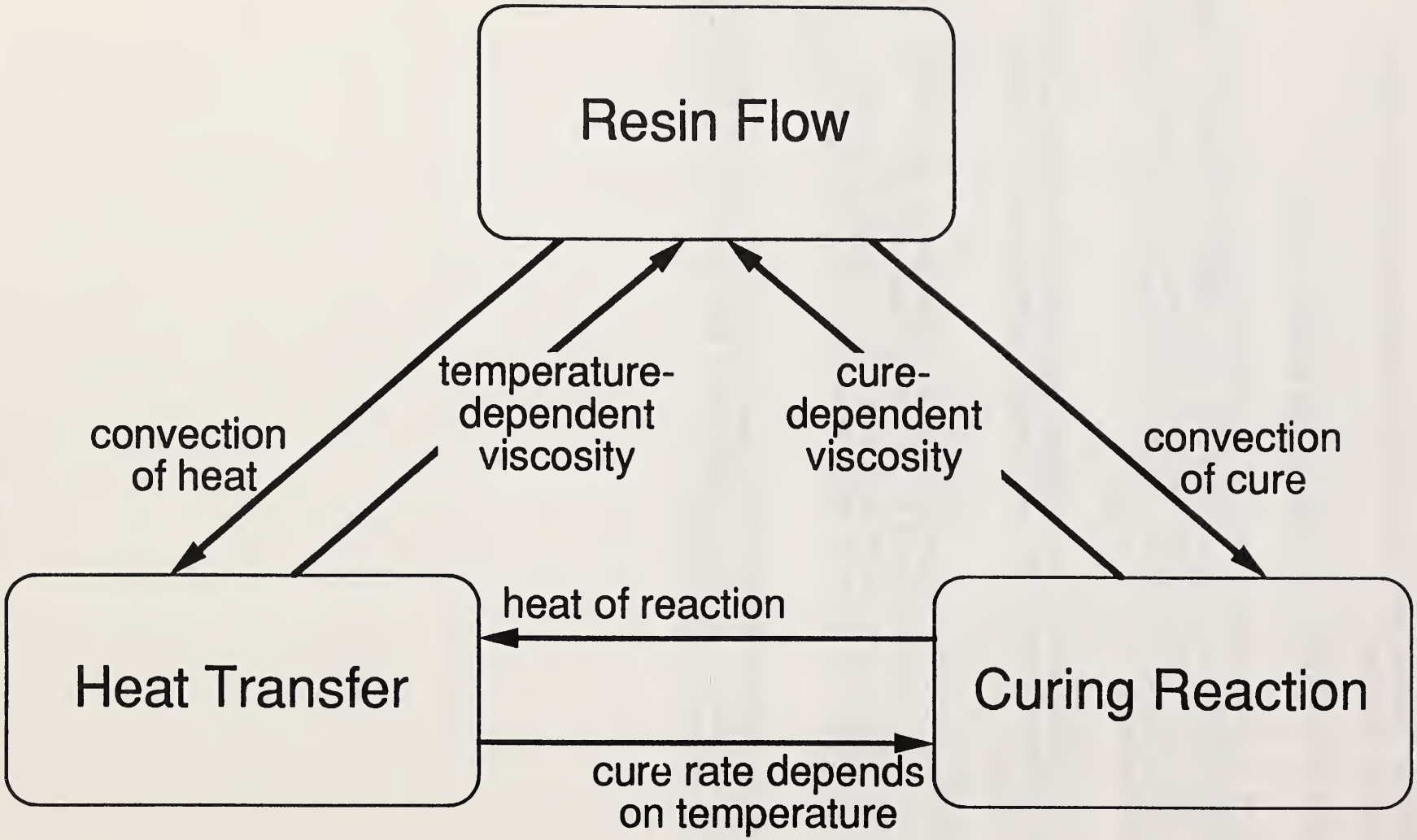
Resin Flow
temperature-
dependent
viscosity
cure-
dependent
viscosity
convection
of heat
convection
of cure
heat of reaction
Heat Transfer
Curing Reaction
cure rate depends
on temperature

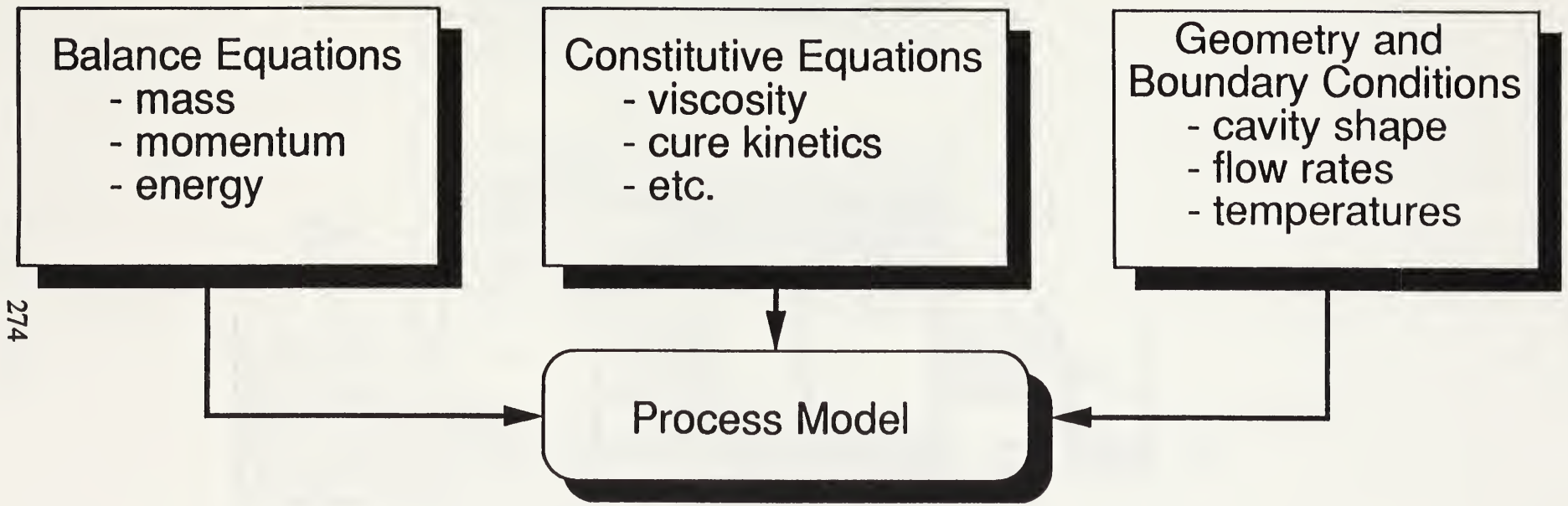
Balance Equations
- mass
- momentum
- energy
Constitutive Equations
- viscosity
- cure kinetics
- etc.
Geometry and
Boundary Conditions
- cavity shape
- flow rates
- temperatures
Process Model

Tucker, Fig. 2

V
S
f
(a)
V
f
(b)
V_f
f
(c)

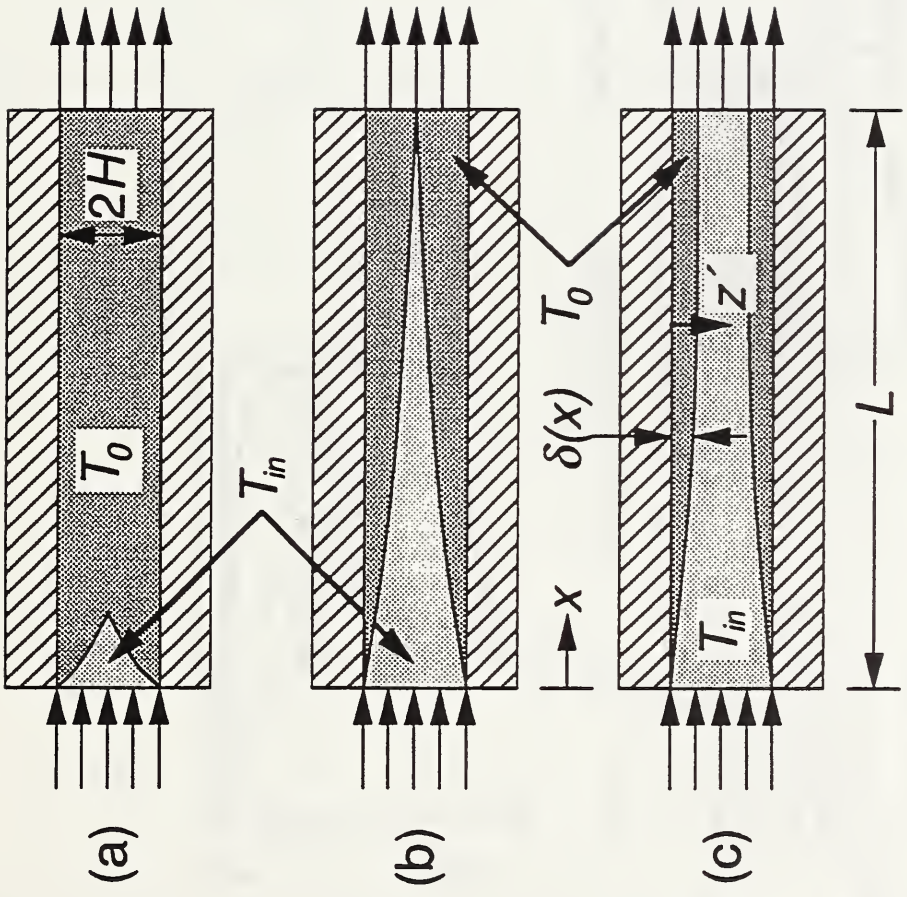
2H
T_0
T_{in}
T_0
$\delta(x)$
x
z'
T_{in}
L
(a)
(b)
(c)

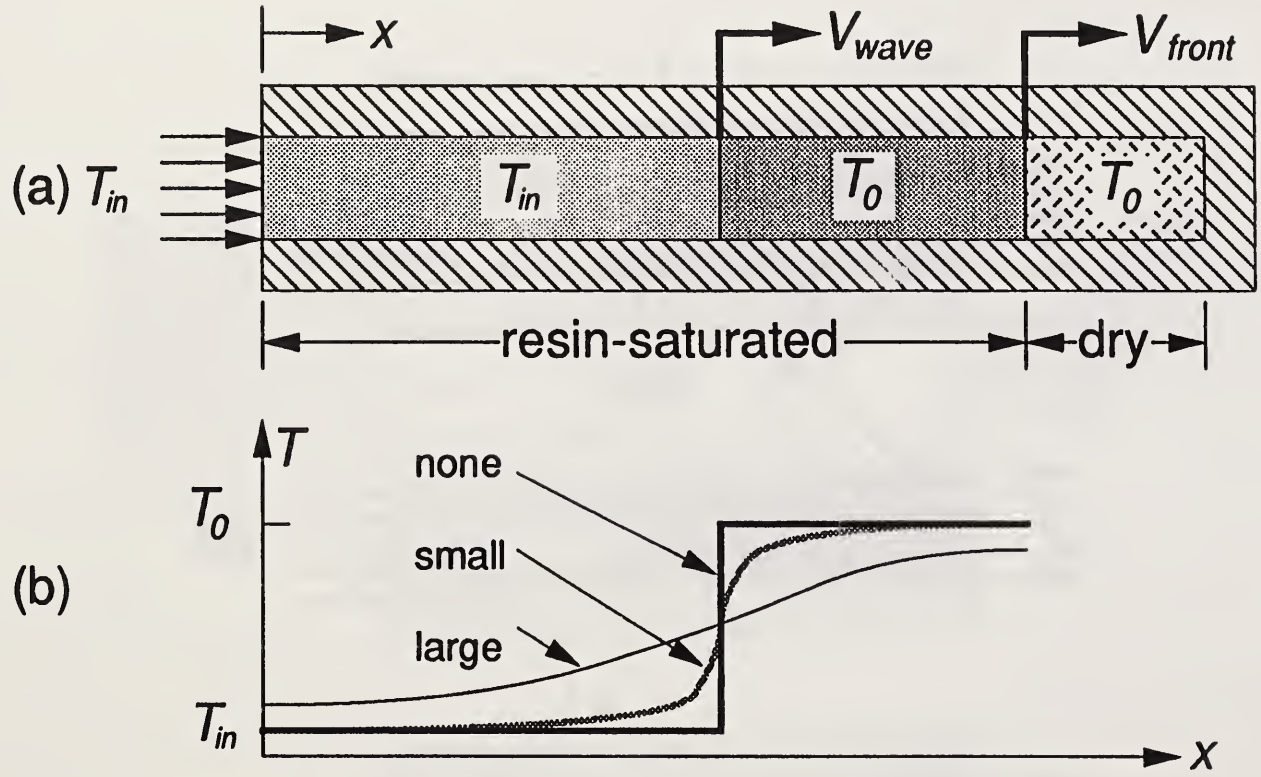
x
V_{wave}
V_{front}
(a) T_{in}
T_{in}
T_0
T_0
resin-saturated
dry
(b)
T
T_0
T_{in}
none
small
large
x

Tucker, Fig. 5

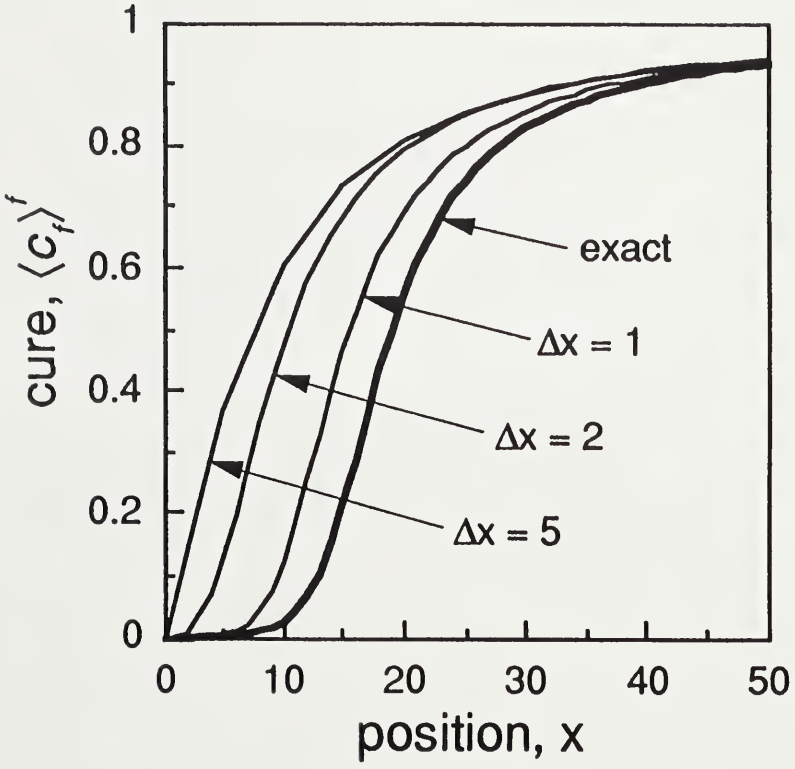

(a)

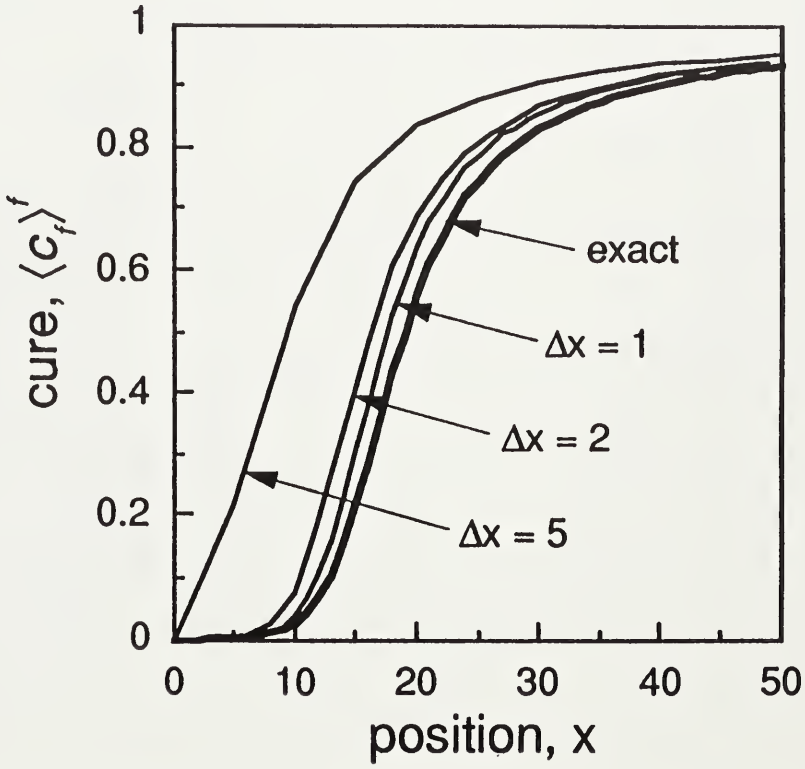

(b)

Tucker, Fig. 6